MITOCHONDRIAL PRECONDITIONING-TRIGGERED

BRAIN TOLERANCE

- IMPLICATIONS FOR ALZHEIMER'S DISEASE AND DIABETES

TOLERÂNCIA CEREBRAL INDUZIDA PELO

PRÉ-CONDICIONAMENTO MITOCONDRIAL

- IMPLICAÇÕES PARA A DOENÇA DE ALZHEIMER E A DIABETES

SÓNIA CATARINA DE SOUSA CORREIA

Universidade de Coimbra

2012

"THE WHOLE OF SCIENCE IS NOTHING MORE THAN A REFINEMENT OF EVERYDAY

THINKING."

ALBERT EINSTEIN

Agradecimentos/ Acknowledgments

Em primeiro lugar, agradeço à minha orientadora, Doutora Paula Moreira, por ter acreditado na realização deste trabalho. Durante esta longa jornada, representou para mim uma fonte de inspiração e motivação. Agradeço o acompanhamento contínuo, as discussões científicas, o incentivo, a confiança e o crescimento científico. Provavelmente, muito ficará por dizer, mas desde já um MUITO OBRIGADO! Hoje acredito na frase: "What does not kill you makes you stronger".

À Doutora Maria Sancha Santos, minha co-orientadora, agradeço toda a confiança depositada neste trabalho e por me receber na "velhinha" Zoologia. Obrigada pelo seu constante apoio, energia, e por ter sido um importante pilar na execução de todo o trabalho experimental desta tese.

Agradeço ainda ao grupo "Molecular Mechanisms of Disease" por todo o apoio e críticas construtivas durante a realização do trabalho experimental. Um obrigado aos meus companheiros de bancada: Raquel, Daniela, Daniel, Diana, Emanuel, Ana Duarte, Ana Plácido, Rosa e Catarina. Agradeço o conhecimento científico partilhado, mas principalmente, a boa disposição e as gargalhadas sonoras (...da Raquel). Um agradecimento muito, muito especial aos colegas de trabalho e amigos, Cristina, Renato e Susana. Durante estes anos aprendemos e partilhamos muitas coisas. No quotidiano, é difícil transmitir-vos o que sinto por vocês... O stress do trabalho, a pressão e os maus resultados (vá e alguns bons lá pelo meio) podem mascarar o que no fundo tem sido uma verdadeira amizade. Sei que posso contar com vocês para a vida toda! Ah, desculpem o meu mau feitio!

To Prof. Mark Smith for giving me the opportunity to work in his laboratory in Cleveland. Thank you for the enthusiasm, the scientific discussions, and foremost for believing in my scientific skills. It was a privilege to work with you!

For her technical insights, generosity, and positive attitude, I am also grateful to Prof. Gemma Casadesus.

I would like to express my gratitude to Prof. Joseph LaManna for promptly accepting me in his laboratory and for all the technical support with the *in vivo* studies.

A very special thanks to Beth Kumar, Sandra Siedlak, Peggy Harris, Sandy Richardson, Julie Wolfram, Wataru Kudo, Hyun-Pil Lee and Frederick Allen for all the helpfulness and for making my stay in Cleveland more enjoyable.

Aos colegas, funcionários e técnicos do Centro de Neurociências e Biologia Celular da Universidade de Coimbra agradeço todo o apoio e auxílio prestado durante a realização do trabalho experimental.

Agradeço ainda a todos os meus amigos (os verdadeiros), que não contribuindo diretamente para a realização deste trabalho, me incentivaram e foram um grande suporte. Particularmente, um obrigado do fundo do coração para a Marta, Áurea, Joana, Filipe, Carlos, Daniela, Marisa, Carolina, Mafalda, Sandra e Rita.

Aos meus pais, um obrigado pelo vosso amor incondicional, dedicação, por acreditarem em mim, e, principalmente, por estarem presentes em todas as fases da minha vida. Mãe, obrigada pelo teu precioso "colinho"! À minha irmã Raquel, agradeço toda a amizade e cumplicidade. Ao meu cunhado José Carlos, um obrigado especial por seres quem és e teres a capacidade de me alegrar. À minha sobrinha Maria Inês, obrigada pelo teu sorriso. Não há nada mais reconfortante…

Ao Ricardo, um agradecimento muito especial por teres estado sempre ao meu lado ao longo destes anos. Obrigado pelo teu amor e por preencheres a minha vida!

Ao Centro de Neurociências e Biologia Celular da Universidade de Coimbra, agradeço por me ter acolhido e concedido todas as ferramentas essenciais para a concretização do trabalho experimental e desta tese.

AOS MEUS PAIS,

À MINHA IRMÃ,

AO RICARDO.

CONTENTS

LIST OF ABBREVIATIONS

2-ME2 - 2-methoxyestradiol

3-NPA - 3-nitropropionic acid

5-HD - 5-hydroxydecanoate

ACh - acetylcholine

AChE - acetylcholine esterase

AD - Alzheimer's disease

ADAD - amyloid-β-binding alcohol dehydrogenase

ADP- adenosine diphosphate

AGEs - advanced glycation end products

AICD - amyloid-β precursor protein intracellular domain

AIF - apoptosis-inducing factor

ANT - adenine nucleotide translocator

APOE 4 - apolipoprotein E4

APP - amyloid-β precursor protein

ATP - adenosine triphosphate

Aβ - amyloid-β

Aβ1-42 - amyloid-β peptide 1-42

BAD - Bcl-2-associated death promoter

BBB - blood-brain barrier

BCA - bicinchoninic acid

BSA - bovine serum albumin

Ca^{2+} - calcium ion

CAA - cerebral amyloid angiopathy

CBF - cerebral blood flow

CBP - cAMP-response element-binding protein-binding protein

CoA - coenzyme A

CoCl₂ - cobalt chloride

CoQ9 - coenzyme Q9

COX - cytochrome *c* oxidase

CSF - cerebrospinal fluid

Cu-Zn SOD - copper-zinc-containing superoxide dismutase

CypD - cyclophilin D

Cyt c - cytochrome c

DCF - 2′-7′-dichlorofluorescein

DCF H2-DA - 2′-7′-dichlorodihydrofluorescein diacetate

DNA - deoxyribonucleic acid

DOC - sodium deoxycholate

DRP1 - dynamin-like protein 1

dsDNA - double stranded deoxyribonucleic acid

DTT - dithiothreitol

eNOS - endothelial nitric oxide synthase

EPO - erythropoietin

ER - endoplasmic reticulum

ETC - electron transport chain

fAD - familial form of Alzheimer's disease

FADH₂ - reduced flavin-adenine dinucleotide

FCCP - carbonyl cyanide-p-trifluoromethoxyphenylhydrazone

Fe²⁺ - iron in ferrous form

FeSO₄ - ferrous sulfate

Fis1 - fission protein 1

GABA - *γ*-aminobutyric acid

GFAP - glial fibrillary acidic protein

GK - Goto-Kakizaki

GLUT - glucose transporter

GPx - glutathione peroxidase

GRed - glutathione reductase

GSH - glutathione

GSK-3β - glycogen synthase kinase-3β

GSSG - glutathione disulfide

GTP - guanosine triphosphate

H_2O_2 - hydrogen peroxide

$HClO_4$ - perchloric acid

HIF-1α - hypoxia inducible factor-1α

$HO^\bullet$ - hydroxyl radical

HP - hypoxic preconditioning

HPLC - high-performance liquid chromatography

HRE - hypoxic response element

icv - intracerebroventricular

IDE - insulin-degrading enzyme

IDH - isocitrate dehydrogenase

IGF-1 - insulin-like growth factor-1

IMM - inner mitochondrial membrane

iNOS - inducible nitric oxide synthase

IP_3 - inositol 1,4,5-triphosphate

IR - insulin receptor

IRS - insulin receptor substrates

KCN - potassium cyanide

LDH - lactate dehydrogenase

LTP - long-term potentiation

MAPK - mitogen-activated protein kinase

MCAO - middle cerebral artery occlusion

MDA - malonaldehyde

MDH -malate dehydrogenase

MitoQ - mitoquinone

mitoK$_{ATP}$ - mitochondrial ATP-sensitive potassium channels

Mn SOD - manganese-containing superoxide dismutase

Mnf - mitofusin

MPP$^+$ - 1-methyl-4-phenylpyridinium ion

mPTP - mitochondrial permeability transition pore

MTCO1 - mitochondrial cytochrome *c* oxidase subunit 1

mtDNA - mitochondrial deoxyribonucleic acid

N$_2$ - nitrogen

NAC - N-acetyl-L-cysteine

NAD$^+$ - oxidized nicotinamide adenine nucleotide

NADH - reduced nicotinamide adenine nucleotide

NADP$^+$ - oxidized nicotinamide adenine dinucleotide phosphate

NADPH - reduced nicotinamide adenine dinucleotide phosphate

NBT - nitroblue tetrazolium

NFTs - neurofibrillary tangles

NIRKO - neuronal-specific insulin receptor knockout mice

NO$^\bullet$- nitric oxide

NO$_2^-$- nitrite

NP-40 - nonyl phenoxypolyethoxylethanol

NRF - nuclear respiratory factor

NT2 - human teratocarcinoma cells

O$_2$ - molecular oxygen

O$_2^{\bullet-}$ - superoxide anion radical

X
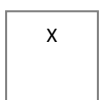
OGD - oxygen-glucose deprivation

OMM - outer mitochondrial membrane

OPA1 - optic atrophy protein 1

OPT - *o*-phthalaldehyde

PBS - phosphate-buffered saline

PD - Parkinson's disease

PDH - pyruvate dehydrogenase

PET - positron emission tomography

PGC-1α - peroxisome proliferator-activated receptor coactivator-1α

PHDs - prolyl hydroxylase enzymes

PHFs - paired helical filaments

PI-3K - phosphatidylinositol 3-kinase

PKB/Akt - protein kinase-B

PKC - protein kinase C

PMSF - phenyl-methylsulfonyl fluoride

PSEN - presenilin

RAGE - receptor for advanced glycation end products

RBE4 - rat brain endothelial cells

RCR - respiratory control ratio

ROS - reactive oxygen species

sAD - sporadic form of Alzheimer's disease

SDH - succinate dehydrogenase

SDS - sodium dodecyl sulfate

Shc - Src-homology-2-containing protein

SIMH - stress-induced mitochondrial hyperfusion

SIRT1 - sirtuin1

SOD - superoxide dismutase

SP- senile plaques

STZ - streptozotocin

T1D - type 1 diabetes

T2D - type 2 diabetes

TBA - thiobarbituric acid

TBARS - thiobarbituric acid reactive substances

TBS - Tris-buffered saline

TCA - citric acid cycle

TFAM - mitochondrial transcription factor A

TIA - transient ischemic attack

TIM - translocase of the inner mitochondrial membrane

TMPD - N,N,N',N'-tetramethyl-p-phenylenediamine

TNF-α - tumor necrosis factor-α

TOM - translocase of the outer membrane

TPP - thiamine pyrophosphate

TPP$^+$ - tetraphenylphosphonium ion

TPR - tetratrico-peptide repeats

UCPs -uncoupling proteins

UDP-GlcNAc - uridine diphosphate-N-acetylhexosamine

VDAC - voltage-dependent anion channel

VEGF - vascular endothelial growth factor

VHL - von Hippel-Lindau protein

α-KGDH - α-ketoglutarate dehydrogenase

ΔΨ$_m$ - mitochondrial membrane potential

ε - molar extinction coefficient

ρ^0- mitochondrial deoxyribonucleic acid-depleted cells

SUMMARY

Alzheimer's disease, the most common form of dementia, is a leading cause of morbidity and mortality in the elderly. Existing in both genetic and sporadic forms, this disease is characterized by severe neurodegeneration associated with the occurrence of two specific pathological hallmarks: the extracellular deposition of amyloid-β in brain parenchyma and cerebral blood vessels and the intracellular accumulation of neurofibrillary tangles composed of hyperphosphorylated tau protein. Several risk factors have been identified that may shed light on the mechanisms that may trigger or facilitate the development of Alzheimer's disease. Among them, type 2 diabetes mellitus has emerged as a major risk factor for sporadic Alzheimer's disease. These two disorders share several common abnormalities including impaired brain glucose and energy metabolism, defective brain insulin signaling and brain mitochondrial dysfunction and oxidative stress. Despite all scientific efforts in Alzheimer's disease field, there are still no effective treatments to prevent or, at least, to effectively modify the course of the disease.

The quote "what does not kill you makes you stronger" perfectly describes the preconditioning phenomenon - a paradigm that affords robust brain tolerance in face of neurodegenerative insults. During the last decades, considerable progress has been made to decipher the mechanistic basis of preconditioning-mediated brain tolerance. However, the knowledge concerning the role of structural and functional adaptations of the brain mitochondrial network in the preconditioning process remained unclear. In this regard, the two major goals of this doctoral research project were to investigate the potential protective effects of preconditioning against diabetes mellitus- and

Alzheimer's disease-related brain malfunction and to unveil the role of mitochondria in this phenomenon.

Data derived from the first part of this study (**Chapter 4**), revealed that the *in vitro* model of preconditioning induced by sub-lethal doses of cyanide (a cytochrome *c* oxidase inhibitor) was effective in protecting both brain endothelial and neuronal cells against high glucose-induced damage by modulating mitochondrial function and network organization and activating the hypoxia-inducible factor-1α signaling pathway. Cyanide preconditioning was reliant on functional mitochondria and mitochondrial reactive oxygen species production, since its cytoprotective effects were abrogated by treating the cells with the antioxidant N-acetyl-L-cysteine and absent in mitochondrial DNA-depleted ρ0 cells, characterized by the absence of functional mitochondria. This study also strength the existence of a crosstalk between mitochondrial-derived reactive oxygen species and hypoxia-inducible factor-1α, which is believed to be the master regulator of the adaptive and pro-survival response underlying the preconditioning process.

In order to validate the rat intracerebroventricularly injected with streptozotocin as a model of sporadic Alzheimer's disease, we evaluated the impact of central insulin resistance induced by streptozotocin in brain mitochondrial dysfunction and oxidative stress, which are considered early events in sporadic Alzheimer's disease (**Chapter 5**). The intracerebroventricular administration of streptozotocin resulted in cognitive deficits and increased levels of amyloid-β peptide 1-42 and hyperphosphorylated tau protein. As expected, the insulin-resistant brain state that characterizes this animal model was intimately associated with impaired brain cortical and hippocampal mitochondrial bioenergetics and increased oxidative stress, highlighting the interplay

between insulin signaling and mitochondria in sporadic Alzheimer's disease pathology. Further, these results support the idea that the rat intracerebroventricularly injected with streptozotocin is a reliable animal model for the study of sporadic Alzheimer's disease.

Then, we tested the hypothesis that hypoxic preconditioning is able to prevent the sporadic Alzheimer's disease-like phenotype induced by the intracerebroventricular administration of streptozotocin in rats (**Chapter 6**). Particularly, our results demonstrated that hypoxic preconditioning avoided learning and memory deficits, brain hypometabolism, mitochondrial dysfunction and oxidative stress. Mechanistically, mitochondrial-derived reactive oxygen species and hypoxia-inducible factor-1 alpha played a role in mediating the hypoxic preconditioning-related protective response.

To further investigate the role of mitochondria in hypoxic preconditioning-triggered brain tolerance, we performed a time-course analysis of the mitochondrial behavior and function in response to hypoxia preconditioning, characterized by repetitive periods of hypoxia-reoxygenation (**Chapter 7**). Interestingly, hypoxic preconditioning induced a more efficient mitochondrial population that could represent a major adaptive strategy in the preconditioning phenomenon. Both brain cortical and hippocampal preconditioned mitochondria displayed an enhanced bioenergetic function, which might be the result of a coordinated interaction between mitochondrial biogenesis and fusion-fission. We observed that immediately after hypoxic preconditioning mitochondrial biogenesis was stimulated, whereas in a latter phase the mitochondrial fusion-fission balance was shifted towards fusion favoring the generation of elongated mitochondria.

Taken together, the results obtained from the *in vitro* and *in vivo/ex vivo* studies revealed that brain mitochondria act as signaling organelles in the preconditioning realm, with reactive oxygen species playing the role of "redox signaling messengers". During preconditioning, mitochondria undergo functional and structural alterations that allow brain cells to survive upon a subsequent, potentially lethal stimulus. So, the reprogramming of mitochondrial biology underlying preconditioning-triggered tolerance represent a potential therapeutic strategy against pathologies associated to central insulin resistance such as diabetes mellitus and Alzheimer's disease.

SUMÁRIO

A doença de Alzheimer, a forma mais comum de demência, é uma das principais causas de morbidade e mortalidade em idosos. Existindo nas formas genética e esporádica, esta doença é caracterizada por uma neurodegenerescência severa associada à presença de dois marcadores patológicos específicos: a deposição extracelular do peptídeo β-amilóide no parênquima cerebral e vasos sanguíneos cerebrais e a acumulação intracelular de tranças neurofibrilares compostos de proteína tau hiperfosforilada. Foram identificados vários fatores de risco, os quais poderão ser uma mais-valia na descoberta dos mecanismos que desencadeiam ou facilitam o desenvolvimento da doença de Alzheimer. A diabetes tipo 2 é um dos principais fatores de risco para a doença de Alzheimer do tipo esporádico. Estas duas doenças partilham várias anomalias, tais como a diminuição do metabolismo energético e da glucose, alteração das vias de sinalização da insulina, disfunção mitocondrial e stress oxidativo. Apesar de todos os esforços científicos feitos na área da doença de Alzheimer, ainda não existem tratamentos eficazes para prevenir ou, pelo menos, modificar o curso da doença.

A citação "o que não nos mata torna-nos mais fortes" descreve perfeitamente o fenómeno do pré-condicionamento - um fenómeno que aumenta significativamente a tolerância do cérebro a estímulos lesivos. Durante as últimas décadas, foram feitos progressos consideráveis para decifrar a base mecanística da tolerância cerebral mediada pelo pré-condicionamento. No entanto, pouco se sabe sobre o papel das adaptações estruturais e funcionais da rede mitocondrial durante o pré-condicionamento. Deste modo, os principais objetivos deste projeto de doutoramento foram: investigar os potenciais efeitos protetores do pré-condicionamento na disfunção

cerebral associada à diabetes e doença de Alzheimer, e desvendar o papel da mitocôndria cerebral neste fenómeno.

Na primeira parte deste estudo (**Capítulo 4**), observámos que o no nosso modelo *in vitro* de pré-condicionamento induzido por doses subletais de cianeto (um inibidor da citocromo c oxidase) foi eficaz a proteger as células endoteliais cerebrais e neuronais dos danos causados por níveis elevados de glucose, através da modulação da função e organização da rede mitocondrial e da indução da via de sinalização mediada pelo fator de transcrição induzido por hipóxia 1α. O pré-condicionamento induzido por cianeto é dependente de mitocôndrias funcionais e da produção de espécies reativas de oxigénio, uma vez que os seus efeitos protetores foram inibidos na presença do antioxidante N-acetil-L-cisteína e inexistente em células depletadas de ADN mitocondrial. Este estudo também mostra a existência de uma interação entre as espécies reativas de oxigénio produzidas pelas mitocôndrias e o fator de transcrição induzido por hipóxia 1α, sendo este fator considerado o regulador da resposta adaptativa associada ao fenómeno do pré-condicionamento.

De forma a validar o uso do modelo animal com insulino-resistência central como uma boa ferramenta experimental para o estudo da doença de Alzheimer do tipo esporádico, fomos avaliar o estado redox e a função de mitocôndrias isoladas de cérebros de ratos sujeitos a uma injeção intracerebroventricular de uma dose sub-diabetogénica de estreptozotocina (**Capítulo 5**). É amplamente reconhecido que a disfunção mitocondrial e o stress oxidativo são alterações que ocorrem na fase inicial da doença de Alzheimer do tipo esporádico. A insulino-resistência central induzida pela administração intracerebroventricular de estreptozotocina induziu défices cognitivos e aumentou os níveis do peptídeo β-amilóide e proteína tau hiperfosforilada. Como

esperado, observámos uma diminuição da bioenergética mitocondrial e stress oxidativo no córtex e hipocampo, comprovando a existência de uma interação entre a via de sinalização da insulina e a função mitocondrial na doença de Alzheimer do tipo esporádico. Este estudo mostrou que este modelo animal é uma boa ferramenta para estudar não só os mecanismos iniciais subjacentes à doença mas também a eficácia de possíveis estratégias terapêuticas.

Desta forma, fomos avaliar o efeito do pré-condicionamento por hipóxia em ratos sujeitos à administração intracerebroventricular de estreptozotocina (**Capítulo 6**). Observámos que o pré-condicionamento por hipóxia preveniu os defeitos de aprendizagem e memória, o hipometabolismo cerebral, a disfunção mitocondrial e o dano oxidativo em ratos tratados com estreptozotocina. Mecanisticamente, as espécies reativas de oxigénio produzidas pelas mitocôndrias e o fator de transcrição induzido por hipóxia 1α parecem desempenhar um papel chave neste efeito do pré-condicionamento por hipóxia.

De forma a clarificar o papel da mitocôndria na tolerância cerebral induzida pelo pré-condicionamento, avaliaram-se as alterações temporais que as mitocôndrias cerebrais sofreram em resposta ao pré-condicionamento por hipoxia, caracterizado por períodos de hipoxia e reoxigenação (**Capítulo 7**). Curiosamente, este estudo mostrou que o pré-condicionamento por hipoxia originou uma população mitocondrial mais eficaz do ponto de vista bioenergético, o que poderá representar uma importante estratégia adaptativa no fenómeno do pré-condicionamento. O pré-condicionamento causou um aumento da função bioenergética, e alterações ao nível da biogénese e da fusão e fissão mitocondrial. Imediatamente após o pré-condicionamento por hipóxia, observou-se que a biogénese mitocondrial foi estimulada, enquanto numa fase mais

tardia o equilíbrio entre fusão e fissão mitocondrial foi alterado a favor da fusão, originando mitocôndrias alongadas.

Em conjunto, os resultados obtidos a partir dos estudos *in vitro* e *in vivo/ex vivo* mostraram que as mitocôndrias cerebrais funcionam como organelos sinalizadores durante o pré-condicionamento, sendo as espécies reativas de oxigénio os mensageiros envolvidos neste processo. Durante o pré-condicionamento, as mitocôndrias sofrem alterações funcionais e estruturais que permitem às células do cérebro sobreviver quando expostas a estímulos potencialmente letais. Assim, podemos especular que a reprogramação da biologia mitocondrial associada à tolerância induzida pelo pré-condicionamento pode representar uma estratégia terapêutica contra a disfunção cerebral associada à diabetes e doença de Alzheimer.

CHAPTER 1

GENERAL INTRODUCTION

1.1 ALZHEIMER'S DISEASE

First described by Alois Alzheimer in 1907, Alzheimer's disease (AD) is the most prevalent age-related neurodegenerative disorder, affecting approximately 35 million people worldwide (Querfurth and LaFerla, 2010). The prevalence of AD increases exponentially with age, rising from 3% in people aged 65-74 to almost 50% in people aged 85 or older (Pahnke et al., 2009). Additionally, it has been predicted that in 2050 more than 140 million people worldwide will suffer from AD (Pahnke et al., 2009).

The clinical symptoms of AD are characterized by a progressive cognitive deterioration, together with impairments in behavior, language, and visuospatial skills, culminating in the premature death of the individual typically 3-9 years after diagnosis (Querfurth and LaFerla, 2010). These traits are accompanied by two distinctive pathological hallmarks, the extracellular deposition of amyloid-β peptides (Aβ) in brain parenchyma (senile plaques, SP) and walls of cerebral arteries and capillaries (cerebral amyloid angiopathy, CAA), and the presence of intracellular neurofibrillary tangles (NFTs), mainly composed of hyperphosphorylated tau protein (Weller et al., 2009) (Fig. 1.1). AD is also characterized by severe neuronal atrophy, which initially occurs in the entorhinal region and the temporal lobe progressing to the limbic system and, subsequently, extending to major areas of the neocortex (Braak and Braak, 1995).
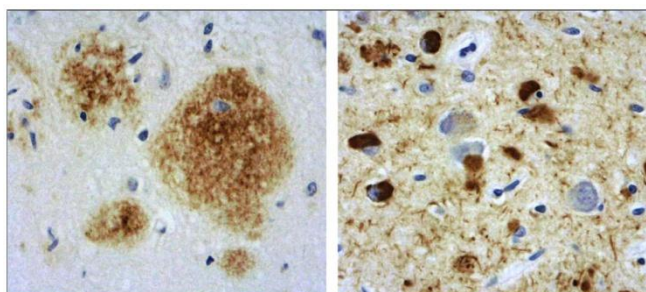
Figure 1.1. Microscopic examination showing the neuropathologic changes in a postmortem hippocampus of a patient with Alzheimer's disease. Left: amyloid-β protein deposits (length 1–42 amino acids; brown staining). Right: phosphorylated tau protein (brown staining). Adapted from Small et al., 2008.

Despite the indistinguishable clinical dementia symptoms, AD cases can be categorized in two main forms, the sporadic late-onset AD (sAD) and the early-onset familial AD (fAD). The great majority of AD cases (95% or more) are sporadic in origin, with aging, type 2 diabetes (T2D) and apolipoprotein E4 (APOE 4) as the main risk factors (Hoyer, 2004a). In a small proportion (5% or less), the disease has a genetic origin and is caused by missense mutations in three genes: amyloid-β protein precursor (APP), presenilin-1 (PSEN1), and presenilin-2 (PSEN2) (Rocchi et al., 2003). Consequently, there is an abnormal and permanent generation of Aβ fragments that aggregate into plaques.

The etiology of AD is complex and multifactorial, and several hypotheses have been proposed over the last decades to answer one of the most intriguing questions: What is the "culprit" of AD? The "amyloid cascade" hypothesis proposes that pathological assemblies of Aβ are the cause of both forms of AD, whereas other neuropathological alterations are downstream consequences of an abnormal Aβ accumulation (Hardy and Selkoe, 2002) (Fig. 1.2). However, Aβ has not been proven to be required for the onset of the sAD (Hoyer, 2004b; Joseph et al., 2001). In this regard, the involvement of brain hypometabolism, defective insulin signaling and mitochondrial dysfunction have been considered potential triggers of AD pathology, a topic that is discussed in detail in the sub-chapter 1.3 of the General Introduction.
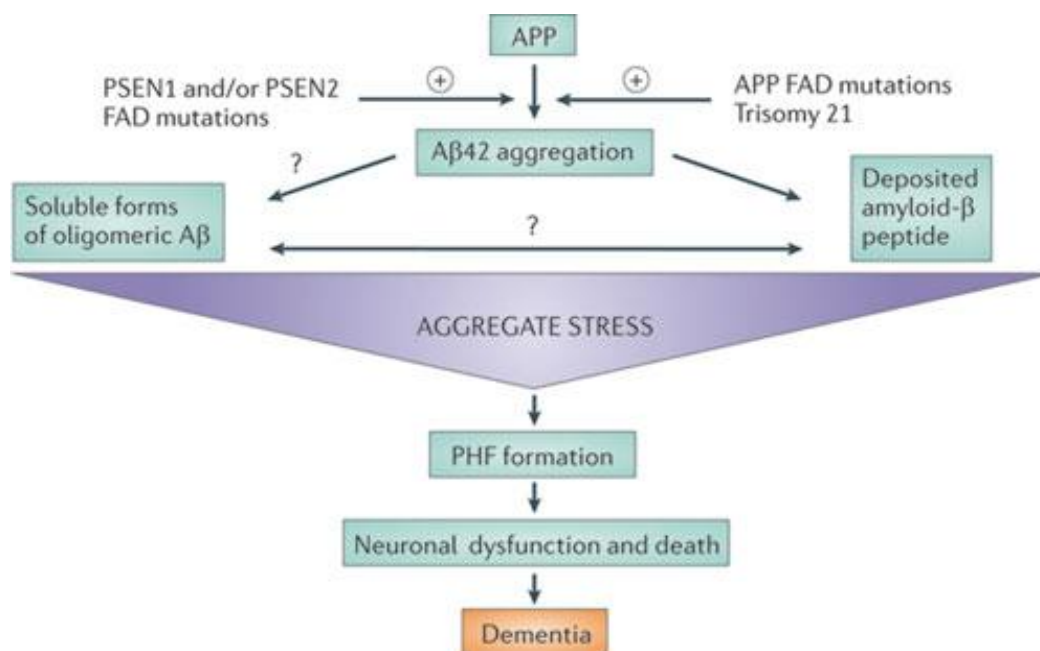
Figure 1.2. Amyloid cascade hypothesis. The amyloid cascade hypothesis posits that the deposition of the amyloid-β (Aβ) peptide in the brain parenchyma is a crucial step that ultimately leads to Alzheimer's disease. Autosomal dominant mutations that cause early onset familial Alzheimer's disease (fAD) occur in three genes: presenilin-1 (PSEN1), presenilin-2 (PSEN2), and amyloid-β precursor protein (APP). This hypothesis has been modified over the years as it has become clear that the correlation between dementia or other cognitive alterations and Aβ accumulation in the brain in the form of amyloid plaques is not linear. The concept of Aβ-derived diffusible ligands or soluble toxic oligomers has been proposed to account for the neurotoxicity of Aβ. These intermediary forms lie somewhere between free, soluble Aβ monomers and insoluble amyloid fibrils, but the exact molecular composition of these oligomers remains elusive. Further, the amyloid cascade hypothesis now suggests that synaptotoxicity and neurotoxicity may be mediated by such soluble forms of multimeric Aβ species. Aβ aggregation leads to the formation of paired helical filaments (PHFs) of tau aggregates and, ultimately, results in neuronal loss. Aβ42, the 42-amino acid form of Aβ. Adapted from Karran et al., 2011.

1.2   DIABETES MELLITUS

Diabetes mellitus is a common metabolic disorder caused by a complex interaction between genetics and environmental factors (Adeghate et al., 2006). The worldwide prevalence of this disorder is rising dramatically, being estimated that 370 million people will be suffering from diabetes in 2030 (Wild et al., 2004) (Fig. 1.3).
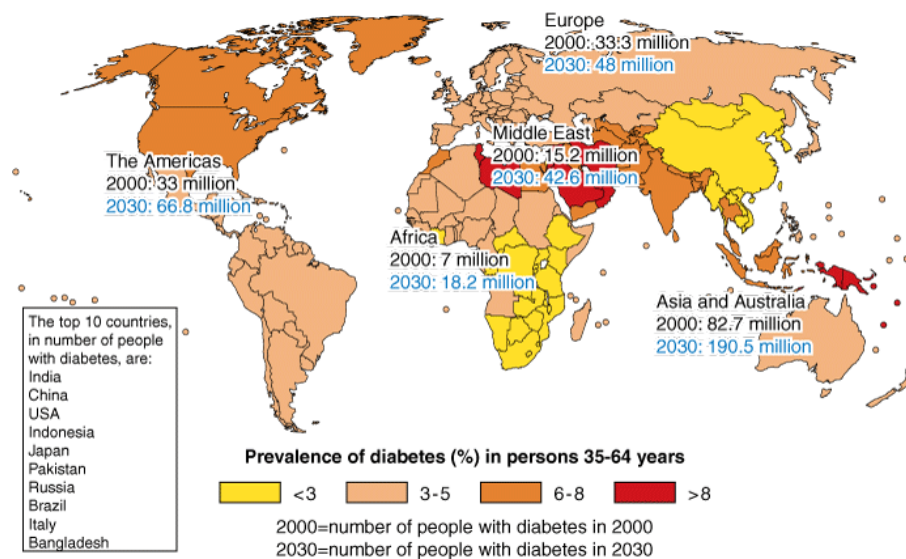
Figure 1.3. Worldwide prevalence of diabetes mellitus. The prevalence of diabetes in 2000 and the projected prevalence in 2030 are shown by geographical region. Adapted from Wild et al., 2004.

Diabetes mellitus is recognized as a group of heterogenous disorders characterized by chronic hyperglycemia and glucose intolerance due to insulin deficiency, impaired effectiveness of insulin action, or both (Umegaki, 2012). Based on its etiology and clinical presentation, diabetes mellitus is classified into two major forms: type 1 (T1D) and type 2 (T2D) diabetes. T1D results from the specific destruction of pancreatic β-cells by the immune system, culminating in hypoinsulinemic and hyperglycemic states. On the other hand, T2D is characterized by insulin resistance and partial insulin deficiency (Umegaki, 2012).

Diabetes mellitus has been posited as a cause of brain atrophy, white matter abnormalities, cognitive impairment (Table 1.1), and is considered a risk factor for dementia (Akisaki et al., 2006; den Heijer et al., 2003; Manschot et al., 2006; Schmidt et al., 2004; Toth et al., 2007). Cognitive deficits, such as impaired learning, memory, problem solving, and mental flexibility have been recognized as being more common in T1D subjects than in the general population (Biessels et al., 2008; Brands et al., 2005), suggesting a detrimental effect of hyperglycemia, and/or hypoinsulinemia on the brain. Along with these deficits, postmortem studies revealed a pronunced degeneration of cerebral cortex and neuronal loss in T1D patients compared to age-matched nondiabetic patients (DeJong, 1977; Reske-Nielsen and Lundbaek, 1963). T2D is related with a greater rate of specific and global cognitive deficits (i.e. decreased executive functions, memory skills and, processing speed) in comparison with the general population (Allen et al., 2004; Roriz-Filho et al., 2009). Moreover, studies on the cerebral structure have evidenced a pronounced cortical, subcortical, and hippocampal atrophy in T2D patients (Roriz-Filho et al., 2009). Thus, diabetes mellitus *per se* can predispose to neurodegenerative conditions, such as AD.

TABLE 1.1 COGNITIVE PROCESSES AFFECTED BY DIABETES MELLITUS

TYPE 1 DIABETES	**TYPE 2 DIABETES**
Information processing	Psychomotor speed
Psychomotor efficiency	Fontal lobe and executive function
Attention	Attention
Visuoconstruction	Verbal fluency
Memory	Memory
Visual-motor skills	Processing speed
Visual-spatial skills	Complex psychomotor functio
Motor speed	
Vocabulary	
General intelligence	
Motor strength	

1.2.1 TYPE 2 DIABETES AS A RISK FACTOR FOR ALZHEIMER'S DISEASE

Since the first Rotterdam study suggesting an increased risk to develop dementia and AD in patients with T2D, numerous clinical and epidemiological studies were undertaken to further strengthen the interplay between both diseases (Kroner, 2009; Ott et al., 1999). In fact, it was revealed that individuals with T2D have nearly a twofold higher risk of AD, independent of the risk for vascular dementia, than nondiabetic individuals (Kroner, 2009). Notably, a study of the Mayo Clinic Alzheimer Disease Patient Registry reported that greater than 80% of AD patients exhibit T2D or abnormal blood glucose levels (Janson et al., 2004), thus AD and T2D could share a common pathogenetic mechanism responsible for the loss of brain cells and β-cells, respectively. Prospective and cross-sectional analyses proposed that diabetes may accelerate the onset of AD, rather than increasing the long-term risk (Pasquier et al., 2006). Meanwhile, some studies failed to demonstrate a correlation between T2D and AD (Bucht et al., 1983; Heitner and Dickson, 1997; Nielson et al., 1996; Wolf-Klein et al., 1988). A postmortem study performed in brains of diabetic patients found no evidence of increased AD pathology compared to age-matched controls (Heitner and Dickson, 1997). However, taking into account that brain functions are extremely reliant on both glucose and insulin levels, we believe that T2D constitute a major risk factor for the development of AD by disrupting cerebral glucose metabolism and insulin signaling and, consequently, promoting brain dysfunction. Furthermore, the risk of AD associated with the APOE ε4 allele has been suggested to be exacerbated by diabetes, as patients with diabetes who are ε4 carriers are twofold more prone to develop AD than nondiabetic individuals who harbor the ε4 allele (Peila et al., 2002). The presence of the ApoE ε4 allele is considered to drastically increase the risk of developing AD by modulating APP

trafficking and processing, and inhibiting Aβ clearance (Sjogren et al., 2006). Overall, this ample epidemiological evidence supports the ideia that T2D is a major risk factor for AD.

1.3 ALZHEIMER'S DISEASE AND TYPE 2 DIABETES: COMMON PATHOGENIC MECHANISMS

In the last decades it has been identified that brain hypometabolism, defective brain insulin signaling and mitochondrial dysfunction are common denominators in AD and diabetes mellitus, and it was proposed that AD may be a brain specific form of diabetes. In this context, this sub-chapter is intended to discuss the most relevant data demonstrating that insulin signaling, glucose metabolism and mitochondria could be mechanistic linkages between AD and T2D.

1.3.1 BRAIN GLUCOSE AND ENERGY METABOLISM

Brain glucose metabolism and utilization are vital for normal neuronal function. Neurons are unable to synthesize or store glucose, which make these cells highly dependent on glucose transport across the blood-brain barrier (BBB), a process mediated by glucose transporters (GLUTs) (Scheepers et al., 2004). GLUT-1 and -3 are the predominant GLUT isoforms found in the brain, with GLUT-1 located in the neurons, cerebrovascular endothelial cells, astrocytes, and oligodendrocytes, while GLUT-3 is specifically expressed in neurons (Vannucci et al., 1997). Compelling evidence demonstrates an association between diabetes-associated abnormal glucose metabolism and memory and synaptic function impairment (Zhao and Townsend, 2009), fostering the idea that disruption of glucose supply, transport, and utilization affects cognitive function. It was recently reported that a reduction in cerebral glucose

metabolism and insulin resistance accompany memory deficits in pre-diabetic and T2D patients (Baker et al., 2011).

Positron emission tomography (PET) studies have demonstrated that brain glucose metabolism is severely impaired in AD pathology, suggesting that the hypometabolic state precedes cognitive symptoms (Mosconi et al., 2008) (Fig. 1.4). Moreover, the hypometabolism is most prominent in the posterior cingulate and parieto-temporal regions in early stages, but spreads to the prefrontal cortex as the disease progresses (Zhao and Townsend, 2009).
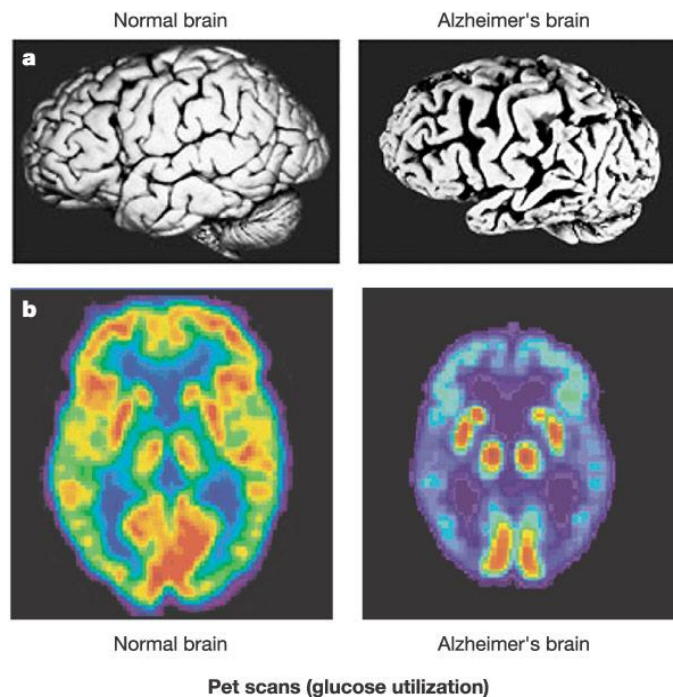
Figure 1.4. Glucose metabolism in normal and Alzheimer's disease brains. a) Compared with the brain of a healthy person, the brain of an AD patient exhibits marked shrinkage of gyri in the temporal lobe (located beneath the Sylvian fissure on both cerebral hemispheres) and frontal lobes (located at the front of the cerebral hemispheres); **b)** positron emission tomography (PET) images showing glucose uptake (red and yellow indicate high levels of glucose uptake) in a normal control subject. The brain of the Alzheimer's patient exhibits a pronounced decline in energy metabolism in the frontal cortex and temporal lobes. Adapted from Mattson, 2004.

In the early stages of AD the cerebral glucose utilization is reduced by 45%, and cerebral blood flow (CBF) by approximately 20%. However, in the later stages of the disease, metabolic and physiological abnormalities aggravate, resulting in 55-65% reductions in CBF (Hoyer and Nitsch, 1989). Interestingly, a similar hypometabolic state was detected in young and middle aged individuals carrying the apolipoprotein APOE ε4 allele (Reiman et al., 2004). It was also found a reduction in brain glucose metabolism in transgenic animal models of AD (Valla et al., 2008). The decrease in the cerebral glucose metabolism correlated with the altered expression and decreased activity of proteins related to mitochondrial energy metabolism, including pyruvate dehydrogenase (PDH), isocitrate dehydrogenase (IDH), and α-ketoglutarate dehydrogenase (α-KGDH); as observed in fibroblasts, platelets, lymphocytes and brain tissue from AD patients (Bubber et al., 2005; Huang et al., 2003). These enzymes are known to be highly susceptible to oxidative modifications and are altered by exposure to a range of pro-oxidants (Tretter and Adam-Vizi, 2000). Bubber and collaborators (2005) observed that all the changes in the activities (specifically that of PDH complex) of tricarboxylic acid cycle (TCA) enzymes were correlated with the degree of clinical disability in AD, suggesting a coordinated mitochondrial alteration. Another decisive pathophysiological consequence of the altered brain glucose metabolism is a decrease in ATP production from glucose by around 50% at the beginning of sAD, compromising the ATP-dependent processes crucial for the normal cell functioning (Mattson et al., 2001; Moreira et al., 2007) Evidence of impaired glucose distribution and utilization in AD was reinforced by the observation that GLUT-1 is significantly reduced in aged humans and in AD transgenic mice, which coincides with hippocampal atrophy (Hooijmans et al., 2007). Similarly, it was demonstrated that both GLUT-1 and -3 were decreased in AD brain, this

decrease being associated with decreased O-GlcNAcylation, the hyperphosphorylation of tau protein, and the density of NFTs (Liu et al., 2008).

The formation of advanced glycation end products (AGEs), as a consequence of impaired glucose metabolism, is also involved in the pathogenesis of AD. Hyperglycemia is known to enhance the formation of AGEs, which are senescent protein derivatives that result from the auto-oxidation of glucose and fructose (Bucala and Cerami, 1992) (Fig. 1.5). The formation and accumulation of AGEs in various tissues occur during normal aging, these processes being extremely accelerated by diabetes mellitus (Goh and Cooper, 2008). AGEs have been detected in vascular walls, lipoproteins and lipid constituents, leading to macro- and microangiopathy and amyloidogenesis (Gasser and Forbes, 2008). It was previously reported that AGEs immunoreactivity is present in both senile plaques and NFTs in AD patients (Sasaki et al., 1998). Indeed, AGE-induced glycation of Aβ and tau protein has been shown to cause Aβ aggregation and the formation of NFTs, respectively, suggesting that AGEs are active participants in the progression of AD pathology (Ledesma et al., 1994). It was also shown that the receptor for AGEs (RAGE) binds Aβ (Yan et al., 1996) increasing its influx into the brain through the BBB (Takuma et al., 2009). A clinical study reported an increase in AGEs immunostaining in postmortem brain slices from diabetic AD patients compared with non-diabetic AD subjects (Girones et al., 2004). Furthermore, diabetic mice exhibiting cognitive deficits, showed increased RAGE expression in neuronal and glial cells when compared with wild-type control mice. It was also demonstrated that RAGE null diabetic mice had significantly less neurodegenerative changes when compared to wild-type diabetic mice (Toth et al., 2006).

12
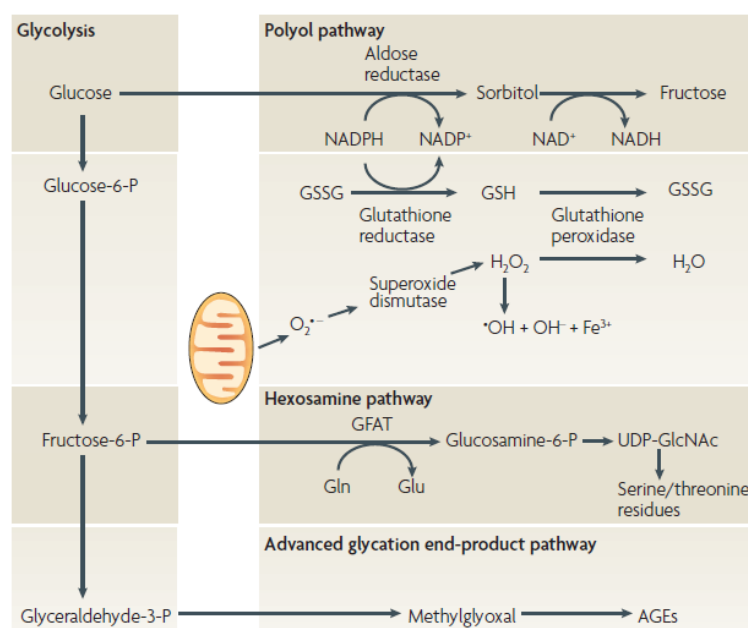
Figure 1.5 Metabolic pathways activated by hyperglycemia. The normal fate of intracellular glucose is the phosphorylation of the number-six-position carbon by hexokinase and entry into glycolysis. However, if high glucose levels saturate hexokinase, glucose is diverted into the polyol pathway, leading to increased consumption of reduced nicotinamide adenine dinucleotide phosphate (NADPH). This can compromise the recycling of glutathione disulphide (GSSG) to glutathione (GSH), which in turn can compromise the conversion of hydrogen peroxide (H_2O_2) to water. Further, fructose-6-phosphate can drive the synthesis of uridine diphosphate-N-acetylhexosamine (UDP-GlcNAc), which can combine with serine and threonine residues on intracellular proteins and compromise the proteins' function (hexosamine pathway). Glyceraldehyde-3-phosphate can be converted to highly reactive methylglyoxal, which is one of the main precursors of AGEs. Adapted from Tomlinson and Gardiner, 2008.

In summary, evidence shows that cerebral glucose metabolism is a mechanistic link between diabetes mellitus and AD. AD is associated with a profound hypometabolic state characterized by reduced cerebral glucose and energy metabolism in highly insulin-sensitive areas, suggesting a role for central insulin resistance in AD pathogenesis. The impairment of cerebral glucose metabolism potentiates AGEs formation, and

consequently Aβ accumulation, tau protein hyperphosphorylation and oxidative stress. In turn, abnormal systemic glucose and insulin metabolism impair cerebral insulin transport and function, which may lead to a deficient cerebral glucose uptake and metabolism predisposing neurons to an energetic crisis and dysfunction. Diabetes-associated AGEs formation exacerbates brain oxidative stress and contributes to the development of AD-related neuropathological hallmarks.

1.3.2 BRAIN INSULIN SIGNALING

Insulin is predominantly involved in the regulation of glucose metabolism in peripheral tissues. However, this hormone also affects numerous brain functions including cognition, memory and synaptic plasticity through complex insulin/insulin receptor (IR) signaling pathways (Zhao and Alkon, 2001) (Fig. 1.6).
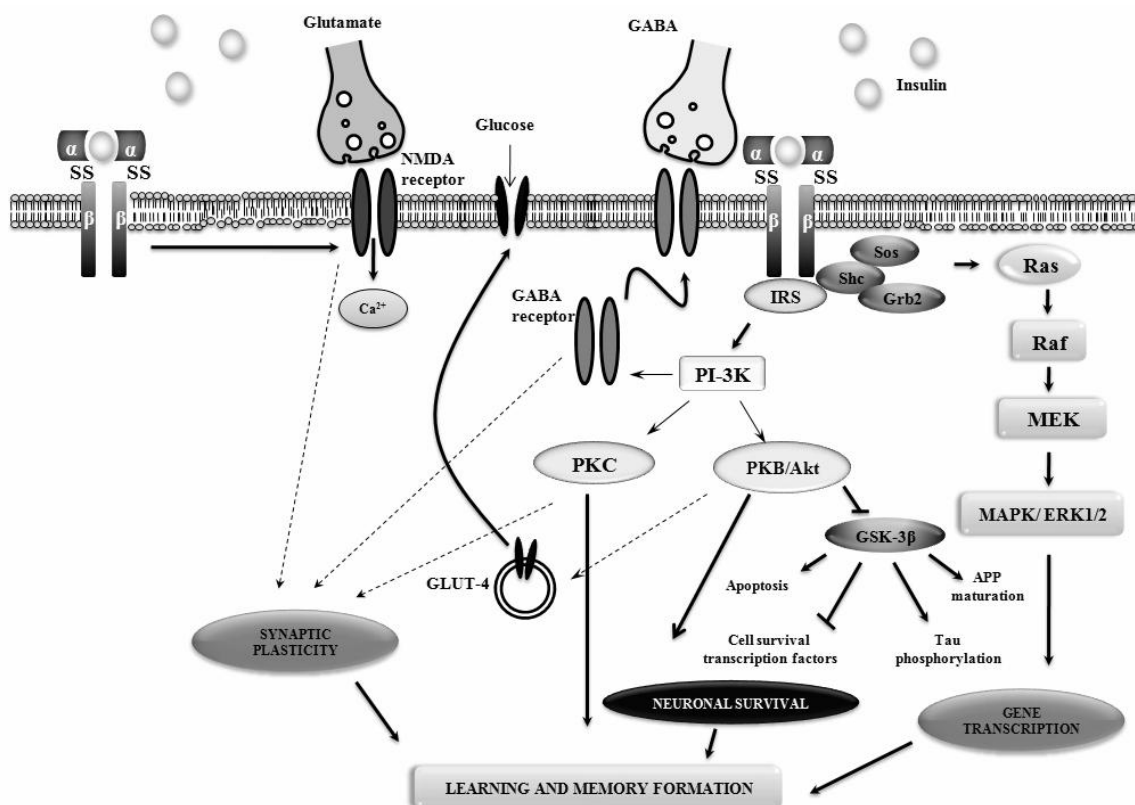
Figure 1.6. Schematic illustration of the potential molecular mechanisms of insulin signaling in the brain. Insulin binds to the insulin receptor activating the intrinsic tyrosine kinase, which phosphorylates endogenous substrates, such as the insulin receptor substrates (IRS) and Src-homology-2-containing protein (Shc), leading to the activation of two major downstream signaling pathways: 1) the phosphatidylinositol 3-kinase (PI-3K) and 2) mitogen-activated protein kinases (MAPK/ERK1/2) pathways. PI-3K mediates the activation of the protein kinase-B (PKB/Akt) favoring neuronal survival. Activated PKB/Akt can interfere with the apoptotic machinery, inactivating the proapoptotic proteins, BAD, and caspase-9. Furthermore, PI-3K/Akt activation inhibits glycogen synthase kinase-3β (GSK-3β). When active, GSK-3β triggers the apoptotic cascade, inhibits the activation of several cell survival transcription factors, and promotes tau protein hyperphosphorylation, and amyloid-β protein precursor (APP) maturation and processing. The PI-3K/Akt signaling cascade also induces the translocation of insulin-sensitive glucose transporter 4 (GLUT-4) to the membrane surface, enhancing glucose uptake. Insulin-mediated PI-3K signaling pathway is implicated in learning and memory, as well as in synaptic plasticity through the regulation of glutamate and GABA (γ-aminobutyric acid) receptors trafficking and channel activity. While the GABAergic receptors mediate the inhibitory synaptic transmission and the glutamatergic receptors mediate the vast majority of the excitatory synaptic transmission, the balance of glutamatergic and GABAergic transmissions is required to maintain normal brain function. Moreover, activation of excitatory glutamatergic synapses induces Ca^{2+} influx at postsynaptic sites, where it acts as a second messenger. Insulin is also able to active the MAPK/ERK1/2 signaling pathway, which is responsible for the activation of several transcription factors that alter protein expression. In summary, insulin has an important role in the regulation of neuronal cell survival/death, synaptic plasticity, learning and memory. Adapted from Cardoso et al., 2009.

Disturbances in insulin function and signaling have been proposed as common mechanistic links between diabetes and AD (Fig. 1.7). Indeed, insulin deficiency contributes to the cognitive deficits found in T1D diabetic patients (Brands et al., 2005). An impaired cognitive performance associated with impaired hippocampal plasticity was observed in the rat model of T1D induced by streptozotocin (STZ) administration (Biessels et al., 1998). The progressive impairment of cognitive function observed in T1D BB/Wor rats was associated with impaired insulin and insulin-like growth factor-1 (IGF-1) actions and neuronal apoptosis in the hippocampus (Li et al., 2002). These alterations were shown to be significantly prevented by the pro-insulin C-peptide, which is known

to modulate the insulin signaling pathway with no effect on glucose levels (Sima and Li, 2005). Studies performed in BBZDR/Wor (a model of T2D) and BB/Wor (a model of T1D) rats showed neuronal loss, neurite degeneration accompanied by perturbations of APP metabolism, hyperphosphorylation of tau protein, and impaired signaling of insulin and IGF-1 (Li et al., 2007a). However, those alterations were more severe in the T2D model, which appear to be associated with insulin resistance.

AD-associated neurodegeneration and cognitive decline are also believed to be partially caused by brain insulin signaling impairment (de la Monte and Wands, 2005). The hypothesis that the disruption of insulin signaling pathway participates in AD etiopathogenesis is supported by the following evidence: 1) reduced insulin levels and IR expression were observed in AD brains (Frolich et al., 1998; Steen et al., 2005), 2) increasing AD Braak stage was associated with progressively reduced levels of mRNA corresponding to insulin, IGF-1, IGF-2 and their receptors (Rivera et al., 2005), 3) AD patients showed increased fasting plasma insulin levels, decreased insulin levels in cerebrospinal fluid (CSF), and/or decreased CSF/plasma insulin ratio, associated with an increase in Aβ levels (Watson and Craft, 2004), which suggest a decrease in insulin clearance that may provoke an elevation of plasma Aβ levels (Li and Holscher, 2007), and 4) administration of insulin and glucose enhanced the memory of AD patients (Manning et al., 1993).

This evidence poses a fundamental question: does abnormal insulin signaling function as a bridge between diabetes mellitus and AD? As aforementioned, peripheral hyperinsulinemia and insulin resistance characterize T2D. High peripheral insulin levels are associated with increased levels of insulin in CSF (Watson et al., 2003). A clear relationship between insulin and Aβ metabolism has been documented (Gasparini et al.,

16

2002; Phiel et al., 2003; Qiu and Folstein, 2006). It was demonstrated that insulin increased the extracellular Aβ concentration by enhancing its trafficking from the endoplasmic reticulum (ER) and trans-Golgi network, the main site for Aβ generation, to the plasma membrane, which significantly reduces the intracellular concentration of Aβ derivatives (Gasparini et al., 2001). Insulin also increased the extracellular Aβ levels by modulating γ-secretase activity (Phiel et al., 2003). On the other hand, insulin-degrading enzyme (IDE), a major Aβ-degrading enzyme, might be competitively inhibited by insulin, resulting in decreased Aβ degradation (Qiu and Folstein, 2006) (Fig 1.6). It was shown that elevated insulin levels in T2D induced Aβ accumulation through competition between insulin and Aβ for IDE (Gasparini and Xu, 2003). Ho and collaborators (2004) observed that AD mice exposed to a dietary regimen that induced insulin resistance and a hyperinsulinemic state present a significant increase in Aβ and a reduction in IDE levels. Conversely, treatment with rosiglitazone, an insulin sensitizer, was shown to reduce $Aβ_{1-42}$ levels and improve learning and memory deficits (Pedersen et al., 2006), suggesting that insulin sensitizers might increase insulin signaling and decrease the levels of insulin available to compete with Aβ for degradation by IDE. Accordingly, the enhancement of IDE activity in IDE and APP double transgenic mice decreased the levels of Aβ in the brain, and prevented the development of AD pathology (Leissring et al., 2003). Prolonged peripheral hyperinsulinemia downregulated BBB functions and IR activity and reduced insulin transport into the brain, leading to an "insulin-resistant brain state", which may explain the lower concentrations of insulin in the CSF of AD patients (Craft et al., 1998; Steen et al., 2005). Brain insulin resistance is known to decrease IDE activity, and it was reported that IDE expression and activity were significantly decreased in the brain of AD patients (Leal et al., 2009), which may result in

insufficient degradation of Aβ and consequent formation of toxic species of this peptide. Thus, the co-existence of brain insulin resistance and insulin deficiency, instead of insulin excess, could be responsible for AD pathology, suggesting that AD may represent a brain-specific form of diabetes, i.e., type 3 diabetes (Kroner, 2009).
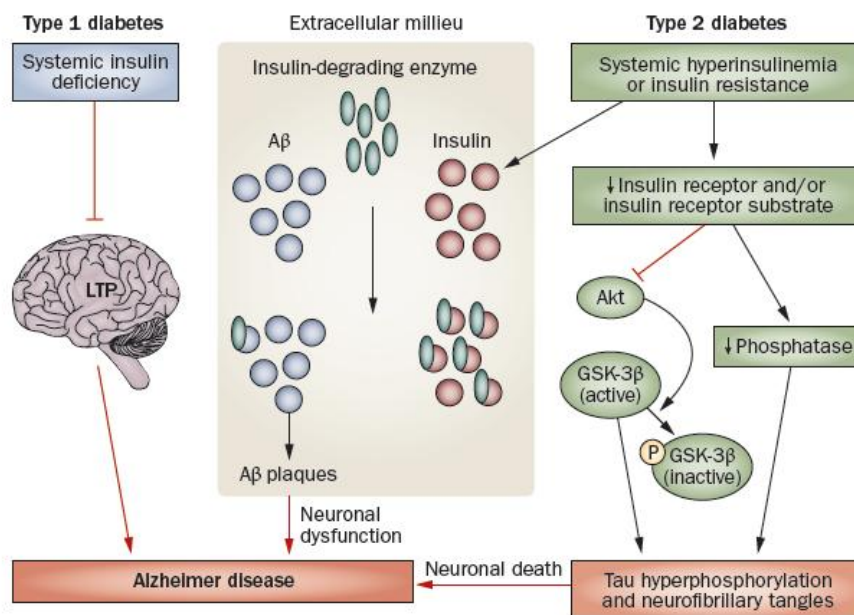
Figure 1.7. Altered insulin signaling in diabetes mellitus contributes to Alzheimer's disease pathophysiology. In type 1 diabetes (T1D), insulin deficiency attenuates long term potentiation (LTP) and might lead to deficits in spatial learning and memory. In type 2 diabetes (T2D), insulin resistance leads to both Aβ plaque formation and tau protein hyperphosphorylation. During hyperinsulinemia, insulin and Aβ compete for insulin-degrading enzyme (IDE), leading to Aβ accumulation and plaque formation. A decrease in insulin receptor signaling leads to inhibition of Akt and dephosphorylation (activation) of glycogen synthase kinase-3β (GSK-3β), which results in tau protein hyperphosphorylation. Adapted from Sims-Robinson et al., 2010.

The regulation of tau protein phosphorylation is another potential mechanism by which insulin links diabetes to AD pathology (Fig. 1.7). Hyperphosphorylated tau protein fails to be transported into axons, accumulating and aggregating into NFTs in neuronal perikarya, which contribute to neurodegeneration by enhancing oxidative stress, and trigger pathophysiological cascades that lead to increased mitochondrial dysfunction,

apoptosis, and necrosis (Sima and Li, 2005). Disturbances in insulin and/or IGF-1 signaling cascades were shown to increase tau protein hyperphosphorylation, potentiating NFTs formation (Cheng et al., 2005). Indeed, primary cortical neurons exposed to insulin or IGF-1 presented a transient increase in the phosphorylation of specific tau residues (Lesort and Johnson, 2000). In insulin receptor substrate-2 (IRS-2)-disrupted mice, a model of T2D, an accumulation of NFTs was detected in the hippocampus (Schubert et al., 2003). Furthermore, neuronal/brain-specific deletion of IR in mice (NIRKO mice) led to tau protein hyperphosphorylation (Schubert et al., 2004). Freude and collaborators (2005) also found that peripherally injected insulin directly targeted the brain causing a rapid cerebral IR signal transduction and site-specific tau protein phosphorylation. Importantly, in insulin-stimulated NIRKO mice, cerebral IR signaling and tau protein phosphorylation were completely abolished (Freude et al., 2005). More recently, it was hypothesized that tau protein modifications caused by insulin signaling dysfunction and hyperglycemia may contribute to the increased incidence of AD in diabetic subjects. Indeed, T1D and T2D contribute to the development of AD pathology through different mechanisms: in T1D insulin deficiency seems to be the major contributing factor for the increased tau protein phosphorylation, whereas the combined effects of hyperglycemia on tau pathology (increased tau protein phosphorylation and cleavage) along with insulin resistance may serve as important linkages between T2D and AD (Kim et al., 2009).

Insulin activates two major signaling pathways implicated in AD pathogenesis: the mitogen-activated protein kinase (MAPK) and the phosphoinositide 3-kinase (PI3-K)/Akt signaling pathways (Cardoso et al., 2009). Postmortem studies in human AD brains revealed that MAPK activation occurred at a very early stage of the disease (Pei et

al., 2001; Sun et al., 2003). Moreover, the intense MAPK immunoreactivity was associated with senile plaques and NFTs-bearing neurons. Indeed, MAPK co-localizes with NFTs in hippocampal and cortical regions in AD brains (Hensley et al., 1999; Munoz and Ammit, 2010). It was also found that transgenic mice with hyperphosphorylared tau protein exhibited a positive correlation between activated MAPK and aggregates of tau protein (Kelleher et al., 2007). Additionally, oligomeric Aβ peptides impaired long-term potentiation (LTP) through RAGE-mediated activation of MAPK (Origlia et al., 2008), an effect that was blocked by antibodies directed against RAGE (Origlia et al., 2008).

A correlation between Akt activity/protein levels and Braak staging has also been documented in human AD postmortem analyses, indicating a pattern of changes relying on PI-3K signaling, which depends on time and insulin stimulation (Pei et al., 2003). PI3-K/Akt phosphorylates and inhibits GSK-3β (Cross et al., 1995) modulating tau protein phosphorylation and Aβ peptide metabolism (Phiel et al., 2003). Loss of insulin-mediated activation of PI3-K and subsequent reduction of phosphorylation of Akt and GSK-3β were shown to cause a substantial increase in the levels of phosphorylated tau protein in the brains of NIRKO mice (Schubert et al., 2004). On the other hand, insulin stimulation reduced tau protein phosphorylation and promoted its binding to microtubules; these effects of insulin were mediated through the inhibition of GSK-3β via the PI3-K/Akt signaling pathway (Hong and Lee, 1997). It was also reported that insulin regulated soluble APP release via PI3-K-dependent pathway, suggesting that PI3-K involvement in APP metabolism may occur at vesicular trafficking level (Noble et al., 2005, Solano et al., 2000). Numerous *in vitro* and *in vivo* studies have also convincingly established that GSK-3β inhibition attenuates the amyloidogenic processing of APP and

inhibits hyperphosphorylated tau protein-associated neurodegeneration (Noble et al., 2005; Phiel et al., 2003; Solano et al., 2000).

Using a mouse model of T1D, Jovialt and colleagues (2008) evaluated the effect of peripheral insulin deficiency on brain insulin signaling, the parallels with AD, and the effect of insulin treatment. The authors observed that reduced insulin signaling, characterized by diminished phosphorylation of Akt and GSK-3β, was associated with a concomitant increase in tau protein phosphorylation and Aβ levels (Jolivalt et al., 2008). Treatment with insulin from onset of diabetes partially restored the phosphorylation of GSK-3β, reduced the level of phosphorylated tau protein, and improved learning ability (Jolivalt et al., 2008). It was recently demonstrated a decreased IR activity and an increased GSK-3β activity associated with an increase in tau protein phosphorylation levels and number of senile plaques in the brain of APP transgenic mice that have concurrent insulin-deficient diabetes (T1D) (Jolivalt et al., 2010).

Overall, diabetes mellitus by compromising insulin metabolism constitutes a risk factor for the development of AD pathology. Peripheral hyperinsulinemia and insulin resistance or deficiency result in an inefficient transport of insulin to the brain as well as reduced IR activity potentiating the deposition of Aβ and hyperphosphorylated tau protein and leading to neuronal and synaptic dysfunction and cognitive decline.

1.3.2.1 Central Administration Of Streptozotocin As An Experimental Approach to the study of Sporadic Alzheimer's Disease

The development of reliable experimental models is critical to uncover the exact pathological events underlying AD and, thus, to design more efficient therapeutic strategies to counteract the progression of the disease. Transgenic mouse models

harboring mutations found in fAD constitute the most widely used *in vivo* approach to study AD (Gotz and Ittner, 2008; Torres-Aleman, 2008, Woodruff-Pak, 2008). In the search for a non-transgenic animal model for sAD, the intracerebroventricular (icv) injection of the diabetogenic agent STZ in rats has emerged as an experimental model mimicking the early pathophysiological changes that occur in sAD (Hoyer, 2004b). As aforementioned, brain insulin signaling dysfunction is a causative event underlying the neurodegenerative events that occur in sAD. In this sense, targeting insulin cascade with icv administration of STZ, inducing an "insulin-resistant brain state", is a suitable strategy to mimic the early alterations that occur in sAD.

In the periphery, the administration of STZ induces a selective destruction of the pancreatic β-cells. It has been postulated that this selective β-cell toxicity induced by STZ is related to the glucose moiety in its chemical structure, which enables STZ to enter into these cells via GLUT-2 (Elsner et al., 2000). Moreover, STZ exerts β-cell toxicity effects mostly by causing alkylation of DNA, which triggers the activation of poly ADP-ribosylation consequently leading to depletion of cellular NAD^+ and ATP, and damaging the main β-cell function - insulin production and secretion (Szkudelski, 2001). Even though the mechanism of action of STZ in the brain is still unknown, it has been speculated to be similar to that occurring in the periphery. Indeed, GLUT-2 is distributed throughout the rat brain, especially in the limbic areas and related nuclei, most concentrated in the ventral and medial regions close to the midline, and involved in glucose sensing and regulation of neurotransmitters release (Arluison et al., 2004a; Arluison et al., 2004b). Compelling evidence demonstrates that a single or multiple injections of low doses of STZ, either uni- or bilaterally into the lateral cerebral ventricles: 1) induces biochemical alterations, characterized by impaired cerebral

glucose and energy metabolism, reduction in CBF, oxidative stress and cholinergic dysfunction; 2) causes morphological alterations resulting in neuronal and oligodendroglial cell damage and loss; and 3) results in a progressive deterioration of learning and memory. That said, the icvSTZ rat model represent a feasible experimental approach to explore the underlying cellular and molecular mechanisms involved in the initial stages of sAD pathology, which are difficult to analyse in the human postmortem brain, and allows the study of novel therapeutic approaches aimed to halt AD progression (Correia et al., 2011a; Grunblatt et al., 2007; Salkovic-Petrisic and Hoyer, 2007).

1.3.3 MITOCHONDRIAL (DYS)FUNCTION

Mitochondria are essencial for neuronal function and survival. Indeed, these organelles are involved in the production of ATP through oxidative phosphorylation and regulation of intracellular calcium (Ca^{2+}) homeostasis (Correia et al., 2010a). Neurons are extremely metabolically active cells with a high energy requirement for synaptic transmission, axonal/dendritic transport, ion channels, and ion pump activity, which are processes with high energy demand (Kann and Kovacs, 2007; Moreira et al., 2009). Functional mitochondria are supplied to the synaptic terminals along microtubules by kinesin (anterograde transport), whereas dysfunctional mitochondria are returned to the soma by dynein (retrograde transport) (Chang et al., 2006; Hollenbeck and Saxton, 2005; Li et al., 2004). The mechanisms that govern mitochondrial dynamics seem to interact with the mitochondrial transport apparatus to control mitochondrial morphology, mass and quality in neurons. During mitochondrial life cycle, new mitochondria result from the division of pre-existing organelles (mitochondrial

biogenesis) and are removed through selective degradation by autophagy (mitophagy), these two processes occurring in the soma. In-between, mitochondria experience successive cycles of fusion and fission that allow the generation of a heterogeneous mitochondrial population (Fig. 1.8). Fusion events are also crucial for the exchange of contents between mitochondria and enable damaged mitochondria to acquire components from healthy mitochondria, while fission is essential for mitochondrial trafficking along axons and sequestration of irreversibly damaged organelles to subsequent degradation by autophagy (Sheng and Cai, 2012; Westermann, 2010). Disruption of mitochondrial dynamics (fission, fusion, motility and turnover) has been postulated to be critically involved in neurodegeneration by inducing distinctive defects in neurons (Chen and Chan, 2009). In addition, the brain is particularly vulnerable to oxidative damage as a consequence of its high levels of polyunsaturated fatty acids, high oxygen consumption, high content in transition metals and poor antioxidant defenses (Nunomura et al., 2006). Therefore, the purpose of this section is to highlight the role of mitochondrial abnormalities in diabetes- and AD-associated neurodegeneration.
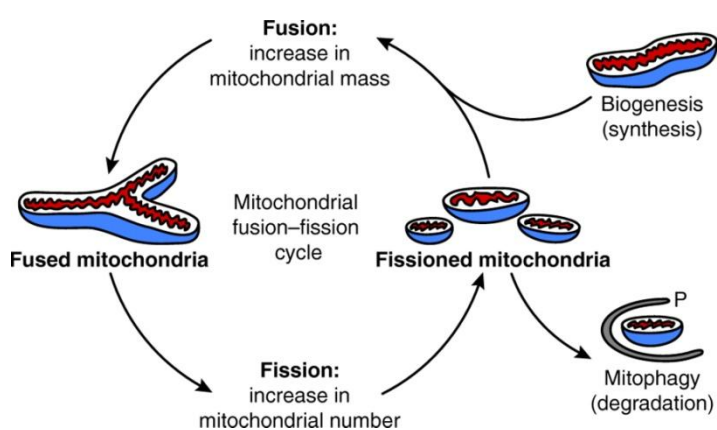
Figure 1.8. Mitochondrial life cycle. The mitochondrial life cycle starts with growth and division of pre-existing organelles (biogenesis) and ends with degradation of impaired or surplus organelles by mitophagy (turnover). In-between, mitochondria undergo frequent cycles of fusion and fission that allow the cell to generate multiple heterogeneous mitochondria or interconnected mitochondrial networks, depending on the physiological conditions. Adapted from Seo et al., 2010.

1.3.3.1 MITOCHONDRIAL BIOENERGETICS IN AD AND DIABETES MELLITUS

Accumulating evidence shows that defective mitochondrial metabolism sets up a cascade of pathological events that underlies neuronal degeneration in AD pathology (Correia et al., 2012a; Moreira et al., 2010; Santos et al., 2010a). In AD, the most consistent defect at the level of mitochondrial electron transport chain (ETC) is the decline in cytochrome c oxidase (COX) activity. In 1990, Parker and collaborators reported for the first time the existence of an impaired COX activity in the platelets of AD patients, this observation being confirmed by subsequent studies performed in lymphocytes and postmortem brain tissue from AD patients (Bosetti et al., 2002; Cardoso et al., 2004; Curti et al., 1997; Kish et al., 1992; Valla et al., 2006). Swerdlow and co-workers (1997) also reported that AD cybrids (a cytoplasmic hybrid cell line generated by the transfer of mitochondria from platelets obtained from AD patients into mitochondrial DNA (mtDNA)-depleted recipient neuron-based cells) presented a widespread defect in mitochondrial function characterized by reduced COX activity and increased free radical production. The impairment in the activities of respiratory chain complexes I and III has also been documented in platelets, lymphocytes, and brain tissue from AD patients (Bosetti et al. 2002, Kish et al. 1992, Parker et al. 1994, Valla et al. 2006). The decline in mitochondrial metabolism is also coupled with exacerbated oxidative damage. Moreira and collaborators (2007a) had depicted a relationship between mitochondrial dysfunction and oxidative damage. The authors observed that AD fibroblasts presented high levels of oxidative stress and apoptotic markers compared to young and age-matched controls. Moreover, AD-type changes could be generated in control fibroblasts by using N-methylprotoporphyrine to inhibit COX assembly, these effects being significantly attenuated by lipoic acid and N-acetyl-L-cysteine (NAC)

(Moreira et al., 2007). These results foster the idea that in AD oxidative damage is associated with mitochondrial dysfunction.

In an attempt to decipher the mechanisms underlying mitochondrial abnormalities, in vitro studies demonstrated that the exposure of cultured neurons to Aβ resulted in increased production of mitochondrial superoxide anion ($O_2^{-\bullet}$), ATP depletion, and increased mitochondrial Ca^{2+} uptake potentiating mitochondrial permeability transition pore (mPTP) opening (a voltage-dependent, high-conductance, non-selective pore located in the inner mitochondrial membrane that is permeable to solutes smaller than 1.5 kDa) and apoptosis (Hashimoto et al., 2003). It was also found that Aβ induced membrane lipid peroxidation and the production of 4-hydroxynonenal (Bruce-Keller et al., 1998) impairing the function of synaptic mitochondria (Keller et al., 1997). Aβ also increased the hydrolysis of membrane sphingomyelin by sphingomyelinases, resulting in the production of ceramides (Cutler et al., 2004), and consequent mitochondria-mediated neuronal death by a mechanism involving dephosphorylation of Akt, Bcl-2-associated death promoter (BAD), and GSK-3β (Stoica et al., 2003). However, one major question for the mitochondria lovers is how mitochondria functioning is further impaired during the course of AD? One possible explanation emerged from the fact that Aβ is able to cross mitochondrial membranes and interact with mitochondrial components, thus exacerbating mitochondrial dysfunction in AD. Aβ was classically documented to be deposited extracellularly; however, cellular and biochemical studies carried out in different models of AD have provided evidence that Aβ can also accumulate inside neurons and target mitochondria (Caspersen et al., 2005; Crouch et al., 2005; Devi et al., 2006; Du et al., 2008; Lin and Beal, 2006; Manczak et al., 2006; Pagani and Eckert, 2011). Hansson-Petersen and

26

collaborators (2008) demonstrated that Aβ peptide is imported into mitochondria via the translocase of the outer membrane (TOM) import machinery and localizes within the mitochondrial cristae. It was also reported an accumulation of full-length and carboxy-terminally truncated APP across mitochondrial import channels in brain tissue from AD patients, which inhibited the entrance of nuclear-encoded COX subunits IV and Vb proteins leading to a decrease in COX activity and an increase in hydrogen peroxide (H_2O_2) levels (Devi et al., 2006). Anandatheerthavarada and colleagues (2003) also found an accumulation of full-length APP in the mitochondrial compartment in a transmembrane-arrested form that impaired mitochondrial functionality and energy metabolism. Conversely, Aβ is able to bind and interact with different molecules upon entering the mitochondria. Aβ also interacts with the mitochondrial protein Aβ-binding alcohol dehydrogenase (ABAD) potentiating mitochondrial failure by increasing the mitochondrial membrane permeability and reducing the activities of enzymes involved in mitochondrial respiration (Lustbader et al., 2004). Aβ can also interact with cyclophilin D (CypD), a critical molecule involved in mPTP formation and cell death, enhancing mitochondrial, neuronal and synaptic stress. Meanwhile, CypD ablation protected neurons from Aβ-induced mPTP formation and mitochondrial and cellular stress (Du et al., 2008), supporting the idea that Aβ interacts with CypD leading to cell damage. The interplay between Aβ and mitochondria was also supported by the observation that Aβ can be produced in mitochondria. In fact, it was reported that APP is a substrate for the mitochondrial γ-secretase and that APP intracellular domain (AICD) is produced inside mitochondria, providing a mechanistic view of the mitochondria-associated APP metabolism where AICD, P3 peptide and potentially Aβ are produced locally and may contribute to mitochondrial dysfunction (Pavlov et al., 2010). Overall, these findings

support the hypothesis that mitochondrial bioenergetics decline associated to an exacerbated oxidative damage play a key role in AD pathogenesis (Fig. 1.9).
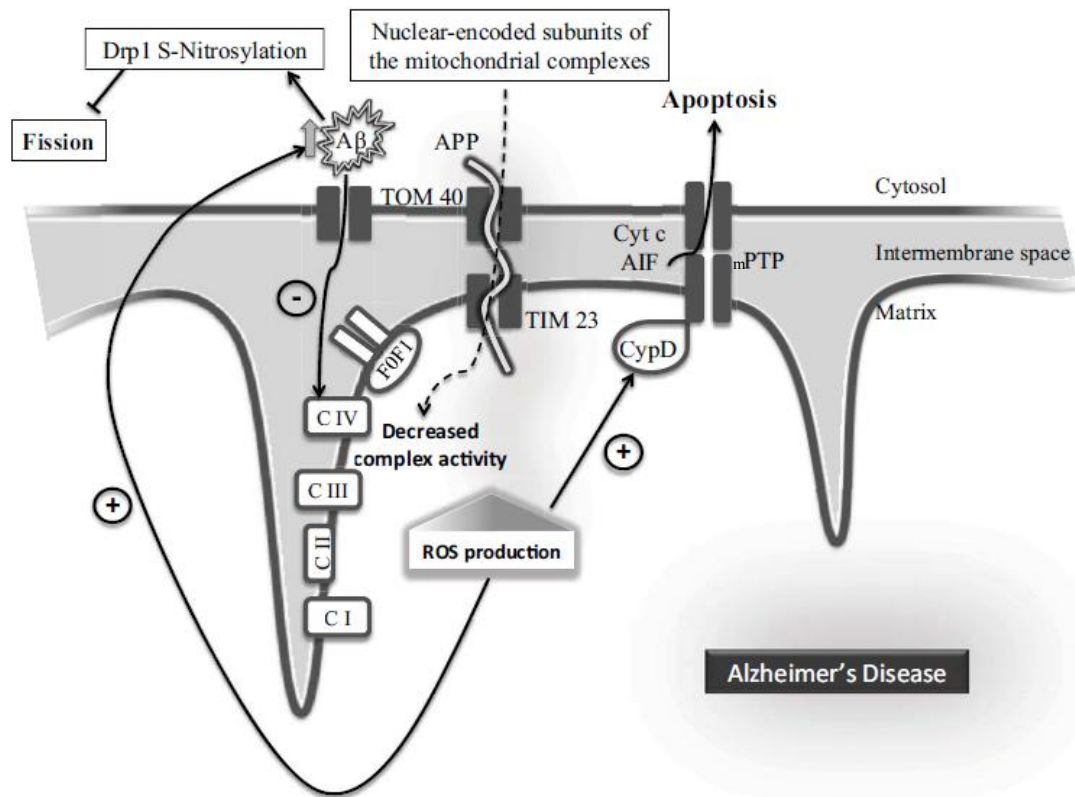
Figure1.9. Mitochondrial abnormalities in Alzheimer's disease. Alzheimer's disease is characterized by a decrease in cytochrome c oxidase (COX) activity that can be partially explained by the blockage of the mitochondrial translocase of the outer mitochondrial membrane (TOM40) and translocase of the inner mitochondrial membrane (TIM23) by amyloid-β (Aβ) precursor protein (APP), which prevents the entry of the nuclear encoded subunits of COX. Furthermore, Aβ also enters mitochondria through the TOM complex and interacts with heme groups in the redox centers of COX decreasing its catalytic activity. The decrease in electron transport chain efficiency increases the production of reactive oxygen species (ROS), which in turn, enhances Aβ production and the cyclophilin D (CypD)-mediated opening of permeability transition pore (mPTP). The opening of mPTP leads to the release of pro-apoptotic factors such as cytochrome c (Cyt c) and apoptosis-inducing factor (AIF) to the cytosol activating the apoptotic cell death. Additionally, Aβ may also induce s-nitrosylation of the dynamin-related protein 1 (Drp1), impairing mitochondrial fission. CI, CII, CIII, mitochondrial electron transport chain complexes I, II and III, respectively; F0F1, ATP synthase. Adapted from Santos et al., 2010.

T1D and T2D are also associated with mitochondrial dysfunction and exacerbated oxidative stress levels. It is now well accepted that inherited defects in mitochondrial DNA cause an insulin-deficient form of diabetes mellitus that resembles T1D (Sims-Robinson et al., 2010). Moreover, the involvement of mitochondria in T2D is emphasized by the finding that mtDNA mutations in humans, as well as pancreatic β-cell-specific deletion of mitochondrial genes in animal models, reduced oxidative phosphorylation capacity and caused diabetes (Silva et al., 2000). Abnormal mitochondrial morphology and function was observed in postmortem pancreatic β-cells from T2D patients (Anello et al., 2005). Additionally, in both types of diabetes, compromised mitochondrial function and morphology, as well as exacerbated mitochondrial oxidative stress, are major mediators of neurodegeneration. This notion is supported by studies showing that sensory neurons and peripheral nerves of animal models of T1D and T2D are characterized by increased ROS generation, lipid peroxidation, protein nitrosylation, and diminished levels of glutathione (GSH) and ascorbate (Fernyhough et al., 2010). Accordingly, it was also demonstrated that brain mitochondria isolated from STZ diabetic rats, a model of T1D, displayed lower levels of coenzyme Q9 (CoQ9), which suggests an impairment of the antioxidant system in diabetic animals (Moreira et al., 2005). Mastrocola and collaborators (2005) showed that brain mitochondria isolated from diabetic STZ rats presented an impairment of the respiratory chain and increased oxidative and nitrosative stress contributing to neuronal injury. The authors observed that hyperglycemia-associated oxidative and nitrosative stress contributed to mitochondrial dysfunction by decreasing the activity of complexes III, IV and V of the respiratory chain and ATP synthesis (Mastrocola et al., 2005). Moreira and collaborators (2006) reported that brain mitochondria isolated from 12-weeks STZ-induced diabetic

rats presented a lower ATP content and ability to accumulate Ca^{2+}. An age-related decline of the respiratory chain efficiency and an uncoupling of oxidative phosphorylation system in brain mitochondria isolated from Goto-Kakizaki (GK) rats, an animal model of T2D, were also observed (Moreira et al., 2003).

1.3.3.2 MITOCHONDRIAL DYNAMICS AND MORPHOLOGY IN AD AND DIABETES MELLITUS

Mitochondria are highly dynamic organelles that move and continuously fuse and divide in response to different stimuli and changes in neuronal metabolic demands by two opposing processes, fusion and fission (Chan, 2006; Chen and Chan, 2005). A shift towards fusion favors the generation of an elongated and interconnected mitochondrial network, whereas a shift towards fission produces a fragmented and disconnected mitochondrial phenotype. The antagonistic and balanced activities of the mitochondrial dynamics machinery are essential to ensure proper neuronal functioning. Indeed, this equilibrium is needed for the maintenance of the respiratory capacity and mtDNA, recruitment of mitochondria to critical subcellular compartments, such as synaptic terminals, content exchange between mitochondria, and control of mitochondrial quality, shape and number (Chen and Chan, 2009). Mitochondrial dynamic morphologic changes are finely orchestrated by at least four conserved dynamin-related GTPases. Mitochondrial fission is regulated by a large cytosolic GTPase that is recruited to the mitochondrial membrane upon a fission-like stimuli, dynamin-like protein 1 (DRP1), and a small mitochondrial molecule located in the outer membrane, denominated mitochondrial fission protein 1 (Fis1). The core components of the mitochondrial fusion machinery are mitofusins 1 and 2 (Mfn1, Mfn2) in the outer membrane and optic

atrophy protein 1 (OPA1) in the inner membrane (Correia et al., 2011b; Santos et al., 2010b) (Fig. 1.10).
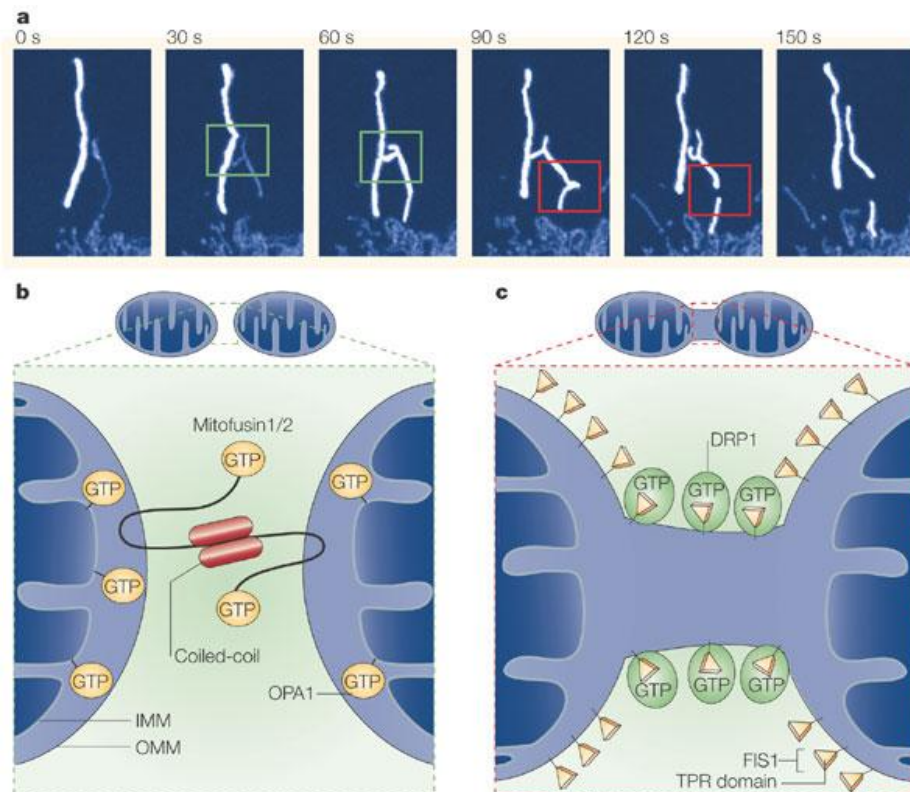
Figure 1.10. Dynamics of the mitochondrial network in mammalian cells. Confocal time-lapse images of mitochondria labelled with mitochondrial-matrix-targeted photoactivatable green fluorescent protein. **a)** Mitochondrial fusion is shown in the green box and fission is shown in the red box following a single mitochondrion photoactivation. The lower panels show schematic cross-sections through mitochondrial fusion **b)** and fission **c)**. During fusion, two mitochondria dock through coiled-coil-domain interactions between mitofusins that are anchored into the outer mitochondrial membrane (OMM; their GTPase domains face the cytosol), whereupon optic atrophy protein 1 (OPA1), which is anchored partially on the inner mitochondrial membrane (IMM), participates in the membrane fusion process **b)**. During fission, fission protein 1 (Fis1) circumscribing the outer mitochondrial membrane recruits the large GTPase and dynamin-like protein 1 (DRP1) through its tetratricopeptide repeats (TPR), which subsequently coalesces into foci at mitochondrial scission sites **c)**. Adapted from Youle and Karbowski, 2005.

Abnormal mitochondrial dynamics with detrimental effects on synaptic and neuronal function have been implicated in the pathogenesis of AD. Ultrastructural alterations in mitochondrial morphology such as reduced size and broken internal membrane cristae were observed in brain tissue from AD patients, suggesting an excessive mitochondrial fragmentation (Baloyannis, 2006; Hirai et al. 2001). *In vitro* studies showed that Aβ oligomers induced excessive mitochondrial fission and neuronal damage in a nitric oxide (NO$^\bullet$)-mediated manner (Barsoum et al., 2006; Yuan et al., 2007). Consistently, long-term exposure of PC12 cells to Aβ$_{25-35}$ induced an increase in mitochondrial number and a decrease in mitochondrial length and size, corroborating the existence of mitochondrial fragmentation in AD (Liu et al., 2010). An exhaustive work of Wang an collaborators (2008a,b; 2009a,b) aimed to dissect the contribution of mitochondrial dynamics to AD pathology revealed a dramatic imbalance in mitochondrial fusion and fission characterized by increased mitochondrial fragmentation and abnormal mitochondrial distribution. A marked reduction of DRP1 levels and elongated mitochondria forming collapsed perinuclear networks were found in fibroblasts from sAD patients (Wang et al., 2008a; 2009a). Further, a reduction in the expression levels of DRP1, OPA1, Mfn1 and 2 and an increase in Fis1 levels were observed in hippocampal tissue from AD subjects (Wang et al., 2009b). Accordingly, APP overexpression in M17 neuroblastoma cells resulted in predominantly fragmented mitochondria, decreased DRP1 and OPA1 levels, and defective neuronal differentiation (Wang et al., 2008b). Manczak and colleagues (2011) documented an increased immunoreactivity of DRP1 in the brains of AD subjects. Interestingly, it was observed that DRP1 interacted with Aβ monomers and oligomers in AD brains, a phenomenon positively correlated with the severity of the disease. These findings suggest that the

32

interaction of Aβ and DRP1 may initiate mitochondrial fragmentation in neurons affected in AD, a situation that was potentiated by the progression of the disease (Manczak et al., 2011). More recently, a physical interaction between phosphorylated tau protein and DRP1 was observed in human brain tissue and transgenic mouse models of AD (Manczak and Reddy, 2012).

Structural abnormalities in mitochondria were observed in dorsal root ganglion neurons of long-term STZ diabetic rats (Schmeichel et al., 2003). Accordingly, it was reported that treatment of cultured dorsal root ganglion neurons with high glucose levels resulted in fragmentation/fission of mitochondria. In an initial phase the up-regulation of the mitochondrial fission protein DRP1 resulted in a protective fission, but in a more advanced stage mitochondrial fragmentation resulted in the activation of Bim and Bax and, subsequently, apoptosis (Leinninger et al., 2006). Edwards and collaborators (2010) demonstrated that diabetes regulated mitochondrial biogenesis and fission in mouse neurons. It was found that dorsal root ganglion neurons from diabetic mice exhibited greater mitochondrial biogenesis in comparison with non-diabetic mice (Edwards et al., 2010). However, the rapid increase in the number of mitochondria appeared to result, at least in part, from mitochondrial fission, since the diabetic state generated small, fragmented mitochondria (Edwards et al., 2010). Accordingly, *in vitro* experiments also revealed that short-term exposure to high glucose increased DRP1 protein levels. Importantly, the inhibition of DRP1-induced fragmentation was neuroprotective and resulted in decreased neuronal susceptibility to high glucose damage (Edwards et al., 2010).

In sum, this sub-chapter provided evidence that mitochondrial dysfunction may constitute a downstream event of diabetes mellitus- and/or AD-associated abnormal

brain insulin and glucose metabolism. Indeed, defective insulin signaling induces a neuronal energy crisis that renders neurons more vulnerable to oxidizing insults, which could promote structural and functional alterations of mitochondria. Aβ and hyperphosphorylated tau protein synergistically impair mitochondrial bioenergetics and potentiate oxidative stress, accelerating the neurodegenerative mechanisms. Overall, central insulin resistance, impaired cerebral glucose metabolism and mitochondria failure may represent a dangerous trio in AD pathophysiology (Fig. 1.10).
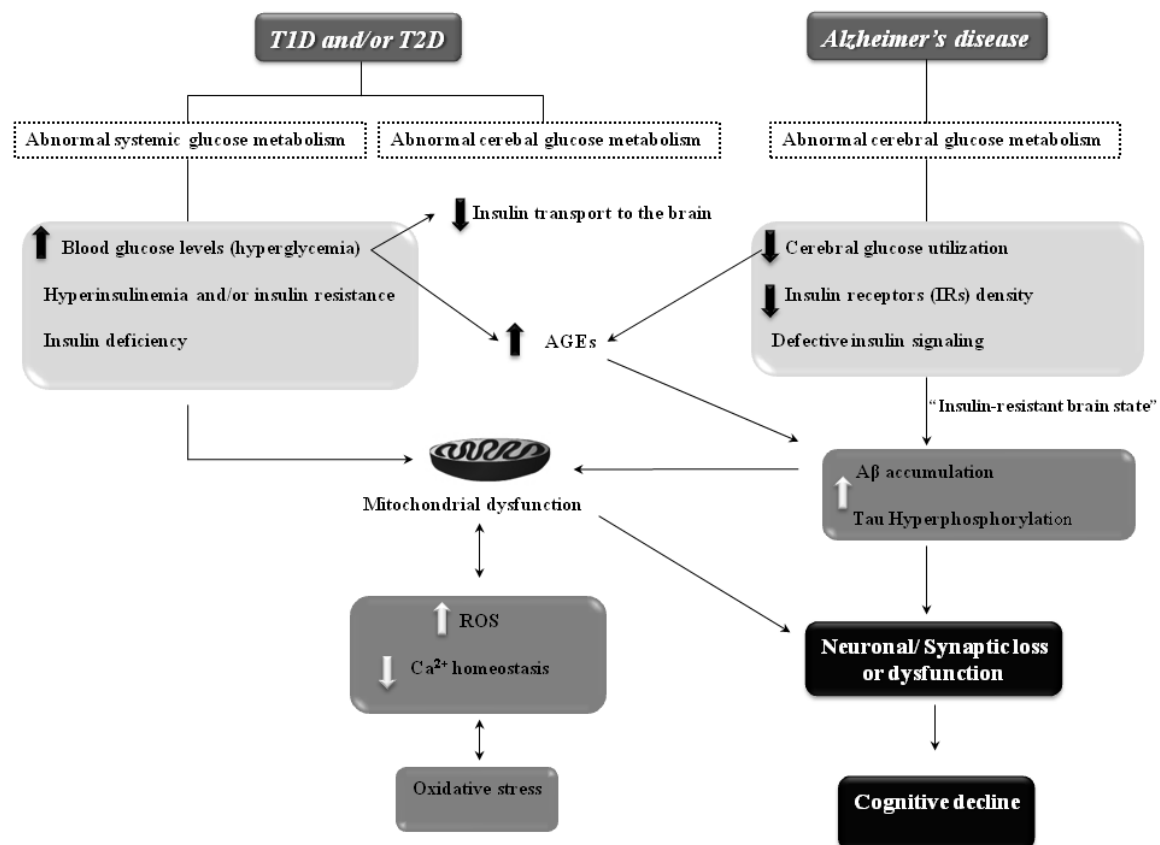
Figure 1.10. Schematic illustration of the pathological mechanisms linking diabetes mellitus and Alzheimer's disease. Abnormalities in systemic glucose/insulin metabolism, characteristic of diabetes mellitus, are amongst the major pathological factors thought to mechanistically influence the onset and/or progression of Alzheimer's disease (AD). Systemic insulin deficiency in type 1 diabetes (T1D) contributes to cognitive deficits. Hyperglycemia, chronic peripheral hyperinsulinemia and insulin resistance, which characterize type 2 diabetes (T2D), result in reduced transport of insulin into the brain and insulin receptors (IRs) activity, compromising brain glucose metabolism and insulin signaling pathway.

Insulin resistance and reduced cerebral glucose metabolism seem to occur in pre-diabetic and T2D patients. Insulin metabolism abnormalities and hyperglycemia-induced glucose auto-oxidation promote the formation of advanced glycation end products (AGEs) and potentiate the occurrence of AD-like neuropathological hallmarks. In the early stages of the disease, AD is also characterized by an impaired brain glucose/energy metabolism in insulin-sensitive areas, suggesting a role for insulin signaling in the AD etiopathogenesis. An "insulin-resistant brain state" has been proposed to form the core of the neuropathological events that occur in AD, including abnormal amyloid-β peptide (Aβ) deposition and tau protein hyperphosphorylation. Abnormal Aβ deposition and tau protein hyperphosphorylation, in turn, promote mitochondrial dysfunction and exacerbate oxidative stress, in a vicious cycle. Mitochondrial impairment and oxidative stress are also contributing factors to diabetes-mediated neuronal damage. Altogether, these neuropathological events contribute to neuronal and synaptic dysfunction, cell death and cognitive decline, characteristics of AD. Adapted from Correia et al., 2012.

1.4   PRECONDITIONING AS A NEUROPROTECTIVE STRATEGY

1.4.1 AN OVERIEW

Preconditioning is an innate protective and adaptive mechanism, whereby a sublethal insult protects against a subsequent lethal insult, a phenomenon remembering one of Nietszche's most memorable quotes "What does not kill you, makes you stronger". The first *in vivo* evidence of preconditioning and tolerance in the brain was provided in 1960's (Dahl and Balfour, 1964). In the late 1980's, several reports again drew attention to ischemic tolerance in the brain (Chopp et al., 1989; Schurr et al., 1986). Since then, the preconditioning phenomenon has been confirmed in many animal models of global (Kitagawa et al., 1991) and focal (Stagliano et al., 1999) ischemia, *in vitro* brain slice preparations (Xu et al., 2002), cultured primary neurons (Bruer et al., 1997), and human beings in the form of short episodes of ischemia without infarction, known as a transient ischemic attack (TIA) (Moncayo et al., 2000). Brain tolerance can be induced by several distinct preconditioning stimuli, such as ischemia, oxidative stress, hypothermia, hypoxia, and low doses of endotoxin (Cadet and Krasnova, 2009). The

existence of multiple, diverse preconditioning stimuli that confer protection result in the well-known phenomenon of "cross-tolerance" (Kirino, 2002). Preconditioning induces two phases of brain tolerance with different temporal profiles and, to some extent, with different mechanisms of protection: early and delayed tolerance. Early tolerance is a short-lasting protection induced within minutes of exposure to preconditioning and wanes within hours. Rapid changes in the activity and posttranslational modifications of existing proteins are involved in this phenomenon. Conversely, preconditioning-induced delayed tolerance needs several hours our even days to manifest and requires gene induction and *de novo* protein synthesis, representing a long-term response through genetic reprogramming (Barone et al., 1998; Correia et al., 2010b, 2011b; Gidday, 2006; Kirino, 2002; Stenzel-Poore et al., 2007).

1.4.2 PRECONDITIONING AND BRAIN TOLERANCE: WHERE DO MITOCHONDRIA FIT IN?

Multiple molecular pathways and protective mechanisms have been identified and continue to be studied in an effort to clarify the mechanisms underlying preconditioning-mediated brain tolerance. In the preconditioning realm, mitochondria have been proposed to be master regulators of preconditioning-triggered endogenous neuroprotection (Busija et al., 2008). The next sub-chapters are aimed to discuss the role of mitochondrial components in the preconditioning paradigm.

1.4.2.1 MITOCHONDRIAL-DERIVED ROS

The mitochondrial respiratory chain is one of the primary sources of cellular ROS. In the mitochondrial respiratory chain, the primary sites of ROS production and release are complexes I and III (Zhang and Gutterman, 2007). While an exacerbated production

of mitochondrial ROS induces mitochondrial dysfunction potentiating cell degeneration and death, evidence shows that low or mild levels of mitochondrial ROS are critically involved in preconditioning-mediated brain tolerance (Dirnagl et al., 2009; Dirnagl and Meisel, 2008; Jou, 2008; Ravati et al, 2000, 2001). In fact, Ravati and collaborators (2001) demonstrated that preconditioning stimulated by moderate ROS levels protected cultured neurons against different damaging agents and prevented the subsequent massive oxygen radical formation, whereas the presence of a radical scavenger abolished ROS-mediated neuronal preconditioning (Ravati et al., 2000). Also, preconditioning with low concentrations of H_2O_2 protected PC12 cells against subsequent lethal oxidative stress levels (Tang et al., 2005a). The mechanisms behind H_2O_2-induced neuroprotective effects involved the maintenance of mitochondrial membrane potential ($\Delta\Psi m$), a mild increase in ROS levels and overexpression of Bcl-2 (Tang et al., 2005b). It was also demonstrated that the generation of H_2O_2 during a brief oxygen-glucose deprivation (OGD) episode was the main trigger involved in the mechanism of preconditioning-induced neuronal protection (Furuichi et al., 2005). More recently, Simerabet and collaborators (2008) reported a preconditioning effect promoted by an *in situ* administration of H_2O_2 in the brain cortex, which suggests a direct implication of ROS during the triggering phase of cerebral preconditioning. A relationship between mitochondrial ATP-sensitive potassium (mitoK$_{ATP}$) channels and ROS has been postulated, since the protection induced by H_2O_2 against cerebral ischemia-reperfusion injury was blocked by mitoK$_{ATP}$ channels antagonists and the antioxidant NAC blocked the protection induced by diazoxide, a mitoK$_{ATP}$ channels opener (Simerabet et al., 2008). The strong relationship between ROS and mitoK$_{ATP}$

places mitochondria centre stage in the neuroprotection induced by cerebral preconditioning (Simerabet et al., 2008).

Inhibition of succinate dehydrogenase (SDH) by 3-nitropropionic acid (3-NPA), an agent known to increase the production of ROS, probably at mitochondrial complex I, was shown to promote tolerance against focal cerebral ischemia (Wiegand et al., 1999), implicating mitochondrial ROS in cerebral preconditioning. It was also shown that 3-NPA was able to induce delayed preconditioning in rats when administered 3 days after transient middle cerebral artery occlusion (MCAO) by reducing infarct volume by about 20% (Horiguchi et al., 2003). NS1619, which inhibits the complex I of mitochondrial respiratory chain, also induced neuronal preconditioning by increasing ROS production and promoting a mild mitochondrial depolarization (Gáspár et al., 2008a; 2009). The neuroprotective effects of NS1619 were significantly reduced in the presence of a ROS scavenger (Gáspar et al., 2009). The same authors also reported that immediate NS1619-mediated preconditioning involved a decrease in Ca^{2+} influx through glutamate receptors, an increase in superoxide dismutase (SOD) activity, a reduced ROS response during glutamate stimulation, and a better preservation of ATP levels (Gáspar et al., 2009). It was also proposed that "minor" mitochondrial ROS generation induced fission and fusion of mitochondria and relocated the mitochondrial network to form a mitochondria free gap, which may play a role in mitochondrial ROS-mediated protective "preconditioning" by preventing the propagation of ROS during the oxidative insult.

Among the multiple signaling pathways that have been proposed to participate in the preconditioning phenomenon, the induction of the hypoxia signaling pathway with the concomitant stabilization and transcriptional activation of the transcription factor hypoxia-inducible factor (HIF)-1 has emerged as one of the major cellular

pathways responsible for brain tolerance. HIF-1 belongs to the basic helix-loop-helix transcription factor family. It is a heterodimeric transcription factor comprised of the constitutively expressed HIF-1β subunit and the oxygen-tension-regulated HIF-1α subunit (Wang et al., 1995; Huang et al., 1996, 1998; Semenza, 2002). HIF-1α accumulates in response to hypoxia and is rapidly degraded upon reoxygenation (Wang et al., 1995). Under normal oxygen conditions, HIF-1α is hydroxylated at two proline residues, Pro402 and Pro564, within the oxygen-dependent degradation domain by a family of prolyl hydroxylase enzymes (PHDs) (Huang et al., 1996; Pugh et al., 1997). Hydroxylation of HIF-1α requires molecular oxygen (O_2), iron in ferrous form (Fe^{2+}), and 2-oxoglutarate as cofactors (Huang et al., 1996; Pugh et al., 1997). The requirement of iron explains the hypoxic-mimetic effects of iron chelators and iron antagonists, such as cobalt chloride ($CoCl_2$). The hydroxylated prolines are recognized by the von Hippel–Lindau protein (VHL), which acts as the recognition component of a multiprotein ubiquitin E3 ligase complex. Then, VHL binds to both hydroxylated HIF-1α and to Elongin-C, which recruits Elongin-B and other subunits of the E3 ubiquitin ligase, targeting the HIF-1α subunit for rapid ubiquitin-mediated proteasomal degradation by the 26S proteasome (Maxwell et al., 1999; Ivan et al., 2001; Jaakkola et al., 2001; Safran and Kaelin, 2003). Under hypoxic conditions or iron chelation, enzymatic inhibition of PHDs abrogates HIF-1α recognition by VHL and proteasomal degradation, resulting in the stabilization of HIF-1α. Consequently, HIF-1α protein translocates and accumulates in the nucleus, where dimerizes with HIF-1β subunits, and recruits the transcription co-activator p300/cAMP-response element-binding protein-binding protein (CBP), forming the active HIF complex (Carrero et al., 2000; Kung et al., 2000; Mole et al., 2001). This complex binds to the hypoxia-responsive element (HRE) in the promoter, up-regulating a

repertoire of target genes, including metabolic enzymes, cytokines, growth factors, receptors, and other signaling proteins (Correia and Moreira, 2010) (Fig. 1.11).
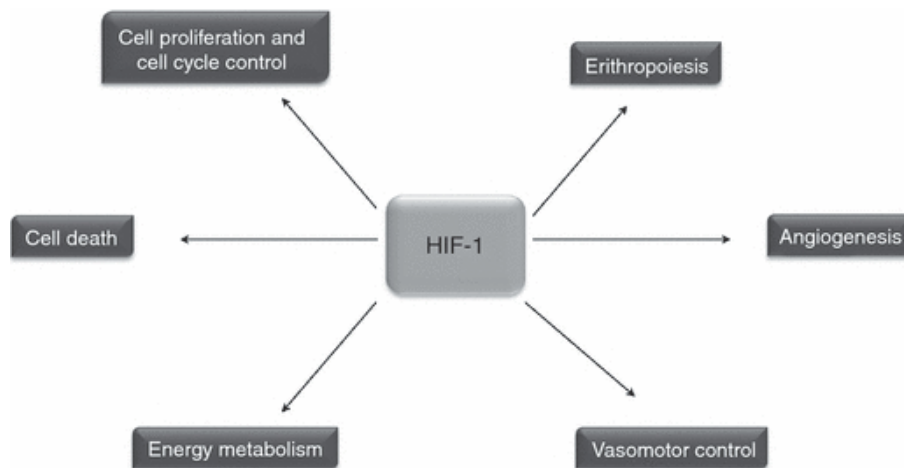
Figure 1.11. Hypoxia-inducible factor 1 (HIF-1) and its targets genes. HIF-1 is a transcriptional complex involved in the molecular and cellular adaptation to hypoxia. HIF-1 regulates the expression of a wide range of genes involved in vasomotor control, angiogenesis, erythropoiesis, iron metabolism, control of cell cycle, cell proliferation and death, and energy metabolism. Adapted from Correia and Moreira, 2010.

HIF-1α activation seems to be strictly bound to the mitochondrial function. Indeed, under hypoxic conditions, mitochondria act as oxygen sensors and convey signals to HIF-1, mitochondrial ROS being the putative signaling molecules between a cellular O_2-sensor and HIF-1. ROS generated by the Q_0 site of mitochondrial complex III have been shown to be critical in the hypoxia-mediated survival signaling (Bell et al., 2007). In accordance, previous studies reported that mitochondrial ROS generation prevented the hydroxylation of HIF-1α, stabilizing HIF-1α and promoting its translocation to the nucleus and dimerization with HIF-1β, initiating the transcription of target genes (Guzy et al., 2005; Bell et al., 2007) (Fig. 1.12). Conversely, mtDNA-depleted (ρ^0) cells, without a functional mitochondrial respiratory chain, failed to increase ROS generation and HIF-1α accumulation under hypoxic conditions (Chandel et al., 1998, 2000). The

exogenous application of H_2O_2 induced HIF-1α under normoxic conditions, whereas ROS scavengers blocked the induction of HIF-1 mediated by hypoxia, which further confirm the involvement of ROS in HIF-1 induction (Guzy et al., 2005; Mansfield et al., 2005). Additionally, the exposure of ρ^0 cells to low levels of H_2O_2 stabilized HIF-1α protein during normoxia (Chandel et al., 2000). These findings show that mitochondrial ROS play a key role in HIF-1α stabilization and activity, a transcriptional regulator of preconditioning-mediated neuroprotective events.
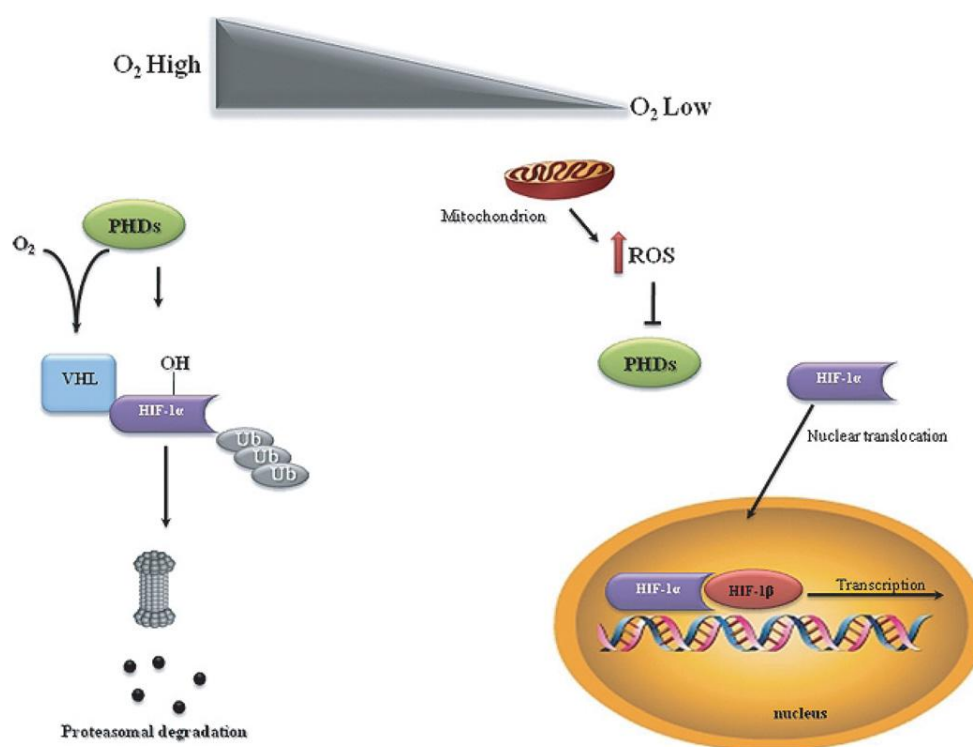
Figure 1.12. Schematic illustration of the involvement of mitochondrial reactive oxygen species (ROS) in hypoxia-inducible factor 1 (HIF-1) stabilization. HIF-1 is a heterodimeric protein composed of a constitutively expressed HIF-1β subunit and an inducible HIF-1α subunit. In the presence of molecular oxygen (O_2), HIF-1α is hydroxylated by prolyl hydroxylase enzymes (PHDs) and rapidly degraded by ubiquitin-proteasome system. Under hypoxic conditions, the generation of ROS by the mitochondrial respiratory chain inhibits PHDs activity, preventing the hydroxylation of HIF-1α, resulting in HIF-1α stabilization and translocation to the nucleus. Consequently, HIF-1α dimerizes with HIF-1β, initiating the transcription of HIF-1-responsiveness genes. Adapted from Correia et al., 2010a.

A crosstalk between mitochondrial ROS and HIF-1 has been proposed to underlie preconditioning-mediated protective events (Correia and Moreira, 2010). It was previously demonstrated that hypoxic preconditioning-induced neuroprotection was associated with ROS production and subsequent induction of HIF-1 and its downstream gene erythropoietin (EPO) (Liu et al., 2005). Accordingly, Chang and co-workers (2008) reported that low levels of exogenous H_2O_2 increased HIF-1α expression and protected primary cortical neurons against the deleterious effects promoted by ischemia.

Collectively, these data indicate that mitochondrial ROS are required for the initiation and maintenance of neuronal preconditioning. As signaling molecules, mitochondrial ROS seem to be triggers and mediators of neuronal preconditioning, by activating important signaling pathways involved in brain tolerance, namely the HIF-1 signaling pathway.

1.4.2.2 MITOCHONDRIAL ATP-SENSITIVE POTASSIUM CHANNELS

There is an ongoing debate about the role of mitoK$_{ATP}$ channels in the preconditioning phenomenon in the brain (Busija et al., 2008). These channels are localized in the inner mitochondrial membrane and regulate mitochondrial function in several tissues, including the brain (Bajgar et al., 2001; Debska et al., 2001; Kulawiak and Bednarczyk, 2005). Brain mitochondria contain seven times more mitoK$_{ATP}$ channels than liver or heart mitochondria, which reflect the importance of these channels in neuronal functionality and integrity (Bajgar et al., 2001). Recent findings suggest that mitoK$_{ATP}$ channels have a key role as both triggers and end effectors in acute and delayed preconditioning-mediated neuroprotection (Busija et al, 2008; Dirnagl and Meisel, 2008). Indeed, the activation of mitoK$_{ATP}$ channels with pharmacological agents

mimicked the preconditioning-associated protective effects (Garlid et al., 1997; Szewczyk and Wojtczak, 2002). Conversely, physiological or chemical preconditioning was abrogated by mitoK$_{ATP}$ channels blockers, such as glibenclamide and 5-hydroxydecanoate (5-HD) (Szewczyk and Wojtczak, 2002). Some progress has been made in the elucidation of the mechanisms underlying mitoK$_{ATP}$ channels-mediated preconditioning. Inoue and collaborators (1991) hypothesized that mitoK$_{ATP}$ channels opening may decrease ΔΨm, promoting an increase in the electron transport chain rate, and, consequently, increasing ATP production. In addition, the activation of mitoK$_{ATP}$ channels induced cerebroprotection by attenuating mitochondrial Ca^{2+} overload and, thus, preventing mPTP induction. It was recently shown that the signal transduction pathways initiated by epsilon protein kinase C (εPKC) mediated preconditioning-induced neuroprotection through the activation of mitoK$_{ATP}$ channels (Raval et al., 2007). Further, the inhibition of mitoK$_{ATP}$ channels or εPKC abolished the beneficial effects of preconditioning (Raval et al., 2007).

It has been reported that diazoxide, a selective mitoK$_{ATP}$ channels opener, induced mild oxidative stress and preconditioning-like neuroprotection (Samavati et al., 2002). However, high doses of diazoxide also inhibited SDH, the complex II of the mitochondrial respiratory chain, leading to the production of ROS in a mitoK$_{ATP}$ channel-independent manner (Kis et al., 2003). It was recently proposed that diazoxide is the most potent inducer of preconditioning-mediated protection due to the combined effects involving mitochondrial membrane depolarization and enhanced ROS production through SDH inhibition (Busija et al., 2008). The immediate preconditioning induced by low doses of diazoxide also protected neuronal and vascular function against the deleterious effects of cerebral ischemia (Domoki et al., 1999). Additionally, this immediate preconditioning

with diazoxide protected against ischemia-reperfusion injury by preventing mitochondrial swelling and Ca^{2+} accumulation in brain cells (Domoki et al., 2004). Diazoxide also induced delayed preconditioning in neurons via acute generation of $O_2^{\bullet-}$ and activation of protein kinases protecting against the oxidative stress induced by OGD, which is a well-established *in vitro* model of cerebral ischemia-reperfusion (Kis et al., 2003). It was also demonstrated that diazoxide protected neurons against ischemia-induced death by increasing mitochondrial Bcl-2 levels and suppressing Bax translocation to mitochondria and subsequent cytochrome c release, suggesting that mitoK$_{ATP}$ channels activation may stabilize mitochondrial function by differentially modulating pro-apoptotic and anti-apoptotic proteins (Liu et al., 2002). Some *in vivo* studies also revealed that diazoxide-mediated acute and delayed preconditioning had a neuroprotective effect against transient focal cerebral ischemia (Shimizu et al., 2002; Mayanagi et al., 2007a). Goodman and Mattson (1996) also demonstrated that diazoxide was effective in protecting hippocampal neurons against oxidative injury induced by exposure to ferrous sulfate (FeSO$_4$) and Aβ, due to the suppression of intracellular peroxide formation. Accordingly, it was observed a protective effect of diazoxide against Aβ-induced cytotoxicity in endothelial cells (Chi et al., 2000). Ma and Chen (2004) reported that diazoxide counteracted the effects of Aβ$_{1-42}$, protecting neurons against the increase of ΔΨm and intracellular ROS levels induced by this amyloidogenic peptide. A recent study reported that Aβ$_{1-42}$ enhanced the expression of K$_{ATP}$ channel subunits in cholinergic neurons, and it was suggested that the change in the composition of K$_{ATP}$ channels may interfere with the function of K$_{ATP}$ channels and membrane excitability (Ma et al., 2009). Moreover, it was demonstrated that neurons pretreated with diazoxide did not present an increase in the expression of K$_{ATP}$ channels

subunits when exposed to $A\beta_{1-42}$ (Ma et al., 2009). In an *in vitro* model of Parkinson's disease (PD), diazoxide protected the neurons against MPP^+-induced cytotoxicity via inhibition of ROS overproduction, which improved mitochondrial function (Xie et al., 2009). Yang and collaborators (2006) also found that this $mitoK_{ATP}$ opener improved both parkinsonian symptoms and neurochemistry alterations occurring in rats treated with rotenone, a model of PD. These results suggest that $mitoK_{ATP}$ activation could represent a new therapeutic strategy for the treatment of early PD. The authors also observed that 5-HD abolished all neurorestorative effects of diazoxide (Yang et al., 2006). This is consistent with previous studies showing that activation of $mitoK_{ATP}$ channels with diazoxide in PC12 cells induced protection against the neurotoxic effects of rotenone, this protection being attenuated by 5-HD (Tai and Truong, 2002; Tai et al., 2003). An *in vitro* study also revealed that diazoxide prevented rotenone-induced microglial activation and the subsequent production of pro-inflammatory factors, such as tumor necrosis factor alpha (TNF-α) and inducible isoform of nitric oxide synthase (iNOS) (Liu et al., 2006).

BMS-191095, a selective $mitoK_{ATP}$ channels opener, is able to induce both immediate and delayed preconditioning in neurons. Kis and collaborators (2004) demonstrated that BMS-191095 led to a remarkable neuroprotection under stress conditions via mechanisms that involved mitochondrial depolarization, PKC activation and attenuated free radical production. It was also found that BMS-191095 depolarized mitochondria without ROS generation, activated the PI3-K signaling pathway, and increased ATP content and catalase expression; these mechanisms playing an important role in the neuroprotective effect afforded by this $mitoK_{ATP}$ channels opener (Gáspár et al., 2008b). Similarly, Mayanagi and collaborators (2007b) examined the effects of BMS-

191095 pretreatment on transient ischemia induced by MCAO in rats and concluded that BMS-191095 afforded protection against cerebral ischemia by delayed preconditioning via selective opening of mitoK$_{ATP}$ channels without ROS generation.

In summary, the activation of mitoK$_{ATP}$ channels seems to be a key event that elicits preconditioning-mediated neuroprotection; these channels representing promising therapeutic targets to counteract neurodegeneration.

1.4.2.3 MITOCHONDRIAL PERMEABILITY TRANSITION PORE

Mitochondria have a high capacity for Ca^{2+} sequestration, which contributes for normal neuronal function (Babcock and Hille, 1998; Rizzuto et al., 2000; Nicholls, 2002). Conversely, mitochondrial Ca^{2+} overload leads to the induction of the mPTP, resulting in osmotic swelling and collapse of the outer mitochondrial membrane. The mPTP, a dynamic multiprotein complex located at the contact site between the mitochondrial inner and outer membranes, is comprised of the voltage-dependent anion channel (VDAC), the adenine nucleotide translocator (ANT), and the regulatory protein CypD. Once open, mPTP allows the release of pro-apoptotic proteins, including cytochrome *c* and apoptosis-inducing factor (AIF), from the mitochondrial intermembrane space into the cytoplasm. Consequently, released cytochrome *c* binds the apoptotic protease-activating factor 1 (Apaf-1) and activates the caspase cascade (Hengartner, 2000; Martinou and Green, 2001; Valko et al., 2007).

Compelling evidence indicates that the inhibition of mPTP opening and its signaling cascade represent crucial events responsible for preconditioning-mediated cytoprotection in both heart and brain (Hausenloy et al., 2002; Javadov et al., 2003; Halestrap et al., 2007; Dirnagl and Meisel, 2008;). Despite the molecular mechanisms underlying these effects are still under investigation, nitrite (NO$_2^-$), a known endogenous

mediator of preconditioning as well as protein kinases, has been proposed as a possible mPTP regulator (Zhao et al., 2006; Shiva et al., 2007). More recently, Halestrap and collaborators (2007) also proposed that a decrease in the oxidation of critical thiol groups of the mPTP, which facilitate the pore opening induced by Ca^{2+}, could be involved in preconditioning-mediated inhibition of mPTP opening. In contrast to heart, the role of mPTP in brain preconditioning remains unclear. However, it was reported that the activation of mitoK_{ATP} channels protected the brain against injury through the attenuation of mitochondrial Ca^{2+} overload and, consequently, prevention of mPTP induction (Wu et al., 2006). It has been proposed that the increase in K^{+} conductance following mitoK_{ATP} opening alkalinizes the mitochondrial matrix and increases the generation of H_2O_2, which in turn activates an mPTP-associated PKCε. In addition, Pérez-Pinzón (2004) and coworkers suggested a pivotal role for PKCε in the tolerance induced by ischemic preconditioning in experimental models of cerebral ischemia. Indeed, ischemic preconditioning promoted a significant increase in synaptic mitochondrial respiration and phosphorylation of respiratory proteins via PKCε (Dave et al., 2008). It was also shown that neurons preconditioned with short periods of OGD contain large mitochondria with dense matrices, increased respiration and an elevated Ca^{2+} loading capacity (Iijima et al., 2008). In accordance, a recent study demonstrated that mitochondrial hyperpolarization that occur after short periods of OGD increased the mitochondrial Ca^{2+} buffering capacity in hippocampal neurons, which suggest that enhanced buffering capacity of the mitochondria may be linked to preconditioning after short-term ischemic episodes (Tanaka et al., 2009). Overall these findings point to a potential role of mPTP in preconditioning-induced brain tolerance.

1.4.2.4 MITOCHONDRIAL UNCOUPLING PROTEINS

In the brain, as well as in the heart, preconditioning is related with a moderate uncoupling of the mitochondrial respiratory chain (Sack, 2006; Dirnagl and Meisel, 2008). Thus, uncoupling proteins (UCPs) are one of the mitochondrial elements believed to be involved in this phenomenon. These proteins, which are located in the inner mitochondrial membrane, dissipate the proton electrochemical gradient between the intermembrane space and the mitochondrial matrix, which uncouple electron transport from ATP synthesis. Thus, UCPs play a critical role in energy balance (Kim-Han and Dugan, 2005). UCP2 is expressed in the brain, essentially in neurons, and it has been proposed to contribute to neuroprotection by reducing mitochondrial ROS generation (Duval et al., 2002; Brand and Esteves, 2005). Indeed, Mattiasson and colleagues (2003) provided evidence of an increased UCP2 mRNA expression in the brain, measured by *in situ* hybridization, after ischemic preconditioning. It was also found that UCP2 prevented neuronal death and diminished brain dysfunction after stroke and brain trauma, which suggest that UCP2 is an inducible protein whose neuroprotective actions may be due to the activation of cellular redox signaling or induction of mild mitochondrial uncoupling that prevents the release of apoptogenic proteins. Accordingly, *in vitro* and *in vivo* experiments performed by Diano and collaborators (2003) revealed that the up-regulation of UCP2 is part of a neuroprotective set of responses to various cellular stresses involved in preconditioning. It was observed that PC12 cells overexpressing UCP2 were protected against free radical-induced cell death. Moreover, in transgenic mice that express UCP2 constitutively in the hippocampus presented a robust reduction in cell death induced by seizures. Since UCP2 increased the number of mitochondria and ATP levels, with a concomitant decrease in free radical-induced damage, the authors

proposed that neuronal preconditioning induced by UCPs involve the dissociation of cellular energy production from that of free radicals generation withstanding the harmful effects of cellular stress occurring in a variety of neurodegenerative disorders (Diano et al., 2003). More recently, it was confirmed that ischemic preconditioning caused increased expression of UCP2 protein *in vivo* preventing ischemia/reperfusion injury in the hippocampus (Liu et al., 2009). In addition, the increase in UCP2 expression in preconditioned brains was blocked by ROS scavengers, which demonstrate an interplay between UCP2 expression and ROS production. These findings are in accordance with previous studies that demonstrated that an excess of ROS production can induce UCP2 overexpression and activation (Busquets et al, 2001; Kim-Han and Dugan, 2005; Echtay and Brand, 2007). Finally, it was shown that both resveratrol and ischemic preconditioning induced neuroprotection against cerebral ischemic damage through an alteration in mitochondrial function via sirtuin1 (SIRT1)-UCP2 pathway (Della-Morte et al., 2009).

1.4.2.5 MITOCHONDRIAL SUPEROXIDE DISMUTASE

To protectmitochondria from $O_2^{\bullet-}$-mediated oxidative damage, cells express a nuclear-encoded mitochondrial enzyme, the manganese superoxide dismutase (Mn SOD) that scavenges $O_2^{\bullet-}$ generated by the mitochondrial electron-transport chain (Hirai et al., 2004). Indeed, previous reports demonstrated that overexpression of MnSOD protected mice against focal cerebral ischemia (Murakami et al., 1998; Noshita et al., 2001). More recently, Scorziello and collaborators (2007) proposed that MnSOD may represent the crucial step through which the NO/Ras/ERK1/2 pathway promoted neuroprotection during preconditioning.

In sum, the sub-chapter 1.3 provides evidence of the critical involvement of mitochondrial biology in preconditioning-triggered brain tolerance.

CHAPTER 2

OBJECTIVES

2.1 Objectives

Mitochondria are fascinating organelles that control cell fate! On the one hand, under physiological conditions, mitochondria are the main producers of ATP and function as signaling organelles orchestrating several intracellular processes through the generation of moderate levels of ROS, among others. On the other hand, defective mitochondrial functioning may initiate a cascade of deleterious events that contribute to cerebrovascular and neuronal degeneration. Mitochondrial abnormalities are considered an upstream event in AD pathology and a mechanistic linkage between AD and diabetes mellitus.

As outlined in **Chapter 1**, preconditioning is a paradigm that affords robust brain tolerance in face of neurodegenerative insults. This tolerance is in part due to the activation of an adaptive reprogramming of mitochondrial biology in response to a noxious stimulus, which in turn will contribute to augment brain adaptive mechanisms. The preconditioning-mediated neuroprotective effects have been extensively reported in experimental models of ischemic stroke; however, little is known about the effectiveness of preconditioning in diseases associated with central insulin resistance such as diabetes and AD.

In this scenario, we hypothesized that preconditioning triggers adaptive mechanisms by stimulating mitochondrial ROS production with the concomitant induction of HIF-1α signaling pathway, which activates protective/survival mechanisms that sustain brain integrity and functionality under potentially lethal conditions.

The general aims of this work were: 1) to investigate if preconditioning is able to induce tolerance against diabetes and AD-associated brain endothelial and neuronal degeneration, and 2) to uncover whether mitochondria act as both signaling organelles and ultimate targets of the protective machinery underlying preconditioning.

Specifically, the aims of this work were as follows:

In **Chapter 4**, we explored the role of mitochondrial ROS and HIF-1α signaling pathway in cyanide-mediated preconditioning of brain endothelial and neuronal cells against hyperglycemia-induced cell damage. Using an *in vitro* approach of preconditioning, rat brain endothelial (RBE4) and human teratocarcinoma (NT2) neuron-like cells were firstly exposed to non-toxic concentrations of cyanide (inhibitor of COX), to produce a mild increase in mitochondrial ROS production, and subsequently exposed to a lethal insult of glucose. To further strength the role of mitochondria and mitochondrial-derived ROS on cyanide preconditioning, we also took advantage of the mtDNA-depleted NT2 cell line (NT2 ρ0) – cells void of functional mitochondria.

To gain additional insights into the role of mitochondria in sAD pathology and their close association with brain insulin resistance, in **Chapter 5** the hippocampal and cortical mitochondrial bioenergetics and oxidative status in the rat model of sAD generated by the icv injection of a sub-diabetogenic dose of STZ were analysed.

In **Chapter 6**, the potential neuroprotective effect of hypoxic preconditioning (HP) against the sAD-like phenotype induced by the icv administration of STZ in rats was evaluated. Particularly, it was ascertained the effect of HP on cognitive function, and brain energy and glucose metabolism in the icvSTZ rat. Preconditioning was achieved by exposing the animals to brief periods of moderate hypoxia (10% O_2 for 2 hours) during a

period of three days. Twenty-four hours after the last episode of hypoxia animals received the icv injection of STZ.

Finally, the study presented in **Chapter 7** aimed to answer the question: What happens to brain mitochondria during HP? A time-course analysis of the brain cortical and hippocampal mitochondrial changes that occurred immediately, 6 and 24 hours after the last hypoxic episode was performed.This investigation focused on the impact of HP on mitochondrial bioenergetics, biogenesis and fusion-fission machinery.

Chapter 2

CHAPTER 3

MATERIALS AND METHODS

3.1 *IN VITRO* STUDIES

3.1.1 CHEMICALS

TABLE 3.1. CHEMICALS

PRODUCT	CATALOG #	SUPPLIER
N-acety-L-cysteine (NAC)	A-7250	SIGMA
D-Glucose	G-8270	
D-Mannitol	M-9546	
2-Methoxyestradiol (2-ME2)	M-6383	
Potassium cyanide (KCN)	60178	FLUKA

All the other chemicals were of the highest grade of purity commercially available.

3.1.2 CELL CULTURE AND CELL MEDIA

The rat brain endothelial cell line (RBE4) was kindly provided by Dr. Jon Holy (University of Minnesota, Duluth, USA). RBE4 cells were maintained as monolayer cultures in collagen-coated T-75 flasks in a humidified atmosphere of 5% CO_2–95% air at 37 °C. RBE4 cells were grown in α-MEM:Ham's F-10 nutrient mixture (1:1), supplemented with 10% FBS, 1 ng/ml bFGF and 300 µg/ml Geneticin (Roux et al., 1994). The medium was changed every 2-3 days until cells reached confluence. Human teratocarcinoma NT2 cells, a committed neuronal precursor cell line, containing mtDNA, and NT2 cells depleted of mtDNA (NT2 ρ0) were grown in T-75 flasks in Optimen Medium containing 10% heat inactivated fetal calf serum, penicillin (50 U/ml), and streptomycin (50 µg/ml); the media for the NT2 ρ0 cells was further supplemented with

uridine (50 µg/ml) and pyruvate (200 µg/ml) (Swerdlow et al., 1997). Both cell lines were maintained in a humidified atmosphere of 5% CO_2-95% air at 37 °C. The medium was changed every 2-3 days until cells reached confluence.

3.1.3 CELL TREATMENTS

Cells were exposed to cyanide (0.01-1 µM) during 1 hour at 37°C. For the evaluation of cell viability, ROS levels and caspase 3 activity, some experiments involved cells pre-treated with 200 µM of NAC or 5 µM of 2-methoxyestradiol (2-ME2) for 24 hours or 30 minutes, respectively, before cyanide exposure. Concerning the experiments with high glucose levels, cells were pre-treated or not with cyanide and then washed with phosphate-buffered saline (PBS) and exposed to 30 mM of D-glucose for 12 hours. Osmotic controls were done with 30 mM mannitol.

3.1.4 CELL VIABILITY ASSAYS

3.1.4.1 ALAMAR BLUE ASSAY

For Alamar blue assay, cells were seeded in 48-well plates at a density of 0.5×10^5 cells/well. After the incubation period, the cells' medium was aspirated and replaced by culture medium containing 10 % (v/v) alamar blue. After 1-2 hours incubation at 37°C, the supernatant was collected and the absorbance was measured at 570 nm and 600 nm using a microplate reader (SpectraMax Plus [384], Molecular Devices) (Neves et al., 2006). Cell viability (% of control) was calculated according to the formula ($A_{570} - A_{600}$) of treated cells x 100 / ($A_{570} - A_{600}$) of control cells.

3.1.4.2 LACTATE DEHYDROGENASE RELEASE

In order to evaluate plasma membrane integrity, lactate dehydrogenase (LDH) activity was measured spectrophotometrically in the cell culture medium and cell lysates as described by Bergmeyer and Bernt (1974), which follows the conversion of NADH to NAD^+ at 340 nm. Briefly, cells were seeded in 12-well plates at a density of 2×10^5 cells/well. After the treatments, the cell culture medium was collected to determine the extracellular LDH, and cells were scrapped in a 15 mM Tris solution (pH 7.4) to determine the intracellular LDH. LDH released to the extracellular medium was expressed as the percentage of total LDH activity (intracellular plus extracellular).

3.1.5 MEASUREMENT OF REACTIVE OXYGEN SPECIES LEVELS

3.1.5.1 2′-7′-DICHLORODIHYDROFLUORESCEIN DIACETATE (DCF H_2-DA) PROBE

Intracellular ROS levels were quantified using the probe $DCFH_2$-DA. This probe is accumulated by cells and hydrolyzed by cytoplasmic esterases to become 2′-7′-dichlorodihydrofluorescein, which then reacts with ROS to generate the fluorescent product 2′-7′-dichlorofluorescein (DCF). Cells were seeded in 48-well plates at a density of 0.5×10^5 cells/well. After that, cells exposed or not to cyanide, in the presence or absence of NAC, were loaded with 20 µM $DCFH_2$-DA in sodium medium containing 132 mM NaCl, 4 mM KCl, 1.2 mM NaH_2PO_4, 1.4 mM $MgCl_2$, 6 mM glucose, 10 mM HEPES-Na, 1 mM $CaCl_2$, pH 7.4, for 30 min at 37°C. After $DCFH_2$-DA incubation, cells were washed and sodium medium was added. Fluorescence was monitored for 1 hour, at 37°C, using a Spectramax GEMINI EM fluorocytometer (Molecular Devices), with excitation and emission wavelengths corresponding to 480 and 550 nm, respectively, with cutoff at 530 nm. The values were expressed as percentage of control.

3.1.5.2 Hydrogen Peroxide Levels

H_2O_2 levels were measured fluorimetrically using a modification of the method described by Barja (1999). Briefly, cell lines exposed or not to cyanide were washed twice with PBS and incubated at 37°C with reaction buffer, pH 7.4, containing 0.1 mM EGTA, 5 mM KH_2PO_4, 3 mM $MgCl_2$, 145 mM KCl, 30 mM Hepes, 0.1 mM homovalinic acid and 6 U/ml horseradish. After 5 minutes, the reaction was stopped with cold stop solution (0.1 M glycine, 25 mM EDTA-NaOH, pH 12). The fluorescence of supernatants was determined at 312 nm excitation and 420 nm emission wavelengths. The H_2O_2 levels were expressed as percentage of control.

3.1.6 Analysis Of Mitochondrial Membrane Potential

3.1.6.1 Rhodamine 123 Probe

Rhodamine 123, a fluorescent cationic dye, was used to monitor changes in ΔΨm. RBE4 cells were seeded in 48-well plates at a density of 0.5×10^5 cells/well. After treatments, cells were washed with PBS and incubated with 1 µM rhodamine 123 in sodium medium for 45 minutes at 37°C, using a Spectramax GEMINI EM fluorocytometer (Molecular Devices). Basal fluorescence was monitored at 505 nm excitation and 525 nm emission wavelengths. At the end of the incubation period, FCCP (6 µM) and oligomycin (0.25 µg/ml) were added in order to establish the maximum retention of Rh123. The difference between the final fluorescence (after oligomycin and FCCP exposure) and the initial fluorescence was used to evaluate ΔΨm. The results were expressed as percentage of control fluorescence.

3.1.7 ANALYSIS OF MITOCHONDRIAL OXYGEN CONSUMPTION

Mitochondria oxygen consumption was determined using the BD Oxygen Biosensor System (BD Biosciences) as previously described (Wilson-Fritch et al., 2004). Cells were resuspended in sodium medium and subsequently transferred to a 96-well plate where the same number of cells (1×10^6) was placed in each well. Levels of oxygen consumption were measured under baseline conditions and in the presence of FCCP (5 μM). Fluorescence was recorded using a Spectramax GEMINI EM fluorocytometer (Molecular Devices) at 1 minute intervals for 60 minutes at an excitation wavelength of 485 nm and emission wavelength of 630 nm.

3.1.8 NUCLEAR HIF-1α ACTIVATION

HIF-1α activation was determined in nuclear extracts. Briefly, RBE4 cells were centrifuged for 5 minutes at 1700 rpm at 4°C (5417R, Eppendorf). The cell pellet was resuspended in nuclear extraction hypotonic buffer (20 mM Hepes, pH 7.5, containing 5 mM NaF, 100 μM Na_2MoO_4, 1 mM EDTA, 0.5 mM dithiothreitol (DTT), and 0.5 mM phenyl-methylsulfonyl fluoride (PMSF)), adjusted to 1% Nonidet P-40, and homogenized. The nuclear cell pellet was resuspended in extraction buffer (10 mM Hepes, pH 7.9, containing 0.1 mM EDTA, 1.5 mM $MgCl_2$, 420 mM NaCl, 0.5 mM DTT, and 0.5 mM PMSF, 20 mM NaF, 1 mM β-glycerophosphate, 10 mM Na_3OV_4, and 20% glycerol) and centrifuged for 15 minutes at 11500 rpm (5417R, Eppendorf), and the supernatant was collected. After that, activation of HIF-1α was quantified by a DNA-binding ELISA kit (Cayman Chemical, France) based on the binding of activated HIF-1 to a specific double stranded DNA (dsDNA) sequence containing the HRE (5'-ACGTG-3').

3.1.9 WESTERN BLOT ANALYSIS

For whole cell extracts, RBE4 cells were plated in petri dishes (10 cm) at a density

of 1×10^6 cells/dish. After treatments, cells were washed twice with PBS, scraped and

resuspended in ice-cold lysis buffer (25 mM Hepes-Na, 2 mM $MgCl_2$, 1 mM EDTA, and 1

mM EGTA) supplemented with 0.1 M PMSF, 0.2 M DTT, and 1:1000 of a protease

inhibitor cocktail (containing chymostatin, pepstatin A, leupeptin, and antipain,

1mg/ml). The cellular extracts were frozen and defrozen three times to favor cells

disruption. For the isolation of cytosolic and mitochondrial fractions, RBE4 cells were

scrapped and homogenized in a buffer containing 250 mM sucrose, 20 mM Hepes, 1 mM

EDTA, 1 mM EGTA, 0.1 M PMSF, 0.2 M DTT, and 1:1000 protease inhibitor cocktail. Cells

were frozen and defrozen three times and the lysate was centrifuged at 2200 rpm

(5417R, Eppendorf) for 12 minutes at 4°C. The resulting supernatant was centrifuged at

9600 rpm for 10 minutes at 4°C. The supernatants represent the cytosolic fractions and

the resulting pellets the mitochondrial fractions. The amount of protein content in the

samples was measured using the Bio-Rad protein dye assay reagent. The samples were

resolved by electrophoresis in 8-12% SDS–polyacrylamide gels and transferred to PVDF

membranes. Non-specific binding was blocked by gently agitating the membranes in 5%

non-fat milk and 0.1% Tween in Tris-buffered saline (TBS) for 1 hour at room

temperature. The blots were subsequently incubated with specific primary antibodies,

overnight at 4 °C, with gentle agitation. Blots were washed three times (15 minutes),

with Tris buffer containing 0.1% non-fat milk and 0.1% Tween (TBS-T) and then were

incubated with secondary antibodies for 2 hours at room temperature with gentle

agitation. After three washes with TBS-T specific bands of immunoreactive proteins

were visualized after membrane incubation with ECF for 5 min in a VersaDoc Imaging

System (Bio-Rad), and the density of protein bands was calculated using the Quantity One Program (Bio-Rad). The antibodies used are listed in Table 3.2.

3.1.10 IMMUNOCYTOCHEMISTRY

RBE4 cells were grown on coverslips in 12-well plates at a density of 2×10^5 cells/well. After incubation with the experimental conditions previously outlined, cells were washed twice with PBS and fixed with 4% paraformaldehyde for 30 minutes at room temperature. Then, cells were permeabilized for 2 minutes at room temperature with 0.2% Triton-X100 in PBS and blocked for 30 minutes in PBS containing 3% bovine serum albumin (BSA). Cells were incubated for 1 hour with primary antibodies prepared in PBS containing 3% of BSA and then washed with PBS and incubated with secondary antibodies conjugated with Alexa Fluor for 1 hour at room temperature. Finally, the cells were washed twice with PBS and treated with Dako Cytomation Fluorescent mounting solution on a microscope slide. Images were acquired on a Zeiss LSM510 META confocal microscope (63× 1.4NA plan-apochromat oil immersion lens) by using Zeiss LSM510 v3.2 software. The antibodies used are listed in Table 3.2.

TABLE 3.2. LIST OF PRIMARY AND SECONDARY ANTIBODIES USED IN THE *IN VITRO* STUDIES

ANTIBODY	CATALOG #	SUPPLIER	HOST SPECIE	DILUTION
Anti-BAX	2772	Cell Signaling	Rabbit	1:7000 (WB); 1:100 (ICC)
Anti-eNOS	sc-654	Santa Cruz	Rabbit	1:200 (WB)
Anti-EPO	sc-7956	Santa Cruz	Rabbit	1:200 (WB); 1:75 (ICC)
Anti-HIF-1α	ab1	Abcam	Mouse	1:400 (WB)
Anti-MTCO1	ab14705	Abcam	Rabbit	1:1000 (WB); 1:50 (ICC)
Anti-TOM 20	sc-11415	Santa Cruz	Rabbit	1:100 (ICC)
Anti-VEGF	PC315	Calbiochem	Rabbit	1:200 (WB)
Anti-α-Tubulin	T-6199	Sigma	Rabbit	1:400 (ICC)
Anti-β-actin	A-5441	Sigma	Mouse	1:5000 (WB)
Alexa Fluor 488 anti-rabbit IgG conjugate	A-11005	Molecular Probes	Goat	1:200 (ICC)
Alexa Fluor 594 anti-mouse IgG conjugated	A-11008	Molecular Probes	Goat	1:200 (ICC)
Anti-mouse IgG alkaline phosphatase conjugate	NIF1316	Amersham Pharmacia Biotech	Goat	1:20000 (WB)
Anti-rabbit IgG alkaline phosphatase conjugate	NIF1317	Amersham Pharmacia Biotech	Goat	1:20000 (WB)

WB - WESTERN BLOT

ICC - IMMUNOCYTOCHEMISTRY

3.1.11 MEASUREMENT OF CASPASE 3-LIKE ACTIVITY

Caspase 3 activation was measured using a colorimetric method described by Cregan et al. (1999). Cells were plated in 6-well plates at a density of 5×10^5 cells/well. After treatment, cells were washed twice with PBS and lysed in cold lysis buffer. Cells were harvested by scraping and frozen and defrozen three times. The lysates were centrifuged for 10 minutes at 14000 rpm (5417R, Eppendorf) at 4°C. The resulting supernatant was stored at -80°C. Protein concentrations were measured by using the Bio-Rad protein dye assay reagent. Cell extracts (50 µg of protein) were incubated at 37°C for 2 hours in 25 mM HEPES, pH 7.5 containing 0.1% CHAPS, 10% sucrose, 2 mM DTT, and 40 µM Ac-DEVD-pNA. Caspase-3-like activity was determined by measuring substrate cleavage at 405 nm in a microplate reader (SpectraMax Plus [384], Molecular Devices).

3.1.12 STATISTICAL ANALYSIS

Results are presented as mean ± SEM of the indicated number of experiments. Statistical significance was determined using the unpaired two-tailed student *t*-test and one-way ANOVA test for multiple comparisons, followed by the posthoc Tukey- Kramer test.

3.2 *IN VIVO* STUDIES

3.2.1 CHEMICALS

STZ was obtained from Sigma (Portugal). All the other chemicals were of the highest grade of purity commercially available.

3.2.2 ANIMAL HANDLING AND PROCEDURES

3.2.2.1 ANIMAL HOUSING

3-month-old male Wistar rats purchased from Charles River were used. Animals were group-housed upon arrival and provided *ad libitum* access to food and water and maintained under controlled light (12-h day/night cycle), temperature (22-24°C) and humidity (50-60%). Animal handling and sacrifice followed the procedures approved by the Federation of European Laboratory Animal Science Associations (FELASA) (**Chapters 5** and **7**) and the Institutional Animal Care and Use Committee (IACUC) of Case Western Reserve University (**Chapter 6**).

3.2.2.2 HYPOXIC PRECONDITIONING PROTOCOL

Wistar rats were randomly divided into two groups: a preconditioned and a non-preconditioned control group. In the HP paradigm, rats were exposed to 2 hours of 10% normobaric hypoxia per day during 3 consecutive days. Non-preconditioned control rats were also placed in the chamber under normoxic conditions. For the experiments described in **Chapter 6**, animals received an icv administration of STZ or vehicle solution 24 hours after the last hypoxic session. For the experiments described in **Chapters 6** and **7**, animals were sacrificed immediately, 6 and 24 hours after the last hypoxic session.

3.2.2.3 INTRACEREBROVENTRICULAR ADMINISTRATION OF STREPTOZOTOCIN

Preconditioned and non-preconditioned Wistar rats were anesthetized with an intraperitonal injection of ketamine (100 mg/kg)/ xylazine (5 mg/kg) (**Chapter 5**) or with isoflurane (2.5% in O_2) in an induction chamber and maintained with 1-2% isoflurane through a nasal cone (**Chapter 6**) and randomly divided into two groups: one group received a single bilateral icv injection of STZ and the other group received the vehicle solution (citrate buffer). The animals were positioned in a stereotaxic apparatus (David Kopf Instruments, Tujunga, CA) and icv injection was given using the following coordinates: 0.8 mm posterior to bregma; 1.5 mm lateral to saggital suture; 3.6 mm ventral from the surface of the brain (Noble et al., 1967). STZ at the dosage of 3 mg/kg and vehicle solution (5 µl) were slowly infused into each cerebral ventricle using a Hamilton microsyringe. 5 weeks after the icv injection, rats were sacrificed and the brains immediately removed.

3.3.3 BEHAVIORAL TESTS

All the behavioral tests were performed at Case Western Reserve University in Cleveland, under the supervision of Prof. Gemma Casadesus.

3.3.3.1 MORRIS WATER MAZE TEST

The Morris water maze test was employed to assess learning and memory of the animals at 4 weeks after icvSTZ injection (Morris, 1984). The Morris water maze is a swimming-based model in which animals learn to escape a pool of water (120 cm in diameter, 50 cm in height, filled to a depth of 30 cm with water at 24 ± 1°C) by a hidden platform. The water was colored with a non-toxic black dye to hide the location of the submerged platform. 4 equally spaced points around the edge of the pool were

designed as North, East, South and West. The rats could climb on the platform to escape from the necessity of swimming. Briefly, rats did 4 trials during 3 daily acquisition sessions. The trial was terminated automatically as soon as the rat reached the platform or when 120 seconds had elapsed. The rat was allowed to stay on the platform for 15 seconds. Mean latency time to reach the platform of each session is shown in **Chapters 5 and 6**. 24 hours after the completion of the acquisition trials, the rats received a single 60 seconds probe trial for memory retention. The rats had one trial with the platform removed from the pool for testing the functioning of long-term memory. At this time, the percentage of time spent in the target area was recorded.

3.3.4 DETERMINATION OF BLOOD GLUCOSE LEVELS

Blood glucose was determined immediately after sacrifice by a glucose oxidase reaction, using a glucometer (Glucometer-Elite, Bayer).

3.3.4 BRAIN TISSUE PROCESSING

After the sacrifice of the animals, the brains were quickly removed and the hippocampus and the cerebral cortex were dissected out on ice. For experiments described in **Chapter 6,** acetylcholine esterase (AChE) activity, oxidative stress parameters, antioxidant defenses and glycolytic enzymes activity were measured in cortical and hippocampal samples homogenized in phosphate buffer (pH 7.4). All the other parameters evaluated in **Chapter 5**, **6** and **7** were performed in mitochondrial preparations from cerebral cortex and hippocampus.

3.3.4.1 PREPARATION OF MITOCHONDRIAL FRACTION

Brain cortical and hippocampal mitochondria were isolated from rats by the method of Moreira et al. (2001), with slight modifications, using 0.02% digitonin to free mitochondria from the synaptosomal fraction. Briefly, after animal decapitation, the hippocampus and cortex were immediately separated and homogenized at 4°C in 10 ml of isolation medium (225 mM mannitol, 75 mM sucrose, 5 mM HEPES, 1 mM EGTA, 1 mg/ml BSA, pH 7.4) containing 5 mg of the bacterial protease (Sigma). Single brain homogenates were brought to 30 ml and then centrifuged at 2500 rpm (Sorvall Evolution RC Superspeed Refrigerated Centrifuge) for 5 minutes. The pellet, including the fluffy synaptosomal layer, was resuspended in 10 ml of the isolation medium containing 0.02% digitonin and centrifuged at 10000 rpm for 10 minutes. The brown mitochondrial pellet without the synaptosomal layer was resuspended again in 10 ml of medium and centrifuged at 10000 rpm for 5 minutes. The pellet was resuspended in 10 ml of washing medium (225 mM mannitol, 75 mM sucrose, 5 mM HEPES, pH 7.4) and centrifuged at 10000 rpm for 5 minutes. The final mitochondrial pellet was resuspended in the washing medium and the protein amount determined by the biuret method calibrated with BSA (Gornall et al., 1949).

3.3.5 MITOCHONDRIAL RESPIRATION MEASUREMENTS

Oxygen consumption of mitochondria was registered polarographically with a Clark oxygen electrode (Estabrook, 1967) connected to a suitable recorder in a thermostated water-jacketed closed chamber with magnetic stirring. The reactions were carried out at 30°C in 1 ml of the standard medium (100 mM sucrose, 100 mM KCl, 2 mM KH_2PO_4, 5 mM Hepes and 10 μM EGTA, pH 7.4) with 0.8 mg of protein. States 4 and

3 respiration were initiated with 5 mM glutamate/2.5 mM malate (mitochondrial complex I energization) or 5 mM succinate in the presence of 2 μM rotenone (mitochondrial complex II energization). Exogenous ADP (155 nmol/mg protein) was added to initiate state 3. In some experiments, oligomycin (2 μg/ml) and FCCP (1 μM) were also added to inhibit passive flux through the ATP synthase and to uncouple respiration, respectively.

FUNDAMENTAL CONCEPTS:

STATE 2 - mitochondrial respiration in the presence of substrate but in the absence of exogenous ADP

STATE 3 - mitochondrial respiration in the presence of substrate and exogenous ADP

STATE 4 - mitochondrial respiration after ADP phosphorylation

RCR - ratio between State 3 and State 4

ADP/O - ratio between the amount of exogenous ADP and the oxygen consumed during State 3

3.3.6 MITOCHONDRIAL MEMBRANE POTENTIAL MEASUREMENTS

$\Delta\Psi_m$ was monitored by evaluating the transmembrane distribution of the lipophilic cation tetraphenylphosphonium (TPP^+) with a TPP^+-selective electrode prepared according to Kamo et al. (1979) using an Ag/AgCl-saturated electrode (Tacussel, model MI 402) as reference. TPP^+ uptake has been measured from the decreased TPP^+ concentration in the medium sensed by the electrode. The potential difference between the selective and reference electrodes was measured with an electrometer and recorded continuously in a Linear 1200 recorder. The voltage response of the TPP^+ electrode to log [TPP^+] was linear with a slope of 59 ± 1, in a good agreement

with the Nernst equation. Reactions were carried out in a chamber with magnetic stirring in 1 ml of the standard medium containing 3 µM TPP$^+$. This TPP$^+$ concentration was chosen in order to achieve high sensitivity in measurements and to avoid possible toxic effects on mitochondria (Jensen and Gunter, 1984). The $\Delta\Psi_m$ was estimated by the equation: $\Delta\Psi_m$ (mV) = 59 log(v/V) - 59 log($10^{\Delta E/59}$-1) as indicated by Kamo et al. (1979) and Muratsugu et al. (1977). v, V, and ΔE stand for mitochondrial volume, volume of the incubation medium and deflection of the electrode potential from the baseline, respectively. This equation was derived assuming that TPP$^+$ distribution between the mitochondria and the medium follows the Nernst equation, and that the law of mass conservation is applicable. A matrix volume of 1.1 µl/mg protein was assumed. No correction was made for the "passive'' binding contribution of TPP$^+$ to the mitochondrial membranes, because the purpose of the experiments was to show relative changes in potentials rather than absolute values. As a consequence, we can anticipate a slight overestimation on $\Delta\Psi_m$ values. However, the overestimation is only significant at $\Delta\Psi_m$ values below 90 mV, therefore, far from our measurements. Mitochondria (0.8 mg/ml) were energized with 5 mM glutamate/2.5 mM malate or 5 mM succinate in the presence of 2 µM rotenone. After a steady-state distribution of TPP$^+$ had been reached (ca. 1 min of recording), $\Delta\Psi_m$ fluctuations were recorded. For the mPTP experiments, mitochondria (0.5 mg/ml) were energized with 5 mM succinate, submitted to two or three pulses of Ca^{2+}(first pulse, 20 nmol Ca^{2+}; second and third pulses, 10 nmol Ca^{2+}), and $\Delta\Psi_m$ was recorded. For the inhibition of mPTP, oligomycin (2 µg/ml) plus ADP (100 µM) were added 2 min before Ca^{2+} addition.

FUNDAMENTAL CONCEPTS:

ADP-INDUCED DEPOLARIZATION - drop in $\Delta\Psi_m$ of energized mitochondria after ADP addition

REPOLARIZATION LEVELS - capacity of mitochondria to re-establish the $\Delta\Psi_m$, after ADP phosphorylation

REPOLARIZATION LAG PHASE - the time required for mitochondria to phosphorylate the amount of ADP added to the reaction medium

3.3.7 DETERMINATION OF ATP LEVELS

For the experiments described in **Chapter 5**, at the end of each $\Delta\Psi m$ measurement, 250 µl of each sample was promptly centrifuged at 14000 rpm (Eppendorf centrifuge 5415C) for 2 minutes with 250 µl of 0.3 M perchloric acid ($HClO_4$). The supernatants were neutralized with 10 M KOH in 5 M Tris and again centrifuged at 14000 rpm for 2 minutes. For the experiments reported in **Chapter 7**, brain cortical and hippocampal homogenates were used. ATP levels in the resulting supernatants were determined with a luminescence assay kit (Invitrogen-Molecular Probes) according to the manufacturer's instructions. The concentration of ATP was calculated using an ATP standard curve and expressed in pmol/mg protein.

3.3.8 NAD$^+$/NADH DETERMINATION

The NAD$^+$/NADH ratio was determined by using the NAD$^+$/NADH Quantification kit (MBL International Corporation). Briefly, brain cortical and hippocampal tissue was homogenized in NAD$^+$/NADH extraction buffer, and centrifuged at 14000 rpm (Eppendorf centrifuge 5415C) for 5 minutes at 4°C. The supernatants corresponded to total NAD$^+$ samples. To detect NADH 200 µl of the supernatants were heated at 60°C for

30 minutes. Following the kit instructions, 50 µl of total NAD$^+$ and NADH cell lysates were incubated with the NAD$^+$ cycling mix for 5 minutes. Then 10 µl of NADH developer was added and the reaction developed for 3 hours. Total NAD$^+$ and NADH were detected at 450nm, and NAD$^+$/NADH ratio was calculated as: <u>Total NAD$^+$ – NADH</u>.

NADH

3.3.9 ANALYSIS OF MITOCHONDRIAL RESPIRATORY CHAIN ENZYME COMPLEXES ACTIVITIES

3.3.9.1 NADH-UBIQUINONE OXIDOREDUCTASE (COMPLEX I) ASSAY

NADH-ubiquinone oxidoreductase activity was assayed spectrophotometrically in 25 mM potassium phosphate buffer (pH 7.2) supplemented with 5 mM MgCl$_2$, 5 mg/ml BSA, 0.8 mM NADH, 240 µM KCN, and 4 µM antimycin A, at 30°C (Barrientos et al., 2009). Briefly, thawed brain cortical mitochondria (50 µg/mL) were added to the reaction medium and the assay was started by the addition of 50 µM of ubiquinone-1 and followed at 340 nm [molar extinction coefficient (ε) = 6.22 mM^{-1}cm^{-1}].

3.3.9.2 CYTOCHROME C OXIDASE (COMPLEX IV) ASSAY

Cytochrome *c* oxidase activity was measured polarographically, at 30°C, in 1 ml of reaction medium (130 mM sucrose, 5 mM KH$_2$PO$_4$, 5 mM MgCl$_2$, 50 mM KCl, 5 mM Hepes-Tris, pH 7.4) supplemented with 2 µM rotenone, 10 µM cytochrome *c* and 100 µg of thawed brain cortical mitochondria. The reaction was initiated by the addition of 5 mM ascorbate plus 0.25 mM N,N,N',N'-tetramethyl-p-phenylenediamine (TMPD) and finished with 1 mM KCN (Moreira et al., 2004).

3.3.10 DETERMINATION OF ATPASE ACTIVITY

ATPase activity was determined spectrophotometrically at 660 nm (Teodoro et al., 2006). The reaction was carried out at 37°C, in 2 ml reaction medium (100 mM NaCl, 25 mM KCl, 5 mM MgCl$_2$, and 50 mM HEPES, pH 7.4). After the addition of thawed brain cortical mitochondria (0.25 mg), the reaction was initiated by adding 2 mM Mg^{2+}-ATP, in the presence or absence of oligomycin (1 µg/mg protein). After 10 minutes, the reaction was stopped by adding 1 ml of 40% trichloroacetic acid and the samples centrifuged for 5 minutes at 3000 rpm (Sigma 3-16K Refrigerated Centrifuge). 2 ml of ammonium molybdate plus 2 ml of distilled water were then added to 1 ml of supernatant. ATPase activity was calculated as the difference in total absorbance and absorbance in the presence of oligomycin. A standard curve was obtained by adding potassium phosphate to the reaction medium.

3.3.11 ANALYSIS OF TRICARBOXYLIC ACID CYCLE ENZYME ACTIVITIES

3.3.11.1 ACONITASE ASSAY

Aconitase activity was determined according to Krebs and Holzach (1952). Briefly, brain mitochondrial fractions (200 µg) were diluted in 0.6 ml buffer containing 50 mM Tris-HCl and 0.6 mM MnCl$_2$ (pH 7.4), and sonicated for 10 seconds. Aconitase activity was immediately measured spectrophotometrically by monitoring at 240 nm the *cis*-aconitase after addition of 20 mM isocitrate at 30°C. The activity of aconitase was calculated using a ε of 3.6 mM^{-1} cm^{-1} and expressed as U/mg protein/min. One unit was defined as the amount of enzyme necessary to produce 1 µM *cis*-aconitate per minute.

3.3.11.2 PYRUVATE DEHYDROGENASE ASSAY

Pyruvate dehydrogenase (PDH) activity was measured spectrophotometrically, as described previously (Humphries and Szweda, 1998). In brief, brain cortical mitochondria (100 μg) were added to the reaction medium (35 mM KH_2PO_4, 5 mM $MgCl_2$, 2 mM KCN, 0.5 mM EDTA, 0.25% X-Triton, pH 7.2) supplemented with 2.5 μM rotenone, 0.5 mM of NAD^+, 0.2 mM thiamine pyrophosphate (TPP), 0.13 mM coenzyme A (CoA), and 1 mM cysteine. The reaction was started by the addition 4 mM sodium pyruvate, and followed at 340 nm at 30°C (ε= 6.22 $mM^{-1}cm^{-1}$).

3.3.11.3 α-KETOGLUTARATE DEHYDROGENASE ASSAY

For ⍺-ketoglutarate dehydrogenase (α-KGDH) activity, brain cortical mitochondria (100 μg) were added to the reaction medium (25 mM KH_2PO_4, 5 mM $MgCl_2$, 2 mM KCN, 0.5 mM EDTA, 0.25% X-Triton, pH 7.25) supplemented with 10 mM $CaCl_2$, 2.5 μM rotenone, 0.2 mM of NAD^+, 0.3 mM TPP, 0.13 mM CoA, and 1 mM cysteine (Starkov et al., 2004). The reaction was started by adding 5 mM of α-ketoglutarate, and the reduction of NAD^+ was followed at at 30°C (ε= 6.22 $mM^{-1}cm^{-1}$).

3.3.11.4 MALATE DEHYDROGENASE ASSAY

Malate dehydrogenase (MDH) activity was determined by the addition of 0.6 mM oxaloacetic acid to the reaction mixture containing 100 mM potassium phosphate (pH 7.4), 0.2 mM NADH and 100 μg of brain cortical mitochondria, at 30°C (Robinson et al., 1987). Changes in absorbance were monitored at 340 nm (ε= 6.22 $mM^{-1}cm^{-1}$).

3.3.11.5 ISOCITRATE DEHYDROGENASE ASSAY

Isocitrate dehydrogenase (IDH) activity was measured spectrophotometrically at 340 nm at 30°C (Robinson et al., 1987). Briefly, brain cortical mitochondria (100 µg) were added to the reaction medium (50 mM Tris, 1 mM $MnCl_2$, 0.5 mM EDTA, pH 7.4) supplemented with 0.25 mM $NADP^+$. The reaction was started by adding 1.6 mM isocitrate (ε= 6.22 $mM^{-1}cm^{-1}$).

3.3.11.6 SUCCINATE DEHYDROGENASE ASSAY

Succinate dehydrogenase activity was assayed by adding brain cortical mitochondria (100 µg) to the reaction medium (100 mM Tris-HCl pH 7.5) supplemented with 0.5 mM EDTA, 2 µM antimycin A, 2 µM rotenone, 10 mM sodium azide and 0.25mM nitroblue tetrazolium (NBT). The reaction was started with 20 mM succinate and the absorbance monitored at 500 nm at 37°C for 60 minutes (ε= 21 $mM^{-1}cm^{-1}$) (Munujos et al., 1993).

3.3.12 ANALYSIS OF GLYCOLYTIC ENZYMES ACTIVITIES

3.3.12.1 LACTATE DEHYDROGENASE ASSAY

Lactate dehydrogenase (LDH) activity was measured spectrophotometrically as described by Bergmeyer and Bernt (1974), which follows the conversion of NADH to NAD^+. Briefly, 100 µg of brain cortical homogenate was added to the reaction medium (0.2 mM NADH and 0.76 mM pyruvate in Tris-NaCl; pH 7.2). Changes in absorbance were monitored at 340 nm at 30 °C (ε= 6.22 $mM^{-1}cm^{-1}$).

3.3.12.2 HEXOKINASE ASSAY

Hexokinase activity was determined by adding 300 µg of brain cortical homogenate to the reaction medium [10 mM $MgCl_2$, 216 mM glucose, 1.2 mM

nicotinamide adenine dinucleotide phosphate (NADP$^+$), 1.1 mM ATP, and 2 U glucose-6-phosphate dehydrogenase in 50 mM Tris–HCl (pH 8)], and following the production of NADPH at 340 nm, 25°C (ε= 6.22 mM^{-1}cm^{-1}) (Leong et al., 1981).

3.3.12.3 GLUCOSE-6-PHOSPHATE DEHYDROGENASE ASSAY

Glucose-6-phosphate dehydrogenase activity was determined by measuring the rate of NADPH production according to Lohr and Waller (1974). Briefly, brain cortical homogenates (25 µg) were added to the reaction medium [5 mM MgCl$_2$, 0.3 mM NADP, and 10 mM glucose-6-phosphate in 50 mM Tris-HCl (pH 7.5)]. NADPH production was continuously monitored at 340 nm, 25°C (ε= 6.22 mM^{-1}cm^{-1}).

3.3.13 OXIDATIVE STRESS EVALUATION

3.3.13.1 NITRITE LEVELS

The levels of nitrite, an indicator of NO$^\bullet$ production, were estimated using the Griess reagent (Green et al., 1981). Brain cortical homogenates (0.1 mg) were added to the Griess reagent (0.1% N-(1-naphthyl) ethylenediamine dihydrochloride, 1% sulfanilamide, and 2.5% phosphoric acid), and the absorbance was determined spectrophotometrically at 540 nm. Nitrite concentration was calculated using a standard curve for sodium nitrite and expressed as µM/mg protein.

3.3.13.2 HYDROGEN PEROXIDE PRODUCTION RATE

H$_2$O$_2$ levels were measured fluorimetrically using a modification of the method described by Barja (1999). Briefly, brain cortical mitochondria (0.2 mg) were incubated at 37°C in 1.5 ml of phosphate buffer, pH 7.4, containing 0.1 mM EGTA, 5 mM KH$_2$PO$_4$, 3 mM MgCl$_2$, 145 mM KCl, 30 mM Hepes, 0.1 mM homovalinic acid and 6 U/ml

horseradish peroxidase. After 15 minutes, the reaction was stopped with 0.5 ml cold stop solution (0.1 M glycine, 25 mM EDTA-NaOH, pH 12). Fluorescence was determined at 312 nm excitation and 420 nm emission wavelengths. The H_2O_2 levels were calculated using a standard curve of H_2O_2 and expressed as pmol/mg protein/15 minutes.

3.3.13.3 THIOBARBITURIC ACID REACTIVE SUBSTANCES LEVELS

Thiobarbituric acid reactive substances (TBARS) levels were determined by using the thiobarbituric acid assay (TBA), according to a modified procedure described by Ernster and Nordenbrand (1967). 0.5 mg of protein was added to 1 ml of reaction medium (175 mM KCl, 10 mM Tris-HCl; pH 7.4) and incubated at 30°C, during 15 minutes, with constantly stirring. After that period the reaction was stopped with 0.5 ml of tricarboxylic acid 40% and 2 ml of TBA 0.67% and the mixture was boiled during 15 minutes. Before reading at 530 nm, the mixture was centrifuged for 7 minutes at 4000 rpm. The measures were made against blanks prepared similarly but in the absence of protein. The amount of TBARS formed was calculated using a ε of 1.56 x 10^5 mol^{-1} cm^{-1} and expressed as nmol TBARS/mg protein.

3.3.13.4 MALONDIALDEHYDE LEVELS

Malondialdehyde (MDA) levels were determined by high-performance liquid chromatography (HPLC) (Wong et al., 1987). Liquid chromatography was performed using a Gilson HPLC apparatus with a reverse phase column (RP18 Spherisorb, S5 OD2). The samples were eluted from the column at a flow rate of 1 ml/min and detection was performed at 532 nm. The MDA content of the samples was calculated from a standard curve prepared using the thiobarbituric acid-MDA complex and was expressed as nmol/mg protein.

3.3.14 ANTIOXIDANT DEFENSES EVALUATION

3.3.14.1 NON-ENZYMATIC ANTIOXIDANT DEFENSES

3.3.14.1.1 GLUTATHIONE AND GLUTATHIONE DISULFIDE LEVELS

Glutathione (GSH) and glutathione disulfide (GSSG) levels were determined with fluorescence detection after reaction of the supernatant containing H_3PO_4/NaH_2PO_4-EDTA or $H_3PO_4/NaOH$, respectively, of the deproteinized mitochondria solution with *o*-phthalaldehyde (OPT), pH 8.0, according to Hissin and Hilf (1976). In brief, 0.5 mg of each sample was resuspended in 1.5 ml phosphate buffer (100 mM NaH_2-PO_4, 5 mM EDTA, pH 8.0) and 500 μl H_3PO_4 4.5% were rapidly centrifuged at 50000 rpm (Beckman, TL-100 Ultracentrifuge) for 30 minutes. For GSH determination, 100 μl of supernatant was added to 1.8 ml phosphate buffer and 100 μl OPT. After thorough mixing and incubation at room temperature for 15 minutes, the solution was transferred to a quartz cuvette and the fluorescence was measured at 420 nm and 350 nm emission and excitation wavelengths, respectively. For GSSG determination, 250 μl of the supernatant were added to 100 μl of *N*-ethylmaleymide and incubated at room temperature for 30 minutes. After the incubation, 140 μl of the mixture were added to 1.76 ml NaOH (100 mM) buffer and 100 μl OPT. After mixing and incubation at room temperature for 15 minutes, the solution was transferred to a quartz cuvette and the fluorescence was measured at 420 nm and 350 nm emission and excitation wavelengths, respectively. The GSH and GSSG contents were determined from comparisons with a linear GSH or GSSG standard curve, respectively.

3.3.14.1.2 VITAMIN E CONTENT

Extraction and separation of vitamin E (α-tocopherol) from brain mitochondria were performed by following a previously described method by Vatassery and Younoszai

(1978). Briefly, 1.5 ml sodium dodecyl sulfate (10 mM) was added to 0.5 mg freshly isolated brain mitochondria, followed by the addition of 2 ml ethanol. Then 2 ml hexane and 50 μl of KCl 3M were added, and the mixture was vortexed for about 3 min. The extract was centrifuged at 2000 rpm (Sorvall RT6000 Refrigerated Centrifuge) and 1 ml of the upper phase, containing n-hexane (n-hexane layer), was recovered and evaporated to dryness under a stream of N_2 and kept at -80°C. The extract was dissolved in n-hexane, and vitamin E content was analyzed by reverse-phase HPLC. A Spherisorb S10w column (4.6 x 200 nm) was eluted with n-hexane modified with 0.9% methanol, at a flow rate of 1.5 ml/min. Detection was performed by an UV detector at 287 nm. The levels of vitamin E were calculated as nmol/mg protein.

3.3.14.2 ENZYMATIC ANTIOXIDANT DEFENSES

3.3.14.2.1 GLUTATHIONE PEROXIDASE ACTIVITY

Glutathione peroxidase (GPx) activity was determined spectrophotometrically at 340 nm by following the method of Flohé and Günzler (1984). Briefly, the activity of GPx was measured upon 5 minutes of incubation, in the dark, of 0.1 mg of each sample with 0.5 mM phosphate buffer (0.25 M KH_2PO_4, 0.25 M K_2HPO_4 and 0.5 mM EDTA, pH 7.0), 0.5 mM EDTA, 1 mM GSH and 2.4 U/ml glutathione reductase (GRed). The quantification occurred after the addition of 0.2 mM NADPH and 1.2 mM *tert*-butyl hydroperoxide, at 30°C with continuous magnetic stirring, for 5 minutes, in a Jasco V560 UV/VIS Spectrophotometer. The measurements were made against blanks prepared in the absence of NADPH. GPx activity was determined using the ε 6.22 mM^{-1} cm^{-1} and expressed as nmol/min/mg protein.

3.3.14.2.2 GLUTATHIONE DISULFIDE REDUCTASE ACTIVITY

For the activity of glutathione disulfide reductase (GRed), 0.1 mg of the sample was incubated for 1 minute with 0.2 mM phosphate buffer (containing 0.2 M K_2HPO_4 and 2 mM EDTA, pH 7.0) and 2 mM NADPH. The measurements were made at 340 nm and initiated with the addition of 20 mM GSSG, at 30°C, with continuous magnetic stirring, for 4 minutes, against blanks prepared in the absence of GSSG, using a Jasco V560 UV/VIS Spectrophotometer (Carlberg and Mannervik, 1984). GRed activity was determined using the molar extinction coefficient ε 6.22 mM^{-1} cm^{-1} and expressed as nmol/min/mg protein.

3.3.14.2.3 CATALASE ACTIVITY

Catalase activity was assayed by the method of Claiborne (1985). Briefly, the assay mixture consisted of 50 mM phosphate buffer (pH 7.0), 19 mM H_2O_2, and 0.1 mg of each sample. The change in absorbance was recorded at 240 nm, using a Jasco V560 UV/VIS Spectrophotometer. Catalase activity was calculated as nmol H_2O_2 consumed/min/mg protein using the ε of 4.36 mM^{-1} cm^{-1}.

3.1.15 DETERMINATION OF Aβ LEVELS

Cortical and hippocampal $A\beta_{1-42}$ levels were assayed using sensitive ELISA detection kits, following the manufacturer's instructions (Invitrogen). Levels of $A\beta_{1-42}$ were expressed in pg/mg protein as deduced from the appropriate standard curve run in parallel with the assay.

3.1.16 HIF-1α ACTIVATION

The determination of HIF-1α activation was performed as described in 3.1.8. However, in this case, brain cortical and hippocampal homogenates were used.

3.1.17 WESTERN BLOT ANALYSIS

Brain cortical and hippocampal samples were homogenized in RIPA buffer (150 mm NaCl, 0.1% sodium dodecyl sulfate (SDS), 1% sodium deoxycholate (DOC), 1% nonyl phenoxypolyethoxylethanol (NP-40), 50 mm Tris, pH 7.4) containing 0.1 M PMSF, 0.2 M DTT, and proteases and phosphatases inhibitors (Roche Applied Science). The crude homogenate was incubated on ice for 15 minutes, frozen and defrozen 3 times to favor disruption, centrifuged at 14000 rpm (Eppendorf centrifuge 5415C) for 10 minutes, at 4°C, and the resulting supernatant collected and stored at -80°C. The amount of protein content in the samples was analyzed by the bicinchoninic acid (BCA) protein assay using the BCA kit (Pierce Thermo Fisher Scientific, Rockford, IL). The Western blot procedure was conducted as described in 3.1.9. The antibodies used are listed in Table 3.3.

TABLE 3.3. LIST OF PRIMARY AND SECONDARY ANTIBODIES USED IN THE *IN VIVO* STUDIES

ANTIBODY	CATALOG #	SUPPLIER	HOST SPECIE	DILUTION
Anti-DRP1	611113	BD Biosciences	Mouse	1:1000 (WB)
Anti-Fis1	IMG-5113A	ImGenex	Rabbit	1:750 (WB)
Anti-Mfn1 (H-65)	sc-50330	Santa Cruz	Rabbit	1:1000 (WB)
Anti-Mnf2	sc-100560	Santa Cruz	Mouse	1:1000 (WB)
Anti-MTCO1	ab14705	Abcam	Rabbit	1:1000 (WB)
Anti-OPA1	612607	BD Biosciences	Mouse	1:1000 (WB)
Anti-PGC-1	sc-13067	Santa Cruz	Rabbit	1:1000 (WB)
Anti-TFAM	sc-23588	Calbiochem	Goat	1:1000 (WB)
Anti-NRF-1	sc-33771	Sigma	Rabbit	1:1000 (WB)
Anti-NRF-2	ab31163	Abcam	Rabbit	1:1000 (WB)
Anti-p-Tau (Ser 396)	sc101815	Santa Cruz	Rabbit	1:750 (WB)
Anti-Tau	MN1010	Thermo Scientific	Mouse	1:1000 (WB)
Anti-β-actin	A-5441	Sigma	Mouse	1:5000 (WB)
Anti-NeuN	MAB377	Millipore	Mouse	1:200 (IHC)
Anti-GFAP	AB5804	Chemicon	Rabbit	1:500 (IHC)
Alexa Fluor 488 anti-rabbit IgG conjugate	A-11005	Molecular Probes	Goat	1:200 (IHC)
Alexa Fluor 594 anti-mouse IgG conjugated	A-11008	Molecular Probes	Goat	1:200 (IHC)
Anti-mouse IgG alkaline phosphatase conjugate	NIF1316	Amersham Pharmacia Biotech	Goat	1:20000 (WB)
Anti-rabbit IgG alkaline phosphatase conjugate	NIF1317	Amersham Pharmacia Biotech	Goat	1:20000 (WB)

WB - WESTERN BLOT

IHC - IMMUNOHISTOCHEMISTRY

3.1.18 IMMUNOHISTOCHEMISTRY

Hemibrain tissue was rinsed in a saline solution and fixed in formalin, at 4°C, overnight. Following fixation, tissue was dehydrated in ethanol gradient, embedded in paraffin wax, and serial sagital sections of 6-μm thickness were obtained. For immunohistochemical staining, tissue sections were deparaffinized in xylene, and rehydrated in a series of graded ethanol. Non-specific binding sites were blocked with 10% normal goat serum during 1 hour. Thereafter, sections were incubated with primary antibodies, at 4°C, for 16 hours. Then, brain sections were stained with secondary antibodies conjugated with Alexa Fluor and the nuclei were counterstained with DAPI. Finally, sections were treated with Dako Cytomation Fluorescent mounting solution on a microscope slide. The antibodies used are listed in Table 3.3.

3.3.19 ELECTRON MICROSCOPY

Mitochondrial pellets obtained after Ca^{2+} experiments or brain cortical and hippocampal tissue were fixed overnight with 3% glutaraldehyde in 0.1 M phosphate buffer (pH 7.3), at 4°C, post-fixed with 1% osmium tetroxide, dehydrated, and embedded in Spurr. Sections were cut on a LKB ultramicrotome Ultrotome III, and stained with a methanolic solution of uranyl acetate plus lead citrate. Electron micrographs were obtained using a Jeol Jem-100SV electron microscope operated at 80 kV.

3.2.20 STATISTICAL ANALYSIS

Results are presented as mean ± SEM of the indicated number of animals/experiments. Statistical significance was determined using the unpaired two-

tailed student t-test or the one-way ANOVA test for multiple comparisons, followed by

the posthoc Tukey- Kramer test.

Chapter 3

88

CHAPTER 4

MITOCHONDRIAL ROS, HIF-1α AND THE PROTECTIVE ROLE

OF CYANIDE PRECONDITIONING

4.1. ABSTRACT

The current study was undertaken to address the role of ROS, and HIF-1α signaling pathway in the protection against high glucose levels in brain endothelial and NT2 neuron-like cells. RBE4 treated with non-toxic concentrations of cyanide ($\leq$ 1 µM; 1 hour) exhibited an increase in ROS levels, particularly H_2O_2. Cyanide also induced a modest mitochondrial depolarization, an increase in oxygen consumption and a structural (smaller mitochondria) and spatial (perinuclear region) reorganization of the mitochondrial network. The stabilization and nuclear activation of HIF-1α in the presence of cyanide was also observed, which resulted in an increase in vascular endothelial growth factor (VEGF), endothelial nitric oxide synthase (eNOS) and EPO protein levels reflecting an adaptive response. Importantly, preconditioning induced by cyanide protected brain endothelial cells against high glucose-mediated damage by the prevention of apoptotic cell death. In NT2 ρ0 cells, cyanide (0.1 µM) was unable to stimulate ROS production and, consequently, protect against glucotoxicity. Conversely, in NT2 cells, the parental cells with functional mitochondria, cyanide significantly increased ROS levels protecting against high glucose-induced neuronal cell loss and activation of caspase-3. The free radical scavenger NAC and the specific HIF-1α inhibitor 2-ME2 completely abolished the protective effects of cyanide preconditioning. Altogether our results demonstrate that mitochondrial preconditioning induced by cyanide triggered a protective response mediated by mitochondrial ROS and HIF-1α activation and signaling, which render brain endothelial and neuronal cells resistant against glucotoxicity.

4.2. INTRODUCTION

Diabetes mellitus is one of the most prevalent metabolic disorders that affects approximately 250 million people worldwide (Cole et al., 2007) and is associated with cognitive deterioration and changes in cerebral anatomy in humans (Biessels et al., 2006, 2008). Indeed, mild-to-moderate impairments of cognitive function have been reported in both T1D and T2D patients (Awad et al., 2004; Biessels et al., 2008). T1D, characterized by a deficit in the production of insulin by the pancreatic β cells, increases cognitive dysfunction and decreases the speed of mental processing (Brands et al., 2005). T2D, which presents as major pathological features peripheral insulin resistance and chronic hyperglycemia, is related with a faster rate in the decline of cognition in comparison with the general population (Allen et al., 2004). In addition, hemoglobin A1c level, a marker of the long-term hyperglycemia, was shown to correlate with cognitive decline in humans (MacLullich et al., 2004). In fact, chronic hyperglycemia has also been proposed to be one of the determinants of diabetes-related cognitive dysfunction by inducing structural and neurochemical abnormalities in the brain and thus, leading to the development of diabetic end-organ damage to the brain (Biessels et al., 2002; Gispen and Biessels, 2000; Kumagai, 1999; Mankovsky et al., 1996).

Preconditioning is a well accepted phenomenon, in which small doses of a noxious stimulus are required to afford robust protective responses against future injury (Correia et al., 2010b). Although the molecular mechanisms underlying the induction and maintenance of preconditioning-induced brain tolerance are complex and remain largely unclear, mitochondrial-centered mechanisms have been proposed to be critical mediators of the preconditioning response (Busija et al., 2008). In fact, compelling evidence indicates that a slight rise of mitochondrial ROS triggers preconditioning-

mediated brain tolerance, suggesting a role for mitochondria on endogenous neuroprotection (Correia et al., 2010b; Dirnagl et al., 2009; Jou, 2008). Conversely, the induction of the hypoxia signaling pathway with the concomitant stabilization and transcriptional activation of the transcription factor HIF-1α has emerged as one of the major cellular pathways responsible for preconditioning-induced neuroprotection (Sharp et al., 2004). HIF-1 is a heterodimeric protein composed of a constitutively expressed HIF-1β subunit and an inducible HIF-1α subunit. Under hypoxic conditions, HIF-1α translocates to the nucleus and recruits HIF-1β, modulates the expression of a wide range of protective genes involved in angiogenesis, metabolism, apoptosis and cell survival, including EPO, VEGF and eNOS (Correia and Moreira, 2010). Additionally, HIF-1α activation seems to be strictly bound to mitochondrial function. Indeed, under hypoxic conditions, mitochondria act as oxygen sensors and convey signals to HIF-1, mitochondrial ROS being the putative signaling molecules between a cellular O_2-sensor and HIF-1 (Correia et al., 2010a, 2010b).

Given the wide scientific evidence that highlights mitochondria as the key regulators of preconditioning (Correia et al., 2010a, 2010b; Correia and Moreira, 2010), we hypothesized that mitochondrial preconditioning induced by cyanide (hereafter called cyanide preconditioning) may afford protection against glucotoxicity by modulating mitochondrial function and network organization and induction of HIF-1α signaling pathway. In the present study, we demonstrated that cyanide preconditioning is effective in protecting both brain endothelial and NT2 neuron-like cells against high glucose-induced damage. Additionally, the cytoprotective effects of cyanide preconditioning are reliant on functional mitochondria, mitochondrial ROS generation and induction of HIF-1α signaling pathway. Elucidation of the role of the mitochondrial

ROS and HIF-1α in the protective mechanisms triggered by preconditioning may offer new avenues for the treatment of diabetes-associated neuronal and endothelial dysfunction.

4.3. RESULTS

4.3.1. CYANIDE STIMULATES MITOCHONDRIAL ROS PRODUCTION IN BRAIN ENDOTHELIAL CELLS WITHOUT AFFECTING CELL VIABILITY

RBE4 cells were subjected to increasing concentrations of cyanide, a specific inhibitor of mitochondrial COX, to stimulate mitochondrial ROS generation. As shown in Fig. 4.1, concentrations of cyanide higher than 0.01 μM significantly increase ROS levels (Fig. 4.1A), particularly H_2O_2 levels (Fig. 4.1B). The free radical scavenger NAC abrogates the increase in ROS levels induced by cyanide (Fig. 4.1A). Interestingly, we observed that all the concentrations of cyanide tested (0.01-1 μM) do not significantly affect either cell viability (Fig. 4.2A) or membrane integrity (Fig. 4.2B). Other mitochondrial modulators were also tested, namely rotenone and antimycin A. Similarly to cyanide, rotenone and antimycin A increase ROS levels without interference with cell viability (data not shown). However, cyanide revealed to be the most efficient mitochondrial modulator.
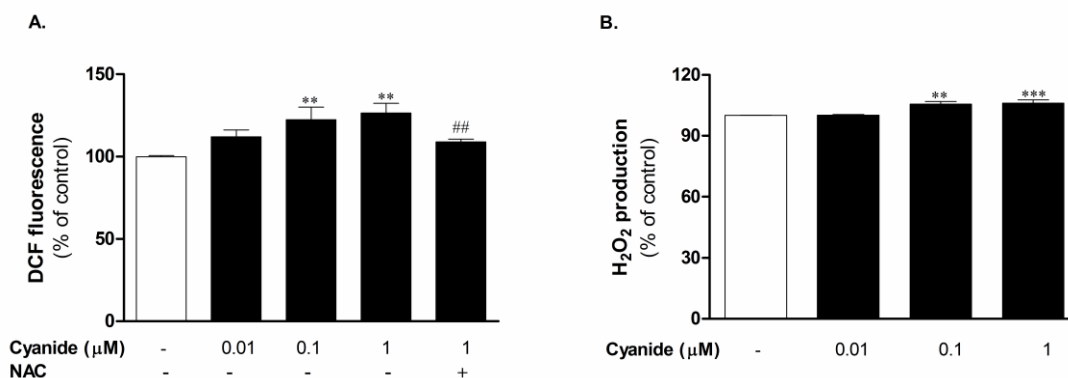
Figure 4.1. Effect of cyanide on intracellular ROS (A) and H$_2$O$_2$ (B) levels in RBE4 cells. Cells were incubated with cyanide (0.01 - 1 µM) for 1 hour at 37°C. ROS production was measured using the H$_2$DCF-DA probe, as described in Material and Methods section. In some experiments cells were pre-treated with the ROS scavenger NAC (200 µM) for 24 hours before mitochondrial modulator exposure. Data are expressed as mean ± SEM of 5-6 independent experiments, performed in triplicate. ** $p<0.01$; *** $p<0.001$ when compared with untreated cells. ## $p<0.01$ when compared with the highest concentration of cyanide.
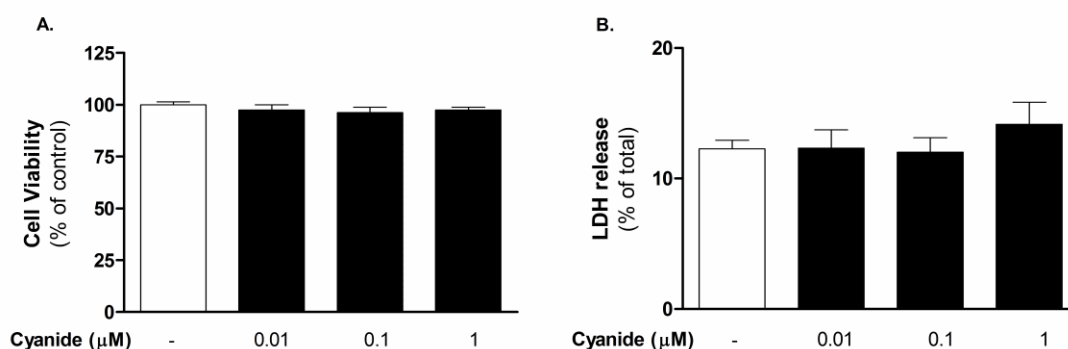
Figure 4.2. Effect of cyanide on RBE4 cells viability. Cells were incubated with increasing concentrations of cyanide (0.01 - 1 µM) for 1 hour at 37°C. Cell viability was determined by following the changes in cell reduction capacity by the Alamar Blue assay **(A)** or by the analysis of plasma membrane integrity through the analysis of LDH release **(B)**. Data are expressed as mean ± SEM of 5-6 independent experiments, performed in triplicate.

4.3.2. Cyanide Induces A Modest Mitochondrial Depolarization And Accelerates Oxygen Consumption In Brain Endothelial Cells

To look more closely at the effect of cyanide on the functioning of mitochondria, we measured $\Delta\Psi_m$ and basal oxygen consumption as well as FCCP-stimulated maximal oxygen consumption. Figure 4.3 shows that 1 µM cyanide causes a modest but significant decrease of $\Delta\Psi_m$. Moreover, RBE4 cells submitted to 0.01 and 1 µM cyanide present a higher rate of basal oxygen consumption in comparison with non-treated cells (Fig. 4.4A). However, for these cyanide concentrations the maximal respiratory capacity remains unaltered (Fig. 4.4B). However, concentrations of cyanide above 1 µM induce a significant decrease of both basal and FCCP-stimulated maximal oxygen consumption (Figs. 4.4A and 4.4B). These findings could be explained by the fact that approximately 60% inhibition of COX is necessary to induce a decrease of cellular respiration (Leavesley et al., 2008). Furthermore, a marked increase in oxygen consumption under conditions of enhanced ROS generation has been attributed to dismutase reactions (Martinez-Redondo et al., 2010).
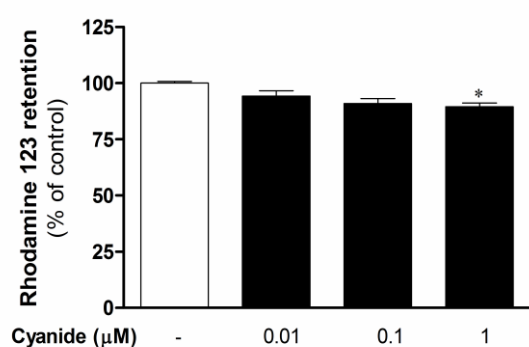
Figure 4.3. Effect of cyanide on mitochondrial membrane potencial in RBE4 cells. Cells were incubated with cyanide (0.01 - 1 µM) for 1 hour at 37°C. Mitochondrial membrane potential was expressed as the percentage of control cells. Data are expressed as mean ± SEM of 5-6 independent experiments, performed in triplicate.* $p < 0.05$ when compared with untreated cells.
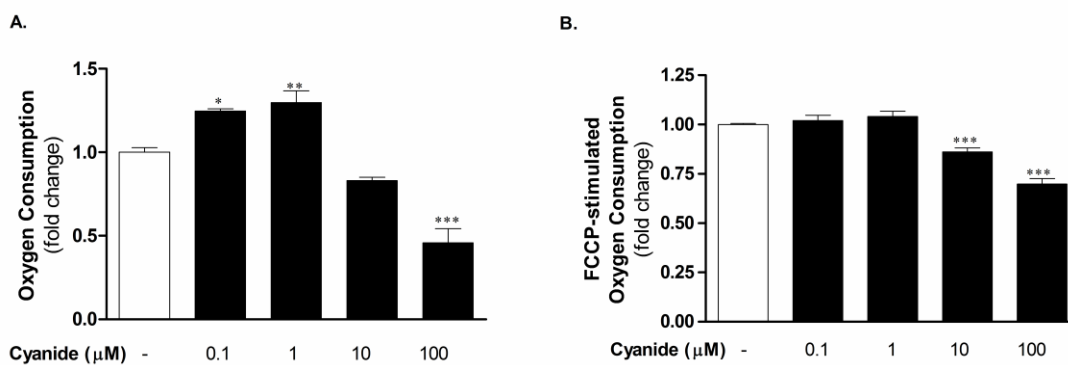
Figure 4.4. Effect of cyanide on mitochondrial oxygen consumption in RBE4 cells. Basal oxygen consumption **(A)** and FCCP-stimulated maximal oxygen consumption **(B)** were monitored at 37°C, in the absence or presence of cyanide (0.1 - 100 μM). Data are expressed as mean ± SEM of 3 independent experiments, performed in triplicate. * $p<0.05$; ** $p<0.01$; *** $p<0.001$ when compared with untreated cells.

4.3.3. Cyanide Induces Spatial And Structural Mitochondrial Network Reorganization In Brain Endothelial Cells

In order to ascertain whether cyanide influences mitochondrial network, we next determined the sequence of changes on mitochondrial distribution and morphology. As seen in Fig. 4.5, non-treated RBE4 cells contain mostly long tubular mitochondria, distributed evenly throughout the whole cell. Cyanide induces a fast alteration in the spatial distribution of mitochondria. Indeed, an asymmetric perinuclear distribution of smaller (fragmented) mitochondria is observed in RBE4 cells treated with both concentrations of cyanide (Fig. 4.5). These alterations in mitochondrial network are suppressed by NAC pre-treatment, implying a role for ROS in this phenomenon (Fig. 4.5).
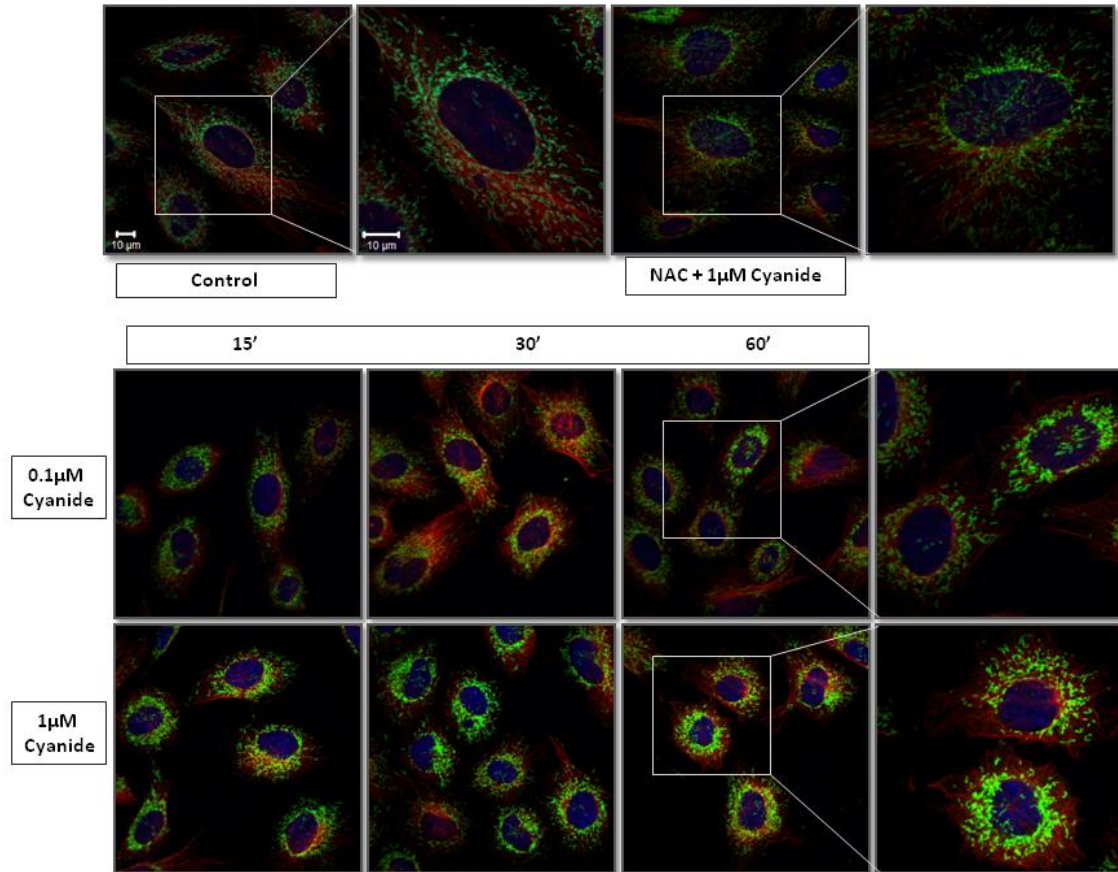
Figure 4.5. Temporal effect of cyanide on mitochondrial network in RBE4 cells. Cells were treated with cyanide (0.1 - 1 µM) for different periods of time (15, 30 and 60 minutes), stained for TOM20 (green) and α-Tubulin (red), and visualized by confocal microscopy. In some experiments cells were pre-treated with the ROS scavenger NAC (200 µM) for 24 hours, before exposure to cyanide during 1 hour. Images are representative of three independent experiments.

4.3.4. CYANIDE PROMOTES HIF-1α EXPRESSION AND ACTIVITY IN BRAIN ENDOTHELIAL CELLS

Since one of the key cellular targets of mitochondrial ROS is the stress response mediated by the transcription factor HIF-1α, we then investigated whether cyanide treatment affects HIF-1α expression and activity as well as the protein levels of HIF-1α-responsive genes: EPO, VEGF and eNOS. Western blot analyses show that the exposure of brain endothelial cells to cyanide for 1 hour results in a rapid activation and up-regulation of HIF-1α protein levels (Fig. 4.6) when compared with non-treated cells (control cells). Cyanide also promotes a significant increase in EPO, VEGF and eNOS protein levels when compared with control cells (Figs. 4.6B and 4.6C). Cells exposed to $CoCl_2$ for 4 hours were used as a positive control, since it has been reported that $CoCl_2$ stabilizes HIF-1α and induces HIF-1 responsive genes. Consistently, cyanide exposure also significantly enhances HIF-1α activation in nuclear extracts compared with non-treated cells (Fig. 4.6A). The effects of cyanide on HIF-1α stabilization and EPO expression were abrogated in the presence of NAC (Fig. 4.6C), further indicating a role for mitochondrial ROS in HIF-1α activation.

A.

B.
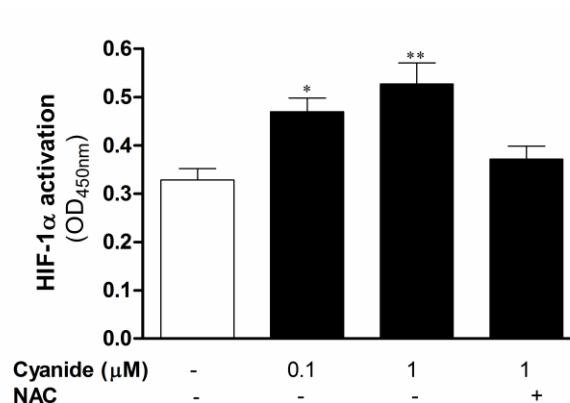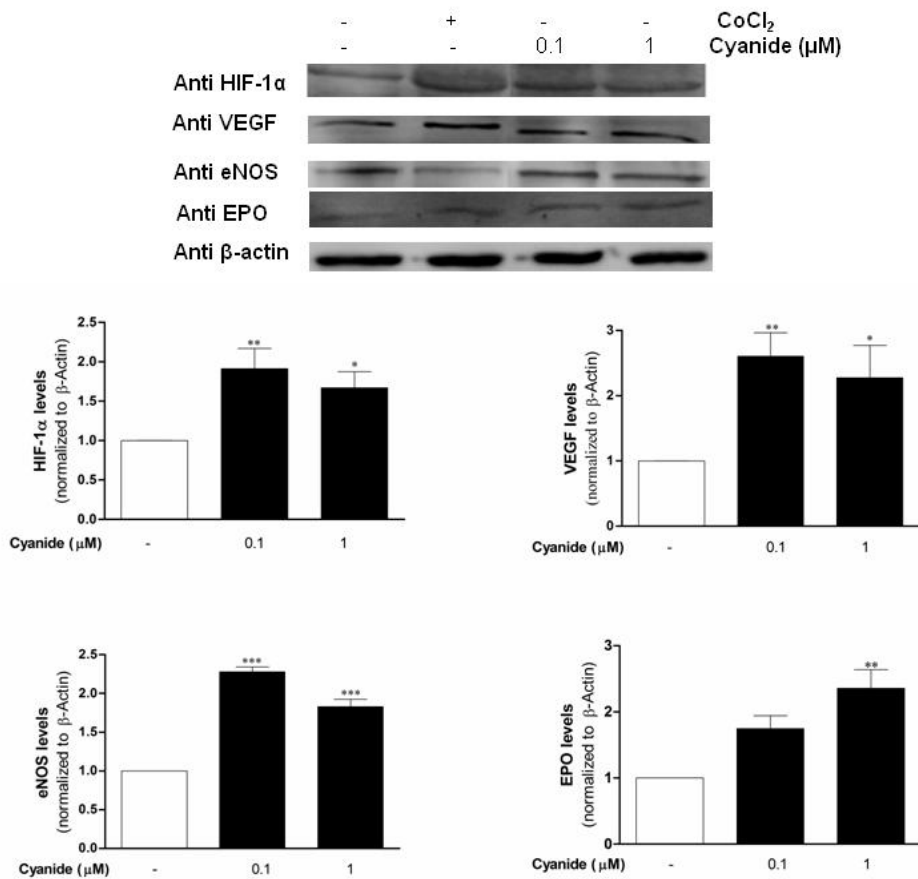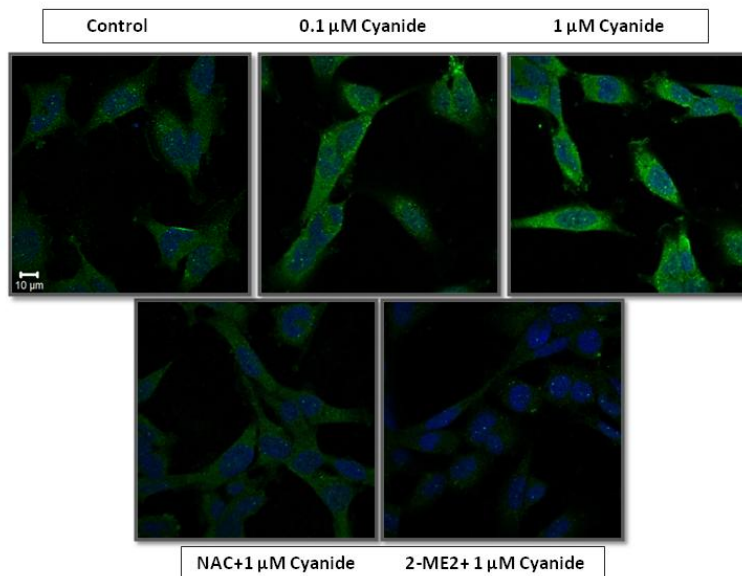
Figure 4.6. Effect of cyanide on nuclear HIF-1α activation and HIF-1α, VEGF, eNOS and EPO protein levels in RBE4 cells. Cells were incubated with cyanide (0.1 or 1 μM) for 1 hour at 37°C. Cells exposed to CoCl$_2$ for 4 hours were used as positive control. Detection of HIF-1α DNA binding by ELISA **(A)**. Western blot analyses of HIF-1α, VEGF, eNOS and EPO protein levels **(B)**. Immunostaining for EPO (green) visualized by confocal microscopy **(C)**. Data in the graph are expressed as mean ± SEM of 3 independent experiments. * p<0.05; ** p<0.01; *** p<0.001 when compared with control cells.

4.3.5. CYANIDE PRECONDITIONING AVOIDS BRAIN ENDOTHELIAL CELLS' MEMBRANE DISRUPTION AND LOSS OF VIABILITY PROMOTED BY HIGH GLUCOSE

As shown in Fig. 4.7, incubation of cells with 30 mM glucose for 12 hours resulted in a significant decrease in cell viability and increase in LDH release when compared with control cells, indicating that this concentration of glucose is toxic to brain endothelial cells. As expected, cells exposed to equimolar concentrations of mannitol (30 mM - osmotic control) did not present significant differences in cell viability and LDH release when compared with control cells (data not shown). On the other hand, it was observed that cyanide preconditioning attenuates high glucose-induced RBE4 cell viability loss and decreases LDH release (Fig. 4.7). Pre-treatment with NAC abrogates the protective effects of cyanide preconditioning against high glucose-induced loss of cell viability and membrane integrity (Fig. 4.7).

Figure 4.7. Effect of high glucose levels and cyanide preconditioning on RBE4 cells viability. Cells were pre-incubated with cyanide for 1 hour and then exposed to high levels of glucose (30 mM) during 12 hours. Cell viability was determined by following changes in cell reduction capacity by the Alamar Blue assay **(A)** or by the analysis of plasma membrane integrity, evaluated by measuring the release of intracellular LDH **(B)**. In some experiments cells were pre-treated with the ROS scavenger NAC (200 µM) for 24 hours before cyanide preconditioning. Data are expressed as mean ± SEM of 5-6 independent experiments, performed in triplicate. * $p < 0.05$; ** $p < 0.01$; *** $p < 0.001$ when compared with untreated cells. # $p < 0.05$; ### $p < 0.001$ when compared with high glucose-treated cells. § $p < 0.05$ when compared with preconditioned cells.

4.3.6. Cyanide Preconditioning Suppresses The Activation Of The Apoptotic Pathway By Inhibiting BAX Translocation To Mitochondria And Caspase-3 Activation Induced By High Glucose Levels In Brain Endothelial Cells

Confocal microscopy analyses revealed that exposure of endothelial cells to 30 mM glucose increased the translocation of BAX to mitochondria (yellow fluorescence) when compared with control cells (Fig. 4.8C). However, the pre-incubation of cells with cyanide avoided the translocation of BAX to mitochondria promoted by glucose (Fig. 4.8C). Accordingly, Western blotting analyses of cytosolic and mitochondrial fractions showed an increase in BAX levels in mitochondrial fractions of cells exposed to high glucose levels, this effect being significantly attenuated in cells pre-incubated with cyanide (Fig. 4.8A and 4.8B).

To further verify the ability of cyanide preconditioning to protect against the activation of the apoptotic cascade induced by high glucose levels we analyzed caspase-3 activation, a crucial executor of apoptosis. As shown in Fig. 4.9, endothelial cells exposed to high levels of glucose presented a significant increase in caspase-3 activation when compared with control cells, this effect being avoided by cyanide pre-treatment.

A.

B.

C.
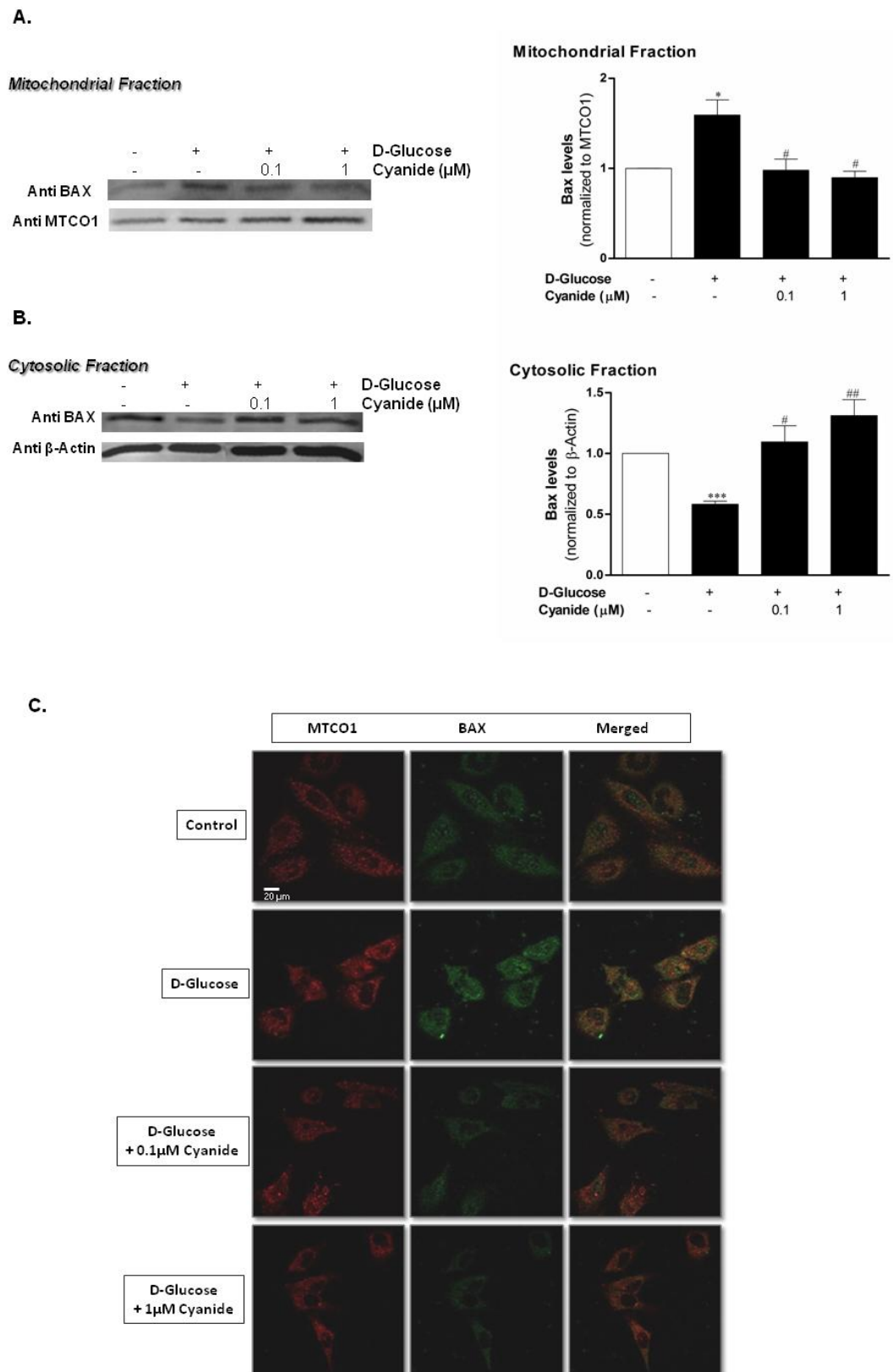
Figure 4.8. Effect of cyanide preconditioning on BAX translocation to mitochondria induced by high-glucose levels. RBE4 cells were pre-incubated with cyanide for 1 hour and then exposed to high levels of

glucose (30 mM) during a period of 12 hours. Western blot analyses of BAX levels in cytosolic **(A)** and mitochondrial **(B)** fractions. Double immunostaining for BAX (green) and MTCO1 (mitochondrial marker - red) visualized by confocal microscopy **(C)**. Data are the mean ± SEM of 3 independent experiments. * $p<0.05$; *** $p<0.001$ when compared with control cells. # $p<0.05$; ## $p<0.01$ when compared with high glucose-treated cells.
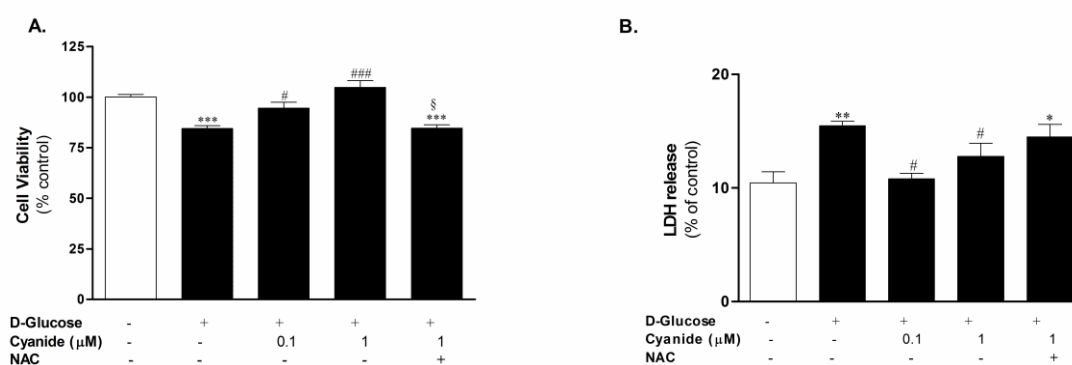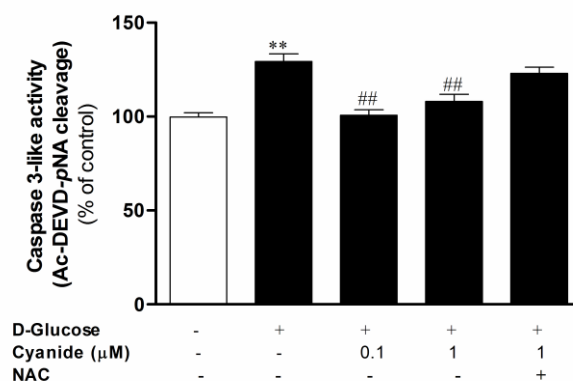

Figure 4.9. Effect of high glucose levels and cyanide preconditioning on caspase-3-like activity. RBE4 cells were incubated with cyanide for 1 hour and then exposed to high levels of glucose (30 mM) during a period of 12 hours. In some experiments cells were pre-treated with the ROS scavenger NAC (200 µM) for 24 hours before cyanide exposure. Caspase activity was measured as described in Material and Methods section. Data are expressed as mean ± SEM of 6 independent experiments, performed in triplicate. ** $p<0.01$ when compared with untreated cells. ## $p<0.01$ when compared with high glucose-treated cells.

4.3.7. FUNCTIONAL MITOCHONDRIA AND ROS PRODUCTION ARE REQUIRED FOR CYANIDE PRECONDITIONING-INDUCED PROTECTION AGAINST GLUCOTOXICITY IN NEURONAL CELLS

To demonstrate the requirement of a functional mitochondrial population in cyanide preconditioning-induced protection against high glucose insult, we performed similar experiments using native human teratocarcinoma NT2 cells and mitochondrial DNA-depleted NT2 ρ0 cells, without functional mitochondria. Cyanide significantly increased ROS production in NT2 cells (Figs. 4.10A and 4.10B), an effect that was not observed in NT2 ρ0 (Figs. 4.10C and 4.10D). Consequently, cyanide preconditioning was able to protect NT2 cells against high glucose-induced neuronal cell loss and activation

of caspase-3 (Figs. 4.11A and 4.11B) but incapable to protect NT2 ρ0 against the same toxic insult (Figs. 4.11C and 4.11D). The protective effects induced by cyanide were abrogated by the antioxidant NAC (Figs. 4.10A, 4.10B, 4.11A and 4.11B). These data indicate that both functional mitochondria and mitochondrial ROS are required for the effectiveness of cyanide preconditioning to protect against glucotoxicity.
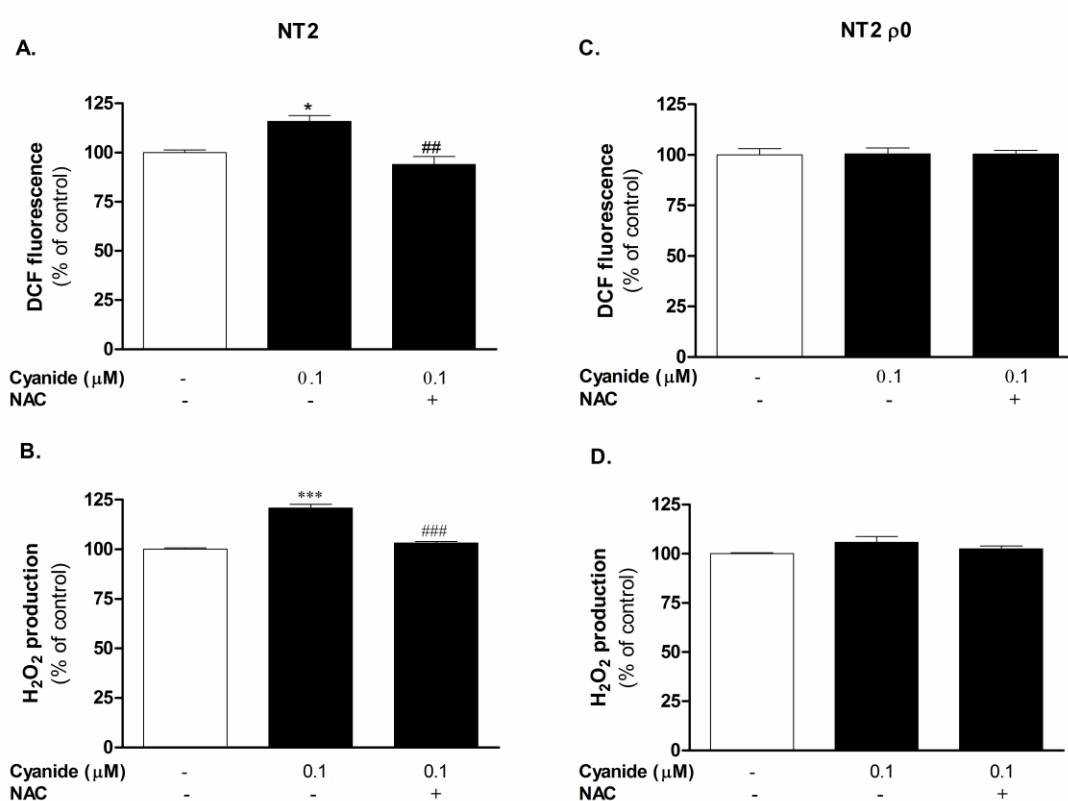
Figure 4.10. Effect of cyanide on intracellular ROS (A) (C) and H₂O₂ (B) (D) levels in NT2 and NT2 ρ0 cell lines. Cells were incubated with cyanide (0.1 μM) for 1 hour at 37°C. ROS production was measured using the H₂DCF-DA probe, as described in Material and Methods section. In some experiments cells were pre-treated with the ROS scavenger NAC (200 μM) for 24 hours before cyanide exposure. Data are expressed as mean ± SEM of 5-6 independent experiments, performed in triplicate. * $p < 0.05$; *** $p < 0.001$ when compared with untreated cells. ## $p < 0.01$; ### $p < 0.001$ when compared with cyanide-treated cells.
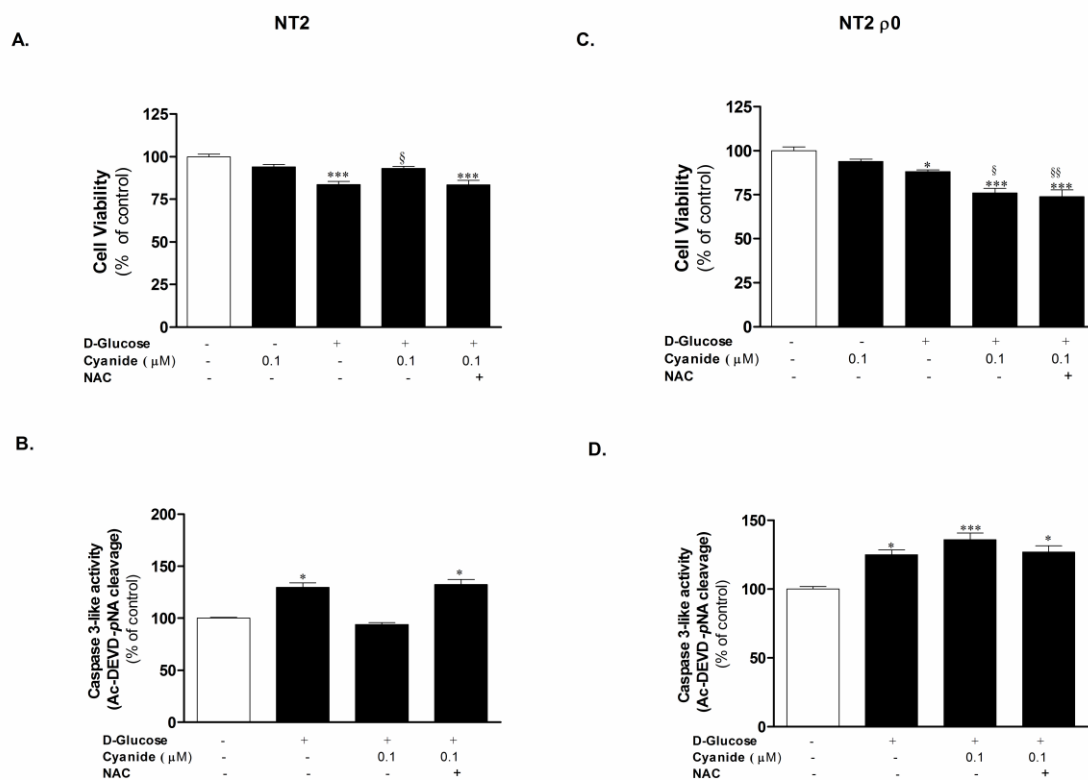
Figure 4.11. Effect of cyanide preconditioning and high glucose levels on NT2 and NT2 ρ0 cells viability and caspase-3-like activity. Cells were pre-incubated with cyanide for 1 hour and then exposed to high levels of glucose (30 mM) during a period of 12 hours. Cell viability was determined by following changes in cell reduction capacity by the Alamar Blue assay **(A) (C)**. Caspase 3 activity was measured as described in Material and Methods section **(B) (D)**. In some experiments cells were pre-treated with the ROS scavenger NAC (200 μM) for 24 hours before cyanide exposure. Data are expressed as mean ± SEM of 5-6 independent experiments, performed in triplicate. * $p<0.05$; *** $p<0.001$ when compared with untreated cells. § $p<0.05$; §§ $p<0.01$ when compared with high glucose-treated cells

### 4.3.8. 2-ME2, A HIF-1α INHIBITOR, ABOLISHES THE PROTECTIVE EFFECTS OF CYANIDE PRECONDITIONING

HIF-1α plays a central stage in preconditioning-induced protection. In a pharmacological approach, we used the HIF-1α inhibitor, 2-ME2, to elucidate the role of HIF-1α signaling pathway in cyanide preconditioning-mediated protection against the deleterious effects induced by high glucose exposure. As shown in Fig. 4.12, pre-treatment of cells with 2-ME2 completely abrogated the cyanide-induced protection

against cell loss and caspase-3 activation promoted by high glucose levels, in both RBE4 (Figs. 4.12A and 4.12B) and NT2 (Figs. 4.12C and 4.12D) cells.
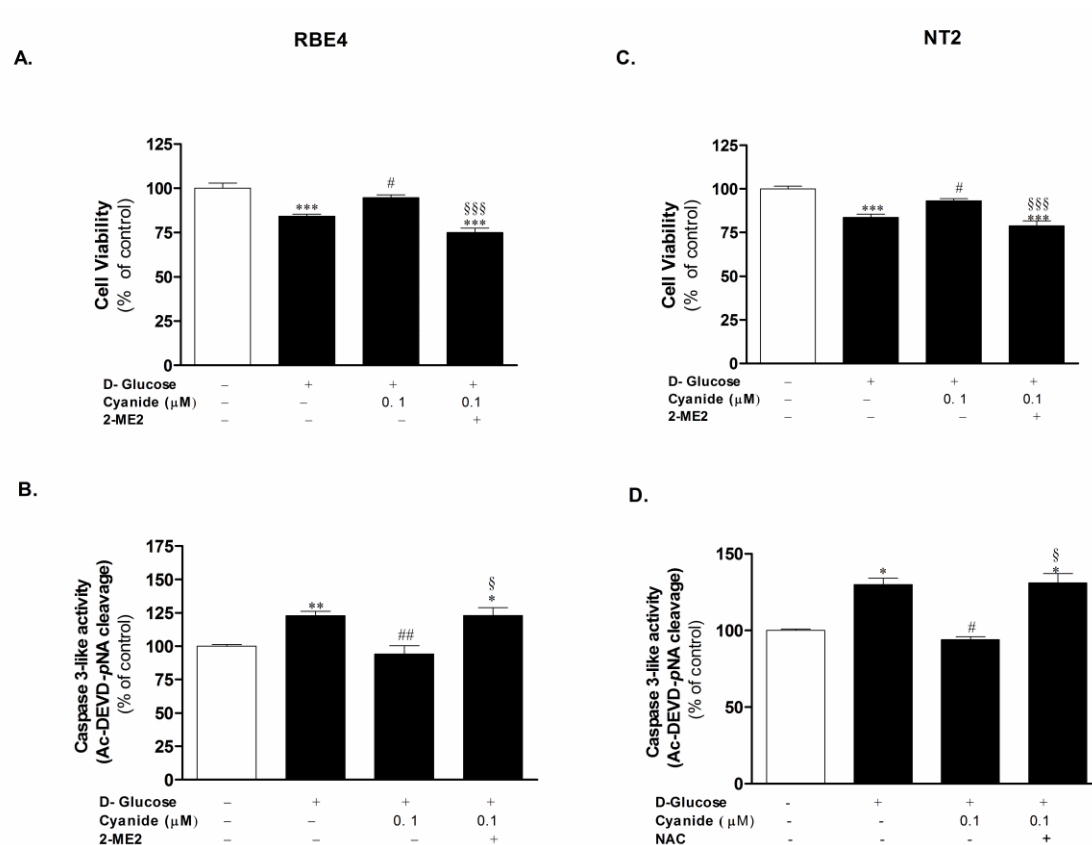
Figure 4.12. Effect of 2-ME2 on cyanide preconditioning-induced protection against glucotoxicity. Brain endothelial and neuronal cells were treated with 2-ME2 (5 μM) before cyanide preconditioning. Cell viability was determined by following changes in cell reduction capacity by the Alamar Blue assay **(A) (C)**. Caspase 3 activity was measured as described in Material and Methods section **(B) (D).** Data are expressed as mean ± SEM of 5-6 independent experiments, performed in triplicate. ** $p < 0.01$; *** $p < 0.001$ when compared with untreated cells. # $p < 0.05$; ## $p < 0.01$ when compared with high glucose-treated cells. § $p < 0.05$; §§§ $p < 0.001$ when compared with preconditioned cells.

4.4. DISCUSSION

The present study shows for the first time that preconditioning of brain endothelial and neuronal cells with the mitochondrial modulator cyanide resulted in protection against high glucose-induced cell damage, a phenomenon not only dependent on the generation of mitochondrial ROS but also dependent on the induction of HIF-1α signaling pathway. In our *in vitro* model of preconditioning, mitochondria seem to adapt to cyanide-induced redox changes by the production of moderate levels of ROS, increased basal oxygen consumption, mitochondrial network reorganization and HIF-1α induction, those alterations suggesting a "metabolic strategy" to restrict cell damage against a subsequent lethal insult.

Traditionally, ROS have been considered the culprit of deleterious events associated with neurovascular dysfunction, a feature of cerebrovascular diseases and neurodegenerative conditions (Iadecola, 2004; Lin and Beal, 2006). However, ROS signaling is a two-edged sword; high ROS levels are involved in processes of cell degeneration and death, while low/mild ROS levels appear to have protective actions involving the recruitment of prosurvival adaptive signaling pathways. Thus, mitochondria, as one of the major sources of intracellular ROS, can act as signaling organelles and are also recognized as master integrators of preconditioning-mediated endogenous protection (Correia et al., 2010b). To determine the possible contribution of mitochondrial ROS in triggering an endogenous defense response against high glucose levels in brain endothelial and neuronal cells, we exposed RBE4, NT2 and NT2 ρ0 cells to cyanide, with the primary purpose of modulating mitochondrial ROS production. Since the sites of $O_2^{\bullet -}$ generation in the ETC are the complexes I and III, the use of

mitochondrial inhibitors can maximize ROS production (Cadenas et al., 1977). Furthermore, it has been reported that mitochondria-derived $O_2^{\bullet-}$ is rapidly dismutated to H_2O_2 by SOD within the mitochondrial matrix and intermembrane space (Loschen et al., 1974). Through dose-response tests we identified concentrations of cyanide (Figs. 4.1A and 4.1B) that enhance ROS production in brain endothelial cells, particularly H_2O_2 levels, without affecting cell integrity and viability (Fig. 4.2). In the same line, we observed that cyanide also promoted a significant increase in intracellular ROS levels in NT2 cells (Figs. 4.10A and 4.10B), with no effects on NT2 ρ0 cells (Figs. 4.10C and 4.10D), indicating that mitochondria are the main source of cyanide-induced ROS generation. In agreement, it was previously shown that mitochondria may be the primary source of ROS, since cyanide inhibits COX that, in turn, stimulates ROS generation at mitochondrial complexes I and III (Chen et al., 2003). FCCP, an uncoupler of oxidative phosphorylation that causes loss of $\Delta\Psi_m$ and abolishes ROS generation from mitochondria, was used to identify the sources of cyanide-induced intracellular ROS generation in dopaminergic neurons (Zhang et al., 2007). The authors observed that cyanide-induced ROS was significantly decreased by FCCP, suggesting that the majority of neuronal ROS had a mitochondrial origin (Zhang et al., 2007).

Mitochondria exist as a dynamic network that often changes shape, through fusion and fission mechanisms, and subcellular distribution. This mitochondrial plasticity allows mitochondria to quickly react to cellular signals (e.g. ROS), which regulate their cellular position, interconnectivity and function. Thus, the dynamic behavior and the precise positioning of mitochondria within the cell play an important role in the ability of these organelles to participate and propagate signaling events (Soubannier and McBride, 2009). Prompted by this evidence, we set out to explore the effect of cyanide

preconditioning on mitochondrial network dynamics in brain endothelial cells. Our findings revealed that cyanide was able to change mitochondrial shape from a mainly tubular, highly interconnected network toward multiple, isolated singular structures (Fig. 4.5). However, these alterations induced by cyanide were suppressed by NAC pre-treatment, suggesting a role of ROS in cyanide-induced rearrangement of mitochondrial network (Fig. 4.5). Similarly, ROS were shown to induce changes in mitochondrial network morphology in endothelial cells and neurons (Barsoum et al., 2006; Jendrach et al., 2008). These observations beg the question: what is the functional meaning of cyanide-mediated mitochondrial fragmentation? It was previously shown that smaller, fragmented mitochondria are more easily transportable, potentiating the rapid mitochondrial trafficking to energy-demanding regions of the cell (Skulachev, 1999). Additionally, mitochondrial activity is reflected in ultrastructural changes of mitochondria, active mitochondria being proposed to be more condensed and to have an electron dense matrix (Hackenbrock, 1966). Moreover, it was previously hypothesized by Yu et al. (2006) that small spherical mitochondria formed after fission may represent condensed, metabolically active mitochondria. This hypothesis is corroborated by our findings, since cyanide treatment promoted an enhancement of ROS production (Fig. 4.1) and mitochondrial respiration (Fig. 4.4), despite the modest mitochondrial depolarization (Fig. 4.3), in parallel with mitochondrial fragmentation (Fig. 4.5), which suggest that cyanide exposure potentiates the formation of smaller metabolically active mitochondria. Rapid fragmentation of mitochondria and concomitant increase of total mitochondrial surface area were also suggested to augment the accessibility of metabolic substrate, and thus facilitating the metabolic input into mitochondria (Yu et al., 2006). Additionally, we found that cyanide-promoted

decomposition of mitochondrial network is accompanied by the translocation of these small mitochondria to the perinuclear area, a situation prevented by the presence of NAC (Fig. 4.5). Thus, we propose that mitochondrial ROS generation during cyanide preconditioning triggers alterations in mitochondrial dynamics that, in turn, represent physiological events underlying cell resistance. As a matter of fact, "minor" mitochondrial ROS generation has been suggested to induce mitochondrial fission and fusion that relocates mitochondrial network to form a mitochondria free gap, i.e., "a firewall", which may play a crucial role in mitochondrial ROS-mediated protective preconditioning (Jou, 2008).

Mitochondria have also been reported to intervene in cellular adaptation via a mitochondria-to-nucleus signaling pathway called retrograde regulation (Butow and Avadhani, 2004). ROS were proposed to act as "energy-state messengers", and thus, retro-regulate the nuclear-encoded energy genes, including HIF-1α (Benard et al., 2010). The important functional link between HIF-1α and mitochondria in preconditioning paradigm is supported by the fact that the generation of ROS by the Q_0 site of complex III is required for the induction of this transcription factor (Bell et al., 2007). Moreover, the use of the mitochondrial-targeted antioxidant mitoquinone (MitoQ) was shown to prevent the increase in cytosolic ROS and stabilization of the HIF-1α protein during hypoxia, which further strength the role for mitochondrial ROS in the activation of HIF pathway (Bell et al., 2007). In this context, we investigated the involvement of cyanide-induced mitochondrial ROS in the expression and nuclear activation of HIF-1α as well as in the expression of its responsive genes: VEGF, eNOS and EPO. Our results demonstrated that cyanide induced nuclear activation of HIF-1α in endothelial cells, a phenomenon suppressed by the ROS scavenger NAC (Fig. 4.6A). These observations

suggest that cyanide-induced mitochondrial ROS serve as redox-signaling molecules that govern nuclear activity of HIF-1 α. Western blot analyses also revealed that endothelial cells under cyanide preconditioning have significantly higher protein levels of HIF-1α, VEGF, eNOS and EPO when compared with non-preconditioned control cells (Figs. 4.6B and 4.6C). Reinforcing the idea that mitochondrial ROS are directly involved in HIF-1α activation and expression of its responsive genes in brain endothelial cells, immunocytochemistry analyses showed the abrogation of cyanide-induced increased EPO expression in cells pre-treated with NAC (Fig. 4.6D). In agreement, Zhang et al. (2007) observed that cyanide induces a rapid surge of intracellular reactive ROS generation, followed by nuclear accumulation of HIF-1α. In addition, the exposure to NAC and catalase, an enzymatic H_2O_2 scavenger, reduced ROS accumulation and inhibited HIF-1 pathway activation, suggesting that ROS are the initiation signal for HIF-1 activation by cyanide (Zhang et al., 2007). Accordingly, Chandel et al. (1998, 2000) also demonstrated that ρ^0 cells, without a functional mitochondrial respiratory chain, failed to increase ROS generation and HIF-1α accumulation under hypoxic conditions. These authors also showed that low levels of exogenous H_2O_2 (40µM) stabilize HIF-1α protein during normoxia and increase HRE-luciferase expression in ρ^0 cells (Chandel et al., 2000), thus attributing a role for ROS and mitochondria in the induction of HIF-1α signaling. Additionally, we hypothesize that the perinuclear distribution of mitochondria promoted by cyanide could in part facilitate the ROS-mediated HIF-1α induction observed in our experiments. This is supported by previous studies showing that retrograde signaling from de-energized mitochondria signals the nucleus to modulate additional adaptive responses (Giannattasio et al., 2005; Guzy et al., 2005). Indeed, it was shown that mitochondria function as oxygen sensors and stabilize HIF-1α and HIF-2α by releasing

ROS to the cytosol (Guzy et al., 2005). In accordance, hypoxic episodes are able to initiate a vectorial movement of mitochondria to the vicinity of the nucleus, which serves to create a ROS-enriched micro-domain important for cellular signaling (Swiger et al., 2007).

It is clear that the brain is one of the targets of diabetic-end organ damage, chronic hyperglycemia emerging as a feasible pathogenetic mechanism underlying cognitive decline and brain structural and functional abnormalities, in both T1D and T2D (Biessels et al., 1994; Gispen and Biessels, 2000). Compelling evidence postulates that hyperglycemic conditions promote mitochondrial dysfunction, oxidative stress and ultimately neuronal dysfunction and death (Russell et al., 2002; Vincent and Feldman, 2004; Vincent et al., 2004, 2005). Our findings demonstrate that exposure of cells to 30 mM D-glucose resulted in a significant decrease in cell viability when compared with control cells (Figs. 4.7, 4.11A and 4.11C), which indicate that high glucose levels are deleterious to brain endothelial and neuronal cells. This is consistent with previous data demonstrating that hyperglycemia is a culprit of apoptosis in neurons (Russell et al., 2002; Vincent et al., 2005) and cultured endothelial cells (Nakagami et al., 2001). It has been demonstrated that translocation of the pro-apoptotic molecule BAX from the cytosol to the mitochondrial membrane is a critical event in apoptosis (Gross et al., 1998). Furthermore, BAX has been shown to induce rapid activation of caspases culminating in apoptosis (Rosse et al., 1998). We observed that high glucose levels induce the translocation of BAX to the mitochondria (Fig. 4.8) and potentiate caspase-3 activation (Figs. 4.9, 4.11B and 4.11D). Accordingly, Lenninger et al. (2006) reported that high glucose causes BAX activation and translocation to mitochondria, and cytochrome *c* loss in dorsal root ganglia neurons. Moreover, a study using human aortic endothelial

cells also demonstrated that high glucose levels induce the expression of BAX protein and its translocation to the mitochondria leading to caspase-3 activation (Nakagami et al., 2002). As hypothesized, our data demonstrate that cyanide preconditioning protects both RBE4 and NT2 cells against high glucose-induced cell damage (Figs. 4.7 and 4.11A), these protective effects being abrogated by cells pre-treatment with the ROS scavenger NAC. However, cyanide preconditioning fails to protect NT2 ρ0 against glucotoxicity (Fig. 4.11C), which further reinforce a role for functional mitochondria and mitochondrial ROS in cyanide preconditioning. Additionally, we also found that cyanide preconditioning blocked the apoptotic cascade activation promoted by high levels of glucose in RBE4 (Figs. 4.8 and 4.9) and NT2 cells (Fig. 4.11B), but not in NT2 ρ0 cells (Fig. 4.11D). Similarly, in a previous study it was demonstrated that preconditioning with a non-toxic concentration of cyanide is able to protect neurons against cyanide-induced neurotoxicity by preserving mitochondrial function (Jensen et al., 2002). Overall, our data indicate that both functional mitochondria and mitochondrial ROS are required for the effectiveness of cyanide-induced preconditioning against glucotoxicity. To determine whether HIF-1α signaling pathway is implicated in cyanide preconditioning-mediated protective response against glucotoxicity in both brain endothelial and neuronal cells, we did a pharmacological approach by inhibiting HIF-1α induction with one of its specific pharmacologic inhibitors, the 2-ME2. Pre-treatment with 2-ME2 completely abolishes the cyanide-induced protection against cell loss and caspase-3 activation potentiated by high glucose levels, in both RBE4 and NT2 cells (Fig. 4.12). It has been proposed that the mechanism of preconditioning-triggered neuroprotection involves sublethal ROS production, which does not damage the neurons, yet may be enough to act as a signal to downregulate the threshold for expression of HIF-1α and its downstream targets (Liu et

al., 2005). Accordingly, Chang et al. (2008) showed that low levels of exogenous H_2O_2 increase HIF-1α expression and induce protection against ischemia in primary cortical neurons. Overall, our data indicate that HIF-1α signaling pathway is a plausible downstream target of cyanide-induced mitochondrial ROS, being essential for the induction of the protective response mediated by cyanide preconditioning.

Altogether, our results show that cyanide preconditioning protects brain endothelial and neuronal cells against high-glucose induced cell damage. Mechanistically, cyanide seems to have a great capacity to mediate preconditioning-induced tolerance through mitochondria-centered mechanisms, the moderate levels of ROS generated during the initial phase of preconditioning being the crucial step for the induction of stress-resistance events. Indeed, the cytoprotective effects of cyanide were completely abolished by the ROS scavenger NAC, which reinforce the idea that ROS are involved in the triggering phase of preconditioning. The lack of cyanide-induced cytoprotective response in cells depleted of mtDNA (NT2 ρ0 cells), indicate that the protection afforded by cyanide is reliant on the presence of functional mitochondria and mitochondrial ROS production. Our results also show that cyanide preconditioning involves a crosstalk between mitochondrial ROS and HIF-1α signaling pathway, whose activation contributes to minimize the deleterious effects of hyperglycemia. Therefore, mitochondria and HIF-1α signaling pathway could represent feasible therapeutic targets to counteract neuronal and vascular dysfunction promoted by diabetes and associated complications. Moreover, a deeper knowledge on the functional role and involvement of mitochondrial dynamics on preconditioning-triggered tolerance could be important to further improve the scientific basis of this new exciting research field.

Chapter 4

CHAPTER 5

MITOCHONDRIAL ABNORMALITIES IN A STZ-INDUCED RAT MODEL OF SPORADIC ALZHEIMER'S DISEASE

5.1 ABSTRACT

This study aimed to show that the rat model of sAD generated by the icv injection of a sub-diabetogenic dose of STZ is characterized by brain mitochondrial abnormalities. Three-month-old male Wistar rats were investigated 5 weeks after a single bilateral icv injection of STZ (3mg/ Kg) or vehicle. icvSTZ administration did not affect blood glucose levels but induced a decrease in brain weight and cognitive decline. icvSTZ administration also resulted in a significant increase in the levels of $A\beta_{1-42}$ in the hippocampus and hyperphosphorylated tau protein in both cortex and hippocampus. Brain mitochondria from icvSTZ rats revealed deficits in their function, as shown by a decrease in $\Delta\Psi m$, repolarization level, ATP content, respiratory state 3, respiratory control ratio and ADP/O ratio and an increase in lag phase of repolarization. Mitochondria from icvSTZ rats also displayed a decrease in PDH, α-KGDH and COX activities and an increase in the susceptibility to Ca^{2+}-induced mPTP. An increase in H_2O_2 and lipid peroxidation levels and a reduction in GSH content were also observed in mitochondria from icvSTZ rats. These results demonstrate that the insulin-resistant brain state that characterizes this rat model of sAD is accompanied by the occurrence of mitochondrial abnormalities reinforcing the validity of this animal model to study sAD pathogenesis and potential therapies.

5.2. INTRODUCTION

AD is the most common form of dementia among older people, affecting approximately 35 million people worldwide (Querfurth and LaFerla, 2010). Neuropathologically characterized by extracellular SP, intracellular NFTs and progressive loss of neurons and synapses in selective brain regions, especially in the hippocampus and cortex, this fatal neurodegenerative disorder is also marked by an initial memory impairment that progresses unrelentingly to a total debilitating loss of mental and physical faculties (Moreira et al., 2009; Selkoe, 2001; Smith, 1998). Etiologically, there are two different types of origin-based AD, despite indistinguishable clinical dementia symptoms. In a small proportion (familial early-onset AD), the disease has a genetic origin, while the vast majority (more than 95%) of AD cases are sporadic in origin (Correia et al., 2011a).

Over the last decades, much effort has been devoted to uncover the "culprit" of sAD development. Although there are a myriad of hypotheses trying to explain sAD ethiopathogenesis, impaired brain insulin functions and glucose metabolism appear to be initial triggers of neurodegenerative events that occur in this disease (Hoyer, 2004a; Hoyer and Lannert, 2007). As a matter of fact, early abnormalities in brain glucose/energy metabolism have been documented in structures with both high glucose demands and high insulin sensitivity, including parietotemporal and frontal areas, in sAD (Henneberg and Hoyer, 1995; Hoyer, 2002, 2004b). Moreover, postmortem AD brain exhibits reduced insulin levels and insulin receptor expression and reduced tyrosine kinase activity (Frolich et al., 1999), reinforcing the idea that abnormalities in brain insulin function and insulin signal transduction are major factors that mechanistically influence the onset of sAD pathology.

Mitochondria are vital organelles involved in energy metabolism and cell survival (Benard et al., 2007). The many functions of mitochondria comprise, but are certainly not restricted to: 1) production of cellular ATP; 2) Ca^{2+} buffering; 3) ROS generation; and 4) the arbitration of apoptosis (Beal, 2005; Mattson et al., 2008). Neurons are particularly vulnerable to bioenergetic crisis and dysfunction of mitochondrial machinery, because of their highly metabolic rate dependence and morphological complexity (Benard et al., 2007). Taking into account that neurons are postmitotic cells with membranes enriched in polyunsaturated fatty acids, they are also highly sensitive to oxidative stress. Mitochondrial dysfunction is also a well documented early feature in vulnerable neurons in sAD (Blass et al., 2000; Bubber et al., 2005).

It was recently shown that the disruption of brain insulin function in rats by icv injection of STZ leads to the development of numerous behavioral, neurochemical and structural features that resemble those found in human sAD (Grunblatt et al., 2007; Salkovic-Petrisic and Hoyer, 2007). However, brain mitochondrial function and oxidative status in this animal model of sAD has not yet been studied. Along this line, this study was undertaken to investigate brain cortical and hippocampal mitochondrial bioenergetics and oxidative status in the rat model of sAD induced by the icv administration of STZ. For this purpose we evaluated the respiratory chain activity [respiratory states 3 and 4, RCR, and ADP/O ratio], oxidative phosphorylation system [ΔΨm, ADP-induced depolarization, repolarization level, repolarization lag phase, and ATP levels], PDH, α-KGDH and COX activities, Ca^{2+}-induced mPTP, H_2O_2 levels, MDA levels (a lipid peroxidation marker), and GSH content (a major non-enzymatic antioxidant defense). Our findings show that the insulin-resistant brain state that

characterizes this animal model is intimately associated with alterations in mitochondrial bioenergetics and oxidative status, considered early events in sAD.

5.3. RESULTS

5.3.1 CHARACTERIZATION OF THE EXPERIMENTAL ANIMALS

As shown in Table 5.1, icvSTZ rats presented a significant decrease in brain weight, and consequently, a decrease in brain-to-body weight ratio (Table 5.1). As expected, the icv administration of STZ, in a sub-diabetogenic dose (3mg/kg), did not affect peripheral blood glucose levels (Table 5.1).

The Morris water maze test, which evaluates the capacity of rodents to learn and retrieve, showed a significant increase in latency times to reach platform, since the first trial session, in icvSTZ-treated rats indicating an impairment of cognitive functions (Fig. 5.1).

Concerning the typical neuropathological hallmarks of AD, Aβ levels were determined by sandwich ELISA assays specific for $A\beta_{1-42}$. As shown in Figure 5.2, five weeks after icv administration of STZ a significant increase in $A\beta_{1-42}$ levels was observed in the hippocampus. In addition, Western blot analyses revealed that icv administration of STZ also promoted an overall increase in phosphorylated tau (p-tau) (Ser 396) protein levels when compared with control sham-operated rats (Figs. 5.3A and 5.3B). Furthermore, no statistically significant differences were found in total tau protein levels between the two experimental groups (Figs. 5.3C and 5.3D). Consequently, a significant increase in the ratio p-tau to total tau was observed in both brain cortex and hippocampus of icvSTZ-treated rats (Fig. 5.3E).

TABLE 5.1. CHARACTERIZATION OF EXPERIMENTAL GROUPS

	SHAM	STZ
BLOOD GLUCOSE LEVELS (MG/DL)	163.4 ± 15.13	144.8 ± 10.93
BRAIN WEIGHT (G)	2.250 ± 0.059	1.870 ± 0.166 *
BRAIN-TO-BODY WEIGHT RATIO	0.004733 ± 0.00019	0.003556 ± 0.00046 *

Data are the mean ± SEM of 10 animals from each condition studied. Statistical significance: *p<0.05 when compared with sham control rats.
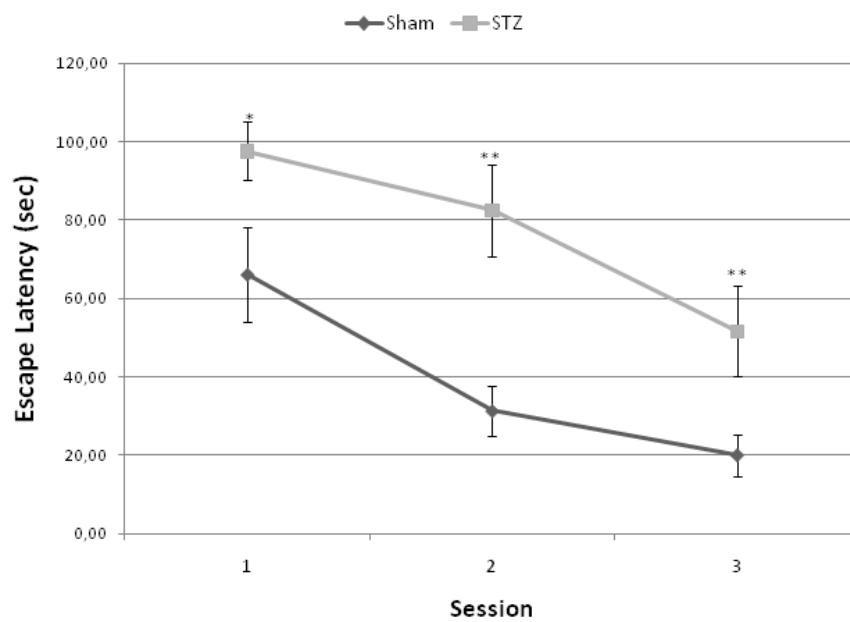
Figure 5.1. Effect of icvSTZ administration on cognitive performance. The capacity of rodents to learn and retrieve was evaluated by the Morris water maze test. Data are the means ± SEM of 8-9 animals from each condition studied. Statistical significance: *p<0.05; **p<0.01 when compared with sham control rats.
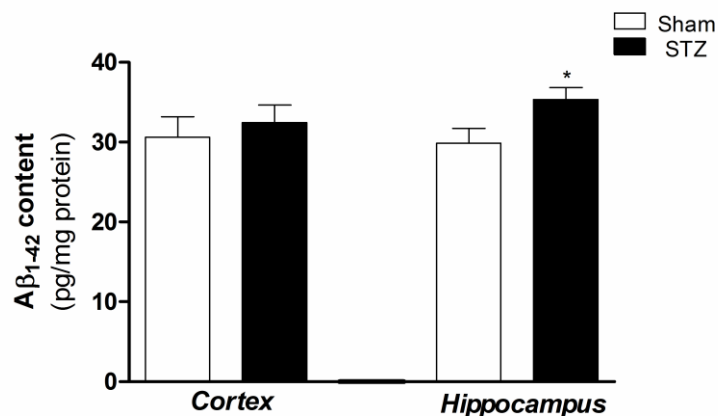
Figure 5.2. Effect of icvSTZ administration on Aβ$_{1-42}$ content in brain cortex and hippocampus. Levels of Aβ$_{1-42}$ from RIPA-extracted homogenates were detected using ELISA and expressed in pg of Aβ/mg of protein. Data are the means ± SEM of 5-7 animals from each condition studied. Statistical significance: *$p < 0.05$ when compared with sham control hippocampus.
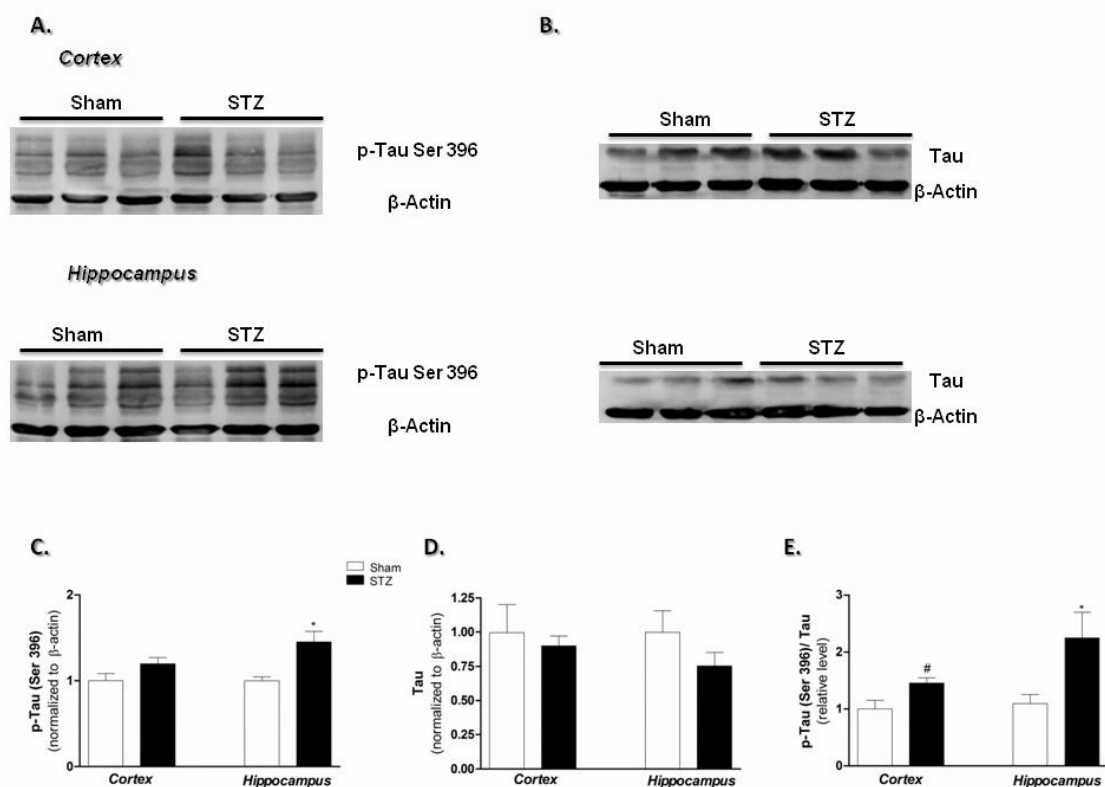
Figure 5.3. Effect of icvSTZ administration on total and phosphorylated tau protein levels in cortex and hippocampus. Brain cortical and hippocampal samples were analyzed for protein levels of phosphorylated tau at serine 396 (p-Tau Ser396) **(A,B)** and total tau **(C,D)** by Western blot. **(E)** The ratio of p-tau to total tau was also calculated. Data are the means ± SEM of 4-5 animals from each condition studied. Statistical significance: #< 0.05 when compared with sham control cortex *$p < 0.05$ when compared with sham control hippocampus.

5.3.2 icvSTZ Administration Drastically Affects Brain Cortical And Hippocampal Mitochondrial Respiratory Chain

In a first approach to evaluate the effect of icvSTZ administration on bioenergetic profile, mitochondrial respiration was determined in freshly isolated brain cortical and hippocampal mitochondria energized with substrates for mitochondrial complexes I and II. As shown in Table 5.2, brain cortical mitochondria from icvSTZ rats energized with glutamate/malate (substrates for complex I) displayed decreased respiratory state 3, RCR and ADP/O ratio, when compared with brain cortical mitochondria isolated from control sham-operated rats. Concerning hippocampal mitochondria from icvSTZ rats energized with glutamate/malate only a significant decrease in RCR was observed. Moreover, RCR and ADP/O ratio were also found to be decreased in both brain cortical and hippocampal mitochondria from icvSTZ rats energized with succinate (substrate for complex II), whereas respiratory state 3 remained unaltered. No significant alterations were observed in respiratory state 4 in brain cortical and hippocampal mitochondria between the two experimental groups with both respiratory substrates.

TABLE 5.2. EFFECT OF icvSTZ ADMINISTRATION ON THE RESPIRATORY FUNCTION OF BRAIN CORTICAL AND HIPPOCAMPAL MITOCHONDRIA

		SHAM		STZ	
		Cortex	*Hippocampus*	*Cortex*	*Hippocampus*
Complex I	**State 3** (nAtgO/min/mg)	93.58 ± 9.19	46.93 ± 7.08	54.6 ± 5.14 [*]	32.9 ± 2.93
	State 4 (nAtgO/min/mg)	27.55 ± 1.78	18.6 ± 1.88	22.69 ± 1.46	20.35 ± 2.4
	RCR	3.43 ± 0.24	2.7 ± 0.26	2.56 ± 0.70 [*]	1.68 ± 0.21 [&]
	ADP/O (nmol ADP/AtgO/min/mg)	2.91 ± 0.17	2.32 ± 0.24	2.08 ± 0.13 [**]	1.81 ± 0.21
Complex II	**State 3** (nAtgO/min/mg)	84.51 ± 7.24	51.15 ± 7.43	64.39 ± 4.95	33.35 ± 2.55
	State 4 (nAtgO/min/mg)	26.34 ± 1.7	19.1 ± 2.73	27.75 ± 2.71	21.33 ± 3.24
	RCR	3.09 ± 0.09	2.68 ± 0.19	2.34 ± 0.25 [#]	1.63 ± 0.17 [§]
	ADP/O (nmol ADP/AtgO/min/mg)	2.28 ± 0.11	2.01 ± 0.04	1.72 ± 0.13 [##]	1.46 ± 0.18 [§]

Mitochondrial respiration parameters were evaluated in freshly isolated brain cortical and hippocampal mitochondrial fractions (0.8 mg) in 1 ml of the reaction medium energized with 5 mM glutamate/2.5 mM malate or with 5 mM succinate in the presence of 2 μM rotenone. Data are the means ± SEM of 3-5 animals from each condition studied. Statistical significance: *p<0.05; **p<0.01, ***p<0.001 when compared with sham control cortical mitochondria energized with the substrate for complex I, glutamate/malate; &p<0.05 when compared with sham control hippocampal mitochondria energized with the substrate for complex I, glutamate/malate; #p<0.05; ##p<0.01 when compared with sham control cortical mitochondria energized with the substrate for complex II, succinate; § p<0.05 when compared with sham control hippocampal mitochondria energized with the substrate for complex II, succinate.

5.3.3 ICVSTZ ADMINISTRATION IMPAIRS BRAIN CORTICAL AND HIPPOCAMPAL OXIDATIVE PHOSPHORYLATION SYSTEM

In the course of electron transfer through the respiratory chain complexes, protons (H^+) are pumped out of the mitochondrial matrix across the inner mitochondrial membrane, whose gradient can establish an electrochemical potential (Δp) resulting in a pH (ΔpH) and a voltage gradient ($\Delta\Psi_m$). Thus, mitochondrial $\Delta\Psi_m$ is fundamental for the phenomenon of oxidative phosphorylation, which results in the conversion of ADP to ATP via ATP synthase, being a highly sensitive indicator of the integrity of the mitochondrial inner membrane. In the presence of glutamate/malate or succinate, brain cortical mitochondria from icvSTZ rats exhibited a decrease in $\Delta\Psi_m$, repolarization level and ATP content and an increase in lag phase of repolarization, when compared with brain cortical mitochondria isolated from control sham-operated rats (Table 5.3). However, no significant differences were observed on ADP-induced depolarization between the two experimental groups with both respiratory substrates. Additionally, hippocampal mitochondria from icvSTZ rats energized with glutamate/malate also presented a significant decrease in repolarization level and ATP content and an increase in lag phase of repolarization, whereas the other parameters remained statistically unchanged when compared with hippocampal mitochondria isolated from control sham-operated rats. Concerning hippocampal mitochondria energized with succinate, no significant differences in the respiratory parameters were observed between the two experimental groups.

TABLE 5.3. EFFECT OF ICVSTZ ADMINISTRATION ON THE MITOCHONDRIAL OXIDATIVE PHOSPHORYLATION SYSTEM

		SHAM		STZ	
		Cortex	*Hippocampus*	*Cortex*	*Hippocampus*
Complex I	**ΔΨm** (−mV)	212.5 ± 2.27	191.8 ± 3.36	202.4 ± 2.02[**]	179.3 ± 6.60
	ADP-induced depolarization (-mV)	22.58 ± 1.32	21.91 ± 1.13	22.14 ± 1.12	23.53 ± 2.15
	Repolarization level (−mV)	211.9 ± 2.85	190.5 ± 2.40	201.8 ± 2.16[*]	172.4 ± 5.79[&]
	Repolarization lag phase (min)	0.44 ± 0.019	0.71 ± 0.066	0.60 ± 0.018[***]	1.01 ± 0.090[&]
	ATP levels (pmol/ mg protein)	41000 ± 2931	39500 ± 1594	31600 ± 2535[*]	30380 ± 1654[&&]
Complex II	**ΔΨm** (−mV)	219.5 ± 3.19	199.2 ± 2.61	208.2 ± 2.72[#]	192.6 ± 6.00
	ADP-induced depolarization (-mV)	33.95 ± 2.46	28.35 ± 2.66	28.35 ± 1.54	24.88 ± 1.59
	Repolarization level (−mV)	218.4 ± 2.85	201.7 ± 3.11	208.1 ± 2.44[#]	188.7 ± 5.37
	Repolarization lag phase (min)	0.51 ± 0.020	0.73 ± 0.045	0.69 ± 0.026[##]	0.96 ± 0.083
	ATP levels (pmol/ mg protein)	44780 ± 1225	40620 ± 2452	33840 ± 1094[###]	34970 ± 2926

The oxidative phosphorylation parameters were evaluated in freshly isolated brain cortical and hippocampal mitochondria (0.8 mg) in 1 ml of the reaction medium supplemented with 3 µM TPP$^+$ and energized with 5 mM glutamate/2.5 M malate or with 5 mM succinate in the presence of 2 µM rotenone. Data are the means ± SEM of 5-6 animals from each condition studied. Statistical significance: *p<0.05; **p<0.01; ***p<0.001 when compared with sham control brain cortical mitochondria energized with the substrate for complex I, glutamate/malate; &p<0.05; &&p<0.01 when compared with sham control hippocampal mitochondria energized with the substrate for complex I, glutamate/malate; #p<0.05; ##p<0.01; ###p<0.01 when compared with sham control brain cortical mitochondria energized with the substrate for complex II, succinate.

5.3.4 ICVSTZ ADMINISTRATION IS ASSOCIATED WITH DECREASED ACTIVITIES OF PDH, α-KGDH, AND COX

Mitochondrial bioenergetic deficits could result from altered activity of mitochondrial metabolic enzymes. Thus, to gain further insight into the effect of icvSTZ administration on mitochondrial bioenergetics, we assessed PDH, α-KGDH and COX activities in isolated brain cortical mitochondria. When compared with control sham-operated rats, brain cortical mitochondria from icvSTZ rats presented a significant decrease in PDH (Fig. 5.4A), α-KGDH (Fig. 5.4B), and COX (Figs. 5.4C and 5.4D) activities, contributing for the "hypometabolic" state that characterizes this animal model of sAD.

Due to sample limitations we were unable to evaluate the activities of these enzymes in hippocampal mitochondria.
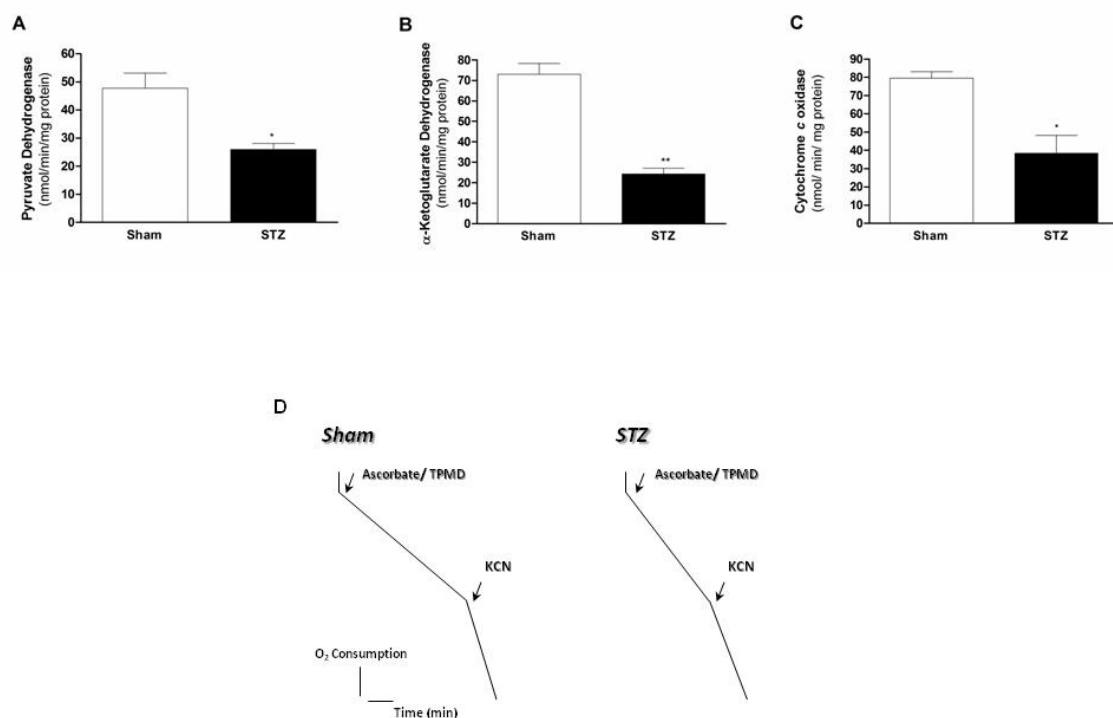
Figure 5.4. Effect of icvSTZ administration on brain cortical mitochondrial enzymatic activities (A) PDH, (B) α-KGDH and (C and D − typical traces) COX. Data are the means ± SEM of 5 animals from each condition studied. Statistical significance: $*p<0.05; **p<0.01$ when compared with sham control rats.

5.3.5 Increased Sensitivity Of Brain Cortical Mitochondria To Ca^{2+}-Induced MPTP Opening In icvSTZ Rats

Increased susceptibility to mPTP opening is linked with mitochondrial function decline. Indeed, excessive levels of ROS and Ca^{2+} could trigger mPTP opening, leading to mitochondrial swelling, membrane depolarization, rupture of mitochondrial membranes and cristae, and the destruction of defective mitochondria by autophagy (Du and Yan, 2010; Kim et al., 2007). As shown in the typical traces (Fig. 5.5A), brain cortical mitochondria from control sham-operated rats energized with succinate presented a $\Delta\Psi_m \approx$ -217 mV. After the addition of the first pulse of exogenous Ca^{2+}, a rapid depolarization was observed followed by an incomplete repolarization. Additionally, the second pulse of Ca^{2+} led to total depolarization of mitochondria followed by a small repolarization, indicating the induction of mPTP (Fig. 5.5A). Concerning brain cortical mitochondria from icvSTZ rats, the addition of succinate produced a $\Delta\Psi_m \approx$ -204 mV (Fig. 5.5B). As in mitochondria from control sham animals, these mitochondria also completely depolarized following the addition of the same two pulses of Ca^{2+}; however, they depolarized more rapidly and were not able to repolarize after the 2nd pulse of Ca^{2+} (Fig. 5.5B). As expected, the presence of the mPTP inhibitors, oligomycin plus ADP, was able to prevent the loss of $\Delta\Psi m$ after the addition of three pulses of Ca^{2+} in mitochondria of both experimental groups, thus preventing the induction of mPTP (Figs. 5.5C and 5.5D).

Consistently, ultrastructural analysis of mitochondria after Ca^{2+} experiments revealed that preparations from icvSTZ rats presented significantly more swollen mitochondria characterized by volume enlargement, loss of typical cristae structure, and

non-dense matrix (Figs. 5.6B and 5.6C), while preparations from control sham-operated rats displayed a preponderance of orthodox mitochondria, with tightly packed thin cristae filling and expanded, more translucent mitochondrial matrix (Figs. 5.6A and 5.6C). Since mitochondria were exposed to an exogenous Ca^{2+} insult, both mitochondrial preparations presented a little extent of mitochondria in a condensed configuration (Fig. 5.6).

Again, and due to sample limitations, we were unable to evaluate these parameters in hippocampal mitochondria.
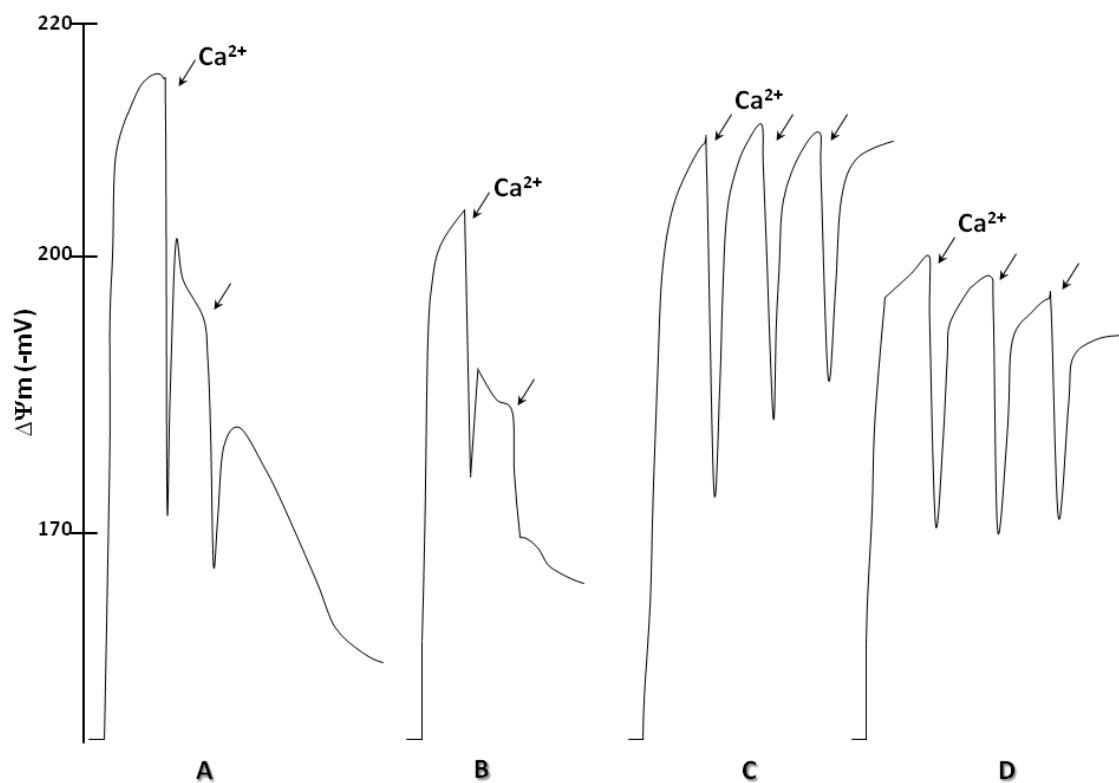
Figure 5.5. Effect of icvSTZ administration on the loss of mitochondrial transmembrane potential ($\Delta\Psi$m) that characterizes Ca^{2+}-induced mPTP. Freshly isolated brain cortical mitochondria (0.5 mg) in 1 ml of the reaction medium supplemented with 3 µl TPP$^+$ were energized with 5 mM succinate. Oligomycin (0.2 µg/ml) plus ADP (100 µM) were added 2 min before Ca^{2+} addition. The traces are typical of 5 experiments. **A**- Sham control brain cortical mitochondria, **B**- icvSTZ-treated brain cortical mitochondria, **C**- Sham

control brain cortical mitochondria in the presence of oligomycin plus ADP; **D**- icvSTZ-treated brain cortical mitochondria in the presence of oligomycin plus ADP. Ca^{2+} pulses: first pulse = 20 nmol Ca^{2+}, second and third pulses = 10 nmol Ca^{2+}.
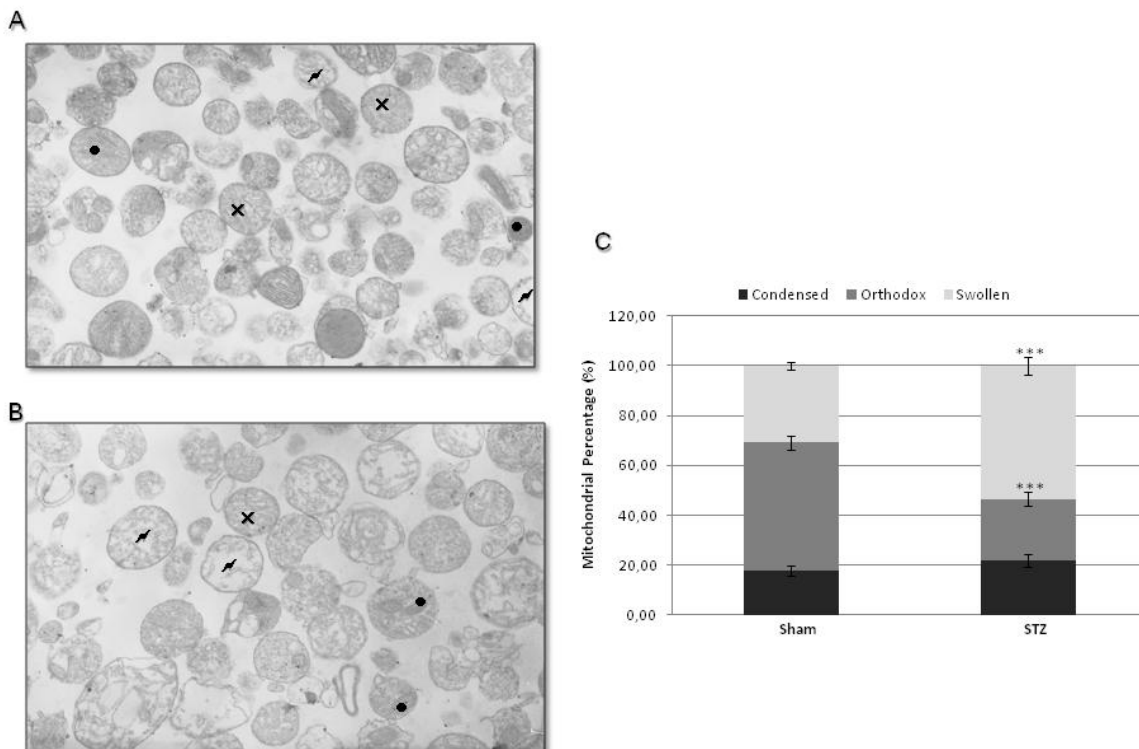
Figure 5.6. Effect of icvSTZ administration on mitochondrial ultrastructure after a Ca^{2+} challenge. Images represent **(A)** sham control brain cortical mitochondria in the presence of Ca^{2+} (60 nmol/mg protein); and **(B)** brain cortical mitochondria from icvSTZ-treated rats in the presence of Ca^{2+} (60 nmol/mg protein) at 10,000x magnification. ●- Condensed mitochondria; ✗- Orthodox mitochondria; ⚡- Swollen mitochondria. **(C)** Graphical representation of mitochondrial morphometric analysis. Statistical significance: ***$p < 0.001$ when compared with sham control brain cortical mitochondria.

5.3.6 ICVSTZ ADMINISTRATION POTENTIATES OXIDATIVE STRESS AND DAMAGE

Mitochondria are one of the major producers of free radicals including H_2O_2, hydroxyl ($HO^{\bullet}$), and $O_2^{\bullet-}$. Thus, we assessed H_2O_2 production in brain cortical mitochondria as an indicator of the pro-oxidant state. As shown in Fig. 5.7A, mitochondria from icvSTZ-treated rats produced significantly higher levels of H_2O_2, when compared with control mitochondria. Accordingly, the levels of MDA, a marker of lipid peroxidation, were found to be significantly increased in icvSTZ rats (Fig. 5.7B).

GSH is a potent endogenous antioxidant scavenger of free radicals and protects against oxidative stress. Figure 5.8 shows that brain cortical and hippocampal mitochondria from icvSTZ-treated rats presented a significant reduction in GSH content and GSH/GSSG ratio compared with mitochondrial preparations from control sham-operated rats.
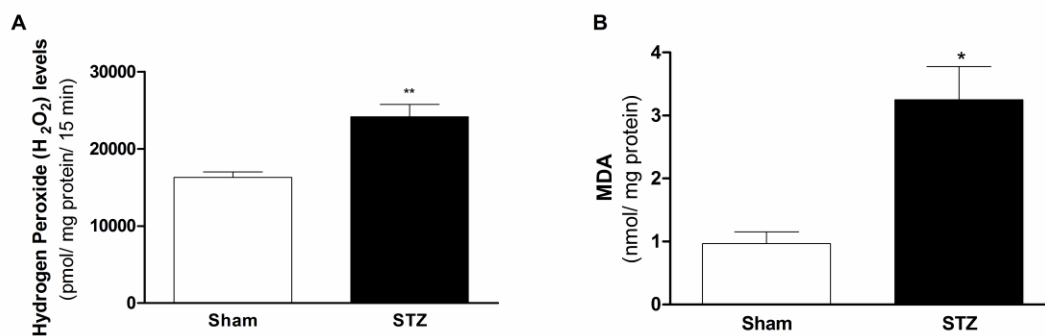
Figure 5.7. Effect of icvSTZ administration on oxidative stress markers: H_2O_2 (A) and MDA (B) levels. H_2O_2 production and MDA levels were measured as described in Material and Methods chapter. Data are the means ± SEM of 5 animals from each condition studied. Statistical significance: *$p<0.05$; **$p<0.01$ when compared with sham control brain cortical mitochondria.
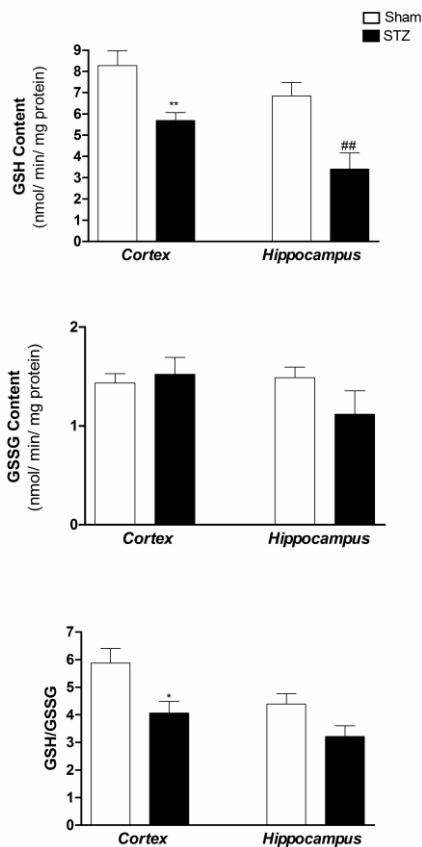
Figure 5.8. Effect of icvSTZ administration on glutathione content. Statistical significance: *p<0.05;**p<0.01 when compared with sham control brain cortical mitochondria; ## p<0.01 when compared with sham control hippocampal mitochondria.

5.4 DISCUSSION

Extensive literature exists showing that the brains of sAD patients are characterized by a decline in glucose/energy metabolism, which is intimately associated to an impairment of insulin signaling and mitochondrial abnormalities (Lin and Beal, 2006; Mattson et al., 2008; Moreira et al., 2009; Reddy, 2009; Wang et al., 2009b). Besides reflecting the insulin resistant brain state that characterizes sAD (Salkovic-Petrisic and Hoyer, 2007), the icvSTZ rat model also presents extensive mitochondrial abnormalities, considered a key early event in the disease progression. Indeed, we show that the icv administration of a sub-diabetogenic dose of STZ promotes a significant decline in both brain cortical and hippocampal bioenergetic function as reflected by

impaired mitochondrial respiration, oxidative phosphorylation system and PDH, α-KGDH and COX activities. An increase in the susceptibility to Ca^{2+}-induced mPTP opening and oxidative stress and damage was also observed in icvSTZ rats.

A significant reduction of gross brain weight and brain-to-body weight ratio was observed five weeks after icv administration of STZ (Table 5.1), probably reflecting brain atrophy. icvSTZ rats also present a cognitive impairment, namely learning deficits marked by the increase in latency time during trial sessions in Morris water maze test (Fig. 5.1), which is in conformity with previous findings (Lannert and Hoyer, 1998). The literature also shows that AD patients present a reduction in total brain weight and atrophy of specific brain regions (DeCarli, 2001). Brain atrophy associated with both synaptic and neuronal loss is a pathological finding in AD patients, reflecting the progressive neurodegeneration that culminates in cognitive decline (Fox et al., 2000). Furthermore, it was detected a significant increase in $A\beta_{1-42}$ content in the hippocampus (Fig. 5.2) and p-tau protein levels in both cortex and hippocampus of icvSTZ-treated rats (Fig. 5.3), considered hallmarks of AD.

As previously indicated, early defects in cerebral glucose utilization and energy metabolism are consistent antecedents of AD development, suggesting that abnormalities in mitochondrial bioenergetics are present at the earliest symptomatic stages of the disease (Blass et al., 2002; Hoyer, 2000). Mitochondria are the central coordinators of energy metabolism, and are responsible for providing more than 90% of the energy required for cellular functions by two linked metabolic processes: the TCA cycle and the ETC (Wallace, 1997). Thus, it is plausible to speculate that "mitoenergetic failure" induced by icvSTZ is intimately associated with central insulin resistance. In fact, we observed that both brain cortical and hippocampal mitochondria from icvSTZ rats

present impaired respiratory chain activity (Table 5.2) and oxidative phosphorylation efficiency (Table 5.3), although the bioenergetic decline was more pronounced in brain cortical mitochondria. Consistently, impairment of mitochondria oxidative phosphorylation was reported in the brain of AD patients (Chagnon et al., 1995). In addition, evidence from the literature also reported decreased ΔΨm and ETC activity in AD cybrids (Cardoso et al., 2004; Cassarino et al., 1998; Khan et al., 2000; Swerdlow et al., 1997), fostering the idea that compromised mitochondrial bioenergetics is a contributing factor in the pathogenesis of sAD. Mitochondrial dysfunction, characterized by decreased mitochondrial respiratory rates, ΔΨm and ATP levels, has also been described in transgenic AD mice models even before extracellular deposition of Aβ, suggesting that mitochondrial function decline precedes the occurrence of AD-like neuropathological hallmarks and is substantially aggravated with aging (Dragicevic et al., 2010; Hauptmann et al., 2009). It was recently shown that vascular Aβ deposits appear only 3 months after the icvSTZ administration (Salkovic-Petrisic et al., 2011). These observations together with our results allow us to suggest that in this non-transgenic animal model of sAD mitochondrial dysfunction is also an early event in AD pathology. It was also demonstrated that decreased mitochondrial bioenergetics triggers Aβ overproduction and nerve cell atrophy (Meier-Ruge and Bertoni-Freddari, 1997; Velliquette et al., 2005). These findings nicely fit in the elegant hypothesis advanced by Smith and colleagues (2002) that proposed that the accumulation of Aβ could represent a protective response to oxidative damage caused by mitochondrial dysfunction.

Another notable aspect of perturbed mitochondrial function induced by icvSTZ administration is the significant decrease observed in the activities of the three mitochondrial respiratory enzymes, PDH and α-KGDH, two enzymes in the rate-limiting

step of the TCA cycle, and COX, the terminal enzyme in the mitochondrial respiratory chain that is responsible for reducing molecular oxygen (Fig. 5.4). Thus, the decrease in the activity of these enzymes could constitute one of the myriad of factors involved in AD-related mitochondrial dysfunction, compromising ECT activity and ATP synthesis (Blass et al., 2000). Altered expression and decreased activity of PDH, α-KGDH and COX were also documented in fibroblasts from AD patients and postmortem AD brain (Bubber et al., 2005; Gibson et al., 1999; Maurer et al., 2000). The impairment in TCA cycle enzymes (specifically PDH) was shown to be correlated with disability in AD brains, suggesting a coordinated mitochondrial alteration (Bubber et al., 2005). Indeed, inactivation of PDH will result in the shortage of ATP and acetylcholine (ACh), which are crucial for neuronal survival and accurate cognitive function (Imahori, 2010). The reduction in α-KGDH activity is also responsible for the impaired brain metabolism; its activity being better correlated with the degree of cognitive impairment than the amount of SP or NFTs (Gibson et al., 1999). Interestingly, it was found that the loss of α-KGDH-enriched neurons is related with the total loss of neurons, suggesting a possible reason for the selective vulnerability in AD brain (Ko et al., 2001). COX deficiency was also found in the regions of brain that show histopathological damage in AD (Schapira, 1996). Finally, these mitochondrial respiratory enzymes are known to be highly susceptible to oxidative modification and are altered by exposure to a range of pro-oxidants (Tretter and Adam-Vizi, 2000).

Mitochondrial bioenergetic metabolism is highly reliant on Ca^{2+}. In the mitochondrial matrix, Ca^{2+} regulates the activity of dehydrogenases coupled to the TCA cycle (e.g. PDH and α-KGDH), promoting an enhanced respiratory chain activity (Gunter et al., 2000; Rizzuto et al., 2000). Mitochondrial matrix Ca^{2+} can also activate the F_0F_1-

ATPase, thus directly determining the rate of ATP production (Rizzuto et al., 2000; Territo et al., 2000). Conversely, mitochondrial Ca^{2+} overload can favor mPTP opening, resulting in mitochondrial depolarization, uncoupling of oxidative phosphorylation, overproduction of ROS, mitochondrial swelling and release of pro-apoptotic proteins to the cytosol. When mPTP opening is persistent and numerous mitochondria are continuously affected, neurons can no longer cope with the stress and apoptosis is initiated (Galluzzi et al., 2009). Persuasive evidence suggests that intracellular Ca^{2+} deregulation is involved in AD pathogenesis, and a sustained increase in cytosolic Ca^{2+} concentrations triggers neurodegeneration (Bezprozvanny and Mattson, 2008; LaFerla, 2002). Our results demonstrate that brain cortical mitochondria from icvSTZ rats have a reduced capacity for Ca^{2+} uptake and, consequently, increased susceptibility for mPTP opening when challenged with several exogenous Ca^{2+} pulses (Figs. 5.5A and 5.5B). This increased susceptibility was further confirmed by ultrastructural analyses. Indeed, mitochondria from icvSTZ rats are more "sensitive" to a Ca^{2+} insult reflected by a higher percentage of swollen mitochondria containing disrupted cristae (Fig. 5.6). Accordingly, it was previously reported that mitochondria isolated from fibroblasts of AD patients have reduced Ca^{2+} uptake compared to age-matched controls, suggesting an impaired Ca^{2+} buffering ability of mitochondria (Kumar et al., 1994). In the "cybrid model" of AD, increased basal Ca^{2+} levels and enhanced inositol 1,4,5-triphosphate (IP_3)-mediated Ca^{2+} release accompanied a decreased mitochondrial Ca^{2+} sequestration (Sheehan et al., 1997). Studies in transgenic models of fAD also show an increased susceptibility of mitochondrial permeability transition evidenced by increased expression and translocation of CypD, a key component of mPTP, and impaired mitochondrial Ca^{2+}-handling capacity (Du et al., 2008, 2011). The failure in the capacity of mitochondria

from icvSTZ rats to retain Ca^{2+} could be correlated with the observed decrease in both

PDH and α-KGDH activities (Figs. 5.4A and 5.4B). Notably, in the presence of the pair

oligomycin plus ADP that efficiently inhibits the mPTP, mitochondria from both

experimental groups are able to maintain $\Delta\Psi$m in the presence of Ca^{2+}, which indicates a

higher Ca^{2+} retention capacity (Figs. 5.5C and 5.5D). This is in accordance with previous

findings demonstrating an increased capacity of brain mitochondria to accumulate Ca^{2+}

by preincubating these organelles with oligomycin plus ADP (Brustovetsky and Dubinsky,

2000; Moreira et al., 2001, 2002, 2004a). Overall, it seems that an inauspicious shift in

the sensitivity of mitochondria to Ca^{2+} load may be one deleterious event underlying

mitochondrial dysfunction in this animal model of sAD.

Oxidative stress is another prominent pathogenic factor of AD that affects both

neuronal and peripheral cells (Cecchi et al., 2002; Zhu et al., 2005). Mitochondrial

abnormalities occurring in AD are believed to be a consequence of the complex nature

and genesis of oxidative damage to key mitochondrial components (Aliev et al., 2003;

Hirai et al., 2001). Mitochondrial oxidative damage impairs oxidative phosphorylation

efficiency, promoting an increased electron leak and, consequently, an increased

production of H_2O_2 potentiating oxidative stress and damage (Reddy and Beal, 2008). In

turn, increased levels of ROS may lead to alterations in mitochondrial morphology and

dynamics (Benard et al., 2007). It was proposed that oxidative stress coupled with

disrupted Ca^{2+} homeostasis and apoptosis underlie synaptic dysfunction and cognitive

decline in AD (Reddy and Beal, 2008). Aside from the decline in mitochondrial

bioenergetic function, we also observed a significant increase in mitochondrial oxidative

stress and damage in icvSTZ rats, characterized by a higher H_2O_2 production (Fig. 5.7A),

lipid peroxidation extent (Fig. 5.7B) and a significant decrease in the antioxidant defense

GSH (Fig. 5.8). It was previously shown that postmortem AD brain present increased lipid peroxidation levels, particularly in the temporal lobe, where histopathologic alterations are very noticeable (Lovell et al., 1995; Marcus et al., 1998; Palmer and Burns, 1994). In a similar fashion, Cardoso et al. (2004) documented increased lipid peroxidation in AD cybrids, which likely reflects enhanced ROS production in this *in vitro* model of AD. In the triple-transgenic mouse model of AD, increased extent of lipid peroxidation and decreased GSH levels were also documented (Resende et al., 2008). A negative correlation between the total antioxidant capacity and disease duration has been proposed in AD patients (Guidi et al., 2006). As a matter of fact, oxidative stress-mediated neuronal loss seems to be instigated by a decline in GSH, which acts as a scavenger of free radicals (Bains and Shaw, 1997). This is supported by evidence demonstrating altered GSH levels in specific regions of the central nervous system of AD patients (Gu et al., 1998). Therefore, the interplay among impaired mitochondrial bioenergetic metabolism, Ca^{2+} misregulation and oxidative damage may constitute a dangerous triangle underlying early mitochondrial abnormalities that occur in sAD.

Altogether, these results strongly suggest that functional and structural mitochondrial defects are mechanistically involved with the "insulin-resistant brain state" that characterizes this rat model of sAD, highlighting the central importance of mitochondrial (dys)function in the pathology of the disease. For these reasons, icvSTZ rats are a reliable tool to explore the mechanisms underlying sAD and evaluate the efficacy of potential therapeutic strategies.

CHAPTER 6

HYPOXIC PRECONDITIONING MEDIATES

NEUROPROTECTION IN A STZ-INDUCED RAT MODEL OF

SPORADIC ALZHEIMER'S DISEASE

6.1 ABSTRACT

Cerebral metabolic changes accompanying an "insulin-resistant brain state" have been hypothesized to form the core of the neurodegenerative events that occur in sAD pathology. This study was conducted to evaluate the effect of HP, one of the most powerful mechanisms of protection, on cognition, cerebral energy metabolism and oxidative status in the icvSTZ-induced model of sAD. For this purpose, male Wistar rats were randomly divided into four groups: 1- Control (sham operation/vehicle administration); 2- STZ (bilateral icv injection of STZ at a dose of 3mg/Kg); 3- HP [exposure to brief periods of moderate hypoxia (10% O_2 for 2 hours) during 3 consecutive days, followed by sham operation/vehicle administration]; 4- HP + STZ (as group 3, but submitted to icvSTZ injection). The severe deficits in learning and memory and the increased activity of AChE resulting from icvSTZ administration were antagonized by HP. HP was also able to significantly attenuate icvSTZ-induced increase in neuroinflammation and oxidative stress, as reflected by increased glial fibrillary acidic protein (GFAP) immunoreactiviy, nitrites, H_2O_2 and TBARS levels and a decrease in the antioxidant defenses. The energy hypometabolism and mitochondrial impairment induced by icvSTZ was also significantly prevented by HP. Mechanistically, mitochondrial-derived ROS and HIF-1α underlaid the pro-survival response triggered by HP. Collectively, these results demonstrate that the sAD-like features induced by icvSTZ administration can be effectively prevented by HP.

6.2 INTRODUCTION

AD is an age-related progressive neurodegenerative condition that affects approximately 35 million people worldwide and is the leading cause of dementia among the elderly (Castellani et al., 2010; Querfurth and LaFerla, 2010). Due to the increase in life expectancy and demographic changes in the population, AD is quickly becoming one of the major universal healthcare problems (Sloane et al., 2002). Currently, there is no cure for AD. So, it is of tremendous importance to provide new and feasible therapeutic targets and strategies capable of arresting or, at least, effectively modify the course of this disease.

Clinical signs of AD are manifested by a progressive decline in memory and cognitive function, and behavioral disturbances. From the neuropathological point of view, this disease is characterized by selective neuronal and synaptic loss in cortical and subcortical regions, deposition of extracellular SP, mainly composed of Aβ peptide, presence of intracellular NFTs containing hyperphosphorylated tau protein, and CAA (Moreira et al., 2009; Selkoe, 2001; Zlokovic, 2011). In general, there are two distinct forms of AD: fAD and sAD (Rocchi et al., 2003; Swerdlow, 2007). Despite the pathogenic road map leading to sAD pathology is still obscure, a large body of knowledge accumulated during the last decades suggests that brain insulin resistance contributes to the initiation and progression of the disease (Correia et al., 2011a). Human postmortem and animal studies revealed that sAD is associated with reduced brain IR density, and defective brain insulin signal transduction (Frolich et al., 1999; Lester-Coll et al., 2006; Moloney et al., 2010) Consistently, AD subjects also exhibit an early impairment in the brain glucose metabolism, fostering the idea that an abnormal brain insulin function occurs in sAD pathology (Azari et al., 1993; Silverman et al., 2001). In this context, the icv

injection of the diabetogenic drug STZ in rats brain has emerged as an experimental model of the early pathophysiological changes in sAD, since it induces an insulin resistant brain state, reproducing several behavioral, neurochemical and structural features that resemble those found in human sAD (Grunblatt et al., 2007; Salkovic-Petrisic and Hoyer, 2007).

Among the existing neuroprotective strategies, the preconditioning phenomenon is currently the strongest procedure to afford robust neuroprotection against lethal insults by triggering endogenous adaptive mechanisms (Correia et al., 2010a,b, 2011b). One well-established model to induce "brain tolerance" relies on the exposure to brief episodes of sublethal hypoxia, known as HP (Dirnagl et al., 2009). In this line, the present study was designed to test the hypothesis that HP is able to prevent the AD-like phenotype induced by the icv administration of STZ in rats. For this purpose, we investigated the potential protective effect of HP on 1) cognitive function, 2) astrogliosis, 3) brain energy/glucose metabolism, 4) brain mitochondrial bioenergetic function, and 5) oxidative status in icvSTZ rats. The results presented herein demonstrate the effectiveness of HP in the protection against the deleterious effects promoted by the icv administration of STZ. From a therapeutic perspective, these data provide the first clue that HP-related molecular mechanisms might be feasible targets for the design of strategies aimed at preventing or delaying sAD pathology.

6.3 RESULTS

6.3.1 HYPOXIC PRECONDITIONING PREVENTS ICVSTZ-INDUCED SPATIAL LEARNING AND MEMORY DEFICITS

In a first approach, the effects of icvSTZ administration and HP on spatial learning and memory were evaluated using the Morris water maze task. As shown in Fig. 6.1A, icvSTZ-treated rats exhibited significantly higher escape latencies (time to reach the platform), when compared with vehicle-treated controls, during the three training days. The cognitive decline in these animals was further confirmed in the retention trial, which showed that icvSTZ-treated rats spent less time in the target quadrant when compared with control sham-operated rats (Fig. 6.1B). HP significantly attenuated the icvSTZ-induced rise in escape latencies time during the acquisition trials and abrogated the icvSTZ-induced decrease in the time spent in the target quadrant on day 4 in the retention trial, reflecting a preventive effect of HP against icvSTZ-induced learning and memory deficits (Fig. 6.1). Notably, HP per se did not affect cognitive function in control rats (Fig. 6.1).

A
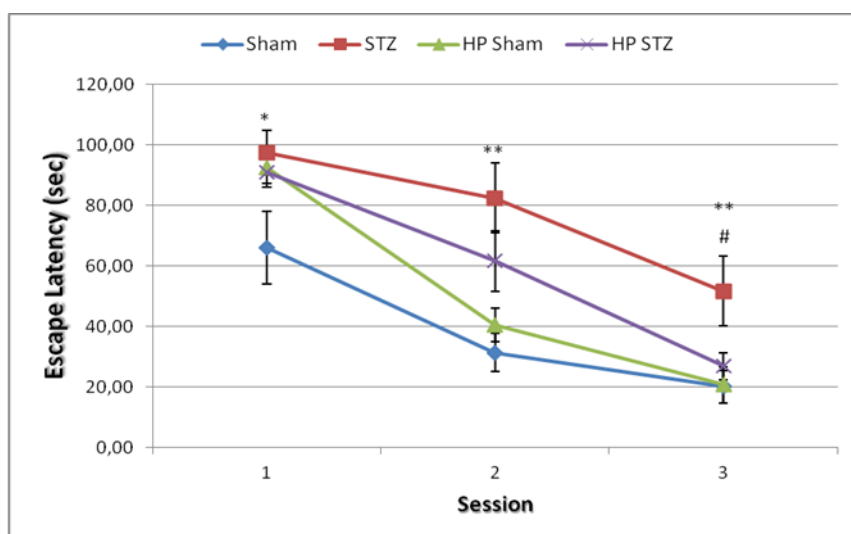
B
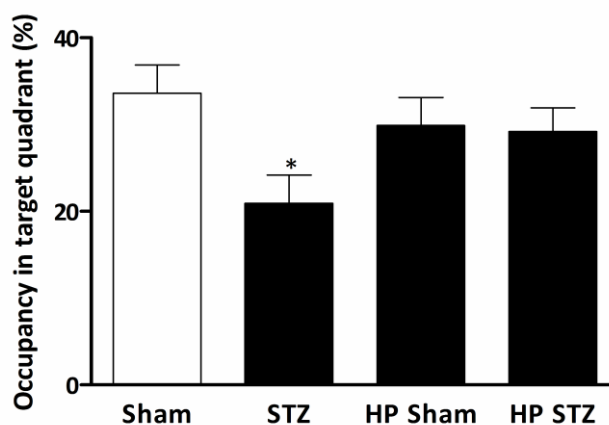
Figure 6.1. Effects of HP and icvSTZ administration on training (A) and retention (B) trials of the Morris water maze task. Data are the means ± SEM of 8-9 animals from each condition studied. Statistical significance: *$p<0.05$; **$p<0.01$ when compared with sham control rats; #$p>0.05$ when compared with preconditioned STZ (HP STZ) rats.

6.3.2 HYPOXIC PRECONDITIONING PREVENTS icvSTZ-INDUCED INCREASE IN AChE ACTIVITY

Since the cholinergic system influences cognitive function, we next examined the activity of brain cortical AChE. As shown in Fig. 6.2, icv administration of STZ in rats produced a significant increase in AChE activity when compared with control sham-operated rats. However, HP significantly inhibited the icvSTZ-induced rise in AChE activity (Fig. 6.2). Additionally, HP per se had no significant effect on AChE activity (Fig. 6.2).
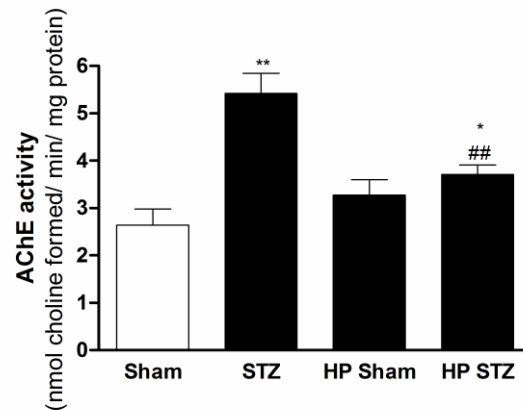
Figure 6.2. Effects of HP and icvSTZ administration on brain cortical AChE activity. Data are the means ± SEM of 5 animals from each condition studied. Statistical significance:*p<0.05; **p<0.01 when compared with sham control rats; ##p<0.01 when compared with icvSTZ rats.

6.3.3 HYPOXIC PRECONDITIONING PREVENTS ICVSTZ-INDUCED ASTROGLIOSIS

An invariant trait of AD is neuroinflammation, characterized by the presence of reactive astrogliosis. In order to explore the effects of icvSTZ administration and HP on astrogliosis extent, we performed double-immunostaining for NeuN (marker of differentiated mature neurons) and GFAP (marker of astrocytes). As shown in Fig. 6.3, immunohistochemistry analyses revealed that the icvSTZ administration promoted a robust increase in the intensity of GFAP-positive cells, an effect that was prevented by HP (Fig. 6.3).
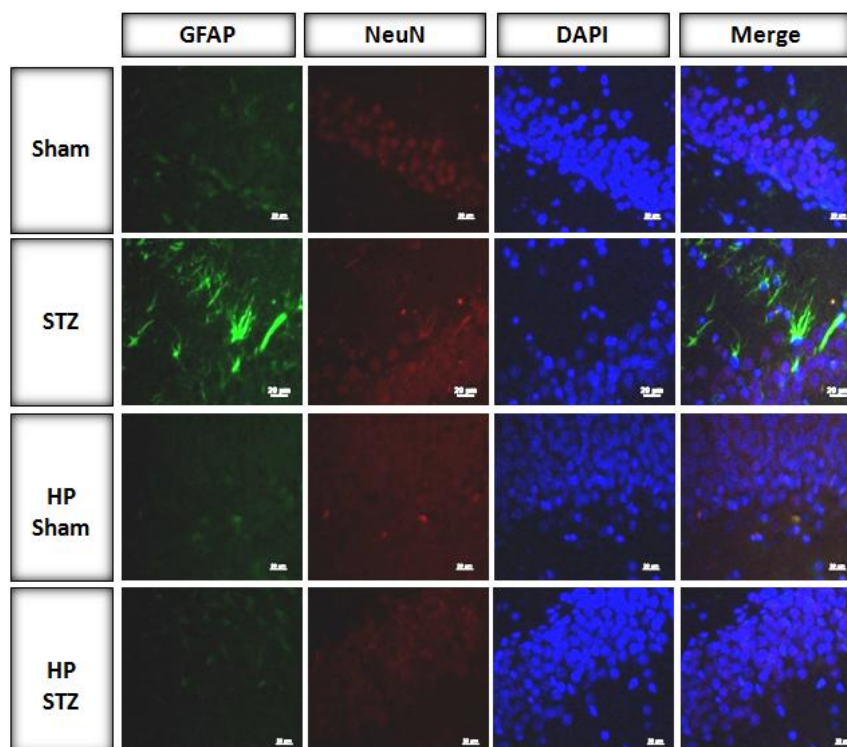
Figure 6.3. Effects of HP and icvSTZ administration on neuroinflammation. Representative fluorescence microscopy images of sagital brain sections immunostained with glial fibrillary acidic protein (GFAP, marker for astrocytes -green) and NeuN (marker of neurons -red) at 40x magnification. Nuclei were counterstained with DAPI (blue).

6.3.4 HYPOXIC PRECONDITIONING PREVENTS ICVSTZ-INDUCED IMPAIRED MITOCHONDRIAL ENERGY METABOLISM

Mitochondrial bioenergetic failure is a prominent feature of sAD pathology. We have previously observed that icvSTZ rats present mitochondrial abnormalities similar to those found in sAD. In the present study, we postulated that HP might prevent icvSTZ-induced mitochondrial deficits. To prove this, we first measured mitochondrial respiration in both freshly isolated brain cortical and hippocampal mitochondria exposed to NADH- and FADH$_2$-linked substrates; energization through mitochondrial complexes I and II, respectively. As shown in Table 6.1, HP prevented the icvSTZ-induced decrease in respiratory state 3, RCR, ADP/O ratio in brain cortical mitochondria energized with

glutamate/malate (substrates for complex I). HP also impeded the icvSTZ-induced reduction in RCR in hippocampal mitochondria energized with glutamate/malate (Table 6.2). Consistently, we found that HP avoided the decrease in RCR and ADP/O ratio in both brain cortical and hippocampal mitochondria from icvSTZ-treated rats energized with succinate (substrate for complex II) (Tables 6.1 and 6.2). All the other parameters remained statistically unchanged among the experimental groups. Overall, these findings indicate that HP prevents the impairment of mitochondrial respiration induced by icvSTZ administration.

TABLE 6.1 - EFFECTS OF HP AND ICVSTZ ON BRAIN CORTICAL MITOCHONDRIAL RESPIRATORY FUNCTION

		SHAM	STZ	HP SHAM	HP STZ
Complex I	**State 3** (nAtgO/min/mg)	93.58 ± 9.19	54.60 ± 5.14[**]	69.22 ± 5.64	78.02 ± 6.66
	State4 (nAtgO/min/mg)	27.55 ± 1.78	22.69 ± 1.46	23.18 ± 1.04	24.66 ± 1.89
	RCR	3.43 ± 0.24	2.56 ± 0.23[*]	3.14 ± 0.14	3.50 ± 0.17
	ADP/O (nmol ADP/AtgO/min/mg)	2.91 ± 0.17	2.08 ± 0.13[**]	2.98 ± 0.17	2.60 ± 0.11
Complex II	**State 3** (nAtgO/min/mg)	84.51 ± 7.24	64.39 ± 4.95	72.77 ± 5.15	81.60 ± 5.84
	State4 (nAtgO/min/mg)	26.34 ± 1.70	27.75 ± 2.71	23.74 ± 1.41	25.14 ± 1.35
	RCR	3.09 ± 0.09	2.34 ± 0.25 [#]	3.07 ± 0.12	3.30 ± 0.18
	ADP/O (nmol ADP/AtgO/min/mg)	2.28 ± 0.11	1.72 ± 0.13 [##]	2.25 ± 0.13	2.49 ± 0.11

Mitochondrial respiration parameters were evaluated in freshly isolated brain cortical mitochondrial fractions (0.8 mg) in 1 ml of the reaction medium energized with 5 mM glutamate/2.5 mM malate (Complex I) or with 5 mM succinate in the presence of 2 μM rotenone (Complex II). Data are the means ± SEM of 5 animals from each condition studied. Statistical significance: *p<0.05; **p<0.01, when compared with sham control brain cortical mitochondria energized with the substrate for complex I, glutamate/malate; #p<0.05; ##p<0.01 when compared with sham control brain cortical mitochondria energized with the substrate for complex II, succinate.

TABLE 6.2 - EFFECTS OF HP AND ICVSTZ ON HIPPOCAMPAL MITOCHONDRIAL RESPIRATORY FUNCTION

		SHAM	STZ	HP SHAM	HP STZ
Complex I	**State 3** (nAtgO/min/mg)	46.93 ± 7.08	32.90 ± 2.93	50.00 ± 7.75	46.70 ± 10.42
	State 4 (nAtgO/min/mg)	18.60 ± 1.88	20.35 ± 2.4	21.10 ± 2.4	16.40 ± 2.24
	RCR	2.70 ± 0.26	1.68 ± 0,21[*]	2.80 ± 0.17	2.77 ± 0.28
	ADP/O (nmol ADP/AtgO/min/mg)	2.32 ± 0.24	1.81 ± 0.21	2.41 ± 0.27	2.43 ± 0.40
Complex II	**State 3** (nAtgO/min/mg)	51.15 ± 7.43	33.35 ± 2.55	50.00 ± 7.75	46.70 ± 10.42
	State 4 (nAtgO/min/mg)	19.10 ± 2.73	21.33 ± 3.24	15.17 ± 1.90	16.88 ± 1.35
	RCR	2.68 ± 0.19	1.63 ± 0.17[#]	2.67 ± 0.28	2.75 ± 0.34
	ADP/O (nmol ADP/AtgO/min/mg)	2.01 ± 0.04	1.46 ± 0.18[#]	2.08 ± 0.12	2.13 ± 0.09

Mitochondrial respiration parameters were evaluated in freshly isolated hippocampal mitochondrial fractions (0.8 mg) in 1 ml of the reaction medium energized with 5 mM glutamate/2.5 mM malate (Complex I) or with 5 mM succinate in the presence of 2 μM rotenone (Compex II). Data are the means ± SEM of 5 animals from each condition studied. Statistical significance: *p<0.05 when compared with sham control hippocampal mitochondria energized with the substrate for complex I, glutamate/malate; #p<0.05 when compared with sham control hippocampal mitochondria energized with the substrate for complex II, succinate.

Additionally, we assessed the enzymatic activity of mitochondrial complex I, COX, and ATPase. As expected, icvSTZ administration promoted a significant decline in complex I, COX and ATPase activities, these decreases being prevented by HP (Fig. 6.4).
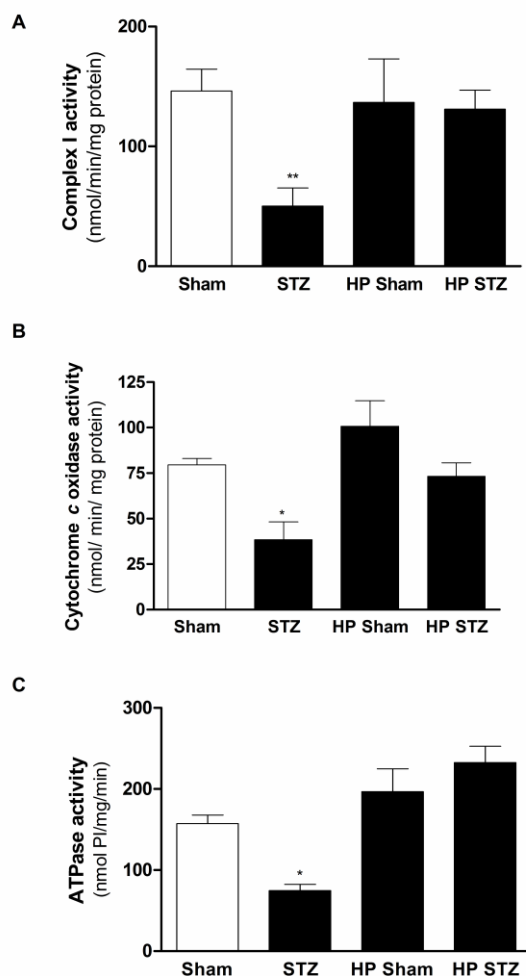
Figure 6.4. Effects of HP and icvSTZ administration on brain cortical mitochondrial enzymatic activities (A) Complex I, (B) Cytochrome *c* oxidase, and (C) ATPase. Data are the mean ± SEM of 5 animals from each condition studied. Statistical significance: *p<0.05;**p<0.01 when compared with sham control rats.

To gain further insight into the effects of icvSTZ administration and HP on brain mitochondrial energy metabolism we evaluated the activity of some enzymes of the TCA cycle. As shown in Table 6.3, diminished aconitase, PDH, α-KGDH and IDH activities occurred in the cortex of icvSTZ-treated rats, when compared with the vehicle-treated control rats. On the other hand, a significant increase in MDH activity was found in icvSTZ-treated rats (Table 6.3). Notably, HP completely abrogated the alterations induced by icvSTZ administration (Table 6.3).

Due to sample limitations, we were unable to evaluate the activities of these enzymes in hippocampal mitochondria.

TABLE 6.3 - EFFECTS OF HP AND ICVSTZ ON THE ACTIVITIES OF TCA CYCLE ENZYMES

	SHAM	STZ	HP SHAM	HP STZ
Pyruvate dehydrogenase (nmol/min/mg protein)	47.7 ± 5.33	25.9 ± 2.17 [*]	44.3 ± 4.93	41.3 ± 5.16 [#]
Aconitase (U/min/mg protein)	135.1 ± 27.49	61.9 ± 2.66 [**]	174.6 ± 31.80	204.4 ± 12.67 [##]
Isocitrate dehydrogenase (nmol/min/mg protein)	37.2 ± 3.81	19.2 ± 3.51 [*]	30.4 ± 1.76	32.5 ± 2.95 [#]
α-Ketoglutarate dehydrogenase (nmol/min/mg protein)	72.9 ± 5.38	24.4 ± 2.75 [**]	46.3 ± 10.83	68.3 ± 7.47 [##]
Malate dehydrogenase (nmol/min/mg protein)	264.8 ± 22.12	375.0 ± 21.99 [**]	304.1 ± 23.55	324.4 ± 19.79

Data are the mean ± SEM of 5 animals from each condition studied. Statistical significance: *$p<0.05$; **$p<0.01$ when compared with sham control rats; #$p>0.05$; ## $p<0.01$ when compared with icvSTZ-treated rats.

6.3.5 HYPOXIC PRECONDITIONING PREVENTS ICVSTZ-INDUCED ALTERED ACTIVITY OF GLYCOLYTIC ENZYMES

Because glycolysis, TCA cycle and mitochondrial respiration are coupled processes; the next step was to evaluate the activity of some key glycolytic enzymes. A marked increase in brain cortical LDH activity was detected in icvSTZ-treated rats (Table 6.5), when compared with vehicle-treated control rats. Conversely, icvSTZ rats exhibited a significant decrease in the activities of hexokinase and glucose-6P dehydrogenase enzymes (Table 6.4), suggesting an impaired cerebral glucose metabolism. Again, HP was

153

able to counteract the effects of icvSTZ administration in the activity of these glucose-metabolizing enzymes (Table 6.4).

Due to sample limitations we were unable to evaluate the activities of these enzymes in hippocampal samples.

TABLE 6.4 - EFFECTS OF HP AND icvSTZ ON THE ACTIVITIES OF GLYCOLYTIC ENZYMES

	SHAM	STZ	HP SHAM	HP STZ
Lactate dehydrogenase (µmol/min/mg protein)	8.1 ± 0.35	11.3 ± 0.58[**]	6.9 ± 1.35	8.0 ± 0.90[#]
Hexokinase (nmol/min/mg protein)	133.5 ± 5.25	87.6 ± 11. 88[**]	121.6 ± 12.97	140.8 ± 11.69[#]
Glucose-6P-dehydrogenase (nmol/min/mg protein)	82.0 ± 4.08	48.9 ± 4.41[**]	66.9 ± 13.14	73.8 ± 5.24[##]

Data are the mean ± SEM of 5 animals from each condition studied. Statistical significance: **$p<0.01$ when compared with sham control rats; #$p>0.05$; ##$p<0.01$ when compared with icvSTZ-treated rats.

6.3.6 HYPOXIC PRECONDITIONING PREVENTS icvSTZ-INDUCED OXIDATIVE IMBALANCE AND DAMAGE

Mitochondrial dysfunction potentiates oxidative damage in AD pathology, leading to a self-perpetuating vicious cycle. Thus, we next examined the impact of icvSTZ administration and HP on oxidative stress markers and non-enzymatic and enzymatic antioxidant defenses. When compared with control sham-operated rats, icvSTZ-treated rats exhibited a significant increase in brain cortical levels of nitrites (Fig. 6.5A), H_2O_2 (Fig. 6.5B) and TBARS (Fig. 6.5C), an indicator of lipid peroxidation extent. All these alterations were efficiently prevented by HP (Fig. 6.5).
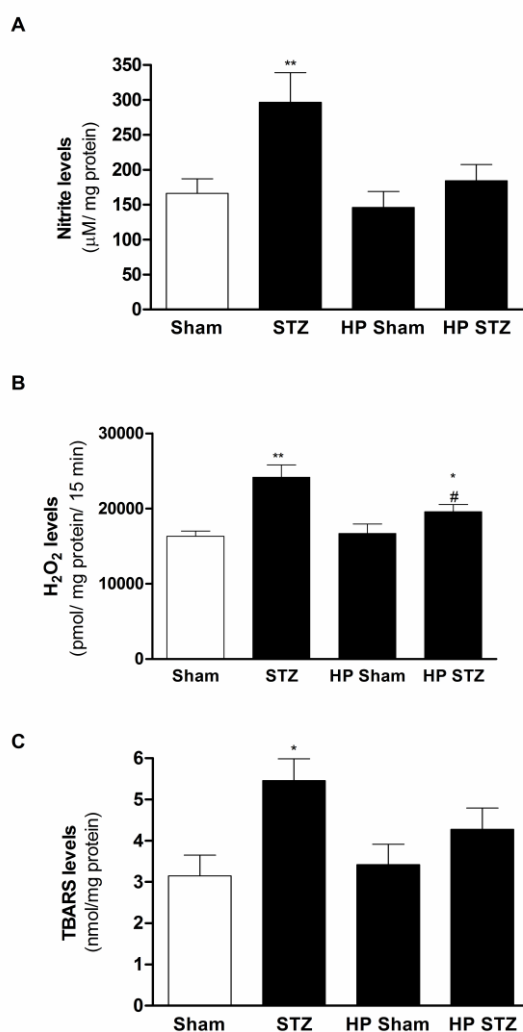
Figure 6.5. Effects of HP and icvSTZ administration on oxidative markers (A) nitrites (B) H$_2$O$_2$, and (C) TBARS levels. Data are the mean ± SEM of 5 animals from each condition studied. Statistical significance: *p<0.05;**p<0.01 when compared with sham control rats; # p<0.05 when compared with icvSTZ-treated rats .

Concerning the non-enzymatic antioxidant defenses, icvSTZ-treated rats presented a significant reduction in brain cortical GSH content, an effect that was significantly prevented by HP (Fig. 6.6A). Interestingly, it was observed a significant

increase in Vitamin E levels in icvSTZ-treated rats, when compared with control sham-operated rats, which was partially prevented by HP (Fig. 6.7).
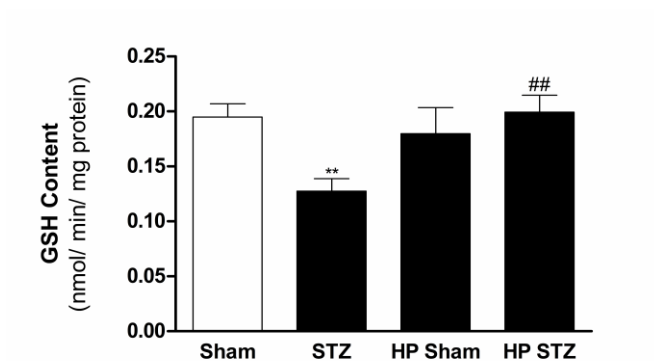
Figure 6.6. Effects of HP and icvSTZ administration on GSH content. Statistical significance: **$p<0.01$ when compared with sham control rats; ## $p<0.01$ when compared with icvSTZ-treated rats.
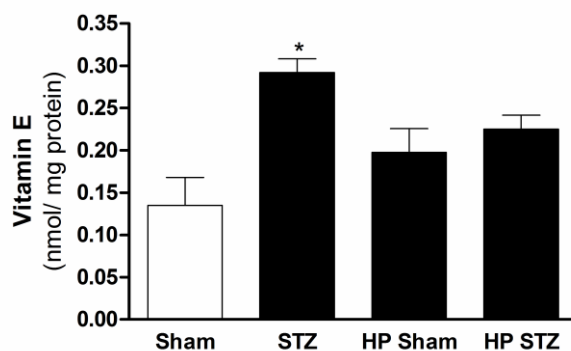
Figure 6.7. Effects of HP and icvSTZ administration on vitamin E levels. Statistical significance: *$p<0.05$ when compared with sham control rats.

icvSTZ administration also promoted a significant decrease in the activity of GRed (Fig. 6.8A) and catalase (Fig. 6.8C) and an increase in GPx (Fig. 6.8B) activity. HP prevented the decrease in the activity of GRed (Fig. 6.8A) and catalase (Fig. 6.8C) enzymes.

Again, and due to sample limitations, we were unable to evaluate these parameters in hippocampal samples.
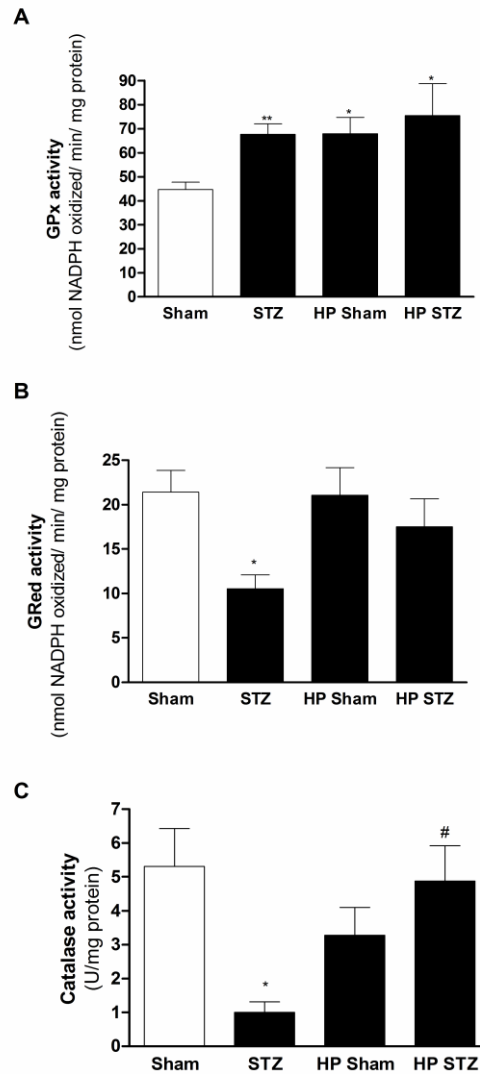
Figure 6.8. Effects of HP and icvSTZ administration on (A) GPx, (B) GRed, and (C) catalase activities. Statistical significance: *p<0.05;**p<0.01 when compared with sham control rats; #p<0.05 when compared with icvSTZ-treated rats.

6.3.7 THE PROTECTIVE EFFECTS EXERTED BY HYPOXIC PRECONDITIONING ARE MEDIATED BY HYDROGEN PEROXIDE AND HIF-1α ACTIVATION

Since mitochondrial ROS have been identified as signaling molecules that actively participate in the preconditioning phenomenon, we next evaluated the impact

of HP on H_2O_2 rate production in both brain cortical and hippocampal mitochondria. As shown in Figure 6.9, HP resulted in a significant increase in H_2O_2 levels in hippocampal mitochondria immediately after the last hypoxic episode, which progressively decline reaching the control levels at 24 hours after the last hypoxic episode (Fig. 6.9B). In brain cortical mitochondria, a slight increase in H_2O_2 levels was also observed immediately after the last hypoxic episode (Fig. 6.9A).
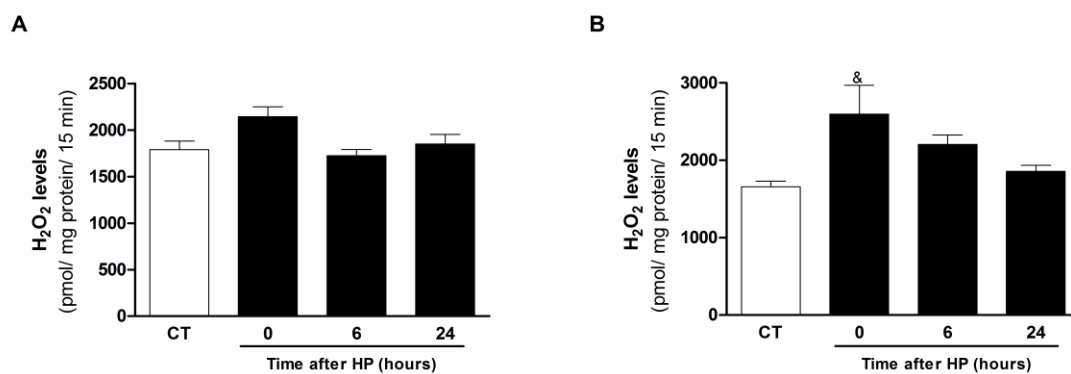
Figure 6.9. Effects of HP on (A) brain cortical and (B) hippocampal mitochondrial H_2O_2 levels. H_2O_2 levels were measured as described in Material and Methods. Data are the means ± SEM of 5 animals from each condition studied. Statistical significance: $\&p<0.05$ when compared with control brain hippocampal mitochondria.

Prompted by these findings, we investigated HIF-1α activation since this transcription factor is considered to be the master regulator of preconditioning-triggered adaptive responses. As shown in Figure 6.10, immediately after the last episode of hypoxia, HIF-1α activation was significantly increased in the hippocampus while a modest increase in HIF-1α activation was observed in brain cortex.
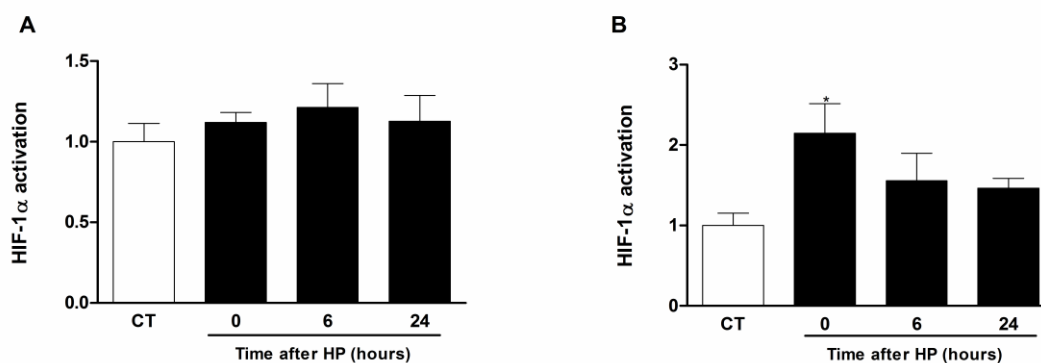
Figure 6.10. Effects of HP on HIF-1α activation in the (A) brain cortex and (B) hippocampus. HIF-1α DNA binding was detected by ELISA. Statistical significance: *$p<0.05$ when compared with hippocampus from control rats.

6.4 DISCUSSION

The cyclic exposure to moderate hypoxia with intervening periods of normoxia has been shown to increase brain resistance against subsequent injurious insults. Meanwhile, less is known about the potential protective effects of HP in AD pathology. In this context, data derived from this study provide evidence that HP prevents the AD-like features induced by icvSTZ administration such as memory and learning deficits, cerebral hypometabolism, mitochondrial abnormalities and oxidative imbalance and damage. Mechanistically, immediately after the last hypoxic episode, an increase in mitochondrial H_2O_2 levels and HIF-1α activation in both brain cortex and hippocampus occur. This is in agreement with our working hypothesis that states that preconditioning triggers adaptive mechanisms, by immediate stimulation of mitochondrial ROS production and concomitant induction of HIF-1α signaling pathway, thereby sustaining brain integrity and functionality.

The impairment of memory is the cardinal and one of the earliest clinical symptoms of AD pathology (Kawas and Corrada, 2006). The icv administration of STZ in

rats produced an impairment in the acquisition and retrieval of memory, as reflected by the higher escape latencies to reach the hidden platform (Fig. 6.1A) and the decrease in the time spent in the target quadrant in the retention trial (Fig. 6.1B). These results are consistent with previous reports demonstrating that the bilateral icv administration of STZ caused learning and memory deficits (Ishrat et al., 2009a,b; Lannert and Hoyer, 1998; Tota et al., 2011). Notably, HP prevented the memory and learning deficits in icvSTZ-treated rats, as demonstrated by the reduction of escape latencies (Fig. 6.1A) and the increase in the percentage of time spent in the target quadrant (Fig. 6.1B). It was previously demonstrated that HP attenuated memory and learning impairments resulting from severe cerebral ischemia (Rybnikova et al., 2005), these effects being related with HP-induced neurogenesis in the hippocampal dentate gyrus (Zhu et al., 2005) and up-regulation of c-Fos, a transcription factor strongly implicated in memory formation (Rybnikova et al., 2009). The deterioration of the cortical cholinergic system is also related with memory failure and cognitive decline in AD (Coyle et al., 1983, Mesulam, 1996). Our icvSTZ-treated rats exhibited a robust increase in brain cortical AChE activity, which was partially prevented by HP (Fig. 6.2). This observation suggests that HP might preserve cognitive abilities in icvSTZ-treated rats, in part by maintaining the functional integrity of the cortical cholinergic system. In agreement, a previous study also demonstrated that HP promoted AChE inhibition and maintenance of ACh levels, which contributed for cell survival (Schetinger et al., 1999).

Glial cells and their resident GFAP integrate neuronal input, modulate synaptic activity and process signals related to learning and memory (Kurosinski and Götz, 2002). Acute and chronic brain insults trigger a specific glial reaction, generally known as reactive astrogliosis, represented by a complex morphofunctional remodelling of

astrocytes (Pekny and Nilsson, 2005). In AD, cognitive impairment due to a severe loss of synapses and neurons is generally believed to be associated with increased GFAP expression in activated astrocytes (Braak et al., 1999; Finch, 2003). Our immunohistochemistry analyses revealed that HP was able to prevent the robust reactive astrogliosis induced by the icv administration of STZ (Fig. 6.3). Accordingly, previous reports documented the ability of preconditioning to attenuate the inflammatory response in the brain during ischemia (Rosenzweig et al., 2004; Lin et al., 2009).

Multiple levels of analysis and experimental paradigms indicate that abnormal glucose metabolism and mitochondrial function are consistent antecedents to the development of AD pathology (Correia et al., 2012a; Gibson and Shi, 2010; Nicholson et al., 2010). As a matter of fact, a decline in brain glucose metabolism and mitochondrial function can appear decades prior to the onset of the histopathological and/or clinical features of AD (Mosconi et al., 2008, 2009, 2011; Reiman et al., 2004). In agreement, the icv administration of STZ induced an impairment of the mitochondrial respiration in both brain cortex and hippocampus (Tables 6.1 and 6.2), accompanied by a drastic alteration in the activity of mitochondrial electron transport chain (Fig. 6.4), TCA cycle (Table 6.3) and glycolytic enzymes (Table 6.4). Remarkably, HP was able to preserve brain mitochondrial function. In accordance, Dave and collaborators (2001) reported that ischemic preconditioning preserved mitochondrial function after cerebral ischemia by maintaining the integrity of mitochondrial oxidative phosphorylation. Subsequent studies also documented that ischemic preconditioning protected mitochondrial energy metabolism during brain ischemia (Perez-Pinzon et al., 2002; Zhang et al., 2003). But, how preconditioning protects mitochondria? One possible explanation could be the up-

regulation of genes related with mitochondria function. For instance, anoxia-induced resistance is associated to the up-regulation of the genes for NADH–ubiquinone oxidoreductase subunit 5 and COX subunit 1, both encoded by mitochondrial genes (Cai and Storey, 1996). Besides the direct effects on mitochondrial function, preconditioning prevented cytochrome *c* release from the mitochondria by maintaining ATP levels (Nakatsuka et al., 1999) and inhibited the translocation of p53 to mitochondria, avoiding mitochondrial-mediated neuronal death (Racay et al., 2007).

Mitochondrial bioenergetics decline is often closely associated with increased free radical production and consequent oxidative stress and damage. Mounting evidence has demonstrated the involvement of oxidative stress during the course of AD (Moreira et al., 2009). Exacerbated free radicals generation and oxidative stress occur before the formation of SP and NFTs, which are partially responsible for memory deficits and hence behavioral impairments in AD (Gibson and Huang, 2005; Guglielmotto et al., 2010; Sultana and Butterfield, 2010; Zafrilla et al., 2006). Data derived from this study demonstrate that icvSTZ-treated rats exhibited increased levels of oxidative markers, including nitrites (Fig. 6.5A), H_2O_2 (Fig. 6.5B), and TBARS (Fig. 6.5C) levels. Moreover, icv administration of STZ promoted an imbalance in both non-enzymatic (Figs. 6.6 and 6.7) and enzymatic (Fig. 6.8) antioxidant defenses. Once again, we found that HP was efficient in preventing both oxidative imbalance and damage. It was previously shown that HP attenuated oxidative damage by upregulating the antioxidant defense system, and attenuating the apoptotic process (Lin et al., 2002; Wang et al., 2005). Omata and collaborators (2006) documented that HP-mediated upregulation of antioxidant enzymes was region-specific, with an elevation of copper-zinc-containing superoxide dismutase (Cu-Zn SOD) and Mn SOD being observed only in the frontal cortex.

The precise mechanisms underlying HP-mediated endogenous neuroprotection remain unclear however, we believe that the induction of the transcription factor HIF-1α mediated by mitochondrial ROS during the HP could represent the master regulator event responsible for the establishment of an adaptive response that increases brain tolerance. Our study revealed that HP resulted in a significant increase in mitochondrial H_2O_2 levels (Fig. 6.9B) and HIF-1α activation (Fig. 6.10B), which were more relevant in the hippocampus (Figs. 6.9A and 6.10A). It is known that physiological concentrations of ROS act as signaling molecules and these species are also recognized as master integrators of preconditioning-mediated endogenous protection (Correia et al., 2010a). Consistent with our results, intermittent hypoxia was found to increase ROS levels in the brain (Jung et al., 2008). Moreover, the administration of the antioxidant NAC during the intermittent hypoxic sessions abrogated the protective effects induced by intermittent hypoxia, suggesting that ROS play a pivotal role in producing brain tolerance (Jung et al., 2008).

We also evaluated the activation of HIF-1α because this transcription factor is a cellular oxygen-sensing, and thereby the central regulator of the hypoxia-mediated adaptive response (Semenza, 2012). Furthermore, under hypoxic conditions, HIF-1α activation was modulated by mitochondrial-derived ROS (Bell et al., 2007), which reinforces the existence of a crosstalk between mitochondrial-derived ROS and HIF-1α in the preconditioning phenomenon. Data from our laboratory also demonstrated that mitochondrial preconditioning induced by cyanide renders brain endothelial and neuronal cells resistant against glucotoxicity, through an adaptive response mediated by mitochondrial-derived ROS and HIF-1α signaling pathway (Correia et al., 2012b). Conversely, the protective effects mediated by cyanide preconditioning were absent in

ρ0 cells and completely abrogated by pre-treating cells with the specific HIF-1α inhibitor 2-ME2, and the antioxidant NAC (Correia et al., 2012b), fostering the crucial involvement of both mitochondrial-derived ROS and HIF-1α in preconditioning-triggered tolerance. Additionally, it was also shown that HIF-1α modulated mitochondrial function and oxygen consumption by increasing the expression of COX subunit 4 to optimize oxidative phosphorylation efficiency (Fukuda et al., 2007). During preconditioning, HIF-1α was also shown to increase the expression and activity of glucose transporters (GLUT1 and GLUT3) and glycolytic enzymes (Jones and Bergeron, 2001) that could represent a mechanism by which HP prevents icvSTZ-induced impaired brain glucose metabolism.

In conclusion, the present study shows that HP exerts powerful neuroprotective effects against icvSTZ-induced sAD-like features. Future studies must be done to explore the mechanisms underlying HP-mediated endogenous neuroprotection, which may have significant implications for the development of novel therapeutic strategies for AD.

CHAPTER 7

TIME COURSE OF THE BRAIN MITOCHONDRIAL

ADAPTIVE RESPONSE TO HYPOXIC PRECONDITIONING

7.1 ABSTRACT

Brief episodes of sublethal hypoxia reprogram brain response to face subsequent lethal stimuli by triggering adaptive and pro-survival mechanisms - a phenomenon denominated by HP. Given the importance of mitochondria in determining cells fate, the present study was devoted to monitor the structural and functional alterations of brain mitochondria in response to a well-established protocol of HP induced by the cyclic exposure to moderate hypoxia (2 hours of 10% O_2) with intervening 24 hours reoxygenation periods, during 3 consecutive days. Therefore, several parameters related with mitochondrial bioenergetic function, biogenesis, and fusion and fission machinery were evaluated in the cortex and hippocampus of adult rats immediately, 6 and 24 hours after the last hypoxic session. HP induced a decrease in respiratory state 2 and an increase in ADP/O ratio in both brain cortical and hippocampal mitochondria. HP also promoted an increase in total ATP content and NAD^+/NADH ratio in brain cortex and hippocampus. Immediately after the last hypoxic episode, a significant increase in the protein levels of nuclear respiratory factor-1 (NRF-1), and mitochondrial transcription factor A (TFAM) was observed. After 24 hours after the last hypoxic episode, a shift in the mitochondrial fusion-fission balance towards fusion occurred, as evidenced by the significant increase in OPA1 protein levels and a decrease in DRP1 protein levels in the cortex, and the significant reduction in the Fis1 protein levels in the hippocampus. Consistently, the electron microscopy analysis revealed that HP generated mitochondria with an elongated phenotype in both brain cortex and hippocampus. Taken together, these results indicate that HP enhances mitochondrial bioenergetic function, probably due to a coordinated interplay between mitochondrial biogenesis and fusion/fission events, increasing brain tolerance.

7.2 INTRODUCTION

HP is a biological paradigm that provides insight into the multivalent protective responses in the brain (Dirnagl et al., 2003; Gidday, 2006; Ran et al., 2005). Mounting evidence demonstrates that cyclic exposure to mild hypoxia with intervening periods of normoxia bolsters brain resistance against noxious stimuli (Bernaudin et al., 2002; Prass et al., 2003; Sharp et al., 2004). The induction of brain tolerance is accompanied by substantial alterations in gene expression and activates several intracellular signaling pathways, which indicates that the preconditioning stimulus arouses a fundamental genomic reprogramming of brain cells that confers protection and survival against subsequent potentially lethal stimuli (Dirnagl et al., 2009; Gidday, 2006; Pignataro et al., 2009). A key regulator of the genomic response mediated by HP is the transcription factor HIF-1α (Semenza, 2000). When activated, this transcription factor modulates the expression of several protective target genes involved in energy metabolism, angiogenesis, erythropoiesis and cell survival (Correia and Moreira, 2010).

Mitochondria are ubiquitious and highly dynamic organelles that orchestrate an extensive repertoire of vital cellular functions, and it is recognized that the strict regulation of mitochondrial structure, function and turnover is an immutable control node for the maintenance of brain integrity and homeostasis (Correia et al., 2011b). These fascinating organelles have been proposed to be master regulators of preconditioning-triggered brain tolerance (Busija et al., 2008). As a matter of fact, mitochondria have been implicated in the transduction of the hypoxic signal, mitochondria-derived ROS being the putative signaling molecules between a cellular O_2-sensor and HIF-1α (Acker, 2005). Evidence from the literature also revealed that

transient exposure of mitochondria to physiological or pathological stimuli, intracellular events, or pharmacological agents, induces mitochondrial changes that ultimately protect neuronal cells and their mitochondria against a variety of lethal insults (Duchen, 2004; Perez-Pinzon et al., 2005). In light of this evidence, it has been proposed that mitochondria constitute a convergence point in the preconditioning paradigm (Correia et al., 2011b).

Previously, we reported the requirement of both functional mitochondria and mitochondrial-derived ROS in an *in vitro* preconditioning-mediated brain endothelial and neuronal cells protection (Correia et al., 2012b). Also, the preservation of mitochondrial function by HP was observed in a STZ-induced rat model of sAD. However, a deeper knowledge on the mitoprotective mechanisms underlying the preconditioning phenomenon is still needed. To further clarify the participation of brain mitochondria in the preconditioning process, this study was conducted to appraise the behavior of mitochondria after HP. Thus, both time- and region-dependent mitochondrial adaptive responses triggered by HP were analyzed in the adult rat brain. Our HP protocol involves repetitive moderate hypoxia and reoxygenation, i.e., 10% O_2 for 2 hours intercalated with 24 hours of reoxygenation, during three consecutive days. The mitochondrial analyses were performed immediately, 6 and 24 hours after the last hypoxic episode. We evaluated the respiratory chain [respiratory states 3 and 4, RCR, and ADP/O ratio], oxidative phosphorylation system [ΔΨm, ADP-induced depolarization, repolarization level, and repolarization lag phase], tissue ATP levels and NAD^+/NADH ratio, and the expression of mitochondrial biogenesis-related proteins [NRF-1 and -2, TFAM, and peroxisome proliferator-activated receptor coactivator-1α (PGC-1α)] and mitochondrial

shaping proteins (Mnf1 and 2, OPA1, DRP1, and Fis1) in both brain cortex and hippocampus.

7.3 RESULTS

7.3.1 CHARACTERIZATION OF THE EXPERIMENTAL ANIMALS

As shown in Table 7.1, HP, characterized by repetitive moderate hypoxia and reoxygenation, did not alter peripheral blood glucose levels, body or brain weight, in comparison with control rats.

TABLE 7.1 – CHARACTERIZATION OF EXPERIMENTAL ANIMALS

		TIME AFTER HP (HOURS)		
	CONTROL	0	6	24
Blood glucose levels (mg/dL)	127.0 ± 8.08	118.4 ± 3.09	110.6 ± 4.16	116.2 ± 3.43
Body weight (g)	303.5 ± 4.14	305.5 ± 8.22	301.3 ± 7.73	306.6 ± 7.06
Brain weight (g)	2.13 ± 0.03	2.11 ± 0.04	2.09 ± 0.04	2.05 ± 0.04

Data are the mean ± SEM of 5 animals from each condition studied.

7.3.2 HYPOXIC PRECONDITIONING ENHANCES BRAIN CORTICAL AND HIPPOCAMPAL RESPIRATORY CHAIN FUNCTION

To investigate whether HP affects brain mitochondrial bioenergetics, we firstly evaluated the effect of repetitive moderate hypoxia and reoxygenation on mitochondrial respiratory chain function. As shown in Table 7.2, a time-dependent decrease in mitochondrial respiration state 2 was observed in both brain cortical and hippocampal mitochondria after HP, reaching statistical significance at 24 hours after the last hypoxic episode. At the same time point, a significant increase in ADP/O ratio in both brain cortical and hippocampal mitochondria (Table 7.2) was also observed. Additionally, at 6 hours after the last hypoxic episode, hippocampal mitochondria also exhibited a significant increase in RCR and ADP/O ratio and a significant decrease in oligomycin-

inhibited respiration (Table 7.2). All the other parameters remained statistically unchanged.

TABLE 7.2 – EFFECT OF HP ON BRAIN CORTICAL AND HIPPOCAMPAL MITOCHONDRIA RESPIRATORY FUNCTION

			TIME AFTER HP (HOURS)		
		CONTROL	0	6	24
CORTEX	State 2 (nAtgO/min/mg)	35.91 ± 2.85	29.41 ± 2.25	27.55 ± 2.33	22.82 ± 2.23[**]
	RCR	3.12 ± 0.28	3.38 ± 0.15	3.45 ± 0.26	3.05 ± 0.19
	ADP/O (nmol ADP/AtgO/min/mg)	2.21 ± 0.14	2.28 ± 0.04	2.02 ± 0.1	2.89 ± 0.13[**]
	Oligomycin-inhibited respiration (nAtgO/min/mg)	32.27 ± 3.51	32.37 ± 2.54	30.79 ± 1.57	31.48 ± 1.37
	FCCP-stimulated respiration (nAtgO/min/mg)	97.9 ± 10.25	109.4 ± 12.86	110.2 ± 4.50	89.2 ± 4.04
HIPPOCAMPUS	State 2 (nAtgO/min/mg)	26.36 ± 2.68	33.05 ± 1.86	25.81 ± 2.26	22.35 ± 2.02[&]
	RCR	2.46 ± 0.51	3.16 ± 0.19	3.82 ± 0.21[&]	2.68 ± 0.20
	ADP/O (nmol ADP/AtgO/min/mg)	2.20 ± 0.25	3.27 ± 0.28	3.39 ± 0.26	4.46 ± 0.25[&&&]
	Oligomycin-inhibited respiration (nAtgO/min/mg)	42.50 ± 6.98	33.37 ± 2.14	24.55 ± 3.64[&]	27.70 ± 2.31
	FCCP-stimulated respiration (nAtgO/min/mg)	93.8 ± 5.40	106.0 ± 7.41	103.9 ± 15.00	86.9 ± 5.64

Mitochondrial respiration parameters were evaluated in freshly isolated brain cortical and hippocampal mitochondrial fractions (0.8 mg) in 1 ml of the reaction medium energized with 5 mM succinate in the presence of 2 μM rotenone. Data are the means ± SEM of 5 animals from each condition studied. Statistical significance: **$p < 0.01$ when compared with control cortical mitochondria; &$p < 0.05$; &&& $p < 0.001$ when compared with control hippocamplal mitochondria.

7.3.3 Hypoxic Preconditioning Does Not Affect Brain Cortical And Hippocampal Oxidative Phosporylation System Efficiency

To gain further insights into the effect of repetitive moderate hypoxia and reoxygenation on brain mitochondrial bioenergetics, we next evaluated the parameters of the oxidative phosphorylation system of brain cortical and hippocampal mitochondria. As shown in Table 7.3, no statistical differences were found in oxidative phosphorylation system parameters of both brain cortical and hippocampal mitochondria energized with succinate (substrate for complex II) among the four experimental groups. Only a modest, but not statistically significant, increase in ΔΨm and a decrease in the repolarization lag phase were observed in both brain cortical and hippocampal mitochondria at 24 hours after the last hypoxic episode, when compared with the respective control mitochondria (Table 7.3).

TABLE 7.3 – EFFECT OF HP ON BRAIN CORTICAL AND HIPPOCAMPAL OXIDATIVE PHOSPORYLATION SYSTEM

			TIME AFTER HP (HOURS)		
		CONTROL	0	6	24
CORTEX	**ΔΨm** (−mV)	207.3 ± 5.03	207.0 ± 2.87	215.7 ± 0.63	212.5 ± 3.02
	ADP-induced depolarization (-mV)	26.5 ± 0.62	26.4 ± 1.26	25.7 ± 0.61	25.6 ± 0.52
	Repolarization level (−mV)	209.5 ± 5.35	209.9 ± 3.05	218.5 ± 0.75	215.3 ± 2.89
	Repolarization lag phase (min)	0.71 ± 0.08	0.65 ± 0.06	0.69 ± 0.02	0.65 ± 0.02
HIPPOCAMPUS	**ΔΨm** (−mV)	199.5 ± 1.74	201.7 ± 2.93	207.2 ± 3.51	211.4 ± 6.88
	ADP-induced depolarization (-mV)	18.2 ± 2.09	17.6 ± 0.68	16.9 ± 1.02	18.7 ± 2.76
	Repolarization level (−mV)	210.0 ± 6.66	204.8 ± 3.14	210.3 ± 3.52	214.0 ± 6.71
	Repolarization lag phase (min)	1.06 ± 0.16	1.09 ± 0.08	1.16 ± 0.13	0.97 ± 0.18

The oxidative phosphorylation system parameters were evaluated in freshly isolated brain cortical and hippocampal mitochondria (0.8 mg) in 1 ml of the reaction medium supplemented with 3 µM TPP^+ and energized with 5 mM succinate in the presence of 2 µM rotenone. Data are the means ± SEM of 5 animals from each condition studied.

7.3.4 HYPOXIC PRECONDITIONING INCREASES BRAIN CORTICAL AND HIPPOCAMPAL ATP LEVELS AND NAD^+/NADH

Since brain cells generate most of the energy in the form of ATP through the oxidative phosphorylation system by the oxidation of NADH (and $FADH_2$-linked substrates), we next determined the impact of HP on total brain cortical and hippocampal ATP content and NAD^+/NADH ratio, two key indicators of the cellular energetic status and redox state. As shown in Figure 7.1, a significant increase in total ATP at all tested time points in the brain cortex and immediately and 6 hours after the last hypoxic episode in the hippocampus was observed (Fig. 7.1). An increase in the

NAD$^+$/NADH ratio was observed at all time points, although only statistically significant immediately (in brain cortex) and 24 hours (both in brain cortex and hippocampus) after the last hypoxic episode (Fig. 7.2).
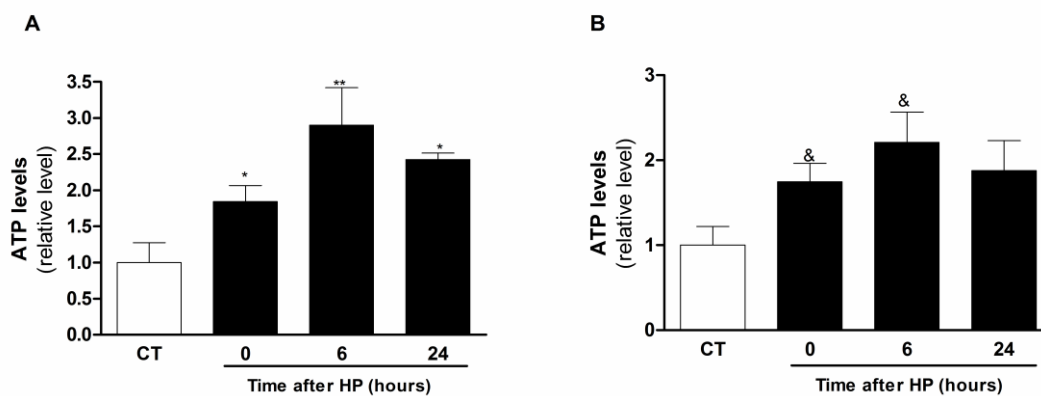
Figure 7.1. Effect of HP on (A) brain cortical and (B) hippocampal ATP levels. Data are the means ± SEM of 5 animals from each condition studied. Statistical significance: *p<0.05 when compared with the brain cortex from control rats; &p<0.05 when compared with the hippocampus from control rats.
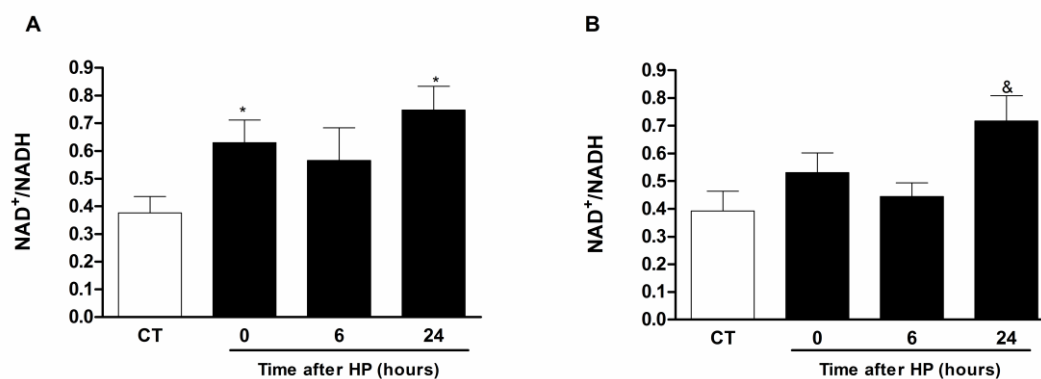
Figure 7.2. Effect of HP on total (A) brain cortical and (B) hippocampal NAD$^+$/NADH ratio. Data are the means ± SEM of 5 animals from each condition studied. Statistical significance: *p<0.05 when compared with the cortex from control rats; &p<0.05 when compared with the hippocampus from control rats.

7.3.5 HYPOXIC PRECONDITIONING POTENTIATES MITOCHONDRIAL ELONGATION BY MODULATION OF FUSION-FISSION MACHINERY

The functional state of mitochondria is accompanied by alterations in mitochondrial morphology. To test if changes in mitochondrial morphology participate in the adaptive response mediated by HP, we analyzed by immunoblotting the levels of the mitochondrial shaping proteins, Fis1 and DRP1, which regulate mitochondrial fission, and Mnf1 and 2 and OPA1 that control the mitochondrial fusion process. Interestingly, a selective and time-dependent increase in OPA1 protein levels was observed in the brain cortex after HP, reaching statistical significance at 24 hours after the last hypoxic episode (Fig. 7.3A). Also, a drastic reduction in brain cortical DRP-1 protein levels was observed at all the time points tested (Fig. 7.3B). No significant alterations occurred in the brain cortical levels of Fis1 protein (Fig. 7.3C). Conversely, only a significant reduction in Fis1 protein levels at 6 and 24 hours after the last hypoxic episode was observed in the hippocampus (Fig. 7.5C). Hippocampal OPA1 and DRP-1 proteins levels remained statistically unchanged (Figs. 7.5A and 7.5B). The levels of Mnf1 and 2 proteins were also analysed in brain cortex and hippocampus but no significant changes were observed (data not shown).

Furthermore, this data was corroborated by electron microscopy analysis, which revealed that HP promoted mitochondrial elongation in both brain cortex (Fig. 7.4) and hippocampus (Fig. 7.6).

These data suggest that during HP, both brain cortical and hippocampal mitochondria acquire an enlarged phenotype however, through distinct mechanisms.

Figure 7.3. Effect of HP on (A) OPA1, (B) DRP1, and (C) Fis1 protein levels in the brain cortex. Data in the graph are expressed as mean ± SEM of 3-5 independent experiments. *$p<0.05$; **$p<0.01$ when compared with the cortex from the control rats.
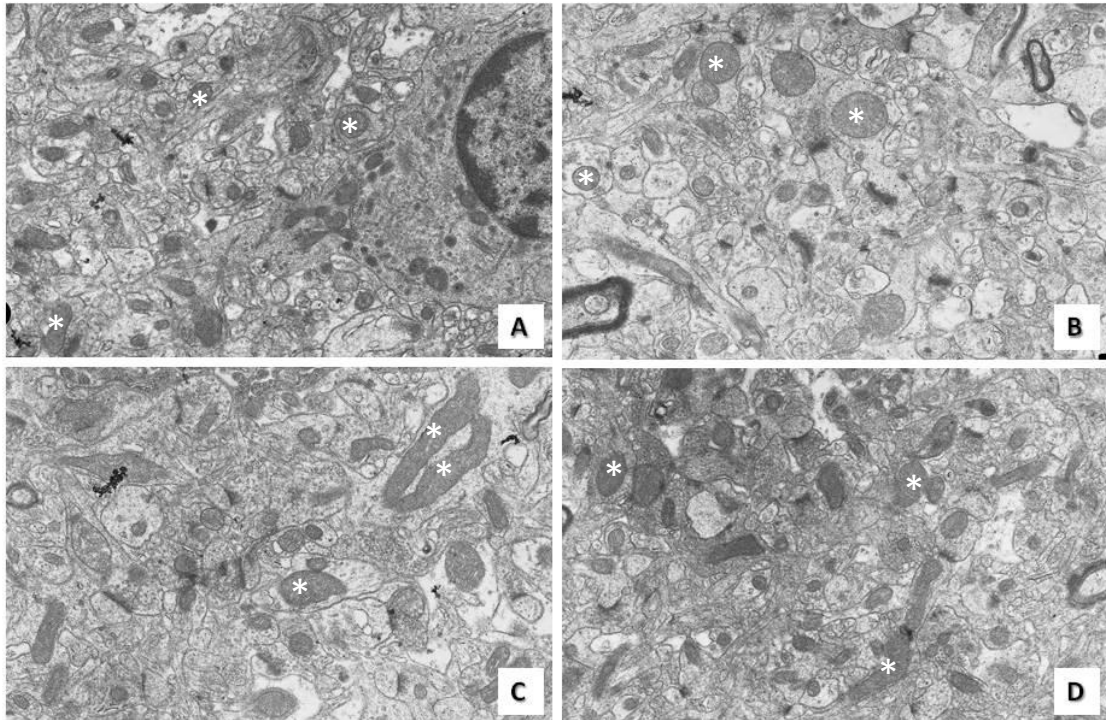
Figure 7.4. Effect of HP on ultrastructural morphology of mitochondria in the brain cortex. Representaive electron microscopy images of brain cortical tissue derived from **(A)** non-preconditioned and preconditioned animals at **(B)** 0, **(C)** 6 and **(D)** 24 hours after the last hypoxic session. Magnification: 8,000x. ***-** mitochondria.
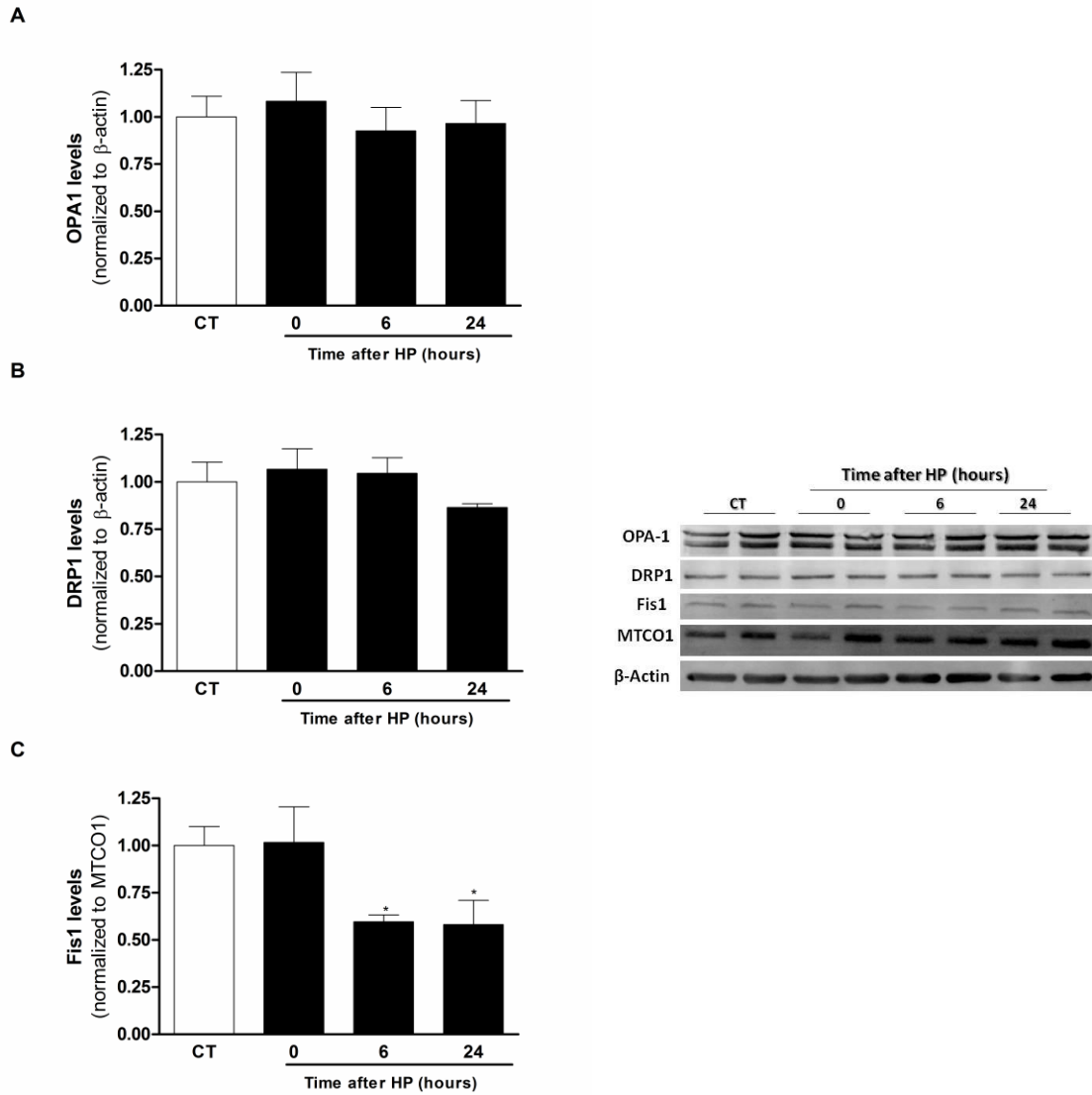
Figure 7.5. Effect of HP on (A) OPA1, (B) DRP1, and (C) Fis1 protein levels in the hippocampus. Data in the graph are expressed as mean ± SEM of 3-5 independent experiments. *p<0.05 when compared with the hippocampus from the control rats.
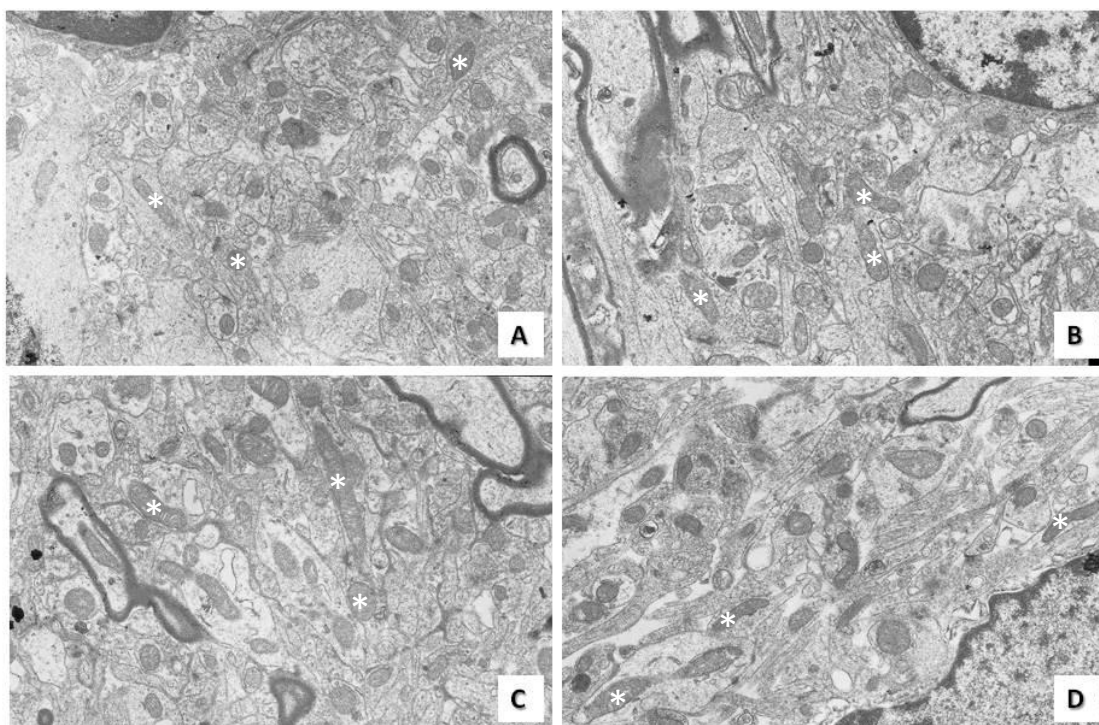
Figure 7.6. Effect of HP on ultrastructural morphology of mitochondria in the hippocampus. Representaive electron microscopy images of brain hippocampal tissue derived from **(A)** non-preconditioned and preconditioned animals at **(B)** 0, **(C)** 6 and **(D)** 24 hours after the last hypoxic session. Magnification: 8,000x. * - mitochondria.

7.3.6 HYPOXIC PRECONDITIONING STIMULATES MITOCHONDRIAL BIOGENESIS

The mitochondrial quantity and quality control is known to be accomplished, in part, by mitochondrial biogenesis. Thus, this last set of experiments was aimed to unveil the contribution of this process in the mitochondrial adaptive response to HP characterized by repetitive moderate hypoxia and reoxygenation. To this end, we evaluated the protein levels of PGC-1α, NRF-1, NRF-2 and TFAM in the brain cortex and hippocampus. As shown in Figures 7.7A and 7.8B, a significant increase in NRF-1 protein

levels was detected immediately after the last hypoxic episode in the two brain regions.

An increase in brain cortical TFAM protein levels at 6 hours (Fig. 7.7C) and immediately

and at 6 hours after the last hypoxic episode in the hippocampus (Fig. 7.8C) was

observed. Surprisingly, no statistically significant changes were observed in both brain

cortical and hippocamal NRF-2 protein levels (Figs. 7.7B and 7.8B) and PGC-1α protein
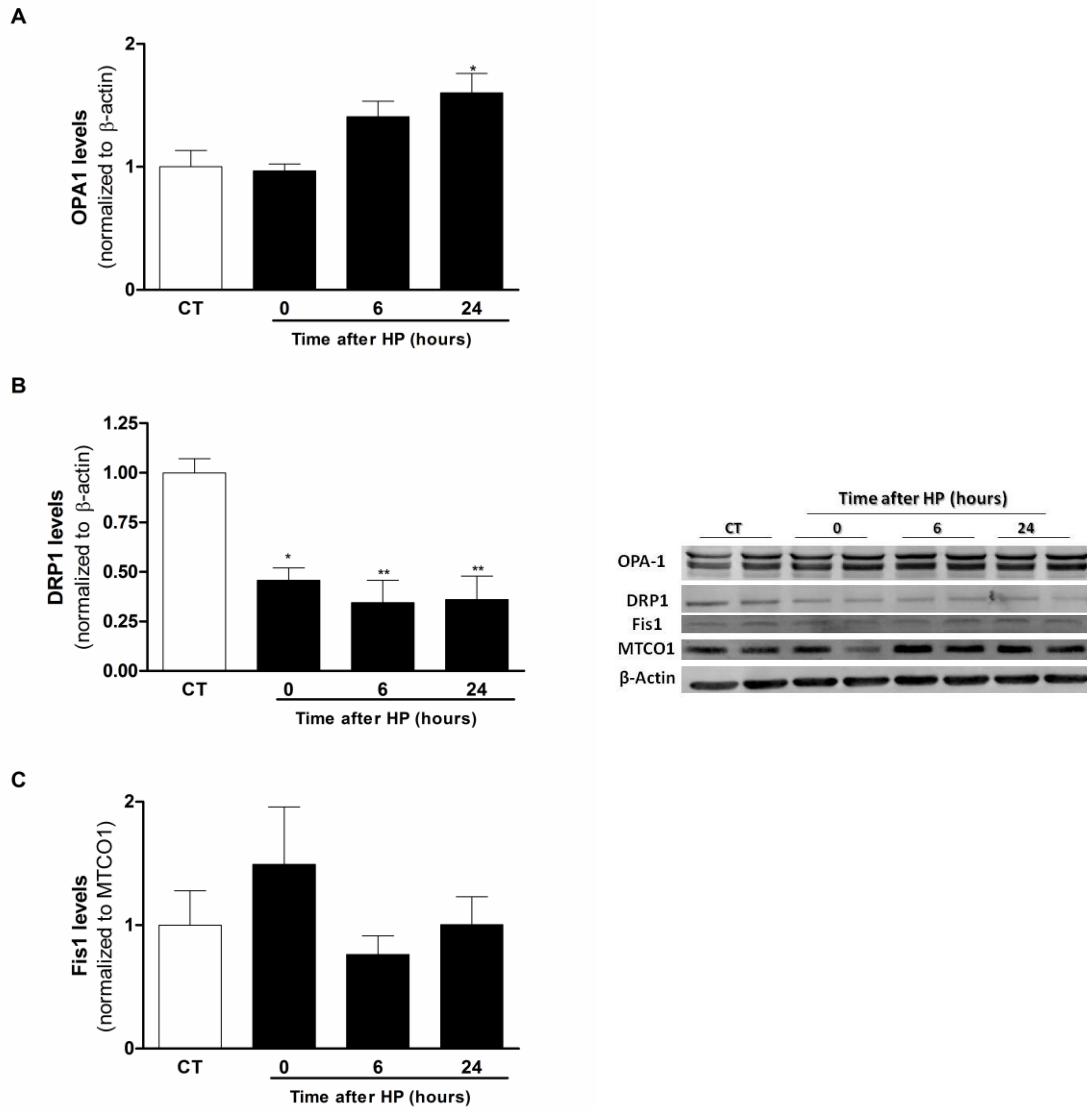
levels (data not shown).
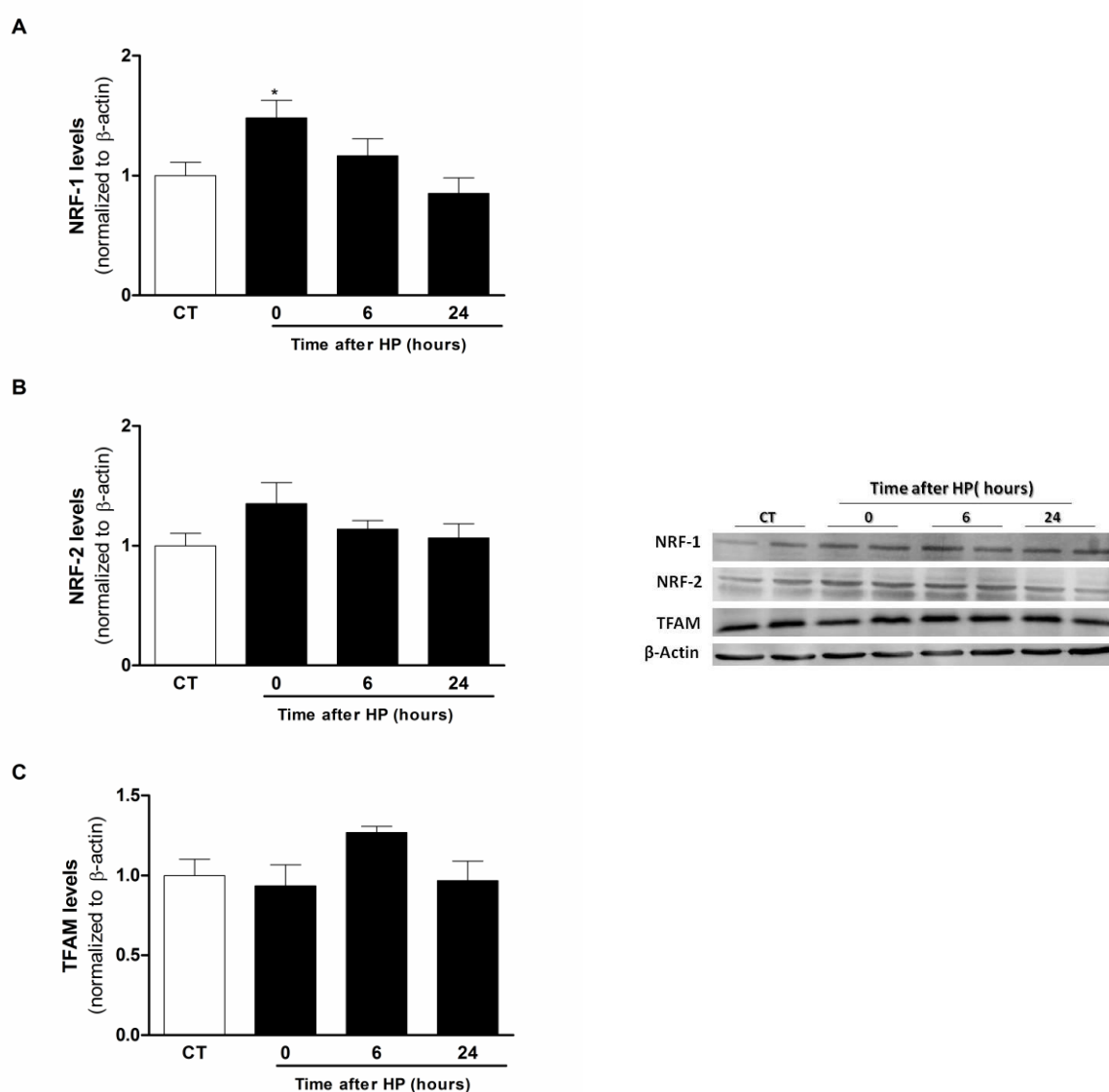
Figure 7.7 Effect of HP on (A) NRF-1, (B) NRF-2, and (C) TFAM protein levels in the brain cortex. Data in the graph are expressed as mean ± SEM of 3-5 independent experiments. *$p < 0.05$ when compared with the brain cortex from the control rats.
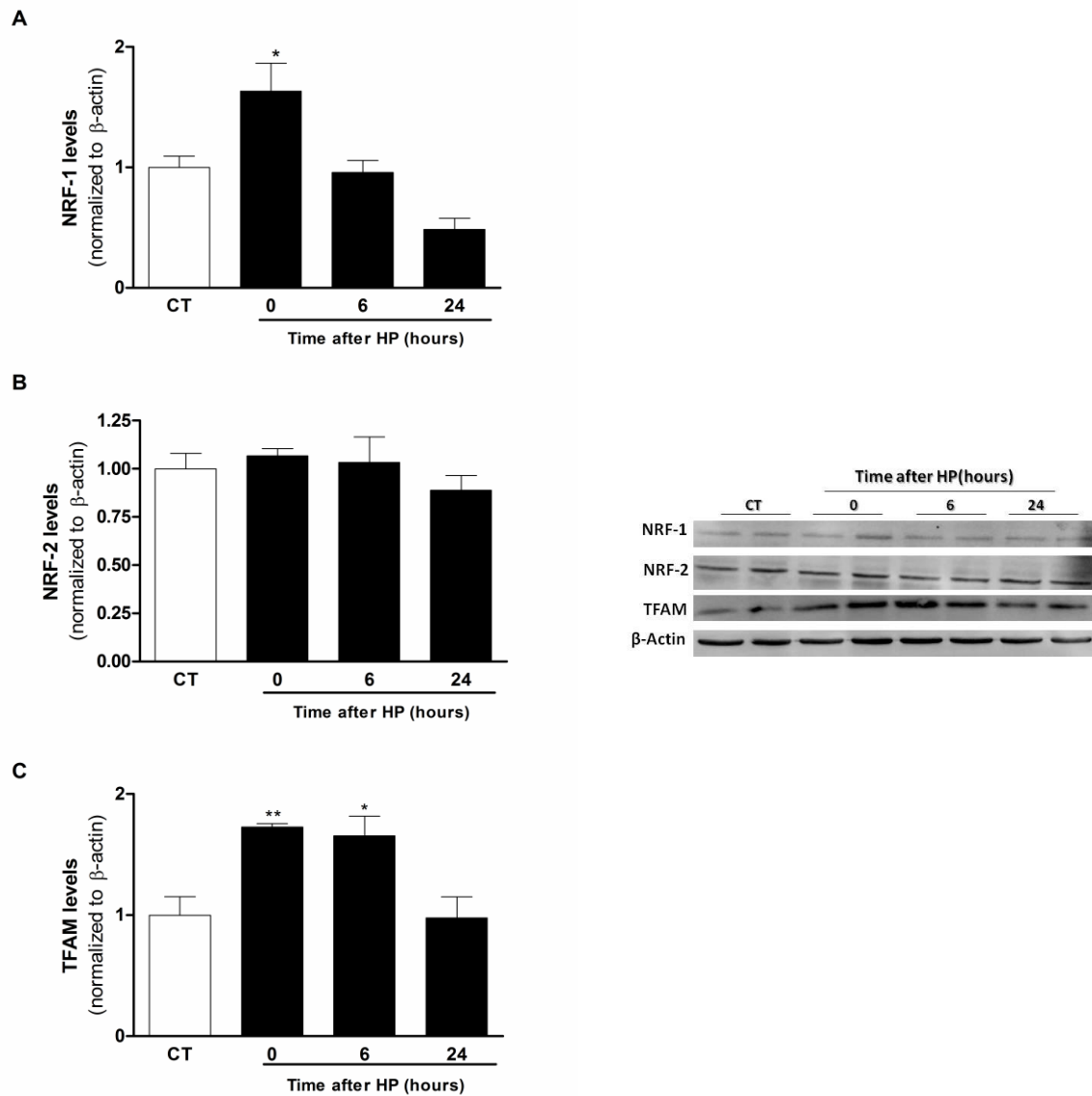
Figure 7.8 Effect of HP on (A) NRF-1, (B) NRF-2, and (C) TFAM protein levels in the hippocampus. Data in the graph are expressed as mean ± SEM of 3-5 independent experiments. *p<0.05. **p<0.01 when compared with the hippocampus from the control rats.

7.4 Discussion

Although the precise cellular mechanisms behind HP-triggered brain tolerance remain largely enigmatic, several lines of research have suggested that mitochondria actively participate in this phenomenon (Correia et al., 2011b). This study extended the current knowledge on the involvement of mitochondria in HP, demonstrating for the first time that HP preconditioning characterized by repetitive moderate hypoxia and reoxygenation: 1) improves brain cortical and hippocampal mitochondrial bioenergetic function, 2) increases tissue ATP content and NAD^+/NADH ratio, 3) stimulates mitochondrial biogenesis by upregulating the levels of NRF-1 and TFAM proteins, and 4) modulates mitochondrial fusion/fission balance, favoring mitochondrial fusion and thus, generating mitochondria with an elongated phenotype in the brain cortex and hippocampus, although presenting a region-specific pattern.

Neurons critically rely on mitochondrial function and oxygen supply, since most of neuronal ATP is produced by the oxidative phosphorylation system (Rugarli and Langer, 2012). Although the mitochondrial phosphorylation system parameters did not change (Table 7.3), a significant increase in ADP/O ratio after HP in both brain cortical and hippocampal mitochondria occurred, indicating an increase in oxidative phosphorylation efficiency (Table 7.2). HP also induced a time-dependent decrease in respiratory state 2 in brain cortical and hippocampal mitochondria (Table 7.2). Furthermore, hippocampal mitochondria from HP animals displayed a reduced basal proton leak as reflected by the significant decrease in the mitochondrial respiration rate after oligomycin addition (Table 7.2). Interestingly, our results demonstrated that total brain cortical and hippocampal ATP levels (Fig. 7.1) and NAD^+/NADH ratio (Fig. 7.2) augmented after the last hypoxic episode. Consistent with our findings, it was reported

that resveratrol preconditioning, which is known to mimic ischemic preconditioning, also promoted an increase of 23% in ATP synthesis and ADP/O ratio in hippocampal mitochondria (Della-Morte et al., 2009). Moreover, preconditioned rat hippocampal slices displayed increased NAD$^+$/NADH ratio (Centeno et al., 1999). Taken together, these data suggest that HP enhances brain cortical and hippocampal respiratory chain function as indicated by the increased mitochondrial coupling and decreased proton leak (Table 7.2) and improvement of the brain energetic status (Fig. 7.1) and redox state (Fig. 7.2), which may underlie brain cells tolerance.

Mitochondrial function depends on mitochondrial mass, morphology, ultrastructure, and coupling efficiency (Hackenbrock et al., 1971; Arnoult et al., 2005; Chen et al., 2005; Gomes et al., 2011). As aforementioned, mitochondria are highly dynamic organelles that undergo continuous cycles of fusion and fission. A shift towards fusion favors the generation of interconnected mitochondria, whereas a shift towards fission produces numerous mitochondrial fragments (Westermann, 2010). Mitochondrial bioenergetics is affected by the degree of mitochondrial connectivity, with a highly connected mitochondrial network being correlated with increased ATP production efficiency (Otera and Mihara, 2012). Indeed, it was theorized that mitochondrial fusion would generate networks of elongated mitochondria with continuous membranes and matrix lumen, allowing a free diffusion of molecules such as ADP, NADH, FADH$_2$, and thus resulting in optimal oxidative phosphorylation efficiency (Skulachev, 2001). Remarkably, our data demonstrated that repetitive moderate hypoxia and reoxygenation promotes a significant increase on OPA1 protein levels (Fig. 7.3A) and a decrease in DRP1 protein levels (Fig. 7.3B) in the brain cortex, and a significant reduction in Fis1 protein levels (Fig. 7.5C) in the hippocampus, which indicates that the

balance of mitochondrial fusion-fission is redirected towards fusion. Consistently, electron microscopy analysis revealed that HP provoked an elongated mitochondrial phenotype in both brain cortex (Fig. 7.4) and hippocampus (Fig. 7.6). Previous studies demonstrated that elongated mitochondria displayed higher levels of ATPase dimers, associated with increased efficiency in ATP production (Strauss et al., 2008). Morphologically, this is mirrored by an increase in the number of mitochondrial cristae, privileged compartments for ATP synthesis (Strauss et al., 2008). In accordance, it was recently demonstrated that under starvation, mitochondrial fission is repressed through DRP1 downregulation, resulting in the elongation of the mitochondria characterized by a higher density of cristae and efficiency of ATP production (Gomes et al., 2011). Further, elongated mitochondria are spared from autophagic degradation sustaining cell viability (Gomes et al., 2011; Rambold et al., 2011). When elongation was genetically or pharmacologically blocked, mitochondria consumed ATP, precipitating starvation-induced cell death (Gomes et al., 2011). Tondera and collaborators (2009) also reported that mitochondria hyperfuse and form a highly interconnected network in cells exposed to modest levels of stress (UV irradiation and actinomycin D), a process designated by stress-induced mitochondrial hyperfusion (SIMH). SIMH is dependent on OPA1 levels, which is known to be responsible for inner mitochondrial membrane fusion and cristae organization (Sesaki et al, 2003; Wong et al, 2003; Cipolat et al, 2006; Frezza et al, 2006), and is accompanied by an increased mitochondrial ATP production, representing an adaptive pro-survival response to counteract stress (Tondera et al., 2009). Furthermore, mitochondria of hypoxic cells undergo a HIF-1α-dependent and Mnf1-mediated change in morphology, acquiring an enlarged phenotype, which make cells resistant to different apoptotic stimuli (Chiche et al., 2010). These enlarged mitochondria are functional and

conserve the ΔΨm and ATP production capacity (Chiche et al., 2010). In line with these findings, we speculate that the enhanced mitochondrial fusion and energy levels observed in our experimental conditions favor cell survival and, thereby represent a critical adaptive step underlying HP-mediated brain tolerance. However, further studies are required to determine whether mitochondrial fusion is critical to HP-mediated brain tolerance through the manipulation of fusion and/or fission proteins. This will elucidate the contribution of mitochondrial fusion/fission in the mitochondrial and cellular adaptive responses during HP. Another interesting aspect that deserves further clarification is the region-specific behavior of mitochondrial adaptive mechanisms.

Since mitochondrial function is also reliant on mitochondrial mass, a complementary explanation for the effects of HP on brain mitochondrial bioenergetics phenotype may be related with alterations in mitochondrial biogenesis. Indeed, induction of mitochondrial biogenesis could represent an attempt of cells to increase their aerobic set point or to maintain a pre-existing aerobic set point in face of a declining mitochondrial function (Onyango et al., 2010). Our findings revealed that NRF-1 protein levels were increased immediately after the last hypoxic episode in both brain cortex and hippocampus (Figs. 7.7A and 7.8A). TFAM protein levels augmented immediately and at 6 hours after the last hypoxic episode in the hippocampus, and at 6 hours after the last hypoxic episode in the brain cortex (Fig. 7.8C). In accordance, it was previously shown that HP stimulated mitochondrial biogenesis (Gutsaeva et al., 2008). Acute transient cerebral hypoxia stimulated mitochondrial biogenesis in the subcortex by activating the nuclear-encoded regulatory program for mitochondrial biogenesis, including the NRF-1 transcription factor, the PGC-1α coactivator, and the mitochondrial transcription factor TFAM. Consequently, this program led to a subsequent increase in

mtDNA transcription and content, followed by structural evidence of neuronal mitochondrial biogenesis (increased neuronal mitochondria number and/or volume density), especially in the hippocampus, a region that is particularly vulnerable to hypoxic injury (Gutsaeva et al., 2008). Overall, these cellular responses seem to participate in a regional adaptive program to optimize oxygen utilization, energy production, and/or mitochondrial phenotype during cerebral oxygen limitation (Gutsaeva et al., 2008). Yin and collaborators (2008) also documented a rapid boost in neuronal mitochondrial biogenesis after neonatal hypoxic-ischemic brain injury, and it was suggested that this phenomenon may constitute a novel component of the endogenous repair mechanisms of the brain. Indeed, it was detected that brain mtDNA content was markedly increased at 6 hours after hypoxic/ischemic stimuli, and continued to increase up to 24 hours (Yin et al., 2008). Paralleling the temporal change in mtDNA content, an increase in total mitochondria number and expression of the mitochondrial heat shock protein 60 (HSP60), COX, and transcription factors NRF-1 and TFAM was observed (Yin et al., 2008). Consistently, the role of mitochondrial biogenesis in the mitochondrial adaptive response to moderate hypoxia is further strength by evidence demonstrating an elevation in the expression and protein levels of nuclear NRF-1 and TFAM, as well as an increase in mtDNA content in the neonatal rat brain (Lee et al., 2008). Overall, these data suggest that the stimulation of mitochondrial biogenesis by repetitive moderate hypoxia and reoxygenation could represent a compensatory mechanism designed to meet the specific energetic demands and, thus to increase the ability of brain cells to survive under stressful conditions.

We have previously found that HP induced an increase in H_2O_2 rate production in both brain cortical and hippocampal mitochondria (**Chapter 6**). A series of studies

reported that mitochondria appear to respond to ROS production by undergoing morphological and/or functional adaptations. Mitochondrial ROS production resulting from complex I inhibition promoted mitochondrial elongation, leading to the formation of a more complex mitochondrial reticulum (Koopman et al., 2005). The antioxidant MitoQ prevented this ROS-mediated mitochondrial outgrowth, which reinforces the idea that mitochondrial morphological alterations represent an adaptive response to ROS generation. It was also reported that ROS-mediated mitochondrial morphological adaptations improved cell ATP production (Aon and Cortassa, 2004; Koopman et al., 2005; Skulachev, 2001). Mitochondrial ROS can also stimulate mitochondrial biogenesis (Butow and Avadhani, 2004). Indeed, mitochondrial-derived ROS trigger a retrograde response that is conveyed to the nucleus, causing the upregulation of nuclear genes encoding mitochondrial proteins and leading to the induction of mitochondrial biogenesis (Butow and Avadhani, 2004). Studies performed in *in vitro* models of oxidative stress, demonstrated that mitochondrial biogenesis, characterized by a marked increase in mitochondrial mass and mtDNA content, was an early response to H_2O_2 exposure (Lee et al., 2000). Compelling evidence provided insight into the mechanisms underlying the crosstalk between mitochondria-derived ROS and mitochondrial biogenesis. It was shown that ROS regulated TFAM expression through phosphorylation of NRF-1 via Akt activation, which promoted the nuclear translocation of NRF-1 and binding to the TFAM promoter (Piantadosi and Sulima, 2006). Mitochondrial ROS-dependent induction of NRF-1 mRNA expression occurred via NRF-2 occupancy of NRF-1 promoter sites to increase NRF-1 expression and activity (Piantadosi et al., 2008). PGC-1α also appeared to be sensitive to the redox status of the cells, since it was demonstrated that exogenous H_2O_2 upregulated PGC-1α mRNA expression via the

transcriptional activation of the PGC-1α promoter, this effect being inhibited by the antioxidant NAC (Irrcher et al., 2009). Moreover, the effect of ROS on PGC-1α promoter activity occurred via AMPK activation (Irrcher et al., 2009). Mitochondrial ROS were also implicated in the induction of the transcription factor HIF-1α, which in turn has been coupled to PGC-1α in HP-mediated neuronal and vascular protection (Zhao et al., 2012).

In summary, we demonstrated herein that the dynamic interplay between mitochondrial biogenesis and mitochondrial fusion-fission in response to repetitive moderate hypoxia contributes to create a "stronger" mitochondrial population with an enhanced bioenergetic function, which can improve the chances of the cell to survive upon a lethal stimulus and thus, represent a major adaptive mechanism triggered by HP. Further studies aimed to understand the mitochondrial adaptive behavior in face to hypoxia-reoxygenation will help clarify the complexity of HP-mediated brain tolerance and may disclose targets for the design of novel therapeutic strategies to fight age-related neurodegenerative diseases.

CHAPTER 8

GENERAL CONCLUSION

8.1 GENERAL CONCLUSION

The work presented in this thesis uncovers the role of mitochondria in preconditioning-triggered brain tolerance. Three major conclusions can be drawn: 1) mitochondria act as signaling organelles during preconditioning, mitochondrial-derived ROS representing key messengers in this process; 2) reshaping of mitochondria and stimulation of mitochondrial biogenesis are critical steps involved in the adaptive response mediated by the preconditioning phenomenon; and 3) mitochondria are also specific targets of the protective machinery underlying preconditioning, since preconditioned mitochondria preserve their functionality when exposed to a deleterious, potentially lethal insult. Taken together, the results of this thesis serve to clarify the brain mitochondrial adaptive response to a preconditioning paradigm.

By modulating mitochondrial ROS production, we developed an *in vitro* model of preconditioning that was able to protect brain endothelial and neuronal cells against high-glucose induced cell damage and death, which relies in a crosstalk between mitochondrial ROS and HIF-1α signaling pathway (**Chapter 4**). Foremost, mitochondrial adaption to cyanide-induced redox changes was characterized by mild ROS generation, increased basal oxygen consumption, mitochondrial network reorganization and HIF-1α induction. We hypothesize that these alterations might constitute a "metabolic strategy" to restrict cell damage and death against a subsequent lethal insult. However, it is important to emphasize that moderate mitochondrial ROS production during the initial phase of cyanide preconditioning seems to be the trigger of cells resistance, since the protective effects mediated by cyanide were abrogated in ρ0 cells or when cells were treated with the antioxidant NAC.

To further strength the link between defective brain insulin signaling and mitochondrial dysfunction in AD, we used a rat model of sAD induced by the icv administration of STZ. Data described in **Chapter 5** demonstrate that abnormal mitochondrial function occurs in both brain cortex and hippocampus of this rat model of sAD. Mitochondria from icvSTZ-treated rats displayed deficits in the respiratory chain and phosphorylation system. An increased susceptibility to Ca^{2+}-induced mPTP opening and oxidative stress was also found in this animal model. These findings demonstrate that icvSTZ rats recapitulate the brain mitochondrial dysfunction described in sAD, reinforcing the idea that the icvSTZ rats is a reliable model to explore the early changes occurring in sAD.

Using a well-established model of HP, we evaluated its potential protective effects in the icvSTZ rat model (**Chapter 6)**. Our analyses revealed that preconditioning prevented cognitive decline and brain hypometabolism in this animal model of sAD. Particularly, we found that HP was able to preserve both brain cortical and hippocampal mitochondrial function in the icvSTZ-induced rat model of sAD. Mechanistically, we observed a modest increase in H_2O_2 production rate in both mitochondrial populations and HIF-1α induction immediately after the last hypoxic episode, which reinforce our hypothesis that a crosstalk between mitochondrial-derived ROS and HIF-1α signaling pathway is the hub of the pro-survival response triggered by HP.

Incited by these exciting findings, a major question invaded our minds: What happens to brain mitochondria during HP? Our findings show that preconditioning could activate an adaptive reprogramming of mitochondrial biology in response to hypoxia-reoxygenation. In fact, data from the **Chapter 7** confirmed this idea, by demonstrating that hypoxia-reoxygenation *per se* improves mitochondrial bioenergetic function,

stimulates mitochondrial biogenesis and alters mitochondrial dynamics, favoring mitochondrial fusion and, thereby generating elongated mitochondria in both brain cortex and hippocampus. All these alterations could illustrate a mitochondrial adaptive response to hypoxia-reoxygenation characterized by a "stronger" mitochondrial population that will allow brain cells to survive upon receiving a lethal stimulus.

An important point that needs to be clarified is the differences at the mitochondrial dynamics observed in our *in vitro* (**Chapter 4**) and *in vivo* (**Chapter 7**) studies. *In vitro*, cyanide preconditioning changed mitochondrial shape of rat brain endothelial cells from a mainly tubular, highly interconnected network toward multiple, isolated singular structures while, *in vivo*, HP increased mitochondrial fusion and generated elongated mitochondria in the adult rat brain cortex and hippocampus. Why this happens? Probably due to the fact that the preconditioning protocols used are different; cyanide exposure represents an immediate preconditioning while HP represents a delayed preconditioning. Thus, depending on the sub-lethal stimulus, duration of the exposure and time of recovery, mitochondria may behave differently. Regarding the importance of mitochondrial dynamics on the preconditioning phenomenon, more studies aimed to manipulate mitochondrial-shaping proteins are required to unveil the real contribution of fusion and fission processes in the preconditioning-mediated brain tolerance.

Despite the present evidences that strongly prove that mitochondrial biology is an integrant and critical component of the adaptive and pro-survival responses elicited by the preconditioning paradigm, further studies are required to achieve more mechanistic insights concerning the link between mitochondria and cell survival. Taking into account that mitochondrial quality and quantity are also regulated by the selective

degradation by autophagy, a process denominated mitophagy, it will be of great interest to decipher how mitochondrial turnover behaves during preconditioning. Evidence from the literature provides clues that mitophagy could be implicated in the preconditioning phenomenon. As a matter of fact, mitochondria-derived ROS, at low or moderate levels, may act as signaling molecules and trigger mitophagy by redox regulation of Atg4, an essential cysteine protease in the autophagic pathway (Scherz-Shouval et al., 2007). It was also reported that HIF-1α, the master regulator of the adaptive response to hypoxia and whose activity is modulated by mitochondrial ROS, enhanced autophagy (Brugarolas et al., 2004; Hardie, 2005; Zhang et al., 2008). In this way, mitophagy could represent an adaptive metabolic response required to eliminate damaged and/or dysfunctional mitochondria preventing a mitoenergetic crisis and bypassing cell death. However, it is plausible to ask ourselves if HP-induced elongated mitochondria are also spared from autophagic degradation. As discussed in the **Chapter 7**, under starvation conditions mitochondria escape from autophagic degradation through extensive fusion into mitochondrial networks, allowing the cells to sustain efficient ATP production and, thereby, to survive (Gomes et al., 2011; Rambold et al., 2011). Hence, more studies are needed to clarify this issue.

In sum, this work proves the crucial role of mitochondria in the preconditioning phenomenon. On the one hand, mitochondria, by acting as signaling organelles, actively participate in the initiation of the adaptive and pro-survival responses underlying brain tolerance. On the other hand, mitochondria are also targeted by preconditioning-related adaptive events. However, a deeper knowledge on the mitochondrial mechanisms underlying the preconditioning phenomenon is required. Future research advances on the role of mitochondrial biology in preconditioning will help to develop novel

therapeutic approaches with the primary goal of modulating mitochondria to enhance

brain tolerance against neurodegenerative events.

Chapter 8

CHAPTER 9

REFERENCES

9.1 REFERENCES

Acker, H., 2005. The oxygen sensing signal cascade under the influence of reactive oxygen species. Philos Trans R Soc Lond B Biol Sci. 360, 2201-10.

Adeghate, E., Schattner, P., Dunn, E., 2006. An update on the etiology and epidemiology of diabetes mellitus. Ann N Y Acad Sci. 1084, 1-29.

Akisaki, T., Sakurai, T., Takata, T., Umegaki, H., Araki, A., Mizuno, S., Tanaka, S., Ohashi, Y., Iguchi, A., Yokono, K., Ito, H., 2006. Cognitive dysfunction associates with white matter hyperintensities and subcortical atrophy on magnetic resonance imaging of the elderly diabetes mellitus Japanese elderly diabetes intervention trial (J-EDIT). Diabetes Metab Res Rev. 22, 376-84.

Aliev, G., Smith, M.A., Obrenovich, M.E., de la Torre, J.C., Perry, G., 2003. Role of vascular hypoperfusion-induced oxidative stress and mitochondria failure in the pathogenesis of Azheimer disease. Neurotox Res. 5, 491-504.

Allen, K.V., Frier, B.M., Strachan, M.W., 2004. The relationship between type 2 diabetes and cognitive dysfunction: longitudinal studies and their methodological limitations. Eur J Pharmacol. 490, 169-75.

Anandatheerthavarada, H.K., Biswas, G., Robin, M.A., Avadhani, N.G., 2003. Mitochondrial targeting and a novel transmembrane arrest of Alzheimer's amyloid precursor protein impairs mitochondrial function in neuronal cells. J Cell Biol. 161, 41-54.

Anello, M., Lupi, R., Spampinato, D., Piro, S., Masini, M., Boggi, U., Del Prato, S., Rabuazzo, A.M., Purrello, F., Marchetti, P., 2005. Functional and morphological alterations of mitochondria in pancreatic beta cells from type 2 diabetic patients. Diabetologia. 48, 282-9.

Aon, M.A., Cortassa, S., O'Rourke, B., 2004. Percolation and criticality in a mitochondrial network. Proc Natl Acad Sci U S A. 101, 4447-52.

Arluison, M., Quignon, M., Nguyen, P., Thorens, B., Leloup, C., Penicaud, L., 2004a. Distribution and anatomical localization of the glucose transporter 2 (GLUT2) in the adult rat brain--an immunohistochemical study. J. Chem. Neuroanat. 28, 117-136.

Arluison, M., Quignon, M., Thorens, B., Leloup, C., Penicaud, L., 2004b. Immunocytochemical localization of the glucose transporter 2 (GLUT2) in the adult rat brain. II. Electron microscopic study. J. Chem. Neuroanat. 28, 137-146.

Arnoult, D., Grodet, A., Lee, Y.J., Estaquier, J., Blackstone, C., 2005. Release of OPA1 during apoptosis participates in the rapid and complete release of cytochrome c and subsequent mitochondrial fragmentation. J Biol Chem. 280, 35742-50.

Awad, N., Gagnon, M., Messier, C., 2004. The relationship between impaired glucose tolerance, type 2 diabetes, and cognitive function. J Clin Exp Neuropsychol. 26, 1044-80.

Azari, N.P., Pettigrew, K.D., Schapiro, M.B., Haxby, J.V., Grady, C.L., Pietrini, P., Salerno, J.A., Heston, L.L., Rapoport, S.I., Horwitz, B., 1993. Early detection of Alzheimer's disease: a statistical approach using positron emission tomographic data. J Cereb Blood Flow Metab. 13, 438-47.

Babcock, D.F., Hille, B., 1998. Mitochondrial oversight of cellular Ca2+ signaling. Curr Opin Neurobiol. 8, 398-404.

Bains, J.S., Shaw, C.A., 1997. Neurodegenerative disorders in humans: the role of glutathione in oxidative stress-mediated neuronal death. Brain Res Brain Res Rev. 25, 335-58.

Bajgar, R., Seetharaman, S., Kowaltowski, A.J., Garlid, K.D., Paucek, P., 2001. Identification and properties of a novel intracellular (mitochondrial) ATP-sensitive potassium channel in brain. J Biol Chem. 276, 33369-74.

Baker, L.D., Cross, D.J., Minoshima, S., Belongia, D., Watson, G.S., Craft, S., 2011. Insulin resistance and Alzheimer-like reductions in regional cerebral glucose metabolism for cognitively normal adults with prediabetes or early type 2 diabetes. Arch Neurol. 68, 51-7.

Baloyannis, S.J., 2006. Mitochondrial alterations in Alzheimer's disease. J Alzheimers Dis. 9, 119-26.

Barja, G., 1999. Mitochondrial oxygen radical generation and leak: sites of production in states 4 and 3, organ specificity, and relation to aging and longevity. J Bioenerg Biomembr. 31, 347-66.

Barrientos, A., Fontanesi, F., Diaz, F., 2009. Evaluation of the mitochondrial respiratory chain and oxidative phosphorylation system using polarography and spectrophotometric enzyme assays. Curr Protoc Hum Genet. Chapter 19, Unit19 3.

Barsoum, M.J., Yuan, H., Gerencser, A.A., Liot, G., Kushnareva, Y., Graber, S., Kovacs, I., Lee, W.D., Waggoner, J., Cui, J., White, A.D., Bossy, B., Martinou, J.C., Youle, R.J., Lipton, S.A., Ellisman, M.H., Perkins, G.A., Bossy-Wetzel, E., 2006. Nitric oxide-induced mitochondrial fission is regulated by dynamin-related GTPases in neurons. EMBO J. 25, 3900-11.

Bell, E.L., Klimova, T.A., Eisenbart, J., Moraes, C.T., Murphy, M.P., Budinger, G.R., Chandel, N.S., 2007. The Qo site of the mitochondrial complex III is required for the transduction of hypoxic signaling via reactive oxygen species production. J Cell Biol. 177, 1029-36.

Benard, G., Bellance, N., James, D., Parrone, P., Fernandez, H., Letellier, T., Rossignol, R., 2007. Mitochondrial bioenergetics and structural network organization. J Cell Sci. 120, 838-48.

Benard, G., Bellance, N., Jose, C., Melser, S., Nouette-Gaulain, K., Rossignol, R., 2010. Multi-site control and regulation of mitochondrial energy production. Biochim Biophys Acta. 1797, 698-709.

Bergmeyer, H.U., Bernt, E., 1974. Lactate dehydrogenase UV-assay with pyruvate and NADH. In Methods of Enzymatic Analysis 574-8.

Bernaudin, M., Nedelec, A.S., Divoux, D., MacKenzie, E.T., Petit, E., Schumann-Bard, P., 2002. Normobaric hypoxia induces tolerance to focal permanent cerebral ischemia in association with an increased expression of hypoxia-inducible factor-1 and its target genes, erythropoietin and VEGF, in the adult mouse brain. J Cereb Blood Flow Metab. 22, 393-403.

Bezprozvanny, I., Mattson, M.P., 2008. Neuronal calcium mishandling and the pathogenesis of Alzheimer's disease. Trends Neurosci. 31, 454-63.

Biessels, G.J., Deary, I.J., Ryan, C.M., 2008. Cognition and diabetes: a lifespan perspective. Lancet Neurol. 7, 184-90.

Biessels, G.J., Kamal, A., Urban, I.J., Spruijt, B.M., Erkelens, D.W., Gispen, W.H., 1998. Water maze learning and hippocampal synaptic plasticity in streptozotocin-diabetic rats: effects of insulin treatment. Brain Res. 800, 125-35.

Biessels, G.J., Kappelle, A.C., Bravenboer, B., Erkelens, D.W., Gispen, W.H., 1994. Cerebral function in diabetes mellitus. Diabetologia. 37, 643-50.

Biessels, G.J., Staekenborg, S., Brunner, E., Brayne, C., Scheltens, P., 2006. Risk of dementia in diabetes mellitus: a systematic review. Lancet Neurol. 5, 64-74.

Biessels, G.J., van der Heide, L.P., Kamal, A., Bleys, R.L., Gispen, W.H., 2002. Ageing and diabetes: implications for brain function. Eur J Pharmacol. 441, 1-14.

Blass, J.P., Gibson, G.E., Hoyer, S., 2002. The role of the metabolic lesion in Alzheimer's disease. J Alzheimers Dis. 4, 225-32.

Blass, J.P., Sheu, R.K., Gibson, G.E., 2000. Inherent abnormalities in energy metabolism in Alzheimer disease. Interaction with cerebrovascular compromise. Ann N Y Acad Sci. 903, 204-21.

Bosetti, F., Brizzi, F., Barogi, S., Mancuso, M., Siciliano, G., Tendi, E.A., Murri, L., Rapoport, S.I., Solaini, G., 2002. Cytochrome c oxidase and mitochondrial F1F0-ATPase (ATP synthase) activities in platelets and brain from patients with Alzheimer's disease. Neurobiol Aging. 23, 371-6.

Braak, E., Griffing, K., Arai, K., Bohl, J., Bratzke, H., Braak, H., 1999. Neuropathology of Alzheimer's disease: what is new since A. Alzheimer? Eur Arch Psychiatry Clin Neurosci. 249, 14-22.

Braak, H., Braak, E., 1995. Staging of Alzheimer's disease-related neurofibrillary changes. Neurobiol Aging. 16, 271-8; discussion 278-84.

Brand, M.D., Esteves, T.C., 2005. Physiological functions of the mitochondrial uncoupling proteins UCP2 and UCP3. Cell Metab. 2, 85-93.

Brands, A.M., Biessels, G.J., de Haan, E.H., Kappelle, L.J., Kessels, R.P., 2005. The effects of type 1 diabetes on cognitive performance: a meta-analysis. Diabetes Care. 28, 726-35.

Bruce-Keller, A.J., Li, Y.J., Lovell, M.A., Kraemer, P.J., Gary, D.S., Brown, R.R., Markesbery, W.R., Mattson, M.P., 1998. 4-Hydroxynonenal, a product of lipid peroxidation, damages cholinergic neurons and impairs visuospatial memory in rats. J Neuropathol Exp Neurol. 57, 257-67.

Bruer, U., Weih, M.K., Isaev, N.K., Meisel, A., Ruscher, K., Bergk, A., Trendelenburg, G., Wiegand, F., Victorov, I.V., Dirnagl, U., 1997. Induction of tolerance in rat cortical neurons: hypoxic preconditioning. FEBS Lett. 414, 117-21.

Brugarolas, J., Lei, K., Hurley, R.L., Manning, B.D., Reiling, J.H., Hafen, E., Witters, L.A., Ellisen, L.W., Kaelin, W.G., Jr., 2004. Regulation of mTOR function in response to hypoxia by REDD1 and the TSC1/TSC2 tumor suppressor complex. Genes Dev. 18, 2893-904.

Brustovetsky, N., Dubinsky, J.M., 2000. Limitations of cyclosporin A inhibition of the permeability transition in CNS mitochondria. J Neurosci. 20, 8229-37.

Bubber, P., Haroutunian, V., Fisch, G., Blass, J.P., Gibson, G.E., 2005. Mitochondrial abnormalities in Alzheimer brain: mechanistic implications. Ann Neurol. 57, 695-703.

Bucala, R., Cerami, A., 1992. Advanced glycosylation: chemistry, biology, and implications for diabetes and aging. Adv Pharmacol. 23, 1-34.

Bucht, G., Adolfsson, R., Lithner, F., Winblad, B., 1983. Changes in blood glucose and insulin secretion in patients with senile dementia of Alzheimer type. Acta Med Scand. 213, 387-92.

Busija, D.W., Gaspar, T., Domoki, F., Katakam, P.V., Bari, F., 2008. Mitochondrial-mediated suppression of ROS production upon exposure of neurons to lethal stress: mitochondrial targeted preconditioning. Adv Drug Deliv Rev. 60, 1471-7.

Busquets, S., Alvarez, B., Van Royen, M., Figueras, M.T., Lopez-Soriano, F.J., Argiles, J.M., 2001. Increased uncoupling protein-2 gene expression in brain of lipopolysaccharide-injected mice: role of tumour necrosis factor-alpha? Biochim Biophys Acta. 1499, 249-56.

Butow, R.A., Avadhani, N.G., 2004. Mitochondrial signaling: the retrograde response. Mol Cell. 14, 1-15.

Cadenas, E., Boveris, A., Ragan, C.I., Stoppani, A.O., 1977. Production of superoxide radicals and hydrogen peroxide by NADH-ubiquinone reductase and ubiquinol-cytochrome c reductase from beef-heart mitochondria. Arch Biochem Biophys. 180, 248-57.

Cadet, J.L., Krasnova, I.N., 2009. Cellular and molecular neurobiology of brain preconditioning. Mol Neurobiol. 39, 50-61.

Cardoso, S., Correia, S., Santos, R.X., Carvalho, C., Santos, M.S., Oliveira, C.R., Perry, G., Smith, M.A., Zhu, X., Moreira, P.I., 2009. Insulin is a two-edged knife on the brain. J Alzheimers Dis. 18, 483-507.

Cardoso, S.M., Proenca, M.T., Santos, S., Santana, I., Oliveira, C.R., 2004. Cytochrome c oxidase is decreased in Alzheimer's disease platelets. Neurobiol Aging. 25, 105-10.

Carlberg, I., Mannervik, B., 1984. Glutathione reductase. Methods Enzymol. 113, 484-490.

Carrero, P., Okamoto, K., Coumailleau, P., O'Brien, S., Tanaka, H., Poellinger, L., 2000. Redox-regulated recruitment of the transcriptional coactivators CREB-binding protein and SRC-1 to hypoxia-inducible factor 1alpha. Mol Cell Biol. 20, 402-15.

Caspersen, C., Wang, N., Yao, J., Sosunov, A., Chen, X., Lustbader, J.W., Xu, H.W., Stern, D., McKhann, G., Yan, S.D., 2005. Mitochondrial Abeta: a potential focal point for neuronal metabolic dysfunction in Alzheimer's disease. FASEB J. 19, 2040-1.

Castellani, R.J., Rolston, R.K., Smith, M.A., 2010. Alzheimer disease. Dis Mon. 56, 484-546.

Cecchi, C., Fiorillo, C., Sorbi, S., Latorraca, S., Nacmias, B., Bagnoli, S., Nassi, P., Liguri, G., 2002. Oxidative stress and reduced antioxidant defenses in peripheral cells from familial Alzheimer's patients. Free Radic Biol Med. 33, 1372-9.

Centeno, J.M., Orti, M., Salom, J.B., Sick, T.J., Perez-Pinzon, M.A., 1999. Nitric oxide is involved in anoxic preconditioning neuroprotection in rat hippocampal slices. Brain Res. 836, 62-9.

Chan, D.C., 2006. Mitochondrial fusion and fission in mammals. Annu Rev Cell Dev Biol. 22, 79-99.

Chandel, N.S., Maltepe, E., Goldwasser, E., Mathieu, C.E., Simon, M.C., Schumacker, P.T., 1998. Mitochondrial reactive oxygen species trigger hypoxia-induced transcription. Proc Natl Acad Sci U S A. 95, 11715-20.

Chandel, N.S., McClintock, D.S., Feliciano, C.E., Wood, T.M., Melendez, J.A., Rodriguez, A.M., Schumacker, P.T., 2000. Reactive oxygen species generated at mitochondrial complex III stabilize hypoxia-inducible factor-1alpha during hypoxia: a mechanism of O2 sensing. J Biol Chem. 275, 25130-8.

Chang, D.T., Honick, A.S., Reynolds, I.J., 2006. Mitochondrial trafficking to synapses in cultured primary cortical neurons. J Neurosci. 26, 7035-45.

Chang, S., Jiang, X., Zhao, C., Lee, C., Ferriero, D.M., 2008. Exogenous low dose hydrogen peroxide increases hypoxia-inducible factor-1alpha protein expression and induces preconditioning protection against ischemia in primary cortical neurons. Neurosci Lett. 441, 134-8.

Chen, H., Chan, D.C., 2005. Emerging functions of mammalian mitochondrial fusion and fission. Hum Mol Genet. 14 Spec No. 2, R283-9.

Chen, H., Chan, D.C., 2009. Mitochondrial dynamics--fusion, fission, movement, and mitophagy--in neurodegenerative diseases. Hum Mol Genet. 18, R169-76.

Chen, H., Chomyn, A., Chan, D.C., 2005. Disruption of fusion results in mitochondrial heterogeneity and dysfunction. J Biol Chem. 280, 26185-92.

Chen, Q., Vazquez, E.J., Moghaddas, S., Hoppel, C.L., Lesnefsky, E.J., 2003. Production of reactive oxygen species by mitochondria: central role of complex III. J Biol Chem. 278, 36027-31.

Cheng, C.M., Tseng, V., Wang, J., Wang, D., Matyakhina, L., Bondy, C.A., 2005. Tau is hyperphosphorylated in the insulin-like growth factor-I null brain. Endocrinology. 146, 5086-91.

Chi, X., Sutton, E.T., Hellermann, G., Price, J.M., 2000. Potassium channel openers prevent beta-amyloid toxicity in bovine vascular endothelial cells. Neurosci Lett. 290, 9-12.

Chiche, J., Rouleau, M., Gounon, P., Brahimi-Horn, M.C., Pouyssegur, J., Mazure, N.M., 2010. Hypoxic enlarged mitochondria protect cancer cells from apoptotic stimuli. J Cell Physiol. 222, 648-57.

Chopp, M., Chen, H., Ho, K.L., Dereski, M.O., Brown, E., Hetzel, F.W., Welch, K.M., 1989. Transient hyperthermia protects against subsequent forebrain ischemic cell damage in the rat. Neurology. 39, 1396-8.

Cipolat, S., Rudka, T., Hartmann, D., Costa, V., Serneels, L., Craessaerts, K., Metzger, K., Frezza, C., Annaert, W., D'Adamio, L., Derks, C., Dejaegere, T., Pellegrini, L., D'Hooge, R., Scorrano, L., De Strooper, B., 2006. Mitochondrial rhomboid PARL regulates cytochrome c release during apoptosis via OPA1-dependent cristae remodeling. Cell. 126, 163-75.

Claiborne, A., 1985. Catalase activity. R.A. Greenwald (Ed.), CRC handbook of methods for oxygen radical research, CRC Press, Boca Raton, 283-284.

Cole, A.R., Astell, A., Green, C., Sutherland, C., 2007. Molecular connexions between dementia and diabetes. Neurosci Biobehav Rev. 31, 1046-63.

Correia, S.C., Cardoso, S., Santos, R.X., Carvalho, C., Santos, M.S., Perry, G., Smith, M.A., Moreira, P.I., 2011b. New insights into the mechanisms of mitochondrial preconditioning-triggered neuroprotection. Curr Pharm Des. 17, 3381-9.

Correia, S.C., Carvalho, C., Cardoso, S., Santos, R.X., Santos, M.S., Oliveira, C.R., Perry, G., Zhu, X., Smith, M.A., Moreira, P.I., 2010a. Mitochondrial preconditioning: a potential neuroprotective strategy. Front Aging Neurosci. 2.

Correia, S.C., Moreira, P.I., 2010. Hypoxia-inducible factor 1: a new hope to counteract neurodegeneration? J Neurochem. 112, 1-12.

Correia, S.C., Santos, R.X., Cardoso, S.M., Santos, M.S., Oliveira, C.R., Moreira, P.I., 2012b. Cyanide preconditioning protects brain endothelial and NT2 neuron-like cells against glucotoxicity: role of mitochondrial reactive oxygen species and HIF-1alpha. Neurobiol Dis. 45, 206-18.

Correia, S.C., Santos, R.X., Carvalho, C., Cardoso, S., Candeias, E., Santos, M.S., Oliveira, C.R., Moreira, P.I., 2012a. Insulin signaling, glucose metabolism and mitochondria: Major players in Alzheimer's disease and diabetes interrelation. Brain Res. 1441, 64-78.

Correia, S.C., Santos, R.X., Perry, G., Zhu, X., Moreira, P.I., Smith, M.A., 2011a. Insulin-resistant brain state: the culprit in sporadic Alzheimer's disease? Ageing Res Rev. 10, 264-73.

Correia, S.C., Santos, R.X., Perry, G., Zhu, X., Moreira, P.I., Smith, M.A., 2010b. Mitochondria: the missing link between preconditioning and neuroprotection. J Alzheimers Dis. 20 Suppl 2, S475-85.

Coyle, J.T., Price, D.L., Delong, M.R., 1983. Alzheimer's disease: a disorder of cortical cholinergic innervations. Science 219, 1184-1190.

Craft, S., Peskind, E., Schwartz, M.W., Schellenberg, G.D., Raskind, M., Porte, D., Jr., 1998. Cerebrospinal fluid and plasma insulin levels in Alzheimer's disease: relationship to severity of dementia and apolipoprotein E genotype. Neurology. 50, 164-8.

Cregan, S.P., MacLaurin, J.G., Craig, C.G., Robertson, G.S., Nicholson, D.W., Park, D.S., Slack, R.S., 1999. Bax-dependent caspase-3 activation is a key determinant in p53-induced apoptosis in neurons. J Neurosci. 19, 7860-9.

Cross, D.A., Alessi, D.R., Cohen, P., Andjelkovich, M., Hemmings, B.A., 1995. Inhibition of glycogen synthase kinase-3 by insulin mediated by protein kinase B. Nature. 378, 785-9.

Crouch, P.J., Blake, R., Duce, J.A., Ciccotosto, G.D., Li, Q.X., Barnham, K.J., Curtain, C.C., Cherny, R.A., Cappai, R., Dyrks, T., Masters, C.L., Trounce, I.A., 2005. Copper-dependent inhibition of human cytochrome c oxidase by a dimeric conformer of amyloid-beta1-42. J Neurosci. 25, 672-9.

Curti, D., Rognoni, F., Gasparini, L., Cattaneo, A., Paolillo, M., Racchi, M., Zani, L., Bianchetti, A., Trabucchi, M., Bergamaschi, S., Govoni, S., 1997. Oxidative metabolism in cultured fibroblasts derived from sporadic Alzheimer's disease (AD) patients. Neurosci Lett. 236, 13-6.

Cutler, R.G., Kelly, J., Storie, K., Pedersen, W.A., Tammara, A., Hatanpaa, K., Troncoso, J.C., Mattson, M.P., 2004. Involvement of oxidative stress-induced abnormalities in ceramide and cholesterol metabolism in brain aging and Alzheimer's disease. Proc Natl Acad Sci U S A. 101, 2070-5.

Dahl, N.A., Balfour, W.M., 1964. Prolonged Anoxic Survival Due to Anoxia Pre-Exposure: Brain Atp, Lactate, and Pyruvate. Am J Physiol. 207, 452-6.

Dave, K.R., DeFazio, R.A., Raval, A.P., Torraco, A., Saul, I., Barrientos, A., Perez-Pinzon, M.A., 2008. Ischemic preconditioning targets the respiration of synaptic mitochondria via protein kinase C epsilon. J Neurosci. 28, 4172-82.

Dave, K.R., Saul, I., Busto, R., Ginsberg, M.D., Sick, T.J., Perez-Pinzon, M.A., 2001. Ischemic preconditioning preserves mitochondrial function after global cerebral ischemia in rat hippocampus. J Cereb Blood Flow Metab. 21, 1401-10.

de la Monte, S.M., Wands, J.R., 2005. Review of insulin and insulin-like growth factor expression, signaling, and malfunction in the central nervous system: relevance to Alzheimer's disease. J Alzheimers Dis. 7, 45-61.

Debska, G., May, R., Kicinska, A., Szewczyk, A., Elger, C.E., Kunz, W.S., 2001. Potassium channel openers depolarize hippocampal mitochondria. Brain Res. 892, 42-50.

DeCarli, C., 2001. The role of neuroimaging in dementia. Clin Geriatr Med. 17, 255-79.

DeJong, R.N., 1977. CNS manifestations of diabetes mellitus. Postgrad Med. 61, 101-7.

Della-Morte, D., Dave, K.R., DeFazio, R.A., Bao, Y.C., Raval, A.P., Perez-Pinzon, M.A., 2009. Resveratrol pretreatment protects rat brain from cerebral ischemic damage via a sirtuin 1-uncoupling protein 2 pathway. Neuroscience. 159, 993-1002.

den Heijer, T., Vermeer, S.E., van Dijk, E.J., Prins, N.D., Koudstaal, P.J., Hofman, A., Breteler, M.M., 2003. Type 2 diabetes and atrophy of medial temporal lobe structures on brain MRI. Diabetologia. 46, 1604-10.

Devi, L., Prabhu, B.M., Galati, D.F., Avadhani, N.G., Anandatheerthavarada, H.K., 2006. Accumulation of amyloid precursor protein in the mitochondrial import channels of human Alzheimer's disease brain is associated with mitochondrial dysfunction. J Neurosci. 26, 9057-68.

Diano, S., Matthews, R.T., Patrylo, P., Yang, L., Beal, M.F., Barnstable, C.J., Horvath, T.L., 2003. Uncoupling protein 2 prevents neuronal death including that occurring during seizures: a mechanism for preconditioning. Endocrinology. 144, 5014-21.

Dirnagl, U., Becker, K., Meisel, A., 2009. Preconditioning and tolerance against cerebral ischaemia: from experimental strategies to clinical use. Lancet Neurol. 8, 398-412.

Dirnagl, U., Meisel, A., 2008. Endogenous neuroprotection: mitochondria as gateways to cerebral preconditioning? Neuropharmacology. 55, 334-44.

Dirnagl, U., Simon, R.P., Hallenbeck, J.M., 2003. Ischemic tolerance and endogenous neuroprotection. Trends Neurosci. 26, 248-54.

Domoki, F., Perciaccante, J.V., Veltkamp, R., Bari, F., Busija, D.W., 1999. Mitochondrial potassium channel opener diazoxide preserves neuronal-vascular function after cerebral ischemia in newborn pigs. Stroke. 30, 2713-8; discussion 2718-9.

Dragicevic, N., Mamcarz, M., Zhu, Y., Buzzeo, R., Tan, J., Arendash, G.W., Bradshaw, P.C., 2010. Mitochondrial amyloid-beta levels are associated with the extent of mitochondrial dysfunction in different brain regions and the degree of cognitive impairment in Alzheimer's transgenic mice. J Alzheimers Dis. 20 Suppl 2, S535-50.

Du, H., Guo, L., Fang, F., Chen, D., Sosunov, A.A., McKhann, G.M., Yan, Y., Wang, C., Zhang, H., Molkentin, J.D., Gunn-Moore, F.J., Vonsattel, J.P., Arancio, O., Chen, J.X., Yan, S.D., 2008. Cyclophilin D deficiency attenuates mitochondrial and neuronal perturbation and ameliorates learning and memory in Alzheimer's disease. Nat Med. 14, 1097-105.

Du, H., Guo, L., Zhang, W., Rydzewska, M., Yan, S., 2011. Cyclophilin D deficiency improves mitochondrial function and learning/memory in aging Alzheimer disease mouse model. Neurobiol Aging. 32, 398-406.

Duchen, M.R., 2004. Roles of mitochondria in health and disease. Diabetes. 53 Suppl 1, S96-102.

Duval, C., Negre-Salvayre, A., Dogilo, A., Salvayre, R., Penicaud, L., Casteilla, L., 2002. Increased reactive oxygen species production with antisense oligonucleotides directed against uncoupling protein 2 in murine endothelial cells. Biochem Cell Biol. 80, 757-64.

Echtay, K.S., Brand, M.D., 2007. 4-hydroxy-2-nonenal and uncoupling proteins: an approach for regulation of mitochondrial ROS production. Redox Rep. 12, 26-9.

Edwards, J.L., Quattrini, A., Lentz, S.I., Figueroa-Romero, C., Cerri, F., Backus, C., Hong, Y., Feldman, E.L., 2010. Diabetes regulates mitochondrial biogenesis and fission in mouse neurons. Diabetologia. 53, 160-9.

Elsner, M., Guldbakke, B., Tiedge, M., Munday, R., Lenzen, S., 2000. Relative importance of transport and alkylation for pancreatic beta-cell toxicity of streptozotocin. Diabetologia. 43, 1528-33.

Ernster, L., Nordenbrand, K., 1967. Microsomal lipid peroxidation. Methods Enzymol. 10, 574-580.

Estabrook, R.E., 1967. Mitochondrial respiratory control and the polarographic measurement of ADP/O ratios. Methods Enzymol. 10,41-7.

Fernyhough, P., Roy Chowdhury, S.K., Schmidt, R.E., 2010. Mitochondrial stress and the pathogenesis of diabetic neuropathy. Expert Rev Endocrinol Metab. 5, 39-49.

Finch, C.E., 2003. Neurons, glia, and plasticity in normal brain aging. Neurobiol Aging. 24 Suppl 1, S123-7; discussion S131.

Flohé, L., Otting, F., 1984. Superoxide dismutase assays. Methods Enzymol. 105, 93-104.

Freude, S., Plum, L., Schnitker, J., Leeser, U., Udelhoven, M., Krone, W., Bruning, J.C., Schubert, M., 2005. Peripheral hyperinsulinemia promotes tau phosphorylation in vivo. Diabetes. 54, 3343-8.

Frezza, C., Cipolat, S., Martins de Brito, O., Micaroni, M., Beznoussenko, G.V., Rudka, T., Bartoli, D., Polishuck, R.S., Danial, N.N., De Strooper, B., Scorrano, L., 2006. OPA1 controls apoptotic cristae remodeling independently from mitochondrial fusion. Cell. 126, 177-89.

Frolich, L., Blum-Degen, D., Bernstein, H.G., Engelsberger, S., Humrich, J., Laufer, S., Muschner, D., Thalheimer, A., Turk, A., Hoyer, S., Zochling, R., Boissl, K.W., Jellinger, K., Riederer, P., 1998. Brain insulin and insulin receptors in aging and sporadic Alzheimer's disease. J Neural Transm. 105, 423-38.

Frolich, L., Blum-Degen, D., Riederer, P., Hoyer, S., 1999. A disturbance in the neuronal insulin receptor signal transduction in sporadic Alzheimer's disease. Ann N Y Acad Sci. 893, 290-3.

Frolich, L., Blum-Degen, D., Riederer, P., Hoyer, S., 1999. A disturbance in the neuronal insulin receptor signal transduction in sporadic Alzheimer's disease. Ann N Y Acad Sci. 893, 290-3.

Fukuda, R., Zhang, H., Kim, J.W., Shimoda, L., Dang, C.V., Semenza, G.L., 2007. HIF-1 regulates cytochrome oxidase subunits to optimize efficiency of respiration in hypoxic cells. Cell. 129, 111-22.

Furuichi, T., Liu, W., Shi, H., Miyake, M., Liu, K.J., 2005. Generation of hydrogen peroxide during brief oxygen-glucose deprivation induces preconditioning neuronal protection in primary cultured neurons. J Neurosci Res. 79, 816-24.

Galluzzi, L., Blomgren, K., Kroemer, G., 2009. Mitochondrial membrane permeabilization in neuronal injury. Nat Rev Neurosci. 10, 481-94.

Garlid, K.D., Paucek, P., Yarov-Yarovoy, V., Murray, H.N., Darbenzio, R.B., D'Alonzo, A.J., Lodge, N.J., Smith, M.A., Grover, G.J., 1997. Cardioprotective effect of diazoxide and its interaction with mitochondrial ATP-sensitive K+ channels. Possible mechanism of cardioprotection. Circ Res. 81, 1072-82.

Gaspar, T., Domoki, F., Lenti, L., Katakam, P.V., Snipes, J.A., Bari, F., Busija, D.W., 2009. Immediate neuronal preconditioning by NS1619. Brain Res. 1285, 196-207.

Gaspar, T., Snipes, J.A., Busija, A.R., Kis, B., Domoki, F., Bari, F., Busija, D.W., 2008a. ROS-independent preconditioning in neurons via activation of mitoK(ATP) channels by BMS-191095. J Cereb Blood Flow Metab. 28, 1090-103.

Gasparini, L., Gouras, G.K., Wang, R., Gross, R.S., Beal, M.F., Greengard, P., Xu, H., 2001. Stimulation of beta-amyloid precursor protein trafficking by insulin reduces intraneuronal beta-amyloid and requires mitogen-activated protein kinase signaling. J Neurosci. 21, 2561-70.

Gasparini, L., Netzer, W.J., Greengard, P., Xu, H., 2002. Does insulin dysfunction play a role in Alzheimer's disease? Trends Pharmacol Sci. 23, 288-93.

Gasparini, L., Xu, H., 2003. Potential roles of insulin and IGF-1 in Alzheimer's disease. Trends Neurosci. 26, 404-6.

Gasser, A., Forbes, J.M., 2008. Advanced glycation: implications in tissue damage and disease. Protein Pept Lett. 15, 385-91.

Giannattasio, S., Liu, Z., Thornton, J., Butow, R.A., 2005. Retrograde response to mitochondrial dysfunction is separable from TOR1/2 regulation of retrograde gene expression. J Biol Chem. 280, 42528-35.

Gibson, G.E., Huang, H.M., 2005. Oxidative stress in Alzheimer's disease. Neurobiol Aging. 26, 575-8.

Gibson, G.E., Shi, Q., 2010. A mitocentric view of Alzheimer's disease suggests multi-faceted treatments. J Alzheimers Dis. 20 Suppl 2, S591-607.

Gidday, J.M., 2006. Cerebral preconditioning and ischaemic tolerance. Nat Rev Neurosci. 7, 437-48.

Gidday, J.M., 2006. Cerebral preconditioning and ischaemic tolerance. Nat Rev Neurosci. 7, 437-48.

Girones, X., Guimera, A., Cruz-Sanchez, C.Z., Ortega, A., Sasaki, N., Makita, Z., Lafuente, J.V., Kalaria, R., Cruz-Sanchez, F.F., 2004. N epsilon-carboxymethyllysine in brain aging, diabetes mellitus, and Alzheimer's disease. Free Radic Biol Med. 36, 1241-7.

Gispen, W.H., Biessels, G.J., 2000. Cognition and synaptic plasticity in diabetes mellitus. Trends Neurosci. 23, 542-9.

Goh, S.Y., Cooper, M.E., 2008. Clinical review: The role of advanced glycation end products in progression and complications of diabetes. J Clin Endocrinol Metab. 93, 1143-52.

Gomes, L.C., Di Benedetto, G., Scorrano, L., 2011. During autophagy mitochondria elongate, are spared from degradation and sustain cell viability. Nat Cell Biol. 13, 589-98.

Goodman, Y., Mattson, M.P., 1996. K+ channel openers protect hippocampal neurons against oxidative injury and amyloid beta-peptide toxicity. Brain Res. 706, 328-32.

Gornall, A.G., Bardawill, C.J., David, M.M., 1949. Determination of serum proteins by means of the biuret reaction. J Biol Chem. 177, 751-66.

Gotz, J., Ittner, L.M., 2008. Animal models of Alzheimer's disease and frontotemporal dementia. Nat Rev Neurosci. 9, 532-44.

Green, L.C., Ruiz de Luzuriaga, K., Wagner, D.A., Rand, W., Istfan, N., Young, V.R., Tannenbaum, S.R., 1981. Nitrate biosynthesis in man. Proc Natl Acad Sci U S A. 78, 7764-8.

Gross, A., Jockel, J., Wei, M.C., Korsmeyer, S.J., 1998. Enforced dimerization of BAX results in its translocation, mitochondrial dysfunction and apoptosis. EMBO J. 17, 3878-85.

Grunblatt, E., Salkovic-Petrisic, M., Osmanovic, J., Riederer, P., Hoyer, S., 2007. Brain insulin system dysfunction in streptozotocin intracerebroventricularly treated rats generates hyperphosphorylated tau protein. J. Neurochem. 101, 757-770.

Gu, M., Owen, A.D., Toffa, S.E., Cooper, J.M., Dexter, D.T., Jenner, P., Marsden, C.D., Schapira, A.H., 1998. Mitochondrial function, GSH and iron in neurodegeneration and Lewy body diseases. J Neurol Sci. 158, 24-9.

Guglielmotto, M., Giliberto, L., Tamagno, E., Tabaton, M., 2010. Oxidative stress mediates the pathogenic effect of different Alzheimer's disease risk factors. Front Aging Neurosci. 2, 3.

Guidi, I., Galimberti, D., Lonati, S., Novembrino, C., Bamonti, F., Tiriticco, M., Fenoglio, C., Venturelli, E., Baron, P., Bresolin, N., Scarpini, E., 2006. Oxidative imbalance in patients with mild cognitive impairment and Alzheimer's disease. Neurobiol Aging. 27, 262-9.

Gunter, T.E., Buntinas, L., Sparagna, G., Eliseev, R., Gunter, K., 2000. Mitochondrial calcium transport: mechanisms and functions. Cell Calcium. 28, 285-96.

Gutsaeva, D.R., Carraway, M.S., Suliman, H.B., Demchenko, I.T., Shitara, H., Yonekawa, H., Piantadosi, C.A., 2008. Transient hypoxia stimulates mitochondrial biogenesis in brain subcortex by a neuronal nitric oxide synthase-dependent mechanism. J Neurosci. 28, 2015-24.

Guzy, R.D., Hoyos, B., Robin, E., Chen, H., Liu, L., Mansfield, K.D., Simon, M.C., Hammerling, U., Schumacker, P.T., 2005. Mitochondrial complex III is required for hypoxia-induced ROS production and cellular oxygen sensing. Cell Metab. 1, 401-8.

Hackenbrock, C.R., 1966. Ultrastructural bases for metabolically linked mechanical activity in mitochondria. I. Reversible ultrastructural changes with change in metabolic steady state in isolated liver mitochondria. J Cell Biol. 30, 269-97.

Hackenbrock, C.R., Rehn, T.G., Weinbach, E.C., Lemasters, J.J., 1971. Oxidative phosphorylation and ultrastructural transformation in mitochondria in the intact ascites tumor cell. J Cell Biol. 51, 123-37.

Halestrap, A.P., Clarke, S.J., Khaliulin, I., 2007. The role of mitochondria in protection of the heart by preconditioning. Biochim Biophys Acta. 1767, 1007-31.

Hansson Petersen, C.A., Alikhani, N., Behbahani, H., Wiehager, B., Pavlov, P.F., Alafuzoff, I., Leinonen, V., Ito, A., Winblad, B., Glaser, E., Ankarcrona, M., 2008. The amyloid beta-peptide is imported into mitochondria via the TOM import machinery and localized to mitochondrial cristae. Proc Natl Acad Sci U S A. 105, 13145-50.

Hardie, D.G., 2005. New roles for the LKB1-->AMPK pathway. Curr Opin Cell Biol. 17, 167-73.

Hardy, J., Selkoe, D.J., 2002. The amyloid hypothesis of Alzheimer's disease: progress and problems on the road to therapeutics. Science. 297, 353-6.

Hashimoto, M., Rockenstein, E., Crews, L., Masliah, E., 2003. Role of protein aggregation in mitochondrial dysfunction and neurodegeneration in Alzheimer's and Parkinson's diseases. Neuromolecular Med. 4, 21-36.

Hauptmann, S., Scherping, I., Drose, S., Brandt, U., Schulz, K.L., Jendrach, M., Leuner, K., Eckert, A., Muller, W.E., 2009. Mitochondrial dysfunction: an early event in Alzheimer pathology accumulates with age in AD transgenic mice. Neurobiol Aging. 30, 1574-86.

Hausenloy, D.J., Maddock, H.L., Baxter, G.F., Yellon, D.M., 2002. Inhibiting mitochondrial permeability transition pore opening: a new paradigm for myocardial preconditioning? Cardiovasc Res. 55, 534-43.

Heitner, J., Dickson, D., 1997. Diabetics do not have increased Alzheimer-type pathology compared with age-matched control subjects. A retrospective postmortem immunocytochemical and histofluorescent study. Neurology. 49, 1306-11.

Hengartner, M.O., 2000. The biochemistry of apoptosis. Nature. 407, 770-6.

Henneberg, N., Hoyer, S., 1995. Desensitization of the neuronal insulin receptor: a new approach in the etiopathogenesis of late-onset sporadic dementia of the Alzheimer type (SDAT)? Arch Gerontol Geriatr. 21, 63-74.

Hirai, K., Aliev, G., Nunomura, A., Fujioka, H., Russell, R.L., Atwood, C.S., Johnson, A.B., Kress, Y., Vinters, H.V., Tabaton, M., Shimohama, S., Cash, A.D., Siedlak, S.L., Harris, P.L., Jones, P.K., Petersen, R.B., Perry, G., Smith, M.A., 2001. Mitochondrial abnormalities in Alzheimer's disease. J Neurosci. 21, 3017-23.

Hirai, K., Hayashi, T., Chan, P.H., Zeng, J., Yang, G.Y., Basus, V.J., James, T.L., Litt, L., 2004. PI3K inhibition in neonatal rat brain slices during and after hypoxia reduces phospho-Akt and increases cytosolic cytochrome c and apoptosis. Brain Res Mol Brain Res. 124, 51-61.

Hissin, P.J., Hilf, R., 1976. A fluorometric method for determination of oxidized and reduced glutathione in tissues. Anal Biochem. 74, 214-26.

Ho, L., Qin, W., Pompl, P.N., Xiang, Z., Wang, J., Zhao, Z., Peng, Y., Cambareri, G., Rocher, A., Mobbs, C.V., Hof, P.R., Pasinetti, G.M., 2004. Diet-induced insulin resistance promotes amyloidosis in a transgenic mouse model of Alzheimer's disease. FASEB J. 18, 902-4.

Hollenbeck, P.J., Saxton, W.M., 2005. The axonal transport of mitochondria. J Cell Sci. 118, 5411-9.

Hong, M., Lee, V.M., 1997. Insulin and insulin-like growth factor-1 regulate tau phosphorylation in cultured human neurons. J Biol Chem. 272, 19547-53.

Hooijmans, C.R., Graven, C., Dederen, P.J., Tanila, H., van Groen, T., Kiliaan, A.J., 2007. Amyloid beta deposition is related to decreased glucose transporter-1 levels and hippocampal atrophy in brains of aged APP/PS1 mice. Brain Res. 1181, 93-103.

Horiguchi, T., Kis, B., Rajapakse, N., Shimizu, K., Busija, D.W., 2003. Opening of mitochondrial ATP-sensitive potassium channels is a trigger of 3-nitropropionic acid-induced tolerance to transient focal cerebral ischemia in rats. Stroke. 34, 1015-20.

Hoyer, S., 2000. Brain glucose and energy metabolism abnormalities in sporadic Alzheimer disease. Causes and consequences: an update. Exp Gerontol. 35, 1363-72.

Hoyer, S., 2002. The brain insulin signal transduction system and sporadic (type II) Alzheimer disease: an update. J Neural Transm. 109, 341-60.

Hoyer, S., 2004a. Causes and consequences of disturbances of cerebral glucose metabolism in sporadic Alzheimer disease: therapeutic implications. Adv Exp Med Biol. 541, 135-52.

Hoyer, S., 2004b. Glucose metabolism and insulin receptor signal transduction in Alzheimer disease. Eur J Pharmacol. 490, 115-25.

Hoyer, S., Lannert, H., 2007. Long-term abnormalities in brain glucose/energy metabolism after inhibition of the neuronal insulin receptor: implication of tau-protein. J Neural Transm Suppl. 195-202.

Hoyer, S., Nitsch, R., 1989. Cerebral excess release of neurotransmitter amino acids subsequent to reduced cerebral glucose metabolism in early-onset dementia of Alzheimer type. J Neural Transm. 75, 227-32.

Huang, H.M., Ou, H.C., Xu, H., Chen, H.L., Fowler, C., Gibson, G.E., 2003. Inhibition of alpha-ketoglutarate dehydrogenase complex promotes cytochrome c release from mitochondria, caspase-3 activation, and necrotic cell death. J Neurosci Res. 74, 309-17.

Huang, L.E., Arany, Z., Livingston, D.M., Bunn, H.F., 1996. Activation of hypoxia-inducible transcription factor depends primarily upon redox-sensitive stabilization of its alpha subunit. J Biol Chem. 271, 32253-9.

Huang, L.E., Gu, J., Schau, M., Bunn, H.F., 1998. Regulation of hypoxia-inducible factor 1alpha is mediated by an O2-dependent degradation domain via the ubiquitin-proteasome pathway. Proc Natl Acad Sci U S A. 95, 7987-92.

Humphries, K.M., Szweda, L.I., 1998. Selective inactivation of alpha-ketoglutarate dehydrogenase and pyruvate dehydrogenase: reaction of lipoic acid with 4-hydroxy-2-nonenal. Biochemistry. 37, 15835-41.

Iadecola, C., 2004. Neurovascular regulation in the normal brain and in Alzheimer's disease. Nat Rev Neurosci. 5, 347-60.

Iijima, T., Tanaka, K., Matsubara, S., Kawakami, H., Mishima, T., Suga, K., Akagawa, K., Iwao, Y., 2008. Calcium loading capacity and morphological changes in mitochondria in an ischemic preconditioned model. Neurosci Lett. 448, 268-72.

Imahori, K., 2010. The biochemical study on the etiology of Alzheimer's disease. Proc Jpn Acad Ser B Phys Biol Sci. 86, 54-61.

Inoue, I., Nagase, H., Kishi, K., Higuti, T., 1991. ATP-sensitive K+ channel in the mitochondrial inner membrane. Nature. 352, 244-7.

Irrcher, I., Ljubicic, V., Hood, D.A., 2009. Interactions between ROS and AMP kinase activity in the regulation of PGC-1alpha transcription in skeletal muscle cells. Am J Physiol Cell Physiol. 296, C116-23.

Ishrat, T., Hoda, M.N., Khan, M.B., Yousuf, S., Ahmad, M., Khan, M.M., Ahmad, A., Islam, F., 2009a. Amelioration of cognitive deficits and neurodegeneration by curcumin in rat model of sporadic dementia of Alzheimer's type (SDAT). Eur Neuropsychopharmacol. 19, 636-47.

Ishrat, T., Parveen, K., Khan, M.M., Khuwaja, G., Khan, M.B., Yousuf, S., Ahmad, A., Shrivastav, P., Islam, F., 2009b. Selenium prevents cognitive decline and oxidative damage in rat model of streptozotocin-induced experimental dementia of Alzheimer's type. Brain Res. 1281, 117-27.

Ivan, M., Kondo, K., Yang, H., Kim, W., Valiando, J., Ohh, M., Salic, A., Asara, J.M., Lane, W.S., Kaelin, W.G., Jr., 2001. HIFalpha targeted for VHL-mediated destruction by proline hydroxylation: implications for O2 sensing. Science. 292, 464-8.

Jaakkola, P., Mole, D.R., Tian, Y.M., Wilson, M.I., Gielbert, J., Gaskell, S.J., Kriegsheim, A., Hebestreit, H.F., Mukherji, M., Schofield, C.J., Maxwell, P.H., Pugh, C.W., Ratcliffe, P.J., 2001. Targeting of HIF-alpha to the von Hippel-Lindau ubiquitylation complex by O2-regulated prolyl hydroxylation. Science. 292, 468-72.

Janson, J., Laedtke, T., Parisi, J.E., O'Brien, P., Petersen, R.C., Butler, P.C., 2004. Increased risk of type 2 diabetes in Alzheimer disease. Diabetes. 53, 474-81.

Javadov, S.A., Clarke, S., Das, M., Griffiths, E.J., Lim, K.H., Halestrap, A.P., 2003. Ischaemic preconditioning inhibits opening of mitochondrial permeability transition pores in the reperfused rat heart. J Physiol. 549, 513-24.

Jendrach, M., Mai, S., Pohl, S., Voth, M., Bereiter-Hahn, J., 2008. Short- and long-term alterations of mitochondrial morphology, dynamics and mtDNA after transient oxidative stress. Mitochondrion. 8, 293-304.

Jensen, B.D., Gunter, T.R., 1984. The use of tertaphenylphosphonium (TPP+) to measure membrane potentials in mitochondria: membrane binding and respiratory effects. Biophys. J. 45,92.

Jensen, M.S., Ahlemeyer, B., Ravati, A., Thakur, P., Mennel, H.D., Krieglstein, J., 2002. Preconditioning-induced protection against cyanide-induced neurotoxicity is mediated by preserving mitochondrial function. Neurochem Int. 40, 285-93.

Jolivalt, C.G., Hurford, R., Lee, C.A., Dumaop, W., Rockenstein, E., Masliah, E., 2010. Type 1 diabetes exaggerates features of Alzheimer's disease in APP transgenic mice. Exp Neurol. 223, 422-31.

Jolivalt, C.G., Lee, C.A., Beiswenger, K.K., Smith, J.L., Orlov, M., Torrance, M.A., Masliah, E., 2008. Defective insulin signaling pathway and increased glycogen synthase kinase-3 activity in the brain of diabetic mice: parallels with Alzheimer's disease and correction by insulin. J Neurosci Res. 86, 3265-74.

Jones, N.M., Bergeron, M., 2001. Hypoxic preconditioning induces changes in HIF-1 target genes in neonatal rat brain. J Cereb Blood Flow Metab. 21, 1105-14.

Joseph, J., Shukitt-Hale, B., Denisova, N.A., Martin, A., Perry, G., Smith, M.A., 2001. Copernicus revisited: amyloid beta in Alzheimer's disease. Neurobiol Aging. 22, 131-46.

Jou, M.J., 2008. Pathophysiological and pharmacological implications of mitochondria-targeted reactive oxygen species generation in astrocytes. Adv Drug Deliv Rev. 60, 1512-26.

Jung, M.E., Simpkins, J.W., Wilson, A.M., Downey, H.F., Mallet, R.T., 2008. Intermittent hypoxia conditioning prevents behavioral deficit and brain oxidative stress in ethanol-withdrawn rats. J Appl Physiol. 105, 510-7.

Kamo, N., Muratsugu, M., Hongoh, R., Kobatake, Y., 1979. Membrane potential of mitochondria measured with an electrode sensitive to tetraphenyl phosphonium and relationship between proton electrochemical potential and phosphorylation potential in steady state. J Membr Biol. 49, 105-21.

Kann, O., Kovacs, R., 2007. Mitochondria and neuronal activity. Am J Physiol Cell Physiol. 292, C641-57.

Karran, E., Mercken, M., De Strooper, B., 2011. The amyloid cascade hypothesis for Alzheimer's disease: an appraisal for the development of therapeutics. Nat Rev Drug Discov. 10, 698-712.

Kawas, C.H., Corrada, M.M., 2006. Alzheimer's and dementia in the oldest-old: a century of challenges. Curr Alzheimer Res. 3, 411-9.

Kelleher, I., Garwood, C., Hanger, D.P., Anderton, B.H., Noble, W., 2007. Kinase activities increase during the development of tauopathy in htau mice. J Neurochem. 103, 2256-67.

Keller, J.N., Mark, R.J., Bruce, A.J., Blanc, E., Rothstein, J.D., Uchida, K., Waeg, G., Mattson, M.P., 1997. 4-Hydroxynonenal, an aldehydic product of membrane lipid peroxidation, impairs glutamate transport and mitochondrial function in synaptosomes. Neuroscience. 80, 685-96.

Kim, B., Backus, C., Oh, S., Hayes, J.M., Feldman, E.L., 2009. Increased tau phosphorylation and cleavage in mouse models of type 1 and type 2 diabetes. Endocrinology. 150, 5294-301.

Kim, I., Rodriguez-Enriquez, S., Lemasters, J.J., 2007. Selective degradation of mitochondria by mitophagy. Arch Biochem Biophys. 462, 245-53.

Kim-Han, J.S., Dugan, L.L., 2005. Mitochondrial uncoupling proteins in the central nervous system. Antioxid Redox Signal. 7, 1173-81.

Kirino, T., 2002. Ischemic tolerance. J Cereb Blood Flow Metab. 22, 1283-96.

Kis, B., Nagy, K., Snipes, J.A., Rajapakse, N.C., Horiguchi, T., Grover, G.J., Busija, D.W., 2004. The mitochondrial K(ATP) channel opener BMS-191095 induces neuronal preconditioning. Neuroreport. 15, 345-9.

Kish, S.J., Bergeron, C., Rajput, A., Dozic, S., Mastrogiacomo, F., Chang, L.J., Wilson, J.M., DiStefano, L.M., Nobrega, J.N., 1992. Brain cytochrome oxidase in Alzheimer's disease. J Neurochem. 59, 776-9.

Kitagawa, K., Matsumoto, M., Kuwabara, K., Tagaya, M., Ohtsuki, T., Hata, R., Ueda, H., Handa, N., Kimura, K., Kamada, T., 1991. 'Ischemic tolerance' phenomenon detected in various brain regions. Brain Res. 561, 203-11.

Ko, L.W., Sheu, K.F., Thaler, H.T., Markesbery, W.R., Blass, J.P., 2001. Selective loss of KGDHC-enriched neurons in Alzheimer temporal cortex: does mitochondrial variation contribute to selective vulnerability? J Mol Neurosci. 17, 361-9.

Koopman, W.J., Verkaart, S., Visch, H.J., van der Westhuizen, F.H., Murphy, M.P., van den Heuvel, L.W., Smeitink, J.A., Willems, P.H., 2005. Inhibition of complex I of the electron transport chain causes O2-. -mediated mitochondrial outgrowth. Am J Physiol Cell Physiol. 288, C1440-50.

Krebs, H. A.; Holzach, O., 1952. The conversion of citrate into cis-aconitate and isocitrate in the presence of aconitase. Biochem. J. 52, 527-528.

Kroner, Z., 2009. The relationship between Alzheimer's disease and diabetes: Type 3 diabetes? Altern Med Rev. 14, 373-9.

Kulawiak, B., Bednarczyk, P., 2005. Reconstitution of brain mitochondria inner membrane into planar lipid bilayer. Acta Neurobiol Exp (Wars). 65, 271-6.

Kumagai, A.K., 1999. Glucose transport in brain and retina: implications in the management and complications of diabetes. Diabetes Metab Res Rev. 15, 261-73.

Kumar, U., Dunlop, D.M., Richardson, J.S., 1994. Mitochondria from Alzheimer's fibroblasts show decreased uptake of calcium and increased sensitivity to free radicals. Life Sci. 54, 1855-60.

Kung, A.L., Wang, S., Klco, J.M., Kaelin, W.G., Livingston, D.M., 2000. Suppression of tumor growth through disruption of hypoxia-inducible transcription. Nat Med. 6, 1335-40.

Kurosinski, P., Gotz, J., 2002. Glial cells under physiologic and pathologic conditions. Arch Neurol. 59, 1524-8.

LaFerla, F.M., 2002. Calcium dyshomeostasis and intracellular signalling in Alzheimer's disease. Nat Rev Neurosci. 3, 862-72.

Lannert, H., Hoyer, S., 1998. Intracerebroventricular administration of streptozotocin causes long-term diminutions in learning and memory abilities and in cerebral energy metabolism in adult rats. Behav Neurosci. 112, 1199-208.

Leal, M.C., Fernandez Gamba, A., Morelli, L., Castano, E.M., 2009. [Cerebral proteolysis of amiloid-b peptide: relevance of insulin-degrading enzyme in Alzheimer's disease]. Medicina (B Aires). 69, 466-72.

Leavesley, H.B., Li, L., Prabhakaran, K., Borowitz, J.L., Isom, G.E., 2008. Interaction of cyanide and nitric oxide with cytochrome c oxidase: implications for acute cyanide toxicity. Toxicol Sci. 101, 101-11.

Ledesma, M.D., Bonay, P., Colaco, C., Avila, J., 1994. Analysis of microtubule-associated protein tau glycation in paired helical filaments. J Biol Chem. 269, 21614-9.

Lee, H.C., Wei, Y.H., 2005. Mitochondrial biogenesis and mitochondrial DNA maintenance of mammalian cells under oxidative stress. Int J Biochem Cell Biol. 37, 822-34.

Lee, H.C., Yin, P.H., Lu, C.Y., Chi, C.W., Wei, Y.H., 2000. Increase of mitochondria and mitochondrial DNA in response to oxidative stress in human cells. Biochem J. 348 Pt 2, 425-32.

Leinninger, G.M., Backus, C., Sastry, A.M., Yi, Y.B., Wang, C.W., Feldman, E.L., 2006. Mitochondria in DRG neurons undergo hyperglycemic mediated injury through Bim, Bax and the fission protein Drp1. Neurobiol Dis. 23, 11-22.

Leissring, M.A., Farris, W., Chang, A.Y., Walsh, D.M., Wu, X., Sun, X., Frosch, M.P., Selkoe, D.J., 2003. Enhanced proteolysis of beta-amyloid in APP transgenic mice prevents plaque formation, secondary pathology, and premature death. Neuron. 40, 1087-93.

Leong, S.F., Lai, J.C., Lim, L., Clark, J.B., 1981. Energy-metabolizing enzymes in brain regions of adult and aging rats. J Neurochem. 37, 1548-56.

Lesort, M., Johnson, G.V., 2000. Insulin-like growth factor-1 and insulin mediate transient site-selective increases in tau phosphorylation in primary cortical neurons. Neuroscience. 99, 305-16.

Lester-Coll, N., Rivera, E.J., Soscia, S.J., Doiron, K., Wands, J.R., de la Monte, S.M., 2006. Intracerebral streptozotocin model of type 3 diabetes: relevance to sporadic Alzheimer's disease. J Alzheimers Dis. 9, 13-33.

Li, L., Holscher, C., 2007. Common pathological processes in Alzheimer disease and type 2 diabetes: a review. Brain Res Rev. 56, 384-402.

Li, Z., Okamoto, K., Hayashi, Y., Sheng, M., 2004. The importance of dendritic mitochondria in the morphogenesis and plasticity of spines and synapses. Cell. 119, 873-87.

Li, Z.G., Zhang, W., Grunberger, G., Sima, A.A., 2002. Hippocampal neuronal apoptosis in type 1 diabetes. Brain Res. 946, 221-31.

Li, Z.G., Zhang, W., Sima, A.A., 2007. Alzheimer-like changes in rat models of spontaneous diabetes. Diabetes. 56, 1817-24.

Lin, A.M., Chen, C.F., Ho, L.T., 2002. Neuroprotective effect of intermittent hypoxia on iron-induced oxidative injury in rat brain. Exp Neurol. 176, 328-35.

Lin, H.Y., Huang, C.C., Chang, K.F., 2009. Lipopolysaccharide preconditioning reduces neuroinflammation against hypoxic ischemia and provides long-term outcome of neuroprotection in neonatal rat. Pediatr Res. 66, 254-9.

Lin, M.T., Beal, M.F., 2006. Alzheimer's APP mangles mitochondria. Nat Med. 12, 1241-3.

Lin, M.T., Beal, M.F., 2006. Mitochondrial dysfunction and oxidative stress in neurodegenerative diseases. Nature. 443, 787-95.

Liu, J., Narasimhan, P., Yu, F., Chan, P.H., 2005. Neuroprotection by hypoxic preconditioning involves oxidative stress-mediated expression of hypoxia-inducible factor and erythropoietin. Stroke. 36, 1264-9.

Liu, X., Feng, L., Yan, M., Xu, K., Yu, Y., Zheng, X., 2010. Changes in mitochondrial dynamics during amyloid beta-induced PC12 cell apoptosis. Mol Cell Biochem. 344, 277-84.

Liu, X., Wu, J.Y., Zhou, F., Sun, X.L., Yao, H.H., Yang, Y., Ding, J.H., Hu, G., 2006. The regulation of rotenone-induced inflammatory factor production by ATP-sensitive potassium channel expressed in BV-2 cells. Neurosci Lett. 394,131-135.

Liu, Y., Chen, L., Xu, X., Vicaut, E., Sercombe, R., 2009. Both ischemic preconditioning and ghrelin administration protect hippocampus from ischemia/reperfusion and upregulate uncoupling protein-2. BMC Physiol. 9, 17.

Liu, Y., Liu, F., Iqbal, K., Grundke-Iqbal, I., Gong, C.X., 2008. Decreased glucose transporters correlate to abnormal hyperphosphorylation of tau in Alzheimer disease. FEBS Lett. 582, 359-64.

Lohr, G.W., Waller, H.D., 1974. Glucose-6-phosphate Dehydrogenase. In Methods of Enzymatic Analysis 636.

Loschen, G., Azzi, A., Richter, C., Flohe, L., 1974. Superoxide radicals as precursors of mitochondrial hydrogen peroxide. FEBS Lett. 42, 68-72.

Lovell, M.A., Ehmann, W.D., Butler, S.M., Markesbery, W.R., 1995. Elevated thiobarbituric acid-reactive substances and antioxidant enzyme activity in the brain in Alzheimer's disease. Neurology. 45, 1594-601.

Lustbader, J.W., Cirilli, M., Lin, C., Xu, H.W., Takuma, K., Wang, N., Caspersen, C., Chen, X., Pollak, S., Chaney, M., Trinchese, F., Liu, S., Gunn-Moore, F., Lue, L.F., Walker, D.G., Kuppusamy, P., Zewier, Z.L., Arancio, O., Stern, D., Yan, S.S., Wu, H., 2004. ABAD directly links Abeta to mitochondrial toxicity in Alzheimer's disease. Science. 304, 448-52.

Ma, G., Chen, S., 2004. Diazoxide and N omega-nitro-L-arginine counteracted A beta 1-42-induced cytotoxicity. Neuroreport. 15, 1813-7.

Ma, G., Gao, J., Fu, Q., Jiang, L., Wang, R., Zhang, Y., Liu, K., 2009. Diazoxide reverses the enhanced expression of KATP subunits in cholinergic neurons caused by exposure to Abeta(1)(-)(4)(2). Neurochem Res. 34, 2133-40.

MacLullich, A.M., Deary, I.J., Starr, J.M., Walker, B.R., Secki, J.R., 2004. Glycosylated hemoglobin levels in healthy elderly nondiabetic men are negatively associated with verbal memory. J Am Geriatr Soc. 52, 848-9.

Manczak, M., Anekonda, T.S., Henson, E., Park, B.S., Quinn, J., Reddy, P.H., 2006. Mitochondria are a direct site of A beta accumulation in Alzheimer's disease neurons: implications for free radical generation and oxidative damage in disease progression. Hum Mol Genet. 15, 1437-49.

Manczak, M., Calkins, M.J., Reddy, P.H., 2011. Impaired mitochondrial dynamics and abnormal interaction of amyloid beta with mitochondrial protein Drp1 in neurons from patients with Alzheimer's disease: implications for neuronal damage. Hum Mol Genet. 20, 2495-509.

Manczak, M., Reddy, P.H., 2012. Abnormal interaction between the mitochondrial fission protein Drp1 and hyperphosphorylated tau in Alzheimer's disease neurons: implications for mitochondrial dysfunction and neuronal damage. Hum Mol Genet.

Mankovsky, B.N., Metzger, B.E., Molitch, M.E., Biller, J., 1996. Cerebrovascular disorders in patients with diabetes mellitus. J Diabetes Complications. 10, 228-42.

Manning, C.A., Ragozzino, M.E., Gold, P.E., 1993. Glucose enhancement of memory in patients with probable senile dementia of the Alzheimer's type. Neurobiol Aging. 14, 523-8.

Manschot, S.M., Brands, A.M., van der Grond, J., Kessels, R.P., Algra, A., Kappelle, L.J., Biessels, G.J., 2006. Brain magnetic resonance imaging correlates of impaired cognition in patients with type 2 diabetes. Diabetes. 55, 1106-13.

Mansfield, K.D., Guzy, R.D., Pan, Y., Young, R.M., Cash, T.P., Schumacker, P.T., Simon, M.C., 2005. Mitochondrial dysfunction resulting from loss of cytochrome c impairs cellular oxygen sensing and hypoxic HIF-alpha activation. Cell Metab. 1, 393-9.

Marcus, D.L., Thomas, C., Rodriguez, C., Simberkoff, K., Tsai, J.S., Strafaci, J.A., Freedman, M.L., 1998. Increased peroxidation and reduced antioxidant enzyme activity in Alzheimer's disease. Exp Neurol. 150, 40-4.

Martinez-Redondo, D., Marcuello, A., Casajus, J.A., Ara, I., Dahmani, Y., Montoya, J., Ruiz-Pesini, E., Lopez-Perez, M.J., Diez-Sanchez, C., 2010. Human mitochondrial haplogroup H: the highest VO2max consumer--is it a paradox? Mitochondrion. 10, 102-7.

Martinou, J.C., Green, D.R., 2001. Breaking the mitochondrial barrier. Nat Rev Mol Cell Biol. 2, 63-7.

Mastrocola, R., Restivo, F., Vercellinatto, I., Danni, O., Brignardello, E., Aragno, M., Boccuzzi, G., 2005. Oxidative and nitrosative stress in brain mitochondria of diabetic rats. J Endocrinol. 187, 37-44.

Mattiasson, G., Shamloo, M., Gido, G., Mathi, K., Tomasevic, G., Yi, S., Warden, C.H., Castilho, R.F., Melcher, T., Gonzalez-Zulueta, M., Nikolich, K., Wieloch, T., 2003. Uncoupling protein-2 prevents neuronal death and diminishes brain dysfunction after stroke and brain trauma. Nat Med. 9, 1062-8.

Mattson, M.P., 2004. Pathways towards and away from Alzheimer's disease. Nature. 430, 631-9.

Mattson, M.P., Gary, D.S., Chan, S.L., Duan, W., 2001. Perturbed endoplasmic reticulum function, synaptic apoptosis and the pathogenesis of Alzheimer's disease. Biochem Soc Symp. 151-62.

Mattson, M.P., Gleichmann, M., Cheng, A., 2008. Mitochondria in neuroplasticity and neurological disorders. Neuron. 60, 748-66.

Maxwell, P.H., Wiesener, M.S., Chang, G.W., Clifford, S.C., Vaux, E.C., Cockman, M.E., Wykoff, C.C., Pugh, C.W., Maher, E.R., Ratcliffe, P.J., 1999. The tumour suppressor protein VHL targets hypoxia-inducible factors for oxygen-dependent proteolysis. Nature. 399, 271-5.

Mayanagi, K., Gaspar, T., Katakam, P.V., Busija, D.W., 2007a. Systemic administration of diazoxide induces delayed preconditioning against transient focal cerebral ischemia in rats. Brain Res. 1168, 106-11.

Mayanagi, K., Gaspar, T., Katakam, P.V., Kis, B., Busija, D.W., 2007b. The mitochondrial K(ATP) channel opener BMS-191095 reduces neuronal damage after transient focal cerebral ischemia in rats. J Cereb Blood Flow Metab. 27, 348-55.

Meier-Ruge, W.A., Bertoni-Freddari, C., 1997. Pathogenesis of decreased glucose turnover and oxidative phosphorylation in ischemic and trauma-induced dementia of the Alzheimer type. Ann N Y Acad Sci. 826, 229-41.

Mesulam, M.M., 1996. The systems-level organization of cholinergic innervation in the human cerebral cortex and its alterations in Alzheimer's disease. Prog Brain Res. 109, 285-97.

Mole, D.R., Maxwell, P.H., Pugh, C.W., Ratcliffe, P.J., 2001. Regulation of HIF by the von Hippel-Lindau tumour suppressor: implications for cellular oxygen sensing. IUBMB Life. 52, 43-7.

Moloney, A.M., Griffin, R.J., Timmons, S., O'Connor, R., Ravid, R., O'Neill, C., 2010. Defects in IGF-1 receptor, insulin receptor and IRS-1/2 in Alzheimer's disease indicate possible resistance to IGF-1 and insulin signalling. Neurobiol Aging. 31, 224-43.

Moreira, P.I., Carvalho, C., Zhu, X., Smith, M.A., Perry, G., 2010. Mitochondrial dysfunction is a trigger of Alzheimer's disease pathophysiology. Biochim Biophys Acta. 1802, 2-10.

Moreira, P.I., Duarte, A.I., Santos, M.S., Rego, A.C., Oliveira, C.R., 2009. An integrative view of the role of oxidative stress, mitochondria and insulin in Alzheimer's disease. J Alzheimers Dis. 16, 741-61.

Moreira, P.I., Rolo, A.P., Sena, C., Seica, R., Oliveira, C.R., Santos, M.S., 2006. Insulin attenuates diabetes-related mitochondrial alterations: a comparative study. Med Chem. 2, 299-308.

Moreira, P.I., Santos, M.S., Moreno, A., Oliveira, C., 2001. Amyloid beta-peptide promotes permeability transition pore in brain mitochondria. Biosci Rep. 21, 789-800.

Moreira, P.I., Santos, M.S., Moreno, A., Rego, A.C., Oliveira, C., 2002. Effect of amyloid beta-peptide on permeability transition pore: a comparative study. J Neurosci Res. 69, 257-67.

Moreira, P.I., Santos, M.S., Moreno, A.M., Proenca, T., Seica, R., Oliveira, C.R., 2004. Effect of streptozotocin-induced diabetes on rat brain mitochondria. J Neuroendocrinol. 16, 32-8.

Moreira, P.I., Santos, M.S., Moreno, A.M., Seica, R., Oliveira, C.R., 2003. Increased vulnerability of brain mitochondria in diabetic (Goto-Kakizaki) rats with aging and amyloid-beta exposure. Diabetes. 52, 1449-56.

Moreira, P.I., Santos, M.S., Oliveira, C.R., 2007. Alzheimer's disease: a lesson from mitochondrial dysfunction. Antioxid Redox Signal. 9, 1621-30.

Moreira, P.I., Santos, M.S., Sena, C., Seica, R., Oliveira, C.R., 2005. Insulin protects against amyloid beta-peptide toxicity in brain mitochondria of diabetic rats. Neurobiol Dis. 18, 628-37.

Morris, K.C., Lin, H.W., Thompson, J.W., Perez-Pinzon, M.A., Pathways for ischemic cytoprotection: Role of sirtuins in caloric restriction, resveratrol, and ischemic preconditioning. J Cereb Blood Flow Metab. 31, 1003-19.

Morris, R., 1984. Developments of a water-maze procedure for studying spatial learning in the rat. J Neurosci Methods. 11, 47-60.

Mosconi, L., de Leon, M., Murray, J., E, L., Lu, J., Javier, E., McHugh, P., Swerdlow, R.H., 2011. Reduced mitochondria cytochrome oxidase activity in adult children of mothers with Alzheimer's disease. J Alzheimers Dis. 27, 483-90.

Mosconi, L., De Santi, S., Li, J., Tsui, W.H., Li, Y., Boppana, M., Laska, E., Rusinek, H., de Leon, M.J., 2008. Hippocampal hypometabolism predicts cognitive decline from normal aging. Neurobiol Aging. 29, 676-92.

Mosconi, L., De Santi, S., Li, J., Tsui, W.H., Li, Y., Boppana, M., Laska, E., Rusinek, H., de Leon, M.J., 2008. Hippocampal hypometabolism predicts cognitive decline from normal aging. Neurobiol Aging. 29, 676-92.

Mosconi, L., Mistur, R., Switalski, R., Tsui, W.H., Glodzik, L., Li, Y., Pirraglia, E., De Santi, S., Reisberg, B., Wisniewski, T., de Leon, M.J., 2009. FDG-PET changes in brain glucose metabolism from normal cognition to pathologically verified Alzheimer's disease. Eur J Nucl Med Mol Imaging. 36, 811-22.

Munoz, L., Ammit, A.J., 2010. Targeting p38 MAPK pathway for the treatment of Alzheimer's disease. Neuropharmacology. 58, 561-8.

Munujos P, Coll-Cantí, J., González-Sastre, F., Gella, F.J., 1993. Assay of succinate dehydrogenase activity by a colorimetric continuous method using iodonitrotetrazolium chloride as electron acceptor. Anal Biochem. 212, 506-509.

Murakami, K., Kondo, T., Kawase, M., Li, Y., Sato, S., Chen, S.F., Chan, P.H., 1998. Mitochondrial susceptibility to oxidative stress exacerbates cerebral infarction that follows permanent focal cerebral ischemia in mutant mice with manganese superoxide dismutase deficiency. J Neurosci. 18, 205-13.

Nakagami, H., Morishita, R., Yamamoto, K., Taniyama, Y., Aoki, M., Yamasaki, K., Matsumoto, K., Nakamura, T., Kaneda, Y., Ogihara, T., 2002. Hepatocyte growth factor prevents endothelial cell death through inhibition of bax translocation from cytosol to mitochondrial membrane. Diabetes. 51, 2604-11.

Nakagami, H., Morishita, R., Yamamoto, K., Yoshimura, S.I., Taniyama, Y., Aoki, M., Matsubara, H., Kim, S., Kaneda, Y., Ogihara, T., 2001. Phosphorylation of p38 mitogen-activated protein kinase downstream of bax-caspase-3 pathway leads to cell death induced by high D-glucose in human endothelial cells. Diabetes. 50, 1472-81.

Nakatsuka, H., Ohta, S., Tanaka, J., Toku, K., Kumon, Y., Maeda, N., Sakanaka, M., Sakaki, S., 1999. Release of cytochrome c from mitochondria to cytosol in gerbil hippocampal CA1 neurons after transient forebrain ischemia. Brain Res. 849, 216-9.

Neves, S.S., Sarmento-Ribeiro, A.B., Simoes, S.P., Pedroso de Lima, M.C., 2006. Transfection of oral cancer cells mediated by transferrin-associated lipoplexes: mechanisms of cell death induced by herpes simplex virus thymidine kinase/ganciclovir therapy. Biochim Biophys Acta. 1758, 1703-12.

Nicholls, D.G., 2002. Mitochondrial function and dysfunction in the cell: its relevance to aging and aging-related disease. Int J Biochem Cell Biol. 34, 1372-81.

Nicholson, R.M., Kusne, Y., Nowak, L.A., LaFerla, F.M., Reiman, E.M., Valla, J., 2010. Regional cerebral glucose uptake in the 3xTG model of Alzheimer's disease highlights common regional vulnerability across AD mouse models. Brain Res. 1347, 179-85.

Nielson, K.A., Nolan, J.H., Berchtold, N.C., Sandman, C.A., Mulnard, R.A., Cotman, C.W., 1996. Apolipoprotein-E genotyping of diabetic dementia patients: is diabetes rare in Alzheimer's disease? J Am Geriatr Soc. 44, 897-904.

Noble, E.P., Wurtman, R.J., Axelrod, J., 1967. A simple and rapid method for injecting H3-norepinephrine into the lateral ventricle of the rat brain. Life Sci. 6, 281-91.

Noble, W., Planel, E., Zehr, C., Olm, V., Meyerson, J., Suleman, F., Gaynor, K., Wang, L., LaFrancois, J., Feinstein, B., Burns, M., Krishnamurthy, P., Wen, Y., Bhat, R., Lewis, J., Dickson, D., Duff, K., 2005. Inhibition of glycogen synthase kinase-3 by lithium correlates with reduced tauopathy and degeneration in vivo. Proc Natl Acad Sci U S A. 102, 6990-5.

Noshita, N., Sugawara, T., Fujimura, M., Morita-Fujimura, Y., Chan, P.H., 2001. Manganese Superoxide Dismutase Affects Cytochrome c Release and Caspase-9 Activation After Transient Focal Cerebral Ischemia in Mice. J Cereb Blood Flow Metab. 21, 557-67.

Nunomura, A., Honda, K., Takeda, A., Hirai, K., Zhu, X., Smith, M.A., Perry, G., 2006. Oxidative damage to RNA in neurodegenerative diseases. J Biomed Biotechnol. 2006, 82323.

Omata, N., Murata, T., Takamatsu, S., Maruoka, N., Yonekura, Y., Fujibayashi, Y., Wada, Y., 2006. Region-specific induction of hypoxic tolerance by expression of stress proteins and antioxidant enzymes. Neurol Sci. 27, 74-7.

Onyango, I.G., Lu, J., Rodova, M., Lezi, E., Crafter, A.B., Swerdlow, R.H., 2010. Regulation of neuron mitochondrial biogenesis and relevance to brain health. Biochim Biophys Acta. 1802, 228-34.

Origlia, N., Righi, M., Capsoni, S., Cattaneo, A., Fang, F., Stern, D.M., Chen, J.X., Schmidt, A.M., Arancio, O., Yan, S.D., Domenici, L., 2008. Receptor for advanced glycation end product-dependent activation of p38 mitogen-activated protein kinase contributes to amyloid-beta-mediated cortical synaptic dysfunction. J Neurosci. 28, 3521-30.

Otera, H., Mihara, K., 2012. Mitochondrial dynamics: functional link with apoptosis. Int J Cell Biol. 2012, 821676.

Pagani, L., Eckert, A., 2011. Amyloid-Beta interaction with mitochondria. Int J Alzheimers Dis. 2011, 925050.

Paganini-Hill, A., Kawas, C.H., Corrada, M.M., 2007. Non-alcoholic beverage and caffeine consumption and mortality: the Leisure World Cohort Study. Prev Med. 44, 305-10.

Pahnke, J., Walker, L.C., Scheffler, K., Krohn, M., 2009. Alzheimer's disease and blood-brain barrier function-Why have anti-beta-amyloid therapies failed to prevent dementia progression? Neurosci Biobehav Rev. 33, 1099-108.

Palmer, A.M., Burns, M.A., 1994. Selective increase in lipid peroxidation in the inferior temporal cortex in Alzheimer's disease. Brain Res. 645, 338-42.

Parker, W.D., Jr., Filley, C.M., Parks, J.K., 1990. Cytochrome oxidase deficiency in Alzheimer's disease. Neurology. 40, 1302-3.

Parker, W.D., Jr., Parks, J., Filley, C.M., Kleinschmidt-DeMasters, B.K., 1994. Electron transport chain defects in Alzheimer's disease brain. Neurology. 44, 1090-6.

Pasquier, F., Boulogne, A., Leys, D., Fontaine, P., 2006. Diabetes mellitus and dementia. Diabetes Metab. 32, 403-14.

Pavlov, P.F., Wiehager, B., Sakai, J., Frykman, S., Behbahani, H., Winblad, B., Ankarcrona, M., 2010. Mitochondrial gamma-secretase participates in the metabolism of mitochondria-associated amyloid precursor protein. FASEB J. 25, 78-88.

Pedersen, W.A., McMillan, P.J., Kulstad, J.J., Leverenz, J.B., Craft, S., Haynatzki, G.R., 2006. Rosiglitazone attenuates learning and memory deficits in Tg2576 Alzheimer mice. Exp Neurol. 199, 265-73.

Pei, J.J., Braak, E., Braak, H., Grundke-Iqbal, I., Iqbal, K., Winblad, B., Cowburn, R.F., 2001. Localization of active forms of C-jun kinase (JNK) and p38 kinase in Alzheimer's disease brains at different stages of neurofibrillary degeneration. J Alzheimers Dis. 3, 41-48.

Pei, J.J., Khatoon, S., An, W.L., Nordlinder, M., Tanaka, T., Braak, H., Tsujio, I., Takeda, M., Alafuzoff, I., Winblad, B., Cowburn, R.F., Grundke-Iqbal, I., Iqbal, K., 2003. Role of protein kinase B in Alzheimer's neurofibrillary pathology. Acta Neuropathol. 105, 381-92.

Peila, R., Rodriguez, B.L., Launer, L.J., 2002. Type 2 diabetes, APOE gene, and the risk for dementia and related pathologies: The Honolulu-Asia Aging Study. Diabetes. 51, 1256-62.

Pekny, M., Nilsson, M., 2005. Astrocyte activation and reactive gliosis. Glia. 50, 427-34.

Perez-Pinzon, M.A., 2004. Neuroprotective effects of ischemic preconditioning in brain mitochondria following cerebral ischemia. J Bioenerg Biomembr. 36, 323-7.

Perez-Pinzon, M.A., Dave, K.R., Raval, A.P., 2005. Role of reactive oxygen species and protein kinase C in ischemic tolerance in the brain. Antioxid Redox Signal. 7, 1150-7.

Phiel, C.J., Wilson, C.A., Lee, V.M., Klein, P.S., 2003. GSK-3alpha regulates production of Alzheimer's disease amyloid-beta peptides. Nature. 423, 435-9.

Piantadosi, C.A., Carraway, M.S., Babiker, A., Suliman, H.B., 2008. Heme oxygenase-1 regulates cardiac mitochondrial biogenesis via Nrf2-mediated transcriptional control of nuclear respiratory factor-1. Circ Res. 103, 1232-40.

Pignataro, G., Scorziello, A., Di Renzo, G., Annunziato, L., 2009. Post-ischemic brain damage: effect of ischemic preconditioning and postconditioning and identification of potential candidates for stroke therapy. FEBS J. 276, 46-57.

Prass, K., Scharff, A., Ruscher, K., Lowl, D., Muselmann, C., Victorov, I., Kapinya, K., Dirnagl, U., Meisel, A., 2003. Hypoxia-induced stroke tolerance in the mouse is mediated by erythropoietin. Stroke. 34, 1981-6.

Pugh, C.W., O'Rourke, J.F., Nagao, M., Gleadle, J.M., Ratcliffe, P.J., 1997. Activation of hypoxia-inducible factor-1; definition of regulatory domains within the alpha subunit. J Biol Chem. 272, 11205-14.

Qiu, W.Q., Folstein, M.F., 2006. Insulin, insulin-degrading enzyme and amyloid-beta peptide in Alzheimer's disease: review and hypothesis. Neurobiol Aging. 27, 190-8.

Querfurth, H.W., LaFerla, F.M., 2010. Alzheimer's disease. N Engl J Med. 362, 329-44.

Racay, P., Tatarkova, Z., Drgova, A., Kaplan, P., Dobrota, D., 2007. Effect of ischemic preconditioning on mitochondrial dysfunction and mitochondrial p53 translocation after transient global cerebral ischemia in rats. Neurochem Res. 32, 1823-32.

Rambold, A.S., Kostelecky, B., Elia, N., Lippincott-Schwartz, J., 2011. Tubular network formation protects mitochondria from autophagosomal degradation during nutrient starvation. Proc Natl Acad Sci U S A. 108, 10190-5.

Ran, R., Xu, H., Lu, A., Bernaudin, M., Sharp, F.R., 2005. Hypoxia preconditioning in the brain. Dev Neurosci. 27, 87-92.

Raval, A.P., Dave, K.R., DeFazio, R.A., Perez-Pinzon, M.A., 2007. epsilonPKC phosphorylates the mitochondrial K(+) (ATP) channel during induction of ischemic preconditioning in the rat hippocampus. Brain Res. 1184, 345-53.

Ravati, A., Ahlemeyer, B., Becker, A., Klumpp, S., Krieglstein, J., 2001. Preconditioning-induced neuroprotection is mediated by reactive oxygen species and activation of the transcription factor nuclear factor-kappaB. J Neurochem. 78, 909-19.

Ravati, A., Ahlemeyer, B., Becker, A., Krieglstein, J., 2000. Preconditioning-induced neuroprotection is mediated by reactive oxygen species. Brain Res. 866, 23-32.

Reddy, P.H., 2009. Amyloid beta, mitochondrial structural and functional dynamics in Alzheimer's disease. Exp Neurol. 218, 286-92.

Reddy, P.H., Beal, M.F., 2008. Amyloid beta, mitochondrial dysfunction and synaptic damage: implications for cognitive decline in aging and Alzheimer's disease. Trends Mol Med. 14, 45-53.

Reiman, E.M., Chen, K., Alexander, G.E., Caselli, R.J., Bandy, D., Osborne, D., Saunders, A.M., Hardy, J., 2004. Functional brain abnormalities in young adults at genetic risk for late-onset Alzheimer's dementia. Proc Natl Acad Sci U S A. 101, 284-9.

Resende, R., Moreira, P.I., Proenca, T., Deshpande, A., Busciglio, J., Pereira, C., Oliveira, C.R., 2008. Brain oxidative stress in a triple-transgenic mouse model of Alzheimer disease. Free Radic Biol Med. 44, 2051-7.

Reske-Nielsen, E., Lundbaek, K., 1963. Diabetic Encephalopathy. Diffuse and Focal Lesions of the Brain in Long-Term Diabetes. Acta Neurol Scand Suppl. 39, SUPPL4:273-90.

Rivera, E.J., Goldin, A., Fulmer, N., Tavares, R., Wands, J.R., de la Monte, S.M., 2005. Insulin and insulin-like growth factor expression and function deteriorate with progression of Alzheimer's disease: link to brain reductions in acetylcholine. J Alzheimers Dis. 8, 247-68.

Rizzuto, R., Bernardi, P., Pozzan, T., 2000. Mitochondria as all-round players of the calcium game. J Physiol. 529 Pt 1, 37-47.

Robinson, J.B., Jr., Brent, L.G., Sumegi, B., Srere, P.A., 1987. An enzymatic approach to the study of the Krebs tricarboxylic acid cycle. In: Darley-Usmar VM, Rickwood D, Wilson MT, editors. Mitochondria: A Practical Approach. IRL Press; Washington, DC: 153-169.

Rocchi, A., Pellegrini, S., Siciliano, G., Murri, L., 2003. Causative and susceptibility genes for Alzheimer's disease: a review. Brain Res Bull. 61, 1-24.

Roriz-Filho, J.S., Sa-Roriz, T.M., Rosset, I., Camozzato, A.L., Santos, A.C., Chaves, M.L., Moriguti, J.C., Roriz-Cruz, M., 2009. (Pre)diabetes, brain aging, and cognition. Biochim Biophys Acta. 1792, 432-43.

Rosenzweig, H.L., Lessov, N.S., Henshall, D.C., Minami, M., Simon, R.P., Stenzel-Poore, M.P., 2004. Endotoxin preconditioning prevents cellular inflammatory response during ischemic neuroprotection in mice. Stroke. 35, 2576-81.

Rosse, T., Olivier, R., Monney, L., Rager, M., Conus, S., Fellay, I., Jansen, B., Borner, C., 1998. Bcl-2 prolongs cell survival after Bax-induced release of cytochrome c. Nature. 391, 496-9.

Roux, F., Durieu-Trautmann, O., Chaverot, N., Claire, M., Mailly, P., Bourre, J.M., Strosberg, A.D., Couraud, P.O., 1994. Regulation of gamma-glutamyl transpeptidase and alkaline phosphatase activities in immortalized rat brain microvessel endothelial cells. J Cell Physiol. 159, 101-13.

Rugarli, E.I., Langer, T., 2012. Mitochondrial quality control: a matter of life and death for neurons. EMBO J. 31, 1336-49.

Russell, J.W., Golovoy, D., Vincent, A.M., Mahendru, P., Olzmann, J.A., Mentzer, A., Feldman, E.L., 2002. High glucose-induced oxidative stress and mitochondrial dysfunction in neurons. FASEB J. 16, 1738-48.

Rybnikova, E., Glushchenko, T., Tyulkova, E., Baranova, K., Samoilov, M., 2009. Mild hypobaric hypoxia preconditioning up-regulates expression of transcription factors c-Fos and NGFI-A in rat neocortex and hippocampus. Neurosci Res. 65, 360-6.

Rybnikova, E., Vataeva, L., Tyulkova, E., Gluschenko, T., Otellin, V., Pelto-Huikko, M., Samoilov, M.O., 2005. Mild hypoxia preconditioning prevents impairment of passive avoidance learning and suppression of brain NGFI-A expression induced by severe hypoxia. Behav Brain Res. 160, 107-14.

Sack, M.N., 2006. Mitochondrial depolarization and the role of uncoupling proteins in ischemia tolerance. Cardiovasc Res. 72, 210-9.

Safran, M., Kaelin, W.G., Jr., 2003. HIF hydroxylation and the mammalian oxygen-sensing pathway. J Clin Invest. 111, 779-83.

Salkovic-Petrisic, M., Hoyer, S., 2007. Central insulin resistance as a trigger for sporadic Alzheimer-like pathology: an experimental approach. J. Neural Transm. Suppl., 217-233.

Salkovic-Petrisic, M., Osmanovic-Barilar, J., Bruckner, M.K., Hoyer, S., Arendt, T., Riederer, P., 2011. Cerebral amyloid angiopathy in streptozotocin rat model of sporadic Alzheimer's disease: a long-term follow up study. J Neural Transm. 118, 765-72.

Samavati, L., Monick, M.M., Sanlioglu, S., Buettner, G.R., Oberley, L.W., Hunninghake, G.W., 2002. Mitochondrial K(ATP) channel openers activate the ERK kinase by an oxidant-dependent mechanism. Am J Physiol Cell Physiol. 283, C273-81.

Santos, R.X., Correia, S.C., Wang, X., Perry, G., Smith, M.A., Moreira, P.I., Zhu, X., 2010a. Alzheimer's disease: diverse aspects of mitochondrial malfunctioning. Int J Clin Exp Pathol. 3, 570-81.

Santos, R.X., Correia, S.C., Wang, X., Perry, G., Smith, M.A., Moreira, P.I., Zhu, X., 2010b. A synergistic dysfunction of mitochondrial fission/fusion dynamics and mitophagy in Alzheimer's disease. J Alzheimers Dis. 20 Suppl 2, S401-12.

Sasaki, N., Fukatsu, R., Tsuzuki, K., Hayashi, Y., Yoshida, T., Fujii, N., Koike, T., Wakayama, I., Yanagihara, R., Garruto, R., Amano, N., Makita, Z., 1998. Advanced glycation end products in Alzheimer's disease and other neurodegenerative diseases. Am J Pathol. 153, 1149-55.

Schapira, A.H., 1996. Oxidative stress and mitochondrial dysfunction in neurodegeneration. Curr Opin Neurol. 9, 260-4.

Scheepers, A., Joost, H.G., Schurmann, A., 2004. The glucose transporter families SGLT and GLUT: molecular basis of normal and aberrant function. JPEN J Parenter Enteral Nutr. 28, 364-71.

Scherz-Shouval, R., Shvets, E., Fass, E., Shorer, H., Gil, L., Elazar, Z., 2007. Reactive oxygen species are essential for autophagy and specifically regulate the activity of Atg4. EMBO J. 26, 1749-60.

Schetinger, M.R., Bonan, C.D., Frassetto, S.S., Wyse, A.T., Schierholt, R.C., Webber, A., Dias, R.D., Sarkis, J.J., Netto, C.A., 1999. Pre-conditioning to global cerebral ischemia changes hippocampal acetylcholinesterase in the rat. Biochem Mol Biol Int. 47, 473-8.

Schmeichel, A.M., Schmelzer, J.D., Low, P.A., 2003. Oxidative injury and apoptosis of dorsal root ganglion neurons in chronic experimental diabetic neuropathy. Diabetes. 52, 165-71.

Schmidt, R., Launer, L.J., Nilsson, L.G., Pajak, A., Sans, S., Berger, K., Breteler, M.M., de Ridder, M., Dufouil, C., Fuhrer, R., Giampaoli, S., Hofman, A., 2004. Magnetic resonance imaging of the brain in diabetes: the Cardiovascular Determinants of Dementia (CASCADE) Study. Diabetes. 53, 687-92.

Schubert, M., Brazil, D.P., Burks, D.J., Kushner, J.A., Ye, J., Flint, C.L., Farhang-Fallah, J., Dikkes, P., Warot, X.M., Rio, C., Corfas, G., White, M.F., 2003. Insulin receptor substrate-2 deficiency impairs brain growth and promotes tau phosphorylation. J Neurosci. 23, 7084-92.

Schubert, M., Gautam, D., Surjo, D., Ueki, K., Baudler, S., Schubert, D., Kondo, T., Alber, J., Galldiks, N., Kustermann, E., Arndt, S., Jacobs, A.H., Krone, W., Kahn, C.R., Bruning, J.C., 2004. Role for neuronal insulin resistance in neurodegenerative diseases. Proc Natl Acad Sci U S A. 101, 3100-5.

Schurr, A., Reid, K.H., Tseng, M.T., West, C., Rigor, B.M., 1986. Adaptation of adult brain tissue to anoxia and hypoxia in vitro. Brain Res. 374, 244-8.

Selkoe, D.J., 2001. Alzheimer's disease results from the cerebral accumulation and cytotoxicity of amyloid beta-protein. J Alzheimers Dis. 3, 75-80.

Semenza, G., 2002. Signal transduction to hypoxia-inducible factor 1. Biochem Pharmacol. 64, 993-8.

Semenza, G.L., 2000. Expression of hypoxia-inducible factor 1: mechanisms and consequences. Biochem Pharmacol. 59, 47-53.

Semenza, G.L., 2012. Hypoxia-inducible factors in physiology and medicine. Cell. 148, 399-408.

Seo, A.Y., Joseph, A.M., Dutta, D., Hwang, J.C., Aris, J.P., Leeuwenburgh, C., 2010. New insights into the role of mitochondria in aging: mitochondrial dynamics and more. J Cell Sci. 123, 2533-42.

Sesaki, H., Southard, S.M., Yaffe, M.P., Jensen, R.E., 2003. Mgm1p, a dynamin-related GTPase, is essential for fusion of the mitochondrial outer membrane. Mol Biol Cell. 14, 2342-56.

Sharp, F.R., Ran, R., Lu, A., Tang, Y., Strauss, K.I., Glass, T., Ardizzone, T., Bernaudin, M., 2004. Hypoxic preconditioning protects against ischemic brain injury. NeuroRx. 1, 26-35.

Sheehan, J.P., Swerdlow, R.H., Miller, S.W., Davis, R.E., Parks, J.K., Parker, W.D., Tuttle, J.B., 1997. Calcium homeostasis and reactive oxygen species production in cells transformed by mitochondria from individuals with sporadic Alzheimer's disease. J Neurosci. 17, 4612-22.

Sheng, Z.H., Cai, Q., 2012. Mitochondrial transport in neurons: impact on synaptic homeostasis and neurodegeneration. Nat Rev Neurosci. 13, 77-93.

Shimizu, K., Lacza, Z., Rajapakse, N., Horiguchi, T., Snipes, J., Busija, D.W., 2002. MitoK(ATP) opener, diazoxide, reduces neuronal damage after middle cerebral artery occlusion in the rat. Am J Physiol Heart Circ Physiol. 283, H1005-11.

Shiva, S., Sack, M.N., Greer, J.J., Duranski, M., Ringwood, L.A., Burwell, L., Wang, X., MacArthur, P.H., Shoja, A., Raghavachari, N., Calvert, J.W., Brookes, P.S., Lefer, D.J., Gladwin, M.T., 2007. Nitrite augments tolerance to ischemia/reperfusion injury via the modulation of mitochondrial electron transfer. J Exp Med. 204, 2089-102.

Silva, J.P., Kohler, M., Graff, C., Oldfors, A., Magnuson, M.A., Berggren, P.O., Larsson, N.G., 2000. Impaired insulin secretion and beta-cell loss in tissue-specific knockout mice with mitochondrial diabetes. Nat Genet. 26, 336-40.

Silverman, D.H., Small, G.W., Chang, C.Y., Lu, C.S., Kung De Aburto, M.A., Chen, W., Czernin, J., Rapoport, S.I., Pietrini, P., Alexander, G.E., Schapiro, M.B., Jagust, W.J., Hoffman, J.M., Welsh-Bohmer, K.A., Alavi, A., Clark, C.M., Salmon, E., de Leon, M.J., Mielke, R., Cummings, J.L., Kowell, A.P., Gambhir, S.S., Hoh, C.K., Phelps, M.E., 2001. Positron emission tomography in evaluation of dementia: Regional brain metabolism and long-term outcome. JAMA. 286, 2120-7.

Sima, A.A., Li, Z.G., 2005. The effect of C-peptide on cognitive dysfunction and hippocampal apoptosis in type 1 diabetic rats. Diabetes. 54, 1497-505.

Simerabet, M., Robin, E., Aristi, I., Adamczyk, S., Tavernier, B., Vallet, B., Bordet, R., Lebuffe, G., 2008. Preconditioning by an in situ administration of hydrogen peroxide: involvement

of reactive oxygen species and mitochondrial ATP-dependent potassium channel in a cerebral ischemia-reperfusion model. Brain Res. 1240, 177-84.

Sims-Robinson, C., Kim, B., Rosko, A., Feldman, E.L., 2010. How does diabetes accelerate Alzheimer disease pathology? Nat Rev Neurol. 6, 551-9.

Sjogren, M., Mielke, M., Gustafson, D., Zandi, P., Skoog, I., 2006. Cholesterol and Alzheimer's disease--is there a relation? Mech Ageing Dev. 127, 138-47.

Skulachev, V.P., 2001. Mitochondrial filaments and clusters as intracellular power-transmitting cables. Trends Biochem Sci. 26, 23-9.

Sloane, P.D., Zimmerman, S., Suchindran, C., Reed, P., Wang, L., Boustani, M., Sudha, S., 2002. The public health impact of Alzheimer's disease, 2000-2050: potential implication of treatment advances. Annu Rev Public Health. 23, 213-31.

Small, G.W., Bookheimer, S.Y., Thompson, P.M., Cole, G.M., Huang, S.C., Kepe, V., Barrio, J.R., 2008. Current and future uses of neuroimaging for cognitively impaired patients. Lancet Neurol. 7, 161-72.

Smith, M.A., 1998. Alzheimer disease. Int Rev Neurobiol. 42, 1-54.

Smith, M.A., Drew, K.L., Nunomura, A., Takeda, A., Hirai, K., Zhu, X., Atwood, C.S., Raina, A.K., Rottkamp, C.A., Sayre, L.M., Friedland, R.P., Perry, G., 2002. Amyloid-beta, tau alterations and mitochondrial dysfunction in Alzheimer disease: the chickens or the eggs? Neurochem Int. 40, 527-31.

Solano, D.C., Sironi, M., Bonfini, C., Solerte, S.B., Govoni, S., Racchi, M., 2000. Insulin regulates soluble amyloid precursor protein release via phosphatidyl inositol 3 kinase-dependent pathway. FASEB J. 14, 1015-22.

Soubannier, V., McBride, H.M., 2009. Positioning mitochondrial plasticity within cellular signaling cascades. Biochim Biophys Acta. 1793, 154-70.

Stagliano, N.E., Perez-Pinzon, M.A., Moskowitz, M.A., Huang, P.L., 1999. Focal ischemic preconditioning induces rapid tolerance to middle cerebral artery occlusion in mice. J Cereb Blood Flow Metab. 19, 757-61.

Starkov, A.A., Fiskum, G., Chinopoulos, C., Lorenzo, B.J., Browne, S.E., Patel, M.S., Beal, M.F., 2004. Mitochondrial alpha-ketoglutarate dehydrogenase complex generates reactive oxygen species. J Neurosci. 24, 7779-88.

Steen, E., Terry, B.M., Rivera, E.J., Cannon, J.L., Neely, T.R., Tavares, R., Xu, X.J., Wands, J.R., de la Monte, S.M., 2005. Impaired insulin and insulin-like growth factor expression and signaling mechanisms in Alzheimer's disease--is this type 3 diabetes? J Alzheimers Dis. 7, 63-80.

Stenzel-Poore, M.P., Stevens, S.L., King, J.S., Simon, R.P., 2007. Preconditioning reprograms the response to ischemic injury and primes the emergence of unique endogenous neuroprotective phenotypes: a speculative synthesis. Stroke. 38, 680-5.

Stoica, B.A., Movsesyan, V.A., Lea, P.M.t., Faden, A.I., 2003. Ceramide-induced neuronal apoptosis is associated with dephosphorylation of Akt, BAD, FKHR, GSK-3beta, and induction of the mitochondrial-dependent intrinsic caspase pathway. Mol Cell Neurosci. 22, 365-82.

Strauss, M., Hofhaus, G., Schroder, R.R., Kuhlbrandt, W., 2008. Dimer ribbons of ATP synthase shape the inner mitochondrial membrane. EMBO J. 27, 1154-60.

Sultana, R., Butterfield, D.A., 2010. Role of oxidative stress in the progression of Alzheimer's disease. J Alzheimers Dis. 19, 341-53.

Sun, A., Liu, M., Nguyen, X.V., Bing, G., 2003. P38 MAP kinase is activated at early stages in Alzheimer's disease brain. Exp Neurol. 183, 394-405.

Swerdlow, R.H., Parks, J.K., Cassarino, D.S., Maguire, D.J., Maguire, R.S., Bennett, J.P., Jr., Davis, R.E., Parker, W.D., Jr., 1997. Cybrids in Alzheimer's disease: a cellular model of the disease? Neurology. 49, 918-25.

Swiger, B. M., Patel, M., Schoultz, T., Pastukh, V., Gillespie, M.N., Al-Mehdi, A.B., 2007. Hypoxia causes mitochondrial translocation to the perinuclear region in pulmonary artery endothelial cells (PAECs): Implications for signal transduction (abstract). The FASEB Journal. 21, 762.2.

Szewczyk, A., Wojtczak, L., 2002. Mitochondria as a pharmacological target. Pharmacol Rev. 54, 101-27.

Szkudelski, T., 2001. The mechanism of alloxan and streptozotocin action in B cells of the rat pancreas. Physiol. Res. 50, 537-546.

Tai, K.K., McCrossan, Z.A., Abbott, G.W., 2003. Activation of mitochondrial ATP-sensitive potassium channels increases cell viability against rotenone-induced cell death. J Neurochem. 84, 1193-200.

Tai, K.K., Truong, D.D., 2002. Activation of adenosine triphosphate-sensitive potassium channels confers protection against rotenone-induced cell death: therapeutic implications for Parkinson's disease. J Neurosci Res. 69, 559-66.

Takuma, K., Fang, F., Zhang, W., Yan, S., Fukuzaki, E., Du, H., Sosunov, A., McKhann, G., Funatsu, Y., Nakamichi, N., Nagai, T., Mizoguchi, H., Ibi, D., Hori, O., Ogawa, S., Stern, D.M., Yamada, K., Yan, S.S., 2009. RAGE-mediated signaling contributes to intraneuronal transport of amyloid-beta and neuronal dysfunction. Proc Natl Acad Sci U S A. 106, 20021-6.

Tanaka, K., Iijima, T., Mishima, T., Suga, K., Akagawa, K., Iwao, Y., 2009. Ca(2+) buffering capacity of mitochondria after oxygen-glucose deprivation in hippocampal neurons. Neurochem Res. 34, 221-6.

Tang, X.Q., Chen, J., Tang, E.H., Feng, J.Q., Chen, P.X., 2005a. Hydrogen peroxide preconditioning protects PC12 cells against apoptosis induced by oxidative stress. Sheng Li Xue Bao. 57, 211-6.

Tang, X.Q., Feng, J.Q., Chen, J., Chen, P.X., Zhi, J.L., Cui, Y., Guo, R.X., Yu, H.M., 2005b. Protection of oxidative preconditioning against apoptosis induced by H2O2 in PC12 cells: mechanisms via MMP, ROS, and Bcl-2. Brain Res. 1057, 57-64.

Teodoro, J., Rolo, A.P., Oliveira, P.J., Palmeira, C.M., 2006. Decreased ANT content in Zucker fatty rats: relevance for altered hepatic mitochondrial bioenergetics in steatosis. FEBS Lett. 580, 2153-7.

Territo, P.R., Mootha, V.K., French, S.A., Balaban, R.S., 2000. Ca(2+) activation of heart mitochondrial oxidative phosphorylation: role of the F(0)/F(1)-ATPase. Am J Physiol Cell Physiol. 278, C423-35.

Tomlinson, D.R., Gardiner, N.J., 2008. Glucose neurotoxicity. Nat Rev Neurosci. 9, 36-45.

Tondera, D., Grandemange, S., Jourdain, A., Karbowski, M., Mattenberger, Y., Herzig, S., Da Cruz, S., Clerc, P., Raschke, I., Merkwirth, C., Ehses, S., Krause, F., Chan, D.C., Alexander, C., Bauer, C., Youle, R., Langer, T., Martinou, J.C., 2009. SLP-2 is required for stress-induced mitochondrial hyperfusion. EMBO J. 28, 1589-600.

Torres-Aleman, I., 2008. Mouse models of Alzheimer's dementia: current concepts and new trends. Endocrinology. 149, 5952-7.

Tota, S., Kamat, P.K., Shukla, R., Nath, C., 2011. Improvement of brain energy metabolism and cholinergic functions contributes to the beneficial effects of silibinin against streptozotocin induced memory impairment. Behav Brain Res. 221, 207-15.

Toth, C., Martinez, J., Zochodne, D.W., 2007. RAGE, diabetes, and the nervous system. Curr Mol Med. 7, 766-76.

Toth, C., Schmidt, A.M., Tuor, U.I., Francis, G., Foniok, T., Brussee, V., Kaur, J., Yan, S.F., Martinez, J.A., Barber, P.A., Buchan, A., Zochodne, D.W., 2006. Diabetes, leukoencephalopathy and rage. Neurobiol Dis. 23, 445-61.

Tretter, L., Adam-Vizi, V., 2000. Inhibition of Krebs cycle enzymes by hydrogen peroxide: A key role of [alpha]-ketoglutarate dehydrogenase in limiting NADH production under oxidative stress. J Neurosci. 20, 8972-9.

Umegaki, H., 2012. Neurodegeneration in diabetes mellitus. Adv Exp Med Biol. 724, 258-65.

Valla, J., Gonzalez-Lima, F., Reiman, E.M., 2008. FDG autoradiography reveals developmental and pathological effects of mutant amyloid in PDAPP transgenic mice. Int J Dev Neurosci. 26, 253-8.

Valla, J., Schneider, L., Niedzielko, T., Coon, K.D., Caselli, R., Sabbagh, M.N., Ahern, G.L., Baxter, L., Alexander, G., Walker, D.G., Reiman, E.M., 2006. Impaired platelet mitochondrial activity in Alzheimer's disease and mild cognitive impairment. Mitochondrion. 6, 323-30.

Vannucci, S.J., Maher, F., Simpson, I.A., 1997. Glucose transporter proteins in brain: delivery of glucose to neurons and glia. Glia. 21, 2-21.

Vatassery, G.T., Younoszai, R., 1978. Alpha tocopherol levels in various regions of the central nervous systems of the rat and guinea pig. Lipids 13, 828-831.

Velliquette, R.A., O'Connor, T., Vassar, R., 2005. Energy inhibition elevates beta-secretase levels and activity and is potentially amyloidogenic in APP transgenic mice: possible early events in Alzheimer's disease pathogenesis. J Neurosci. 25, 10874-83.

Vincent, A.M., Feldman, E.L., 2004. New insights into the mechanisms of diabetic neuropathy. Rev Endocr Metab Disord. 5, 227-36.

Vincent, A.M., McLean, L.L., Backus, C., Feldman, E.L., 2005. Short-term hyperglycemia produces oxidative damage and apoptosis in neurons. FASEB J. 19, 638-40.

Vincent, A.M., Russell, J.W., Low, P., Feldman, E.L., 2004. Oxidative stress in the pathogenesis of diabetic neuropathy. Endocr Rev. 25, 612-28.

Wallace, D.C., 1997. Mitochondrial DNA in aging and disease. Sci Am. 277, 40-7.

Wang, C.H., Chang, A., Tsai, M.J., Cheng, H., Liao, L.P., Lin, A.M., 2005. Kainic acid-induced oxidative injury is attenuated by hypoxic preconditioning. Ann N Y Acad Sci. 1042, 314-24.

Wang, G.L., Jiang, B.H., Rue, E.A., Semenza, G.L., 1995. Hypoxia-inducible factor 1 is a basic-helix-loop-helix-PAS heterodimer regulated by cellular O2 tension. Proc Natl Acad Sci U S A. 92, 5510-4.

Wang, X., Su, B., Fujioka, H., Zhu, X., 2008a. Dynamin-like protein 1 reduction underlies mitochondrial morphology and distribution abnormalities in fibroblasts from sporadic Alzheimer's disease patients. Am J Pathol. 173, 470-82.

Wang, X., Su, B., Lee, H.G., Li, X., Perry, G., Smith, M.A., Zhu, X., 2009a. Impaired balance of mitochondrial fission and fusion in Alzheimer's disease. J Neurosci. 29, 9090-103.

Wang, X., Su, B., Siedlak, S.L., Moreira, P.I., Fujioka, H., Wang, Y., Casadesus, G., Zhu, X., 2008b. Amyloid-beta overproduction causes abnormal mitochondrial dynamics via differential

modulation of mitochondrial fission/fusion proteins. Proc Natl Acad Sci U S A. 105, 19318-23.

Wang, X., Su, B., Zheng, L., Perry, G., Smith, M.A., Zhu, X., 2009b. The role of abnormal mitochondrial dynamics in the pathogenesis of Alzheimer's disease. J Neurochem. 109 Suppl 1, 153-9.

Watson, G.S., Craft, S., 2004. Modulation of memory by insulin and glucose: neuropsychological observations in Alzheimer's disease. Eur J Pharmacol. 490, 97-113.

Watson, G.S., Peskind, E.R., Asthana, S., Purganan, K., Wait, C., Chapman, D., Schwartz, M.W., Plymate, S., Craft, S., 2003. Insulin increases CSF Abeta42 levels in normal older adults. Neurology. 60, 1899-903.

Weller, R.O., Boche, D., Nicoll, J.A., 2009. Microvasculature changes and cerebral amyloid angiopathy in Alzheimer's disease and their potential impact on therapy. Acta Neuropathol. 118, 87-102.

Westermann, B., 2010. Mitochondrial fusion and fission in cell life and death. Nat Rev Mol Cell Biol. 11, 872-84.

Westermann, B., 2010. Mitochondrial fusion and fission in cell life and death. Nat Rev Mol Cell Biol. 11, 872-84.

Wiegand, F., Liao, W., Busch, C., Castell, S., Knapp, F., Lindauer, U., Megow, D., Meisel, A., Redetzky, A., Ruscher, K., Trendelenburg, G., Victorov, I., Riepe, M., Diener, H.C., Dirnagl, U., 1999. Respiratory chain inhibition induces tolerance to focal cerebral ischemia. J Cereb Blood Flow Metab. 19, 1229-37.

Wild, S., Roglic, G., Green, A., Sicree, R., King, H., 2004. Global prevalence of diabetes: estimates for the year 2000 and projections for 2030. Diabetes Care. 27, 1047-53.

Wilson-Fritch, L., Nicoloro, S., Chouinard, M., Lazar, M.A., Chui, P.C., Leszyk, J., Straubhaar, J., Czech, M.P., Corvera, S., 2004. Mitochondrial remodeling in adipose tissue associated with obesity and treatment with rosiglitazone. J Clin Invest. 114, 1281-9.

Wolf-Klein, G.P., Siverstone, F.A., Brod, M.S., Levy, A., Foley, C.J., Termotto, V., Breuer, J., 1988. Are Alzheimer patients healthier? J Am Geriatr Soc. 36, 219-24.

Wong, E.D., Wagner, J.A., Scott, S.V., Okreglak, V., Holewinske, T.J., Cassidy-Stone, A., Nunnari, J., 2003. The intramitochondrial dynamin-related GTPase, Mgm1p, is a component of a protein complex that mediates mitochondrial fusion. J Cell Biol. 160, 303-11.

Wong, S.H., Knight, J.A., Hopfer, S.M., Zaharia, O., Leach, C.N., Jr., Sunderman, F.W., Jr., 1987. Lipoperoxides in plasma as measured by liquid-chromatographic separation of malondialdehyde-thiobarbituric acid adduct. Clin Chem. 33, 214-20.

Wu, L., Shen, F., Lin, L., Zhang, X., Bruce, I.C., Xia, Q., 2006. The neuroprotection conferred by activating the mitochondrial ATP-sensitive K+ channel is mediated by inhibiting the mitochondrial permeability transition pore. Neurosci Lett. 402, 184-9.

Xie, J., Duan, L., Qian, X., Huang, X., Ding, J., Hu, G., 2009. K(ATP) channel openers protect mesencephalic neurons against MPP+-induced cytotoxicity via inhibition of ROS production. J Neurosci Res. 88, 428-37.

Xu, G.P., Dave, K.R., Vivero, R., Schmidt-Kastner, R., Sick, T.J., Perez-Pinzon, M.A., 2002. Improvement in neuronal survival after ischemic preconditioning in hippocampal slice cultures. Brain Res. 952, 153-8.

Yan, S.D., Chen, X., Fu, J., Chen, M., Zhu, H., Roher, A., Slattery, T., Zhao, L., Nagashima, M., Morser, J., Migheli, A., Nawroth, P., Stern, D., Schmidt, A.M., 1996. RAGE and amyloid-beta peptide neurotoxicity in Alzheimer's disease. Nature. 382, 685-91.

Yang, Y., Liu, X., Long, Y., Wang, F., Ding, J.H., Liu, S.Y., Sun, Y.H., Yao, H.H., Wang, H., Wu, J., Hu, G., 2006. Activation of mitochondrial ATP-sensitive potassium channels improves rotenone-related motor and neurochemical alterations in rats. Int J Neuropsychopharmacol. 9, 51-61.

Yin, W., Signore, A.P., Iwai, M., Cao, G., Gao, Y., Chen, J., 2008. Rapidly increased neuronal mitochondrial biogenesis after hypoxic-ischemic brain injury. Stroke. 39, 3057-63.

Yu, T., Robotham, J.L., Yoon, Y., 2006. Increased production of reactive oxygen species in hyperglycemic conditions requires dynamic change of mitochondrial morphology. Proc Natl Acad Sci U S A. 103, 2653-8.

Yuan, H., Gerencser, A.A., Liot, G., Lipton, S.A., Ellisman, M., Perkins, G.A., Bossy-Wetzel, E., 2007. Mitochondrial fission is an upstream and required event for bax foci formation in response to nitric oxide in cortical neurons. Cell Death Differ. 14, 462-71.

Zafrilla, P., Mulero, J., Xandri, J.M., Santo, E., Caravaca, G., Morillas, J.M., 2006. Oxidative stress in Alzheimer patients in different stages of the disease. Curr Med Chem. 13, 1075-83.

Zhang, D.X., Gutterman, D.D., 2007. Mitochondrial reactive oxygen species-mediated signaling in endothelial cells. Am J Physiol Heart Circ Physiol. 292, H2023-31.

Zhang, H., Bosch-Marce, M., Shimoda, L.A., Tan, Y.S., Baek, J.H., Wesley, J.B., Gonzalez, F.J., Semenza, G.L., 2008. Mitochondrial autophagy is an HIF-1-dependent adaptive metabolic response to hypoxia. J Biol Chem. 283, 10892-903.

Zhang, H.X., Du, G.H., Zhang, J.T., 2003. Ischemic pre-conditioning preserves brain mitochondrial functions during the middle cerebral artery occlusion in rat. Neurol Res. 25, 471-6.

Zhang, L., Li, L., Liu, H., Prabhakaran, K., Zhang, X., Borowitz, J.L., Isom, G.E., 2007. HIF-1alpha activation by a redox-sensitive pathway mediates cyanide-induced BNIP3 upregulation and mitochondrial-dependent cell death. Free Radic Biol Med. 43, 117-27.

Zhao, H., Sapolsky, R.M., Steinberg, G.K., 2006. Phosphoinositide-3-kinase/akt survival signal pathways are implicated in neuronal survival after stroke. Mol Neurobiol. 34, 249-70.

Zhao, J., Li, L., Pei, Z., Li, C., Wei, H., Zhang, B., Peng, Y., Wang, Y., Tao, Y., Huang, R., 2012. Peroxisome proliferator activated receptor (PPAR)-gamma co-activator 1-alpha and hypoxia induced factor-1alpha mediate neuro- and vascular protection by hypoxic preconditioning in vitro. Brain Res. 1447, 1-8.

Zhao, W.Q., Alkon, D.L., 2001. Role of insulin and insulin receptor in learning and memory. Mol Cell Endocrinol. 177, 125-34.

Zhao, W.Q., Townsend, M., 2009. Insulin resistance and amyloidogenesis as common molecular foundation for type 2 diabetes and Alzheimer's disease. Biochim Biophys Acta. 1792, 482-96.

Zhu, L.L., Zhao, T., Li, H.S., Zhao, H., Wu, L.Y., Ding, A.S., Fan, W.H., Fan, M., 2005. Neurogenesis in the adult rat brain after intermittent hypoxia. Brain Res. 1055, 1-6.

Zlokovic, B.V., 2011. Neurovascular pathways to neurodegeneration in Alzheimer's disease and other disorders. Nat Rev Neurosci. 12, 723-38.

ADDENDUM

PAPERS PUBLISHED AFTER THE SUBMISSION OF THE THESIS

1. **Correia SC**, Santos RX, Santos MS, Casadesus G, Lamanna JC, Perry G, Smith MA, Moreira PI. Mitochondrial abnormalities in a streptozotocin-induced rat model of sporadic Alzheimer's disease. Curr Alzheimer Res. 2012 (*in press*).

2. Cardoso S, Santos RX, **Correia SC**, Carvalho C, Santos MS, Baldeiras I, Oliveira CR, Moreira PI. Insulin-induced recurrent hypoglycemia exacerbates diabetic brain mitochondrial dysfunction and oxidative imbalance. Neurobiol Dis. 2012 (*in press*).

3. Cardoso S, **Correia S**, Santos RX, Carvalho C, Candeias E, Duarte AI, Plácido AI, Santos MS, Moreira PI. Hyperglycemia, hypoglycemia and dementia: role of mitochondria and uncoupling proteins. Curr Mol Med. 2012 (*in press*).

4. **Correia SC**, Santos RX, Cardoso S, Carvalho C, Candeias E, Duarte AI, Plácido AI, Santos MS, Moreira PI. Alzheimer disease as a vascular disorder: Where do mitochondria fit? Exp Gerontol. 2012 (*in press*).